Quantifying and Optimizing the Complexity: A Comprehensive Method to Modeling and Simulation in Electrical DC Systems

- A Maritime and Mechatronic Case Study

Vom Promotionsausschuss der
Technischen Universität Hamburg
zur Erlangung des akademischen Grades
Doktor-Ingenieurin (Dr.-Ing.)

genehmigte Dissertation (Monografie)

von
Jana Ihrens

aus
Hamburg

2026

1. Gutachter: Prof. Dr.-Ing. Thorsten A. Kern
2. Gutachter: Prof. Dr.-Ing. Christian Becker
Vorsitzender des Prüfungsausschusses: Prof. Dr.-Ing. Nikola Bursac

Tag der mündlichen Prüfung: 13.02.2026

ORCID: Jana Ihrens
https://orcid.org/0000-0002-1523-9511

DOI: https://doi.org/10.15480/882.16743

Foreword

This dissertation is the result of my work as a research associate at the Institute of Mechatronics in Mechanics at Hamburg University of Technology.

My sincere gratitude goes to Prof. Dr.-Ing. Thorsten Alexander Kern for his expert guidance, his enduring support, the confidence he showed in me, for fostering an environment of academic freedom and excellence, and the excellent working conditions. I would also like to thank Prof. Dr.-Ing. Becker for the fruitful collaboration in the SuSy project and for his willingness to serve as the second examiner for my dissertation. Furthermore, I thank Prof. Dr.-Ing. Nikola Bursac for chairing the examination committee.

I am deeply grateful to all my colleagues for the many insightful discussions, their unwavering support, their creative ideas, and the good humor and fun they brought even during stressful times. I especially want to highlight Mattis Molinski, Christoph Klie, Robert Annuth, and Timon Hartwich. The collaboration with them in the project and the lab, as well as our many discussions both within and beyond our academic fields, were invaluable. I also wish to thank all the students I had the pleasure of working with, whose research results have contributed to this thesis.

Finally, my deepest thanks are reserved for my family and friends, who have given me the necessary self-confidence and support to complete this work over the past years. I want to thank my parents, Britta and Stefan, and my siblings, Nina and Finn, for their constant encouragement and for supporting my path. A huge thank you is owed to Felix and Piet for providing welcome distractions and much joy, especially in stressful times. Felix, in particular, contributed immensely to the success of this work through his dedication, encouragement, and understanding. Thank you!

Jana Ihrens

Abstract

**Quantifying and Optimizing the Complexity:
A Comprehensive Method to Modeling and Simulation in Electrical DC Systems
- A Maritime and Mechatronic Case Study**

In the light of the climate crisis, the maritime industry is faced with the urgent need to reduce their greenhouse gas emissions. The development of maritime electrical energy systems is a key technology for sustainable shipping as it can improve energy efficiency. Designing new grids entails simulations due to the rare availability of prototypes in ship design, thereby prompting the need to prevent excessively complex simulations and models while maintaining a balance between complexity and accuracy. Achieving this balance is of paramount importance to ensure that simulations remain computationally feasible while providing reliable results for decision-making in ship design. A comprehensive methodology to optimize towards the correct level of accuracy in creating models and simulations of electrical DC power systems is proposed in this work. The relationship between accuracy and the level of detail in commonly used electrical grid component models is investigated by analyzing various models and component measurements. The results form a crucial basis for the optimization methodology developed. This methodology is predicated on a specific cost function for maritime electric grids that integrates computational and structural complexity of simulations respectively models with accuracy requirements for a range of commonly used components. This integration facilitates tailored optimization for various components and application areas. The efficacy of the methodology is demonstrated by an exemplary application to the grid of an existing ship, achieving sufficient accuracy while reducing simulation costs. The methodology's versatility is further validated through its successful application to a mechatronic system, proving its potential for broader use across domains.

Contents

Symbols

Symbol	Description	Unit
A_{Comp}	Simulation accuracy of component	-
$A_{\text{Comp,tot}}$	Total accuracy of a component	-
$A_{\text{min,Comp}}$	Calculated minimal accuracy of the investigated component	-
$A_{\text{min,sys}}$	Minimal system simulation accuracy	-
A_{Sys}	Simulation accuracy without influence of resolution	-
$A_{\text{Sys,tot}}$	Simulation accuracy including influence of resolution	-
B	Binomial distribution	-
b	Sample size	-
β	Factor to estimate the working time according to parameters, multiplicity, and cyclomatic complexity	-
C	Informational entropy complexity	-
C_{Bat}	Cost of the installed battery capacity	€
C_{Calc}	Computation costs	€
C_{Dev}	Development costs	€
C_{diode}	DC/DC-converter diode capacitance	F
C_{ds}	DC/DC-converter MOSFET drain-source capacitance	F
C_{elec}	Capacitance in electrical system	F
C_{ESL}	DC/DC-converter capacitor series inductance	H
C_{ESR}	DC/DC-converter capacitor series resistance	Ω
C_{Fix}	Fixed costs	€
C_{gd}	DC/DC-converter MOSFET drain-gate capacitance	F
C_{gs}	DC/DC-converter MOSFET gate-source capacitance	F
χ^2	Chi-squared distribution for statistical hypothesis testing	-
C_{in}	DC/DC-converter input capacitance	F
c_{int}	Capacitive component of the internal mass-spring-damper system of actuator	F
C_{Lic}	Licence costs for simulation software	€
c_{M}	Internal compliance of the actuator represented as a capacitance	F

Symbol	Description	Unit
c_{mech}	Compliance in mechanical system	mN^{-1}
C_{out}	DC/DC-converter output capacitance	F
C_{Risk}	Risk costs	€
C_{Sal}	Salary of engineers per hour	€
C_{Sav}	Potential for savings	€
C_{Serv}	Server costs	€
C_{Ship}	Total cost of ship	-
C_{tot}	Total costs	€
C_{Vol}	Price for volume reduction	€
c_{W}	Capacitive component of environment of actuator represented as a load	F
D_i	Detectability of the failure	-
d_{int}	Conductive component of the internal mass-spring-damper system of actuator	$\text{mN}^{-1}\text{s}^{-1}$
d_{M}	Internal damping of actuator represented as a conductance	$\text{mN}^{-1}\text{s}^{-1}$
D_{max}	Maximum detectability value of all FMEA failure cause, effect, and mode combinations	-
d_{mech}	Damping/friction in mechanical system	$\text{mN}^{-1}\text{s}^{-1}$
D_{PID}	DC/DC-converter controller derivative term	-
d_{W}	Conductive component of environment of actuator represented as a load	$\text{mN}^{-1}\text{s}^{-1}$
D_{x}	DC/DC-converter diodes with $x = 1,2,3$	-
e	Edges	-
$\eta(G)$	Cyclomatic complexity	-
F_{Bat}	Influence of the battery capacity on F_{ts}	-
f_{Bidirect}	Influence of bidirectionality on computation time	-
F_{Imp}	Factor for number of implementations	-
F_{mech}	Force in mechanical system	N
f_{PWM}	PWM controller frequency of DC/DC-converter	Hz
F_{ts}	Influence of the simulation resolution on the accuracy	-
f_{U}	Factor to ensure maximum simulation accuracy	-
h	Number of real measured values	-
H	H-value of Kruskal-Wallis test	-
I	Current	A
I_{elec}	Current in electrical system	A
I_{ent}	Informational entropy	-
I_{PID}	DC/DC-converter controller integral term	-
j	Number of model parameters	-

Symbol	Description	Unit
k	Number of quantities x	-
k_i	Number of cases in group i	-
L	DC/DC-converter output inductance	H
L_{DCR}	DC/DC-converter inductor series resistance	Ω
L_{elec}	Inductance in electrical system	H
L_{EPC}	DC/DC-converter inductor parallel capacitance	F
L_{m}	DC/DC-converter magnetic inductance	H
$L_{\mathrm{on,diode}}$	DC/DC-converter diode on-inductance	H
$L_{\mathrm{on,MOSFET}}$	DC/DC-converter MOSFET on-inductance	H
$l(p)$	Number of instructions	-
m	Number of quantities y	-
m_i	Measured reference value at index i	V or A
m_{int}	Inductive component of the internal mass-spring-damper system of actuator	kg
M_{max}	Maximum of measured reference value	V or A
m_{mech}	Mass in mechanical system	kg
μ_{U}	Mean value of the U-distribution	-
m_{W}	Inductive component of environment of actuator represented as a load	kg
n	Number of nodes	-
$N1$	Number of primary windings of transformer in DC/DC-converter	-
$N2$	Number of secondary windings of transformer in DC/DC-converter	-
N_{Cabins}	Number of Cabins	-
$N_{\mathrm{C,diff}}$	Number of different components developed	-
N_{Comp}	Implemented number of investigated components	-
$N_{\mathrm{Comp,imp}}$	Number of components that are implemented in the simulation	-
$N_{\mathrm{Comp,Mult}}$	Factor to estimate the additional work for multiple implementations of the same component	-
$N_{\mathrm{Const.Load}}$	Number of constant loads	-
N_{enc}	Size of the used encoding alphabet	-
n_{error}	Allowed number of 'false' simulated components	-
n_{false}	Maximum number of components that are permitted to be falsely simulated	-
N_{Para}	Number of parameters implemented	-
N_{ParaBatt}	Number of parameters of battery simulation model	-

Symbol	Description	Unit
N_{ParaDCDC}	Number of parameters of DC/DC-converter simulation model	-
$\mathcal{O}$	Big $\mathcal{O}$ notation of number of operations	-
O_i	Occurence of the failure	-
$\omega(s,x)$	Number of equivalent descriptions with meaning x of a maximum size of s	-
P	Maximum power of DC/DC-converter	W
p	Connected components	-
P_{Ind}	Scaling factor according to the kind of industry	-
P_{PID}	DC/DC-converter controller proportional term	-
$P(s)$	Solomonoff-Levin distribution	-
$p(x_i)$	Probability of occurring in the message x_{i}	-
R	Pearson correlation coefficient	-
R^{-1}	Conductance in electrical system	Sm^{-1}
R_0	Battery internal resistance	Ω
R_i	Rank sum of group i	-
$R_{\text{on,diode}}$	DC/DC-converter diode on-resistance	Ω
$R_{\text{on,MOSFET}}$	DC/DC-converter MOSFET on-resistance	Ω
R_{winding}	DC/DC-converter transformer winding resistance	Ω
S_i	Severity of the failure	-
S_0	Battery initial state of charge	-
S_{av}	Average severity of all FMEA failure cause, effect, and mode combination	-
s_i	Simulated value at index i	V or A
σ_{U}	Standard error of U-Value	-
SOC	Battery state of charge	-
s_{Turing}	Particular string put out by Turing machine	-
T	Sum of ranks of larger quantity	-
t_{Calc}	Computation time of one single component	s
$t_{\text{Calc,Comp.}}$	Computation time, complex model	s
$t_{\text{Calc},i}$	Computation time for the i-th component	s
$t_{\text{Calc,Simp.}}$	Computation time, simplified model	s
$t_{\text{Calc,tot}}$	Cumulative computation time	s
t_{Dev}	Time needed for the development of the first implemented component model	-
$t_{\text{on,max}}$	Maximum on-time of the MOSFET in the DC/DC-converter	sec
t_{s}	Simulation temporal resolution	s
T_{Ship}	Life cycle of a (cruise)ship	years

Symbol	Description	Unit
t_{sim}	Duration of the simulation	s
$t_{\text{sim,test}}$	Test simulation duration	s
$t_{\text{s,test}}$	Test simulation resolution	s
U	U-statistic	-
V	Voltage	-
V_0	No-load battery voltage	V
V_{cyc}	Cyclomatic complexity	-
V_{elec}	Voltage in electrical system	V
V_{f}	DC/DC-converter diode forward voltage	V
V_{in}	DC/DC-converter input voltage	V
V_{out}	DC/DC-converter output voltage	V
V_{Sav}	Savings through reduced volume	m^3
w_i	Weight for the i-th data point	-
$\dot{x}$	Velocity in mechanical system	-
x_i	Message of symbols	-
Z	Z-Standardization	-

Abbreviations

AC	Alternating Current
AIC	Algorithmic Information Complexity
CAT	Control and Transformation Metric
CHiL	Controller Hardware-in-the-Loop
CPU	Central Processing Unit
DC	Direct Current
FMEA	Failure Mode and Effects Analysis
FMU	Functional Mock-up Unit
FZ	Fire-Zone
GHG	Greenhouse Gas
HV	High Voltage
HVAC	Heating, Ventilation and Air Conditioning
iMEK	Institute for Mechatronics in Mechanics
IMO	International Maritime Organization
LED	Light-emitting Diode
LoD	Level of Detail
LRA	Linear-Resonant-Actuator
LV	Low Voltage
LVDC	Low Voltage Direct Current
MAPE	Mean Average Percentage Error
MARPOL	International Convention for the Prevention of Pollution from Ships
MOSFET	Metal–Oxide–Semiconductor Field-Effect Transistor
MV	Medium Voltage
MVDC	Medium Voltage Direct Current
PCB	Printed Circuit Board
PHiL	Power Hardware-in-the-Loop
PV	Photovoltaics
PWM	Pulse Width Modulation
RE	Renewable Energies
RES	Renewable Energy Sources
RMSE	Root Mean Squared Error
RPN	Risk Priority Number
SLD	Single-Line Diagram
SOC	State of Charge
SOLAS	International Convention for the Safety of Life at Sea
SSCB	Solid-State Circuit Breaker
SuSy	Sustainable DC-Systems

1 Introduction

The impacts of the climate crisis are becoming increasingly apparent, prompting various nations and organizations, including the United Nations, to set ambitious emission reduction targets. The maritime sector, contributing significantly to Greenhouse Gas (GHG) emissions with approximately 2.89 % of total worldwide GHG emissions in 2018 [1], has committed to the IMO objectives of achieving net zero GHG emissions around 2050 [2]. Achieving this goal requires leveraging multiple strategies within the maritime sector, as the adoption of fossil-free propulsion systems in shipping presents greater challenges compared to land-based systems. In this context, diverse stakeholders, including shipyards, suppliers, shipping companies, classification societies, flag states, and international organizations, often have conflicting interests.

Beyond the choice of propulsion systems or fuels, onboard power grids play a particularly critical role, especially on large vessels such as ferries and cruise ships, where energy demands can easily reach a small city's scale. The use of Direct Current (DC) grids offers numerous advantages, including facilitating the integration of renewable energy sources and reducing energy losses through fewer conversion steps [3]. However, due to the lack of ship prototypes (particularly at this scale) and limited opportunities for field testing in real DC systems, simulation plays a major role in the development of DC grids for ships.

Simulating microgrids is computationally demanding, complex, and dynamic, requiring substantial computational resources, particularly when analyzing a large number of alternative designs [4]. Due to the limited practical experience with DC grids on ships, a validation challenge arises. It remains unclear how complex simulation models need to be to achieve sufficiently accurate results while avoiding overly expensive and unnecessarily complex simulations and models. Moreover, less complex models often achieve similar levels of accuracy as more intricate ones while offering greater transparency, easier communication, reduced data requirements, less error propagation, and a greater likelihood of fostering causal understanding [5]. Therefore, simulation models should always be as simple as possible for the specific application [6].

Historically, the increasing complexity of simulations was previously offset by the increasing speed of Central Processing Units (CPUs)s, as predicted by Moore's law, stating that the number of transistors per chip doubles approximately every two years. However, recently, this growth has slowed as miniaturization approaches its physical limits [7, 8]. This shift places greater emphasis on software, algorithms, hardware architecture, the number of processors used, and the parallelization of programs.

To achieve an optimal balance between accuracy and complexity in simulation models, it is essential to determine the appropriate level of model complexity for a given application before the modeling process begins. This dissertation makes two principal contributions: the development of a generalized methodology to identify the optimal complexity for various use cases, and the development of a specific cost function tailored to the application in the context of maritime DC grid development. The methodology proposes and optimizes a cost function prior to simulation and modeling that incorporates all the resources required for simulation and modeling, as well as the risk cost associated with insufficient accuracy.

The derived methodology is not limited to maritime DC grids and can be applied to other fields. For example, a similar cost function could be formulated and optimized for land-based electrical grids. Additionally, other domains, such as the simulation of mechatronic actuators using analogies to electrical components, could benefit from this approach. Another example is climate dynamics simulations, requiring enormous computational power and infrastructure due to their high resolution, reaching up to 8 km on the earth's surface and 50 km in the atmosphere [9]. In this field, a similar methodology could be employed to reduce the resources needed for simulation.

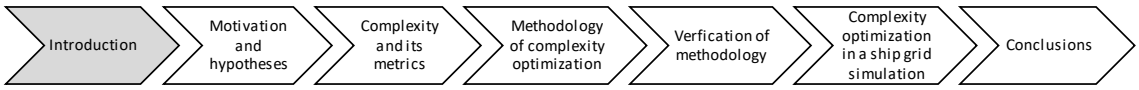

Figure 1: *Visual outline of the thesis*

In this work, visually outlined in Fig. 1, the possibilities for analyzing the accuracy and measuring the complexity of simulations and models are first examined and then tailored to the specific application of DC grids in Chapter 3. In Chapter 4, a methodological approach for optimizing the complexity of simulations and models is developed, based on the use of a cost function. Since the cost function relies on the relationship between model complexity and accuracy, an appropriate data foundation is required. For this purpose, measurements are conducted on various components and setups commonly used in DC grids as presented in Chapter 4.2. Furthermore, the influence of topology, bidirectionality, and the potential for model partitioning are analyzed in Chapter 4.3 and incorporated into the optimization process. The concept is subsequently applied to a scaled-ship grid and a mechatronic use case to demonstrate its feasibility as presented

in Chapter 5. To further validate the approach, the cost function is tested through an exemplary calculation for the development of a ship grid for an existing ship. The methodology developed is expected to provide a systematic approach to balancing accuracy and complexity in simulation, and achieve more efficient simulation practices in the context of maritime DC grids, while offering potential applications in other domains.

2 Simulations and Models in Electrical Energy Systems

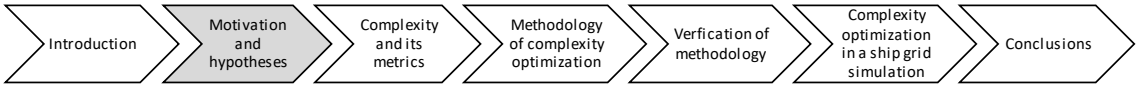

In this chapter, the importance of models and simulations for the development of maritime electrical energy systems is described. Commencing with the general design process for ships and the use of models and simulations within it, the applications of modeling and simulation are explained. Subsequently, the implications of simulation and laboratory tests in maritime grid development are presented and their properties defined. Finally, the chapter concludes with the aim of the work and the hypotheses, serving as a foundation for the subsequent investigation.

2.1 Shipboard DC Grids

As part of the ship grid design process, the evolution of shipboard electrical grids, including the transition from Alternating Current (AC) to DC systems, plays a critical role in shaping modern ship grid design. Since the introduction of shipboard electricity in 1880 as a DC lighting system on the passenger ship SS Columbia [3, 10], the presence of electrical AC grids on ships has become widely adopted [3] and has undergone substantial advancements. Electric propulsion, first introduced in 1988 on the ocean liner Queen Elizabeth II, is a widely used and fuel-efficient drive system that has gained increasing popularity over time [11, 12]. With increasing power levels and more critical components connected to the electrical grid, the grid's complexity increases [13], thus increasing the significance of simulations and their accuracy for ship grid design. This development facilitated further advancements such as the launch of the first battery-driven ferry, Ampere, in 2015, followed by other vessels such as the FCS Alsterwasser[1], the Tycho Brahe and Aurora ferries[2] [3, 10], that marked a shift toward

[1] ferry with a combination of fuel cell and battery power system, 2012, [14]
[2] HH ferries car ferry, 2017, ABB

hybrid AC/DC grids featuring DC main buses. However, the number of readily available solutions remains limited [15]. These grids are designed to accommodate batteries and other energy storage systems connected to the main bus. As the integration of distributed Renewable Energy Sources (RES) and energy storage systems across ships increases, additional lower level DC grid segments and buses are being developed and implemented [10], as demonstrated in the DAMEN waterbus [16].

The increased use of DC grids, particularly in maritime environments, offers several advantages, including a more flexible distributed system [17–19], eliminating synchronization problems and reactive power losses [3, 10, 20]. Driven by stricter environmental regulations and the advancing integration of (battery) storage, renewable energy, and the availability of semiconductor switching devices and power electronics [21], DC grid technology is gaining importance [15, 17]. There are particular advantages in the maritime sector, as DC grids can be implemented more easily on ships than on shore, due to the inherent island nature of the grid [22]. Compared to AC grids, power electronic DC/DC-converters provide more efficient conversion, allowing large ferromagnetic transformers to be replaced by more compact units [17, 23]. This results in higher efficiency by eliminating conversions at the component level, especially for DC loads such as Light-emitting Diode (LED) lighting and batteries [11, 24] where a conversion can be eliminated. The use of distributed systems and bus layouts in DC systems can reduce wiring and safety installation costs while maintaining system safety [11, 25]. A reduction in cable cross sections is possible due to the irrelevance of the skin and proximity effects for direct current grids [11]. This reduction in cable cross section in combination with the different grid structure leads to a decrease in necessary space and weight [10, 25]. Other benefits include generator operation at optimized operating points at variable frequencies, leading to a reduction in fuel oil consumption [3, 10, 11, 26] and simplified motor control [27]. Even for variable frequency generators in AC, the adoption of a DC system eliminates one conversion step from AC to DC. Consequently, due to efficiency gains in these various aspects, the global efficiency of a DC system is greater than for comparable AC systems, thus reducing CO_2 emissions [28].

The integration of renewable energies, including fuel cells, photovoltaics, and battery storage, is facilitated by the use of DC grids [10, 11, 26]. However, despite promising benefits, DC grids present challenges. Fault protection requires special semiconductor circuit breakers, as the lack of a natural zero crossing requires more complex arc extinguishing [3]. Short circuits can have more serious consequences in DC grids [29, 30], but interruption of short circuits can be achieved faster due to the use of Solid-State Circuit Breakers (SSCBs) [25]. Nevertheless, the selectivity of fault protection devices in bidirectional DC grids is more complex as a result of the presence of bidirectional power flows. The control of power flows and power quality requires using droop control instead of frequency and reactive power flow for control functions [3]. Furthermore,

voltage ripples induced by converters and load transients can lead to issues regarding power quality [3].

Suitable grounding [30], the limited availability of components, and the increased complexity of power electronic components for protection and switching are further challenges [21]. Direct connection of bidirectional components to the grid requires extensive modeling due to the possible power flows in fault scenarios and the more complex power flow, making grid interconnection and simulation considerably more complex. For DC grids, simulation plays an even more critical role compared to AC grids due to several factors. The lack of prototypes and limited practical experience with DC grids increases the reliance on simulation for design and analysis. Additionally, the inherent risks associated with new grid designs can be mitigated through simulation. Despite these challenges, DC technology remains a promising area for its potential benefits, but requires further effort in developing simulation methodologies for achieving optimal simulation models.

An example of a traditional AC main grid for a cruise ship is illustrated in Fig. 2 as a Single-Line Diagram (SLD) [19]. It includes two main buses, main generators, propulsion machines, as well as fuel cells and batteries as additional energy sources. The entire system is designed with redundant connections, including the five Fire-Zone (FZ) Low Voltage (LV) distributions, that are connected via transformers.

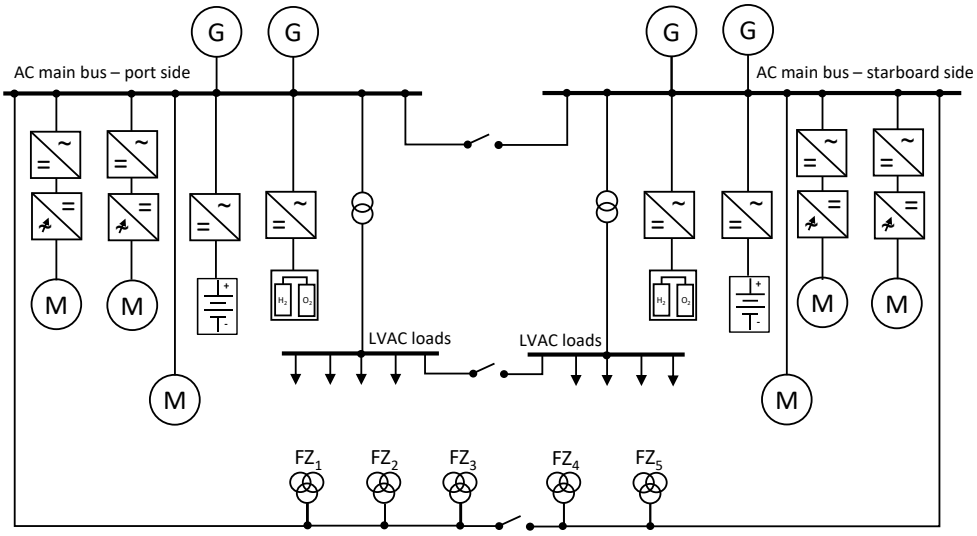

Figure 2: *SLD of Conventional AC Grid of five FZs, with two main buses, main generators, propulsion machines, and fuel cells and batteries as additional energy sources in a redundant setup*

Some DC grid topologies are presented in the literature; however, with few real ships utilizing DC grids, there is currently no established standard. Within the project *SuSy - Sustainable DC Systems - Direct Current Energy Supply on Ships* [31], new concepts

for hybrid ship grids were developed, providing valuable insights. Based on these findings, this dissertation proposes DC grid setups. Fig. 3 presents a comparable DC grid for a cruise ship in a ring topology, featuring starboard and port-side buses, main generators, propulsion machines, and the same additional energy sources. The entire grid, including the LV FZ distributions connected via DC/DC-converters, is designed redundant.

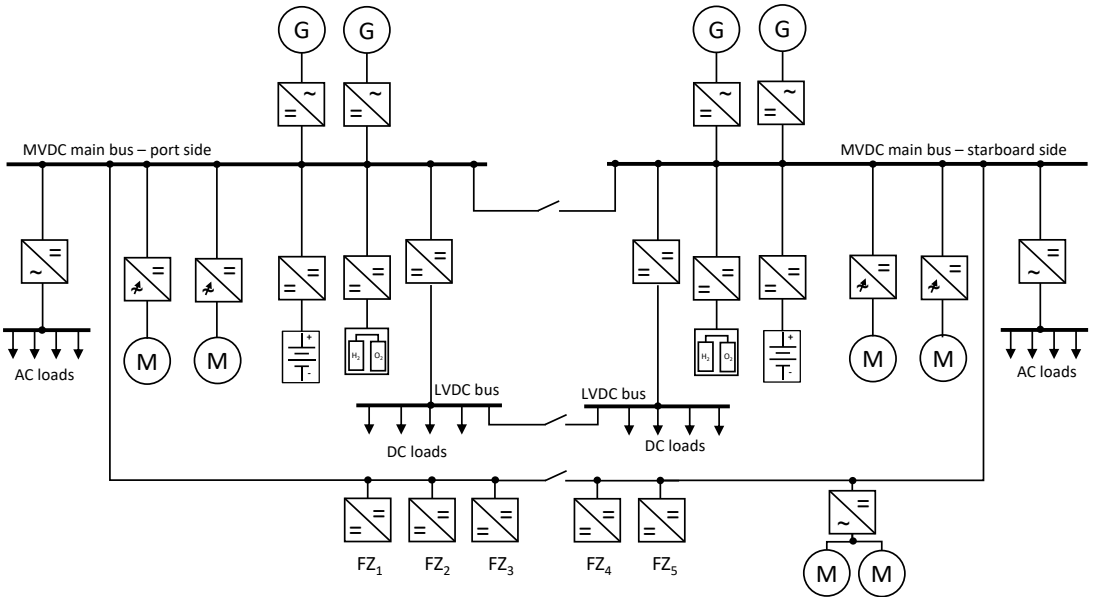

Figure 3: *SLD of proposed DC grid in ring topology, with a starboard and a port-side main bus, each with main generators, propulsion machines, and fuel cells and batteries as additional energy sources. Redundancy is maintained by switches that link both main buses.*

An alternative DC grid in a zonal topology similar to the grid presented in [18, 32] is shown in Fig. 4, containing the same components connected to two main buses. The LV FZ distributions are again linked via DC/DC-converters, and the entire system maintains redundancy.

In low voltage distribution, bipolar DC grids, proposed as an alternative to unipolar grids, offer increased power density and greater flexibility compared to unipolar systems [33, 34] by providing two distinct voltage levels for loads with different requirements in terms of power and voltage level. However, as a relatively new grid concept, bipolar grids currently lack established standards [33]. Challenges such as power balancing, protection, and voltage stability remain barriers to their widespread adoption. An example of a FZ power grid architecture for a unipolar and bipolar DC grid is shown in Fig. 5.

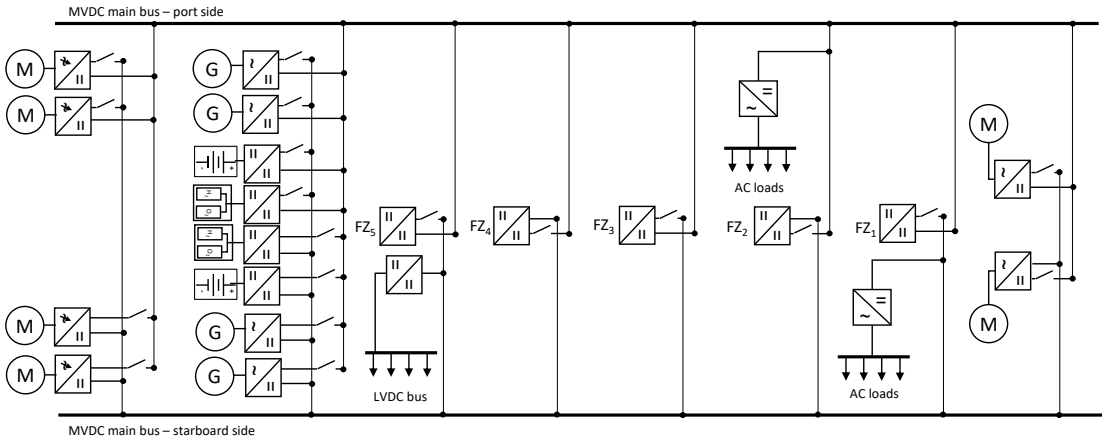

Figure 4: *SLD of proposed DC grid of Fig. 3 in zonal topology, with all safety-relevant components permanently connected to one main bus and, for redundancy, additionally connected to the other main bus via a switch.*

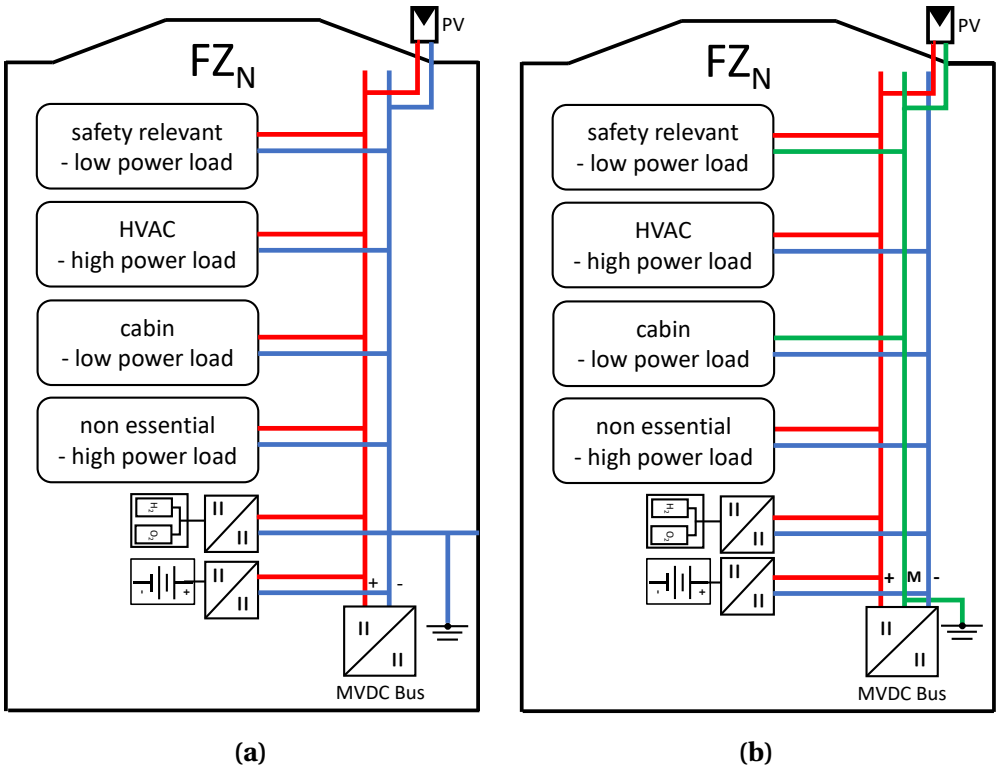

Figure 5: *Low Voltage Direct Current (LVDC) FZ distribution system (a) unipolar architecture (b) bipolar architecture with red as the positive and blue as the negative pole, the grounded neutral (M) depicted in green*

One strategy proposed to increase the versatility of DC grids for various maritime applications is streamlining the design through modularization and standardization of power

systems [17]. Modularization, a well-established method in complexity management [35] and systems engineering [36], involves clustering commonly used components into modules and connecting them via standardized interfaces to meet the majority of modern ship requirements. The implementation of this modularization concept is illustrated in Fig. 6.

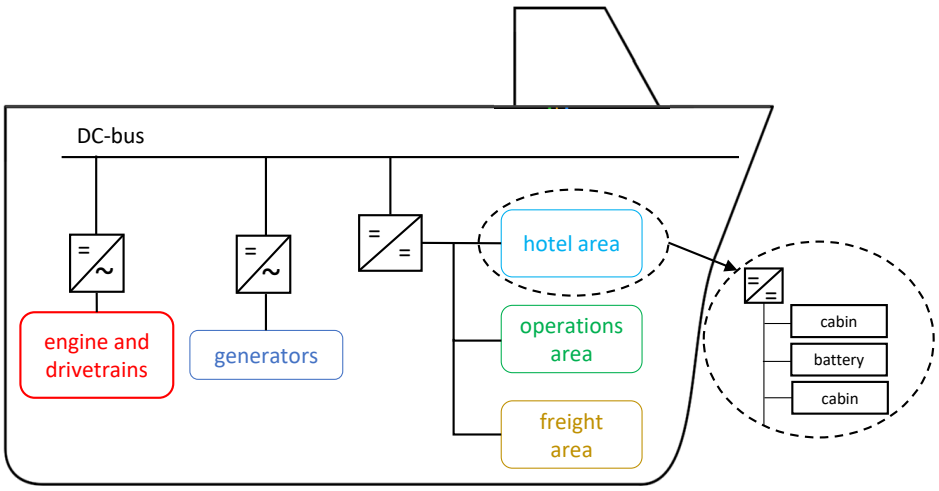

Figure 6: *Modularization of a shipboard energy system*

To fully benefit from modularization, structuring simulation models according to the modular system can simplify and enhance the simulation process in ship grid design.

2.2 Ship Grid Design Methodology

Maritime electrical energy systems are uniquely designed complex systems and specific for each ships' operating conditions [37]. The shipbuilding industry has a complex value creation chain involving various stakeholders. Shipyards play a central role in coordinating other stakeholders and constructing the ships, involving the use of additional subcontractors and suppliers. These subcontractors and suppliers, ranging from engine and electrical system integrators to balcony or window manufacturers, contribute to value creation by providing highly specialized components. Engineering companies are often used for technical planning and optimization. Owners, whether private or corporate, finance the project and have specific requirements for the ship's later use. Ship classification societies certify that the ship's construction complies with all relevant standards, enabling it to be registered with the desired flag state's ship registry and obtain insurance. In the European shipbuilding industry, the vast majority of ships are custom solutions and designs, leading to a development aligned to the customers' wishes [37–39]. Additionally, complying with the strict rules and regulations for modern

vessels and their quality of service as stated by the International Maritime Organization (IMO), International Convention for the Safety of Life at Sea (SOLAS), International Convention for the Prevention of Pollution from Ships (MARPOL), national agencies and classification societies add further requirements [12]. For the compliance with maritime regulations and to guarantee safety and redundancy, ships are typically divided into decks and FZs as depicted in Fig. 7.

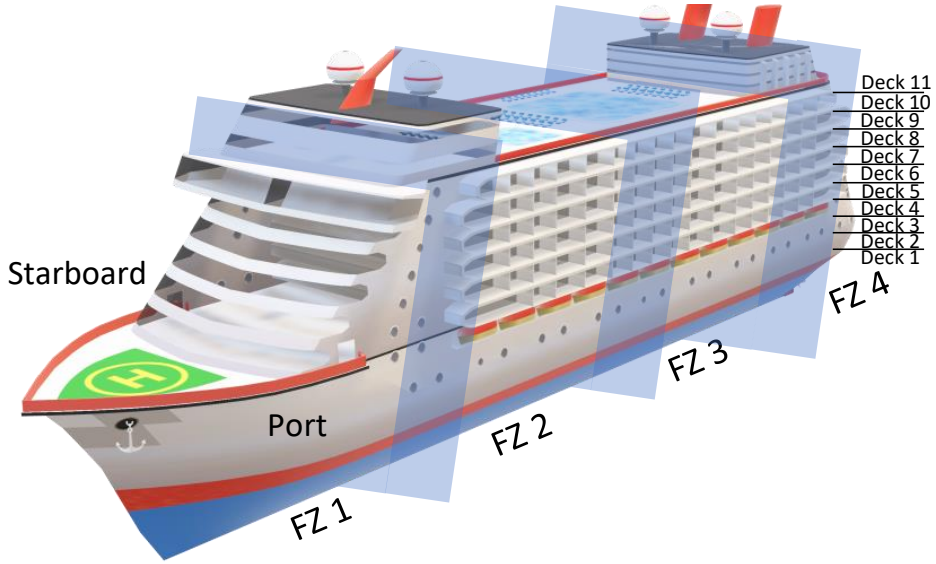

Figure 7: *Visualization of deck levels and FZs on a cruise ship (base drawing adapted from [40])*

Ship design shows a unique relationship between design complexity and project duration. Although characterized by higher complexity, there are comparatively shorter timelines than those observed in the development of cars, airplanes, and power plants [38]. The traditional sequential ship design approach as depicted in Fig. 8 consists of concept, preliminary, contract, and detailed design phases [12, 41], that applies to a complex set of objectives from the ships' dimensions and hull form to machinery, structural elements, electrical and thermal grids, while keeping the costs as low as possible. Due to the complexity of each of these objectives and their - partly contradictory - relationships [41], a linear design process is unfeasible, and an iterative approach is required [42]. The design spiral, the iterative process introduced by Evans in 1959 [43], has since been used to design ships in various iterative steps. This highlights the iterative nature of ship design, where interdependencies between all systems and their requirements must be considered. Multiple iterations through the various systems are required, with each cycle bringing the design closer to its final form. It has been updated to more modern approaches, such as the 3D design spiral depicted in Fig. 9. This approach emphasizes communication of all stakeholders between loops, the possibility of each phase requiring several complete turns [44], and it allows focus shifts between the phases.

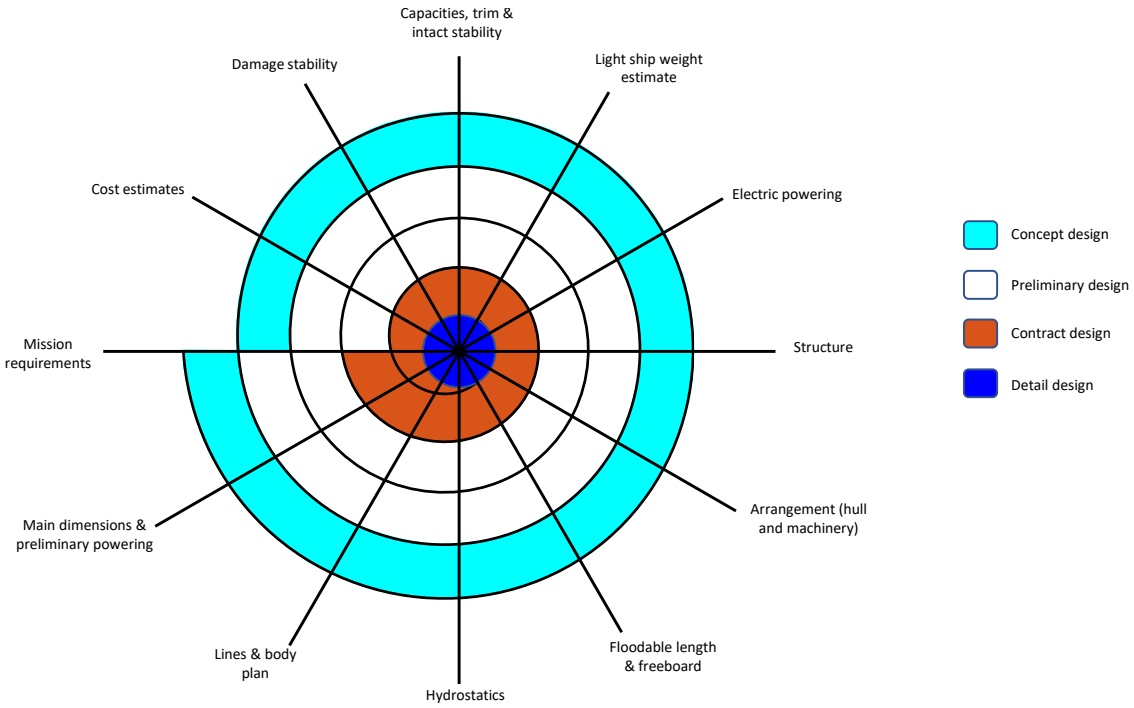

Figure 8: *Traditional design spiral for ship design with each cycle refining the design. Own visualization based on Evans [43]*

The design spiral was and still is often used as a method for developing a complete ship design as well as a particular part of ship design, e.g., the electrical grid design. However, as ships are no longer designed for a single operation point but a multipoint operation, recent investigations show that the traditional design spiral is no longer a good representation of the ship design process [44]. Furthermore, the process is time-consuming and prone to stagnation in local optima[45]. *Simulation-driven ship design* [46, 47] or integrated multi-objective optimization [44, 48] as a modern, integrated design method are increasingly focussed instead. Nevertheless, the design spiral remains a popular design method in the shipbuilding industry. The integration of simulation into the methodology and design of shipboard electrical systems is slowly gaining traction and provides the ability to improve efficiency, reliability, and safety. The contract design phase is of primary importance for incorporating the ship's electrical systems into the design. During this phase, the preliminary design is further developed to provide a more precise estimate of the ship's technical and economic performance, while the auxiliary grids, utility grids, and the ship's electrical grid are designed. In contrast, the preliminary design phase focuses primarily on the dimensioning of the most relevant electrical components.

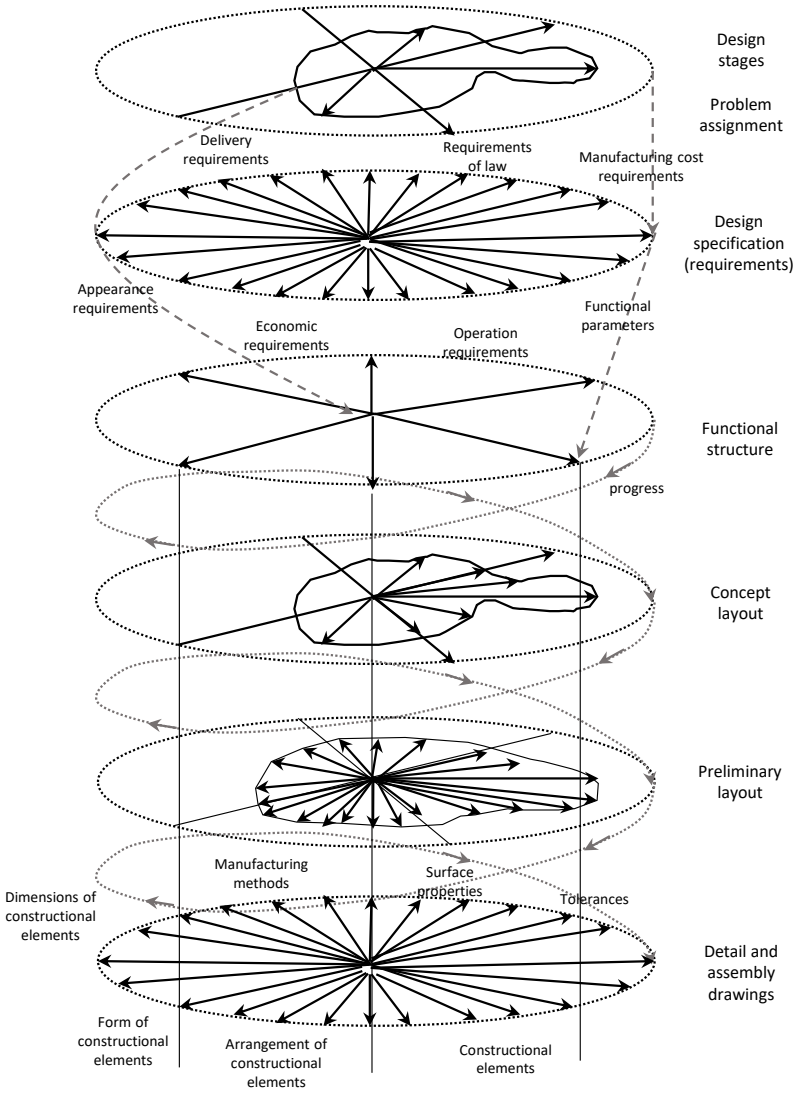

Figure 9: *Own visualization of 3D design spiral adapted from Papanikolaou [41], allowing focus shifts and multiple loops per phase with enhanced dialogue and flexibility within the iterative process.*

2.3 Inherent Simulation and Model Properties

The use of simulation models facilitates understanding of the behavior of complex real systems, be it a technical, social, or other system, and to develop operation strategies [49, 50]. For this, a simulation can run possible scenarios to predict the system's response [49, 50]. In the context of shipboard DC grids, simulations are essential for evaluating design choices and optimizing their performance in various operational scenarios. This section provides a discussion of simulations, models, and their characteristics. The initial step in this process is to establish a clear definition of the concept of simulation complexity

and the level of detail in the modeling. A systematic literature search is presented in Chapter 2.3.2 to provide an overview of the scientific sources and to identify research gaps. Subsequently, the requirements for simulations that are necessary for efficient modeling are presented. In addition, the uncertainties incorporated in the simulation models are addressed, and a metric is presented for the quantification of the accuracy of the model. Finally, the application scope of simulations is examined.

The basis for the simulation is the model, a static representation of a real system [51], that can be executed on a computer [52]. Models can be grouped into continuous, discrete, or discrete-continuous models [6], as this work focuses on models for maritime electrical grids and their modeling in *MATLAB Simulink Simscape*®, this work focuses only on discrete models, although the outcome of this thesis may also apply to other groups of models. Additionally, models are characterized by their input and output variables that are linked by differential algebraic equations, state graphs or automata, and (usually fixed) internal parameters [6, 53]. When developing a model of a system, the first step is defining the model's boundary and the necessary accuracy [50, 53]. Subsequently, in- and output variables need to be set and the structure to link both needs to be developed and parameters need to be set, using optimization, datasheets, measurements, or other additional sources [50, 54]. The development of models is defined in the literature, as depicted in Fig. 10. Obtaining a concept-model from the real system is achieved through analyzing the real system and then qualifying the concept-model against reality. A concept-model can then be implemented as an executable model, that needs to be verified against the concept-model. The executable model is then simulated to obtain information about the behavior of the real system. Simulation is defined by changing one or multiple variables of a model and observing the results [55]. This simulation is used to answer questions about the system that it is representing. It needs to be validated against the real system, whether it displays a sufficiently similar behavior to the real system to obtain meaningful results [56].

Verification is defined here as determining the correct implementation of a model and confirming its compliance with previously defined requirements [5, 56, 57]. Whereas, validation is defined as determining the accurate representation of the real system by the model and a satisfactory accuracy for its intended application [5, 56]. If the real system to be represented by the model does not yet exist or data are not available, conceptual model validation is used to test the structure, logic, and mathematical and causal relationships of the model [56]. The numerical result must always be judged by the user [58].

There are few quantified statements regarding the accuracy of simulation models. However, strong qualitative assertions exist, emphasizing that all models are, to some extent, inherently wrong [59], as not all physical phenomena can be fully explained and implemented into a model. Choosing an appropriate Level of Detail (LoD) for the specific

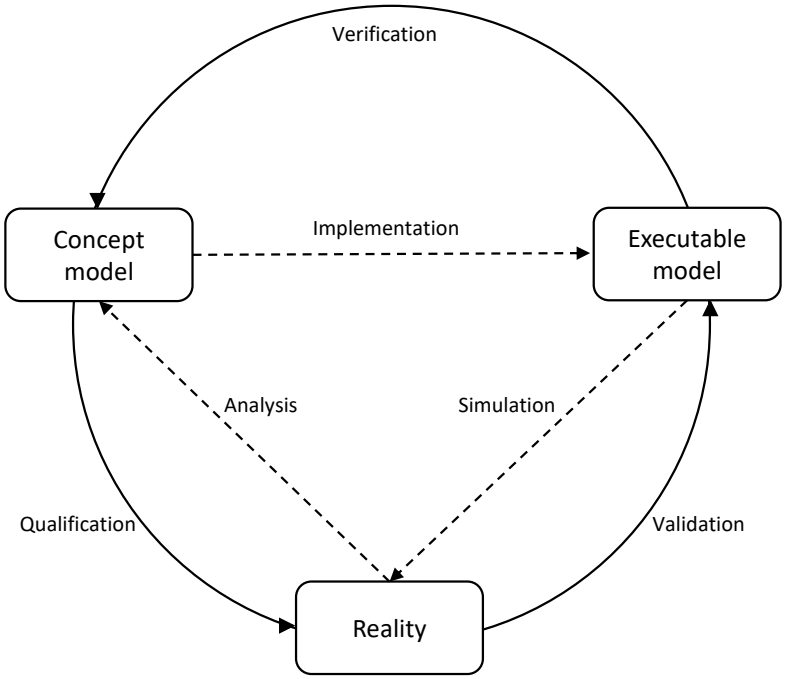

Figure 10: *Model development and simulation process, own visualization based on Sargent [56]*

application and objectives, while keeping the complexity of the model as low as possible, is therefore essential to obtain meaningful results [6, 60]. The use of simulation models is often the only way to study certain electrical grids, because experiments during operation can be dangerous and forbidden, too expensive, or the grid to be studied does not exist yet. However, apart from these constraints that lead to the use of simulations, there are other advantages that simulations offer: They provide the opportunity to choose different setups, to compress and expand time, and to explore different possibilities for the system [51, 55]. A better understanding can be obtained through their use, making them a suitable option for training and convincing others through visualization [51, 61]. Problems can be diagnosed and constraints or requirements can be identified through the use of simulation [51]. However, simulations can also entail disadvantages [51, 55]: Simulations may be cheaper than field tests and experiments, but can still be time-consuming and costly. They can be used in cases where they do not produce meaningful results, or the interpretation of the results can be difficult, and special training is needed to build suitable simulation models. Using models with an inappropriate LoD for the simulation's objective can additionally endanger the success of a simulation [55]. However, simulations can never provide a complete representation of reality, since they rely on simplifications and assumptions that may not fully reflect the complexity of real systems. Therefore, several levels of abstraction and simplification for models are necessary to achieve a balance between capturing important system dynamics and maintaining computational efficiency [58]. A similar challenge arises in the design of avionics systems, where models are inherently complex and feature a vast degree of

freedom, leading to substantial computational resource demands. This avionics system complexity can be effectively managed through interconnected meta-models, that facilitate seamless transitions between abstraction levels while ensuring consistency and coherence across the system [62].

2.3.1 Simulation Complexity

Complexity is not universally defined in the context of simulations of technical systems, although an intuitive concept of complexity is widely understood [63, 64]. Both the represented real system and the simulation of this system can be assigned a complexity, but in this thesis only the complexity of the simulation is considered. This is divided into two aspects as shown in Fig. 11. On the one hand the computational complexity, that is relevant to the execution of the simulation. On the other hand the structural complexity of the simulation model, that is related to the computational complexity, but primarily affects the development and understanding of the simulation [64]. Structural and computational complexity can be combined in one definition if they are understood as the resource requirements of the simulation process from model creation to evaluation. This leads to the definition of simulation complexity as a measure of the resources required to develop and understand a model or its corresponding underlying system, to simulate the model and the necessary computational resources, and to analyze the simulation results.

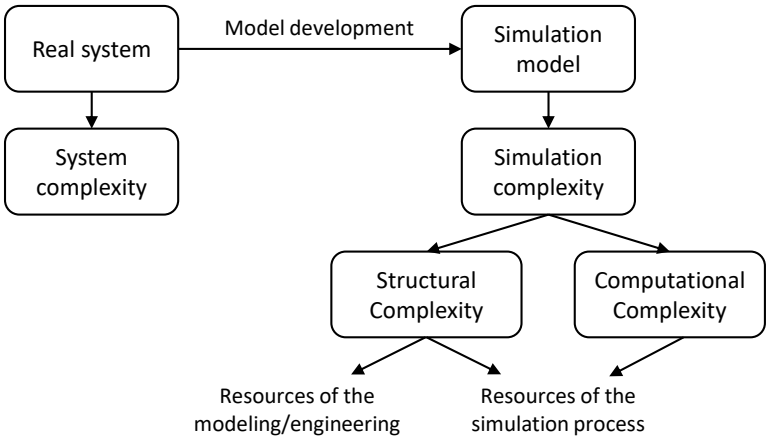

Figure 11: *Complexity of the real system and the respective simulation model*

Even if the complexity of the model is generally independent of that of the real system, it can be assumed that the complexity of the simulation increases with the complexity of the real system, as f.i., simple models of complex systems are possible. Since the resources required are directly related to the cost of the simulation and the hardware used, the cost of a simulation is determined by its complexity [63, 65]. With regard to the

complexity of simulations and models, it is relevant to distinguish between complexity and LoD. The LoD refers to the particular properties of the modeled components and the detailed physical effects, whereas the complexity refers only to the structure of the model and its execution. A high level of complexity is indicated by many components, connections, parameters, or a long computation time [60].

Simulations cannot fully represent real systems, otherwise infinite simulation times would be necessary [58]. Instead, simulations and simulation models should only have a LoD as high as necessary to be suitable for the particular application [5, 6]. Models with higher LoD do not necessarily lead to better results, but may contain more errors due to their complexity and the associated difficulties for verification and validation [64, 66]. Models with a lower LoD allow more transparency, require fewer data for parameterization, verification and validation, reduce error propagation and facilitate application understanding [5], but may result in lower accuracy [67]. Complexity of simulations on the other hand should always be kept as low as possible while maintaining sufficient LoD to achieve the model objectives.

2.3.2 State of the Art

A focused systematic literature search is conducted to obtain an extensive overview of scientific sources concerning the complexity of models and simulations, an overview of publications is shown in Table 3. This comprehensive search is carried out using selected keywords as outlined in Appendix A. As highlighted by Brooks *et al.* [63] in 1996, there is a lack of research on selecting appropriate models and achieving the optimal LoD for specific applications, despite the critical importance of this topic. In 2016, Ahmed *et al.* [68] noted that research interest in defining simulation model complexity remains limited, despite the growing size and complexity of models driven by increasing computational power [64, 68–71]. This gap is concerning, as several authors have raised issues regarding the consequences of increasing model complexity, including challenges in verification and validation [69], higher costs [72], and potentially reduced predictability [73]. There is broad consensus among researchers that models should adhere to the principle of parsimony [49, 59, 63, 64, 72–74].

The publications reviewed span from foundational works in the 1980s, through a larger volume of research in the 1990s, to a concentrated block of studies around 2015. This distribution explains the inclusion of older publications in this analysis, as they provide essential context and foundational information. This lack of research and the associated challenges constitute the reason for the focus on the topic of optimization of simulation complexity in this work. A graphical representation of citation connections and topics is provided in Fig. 12.

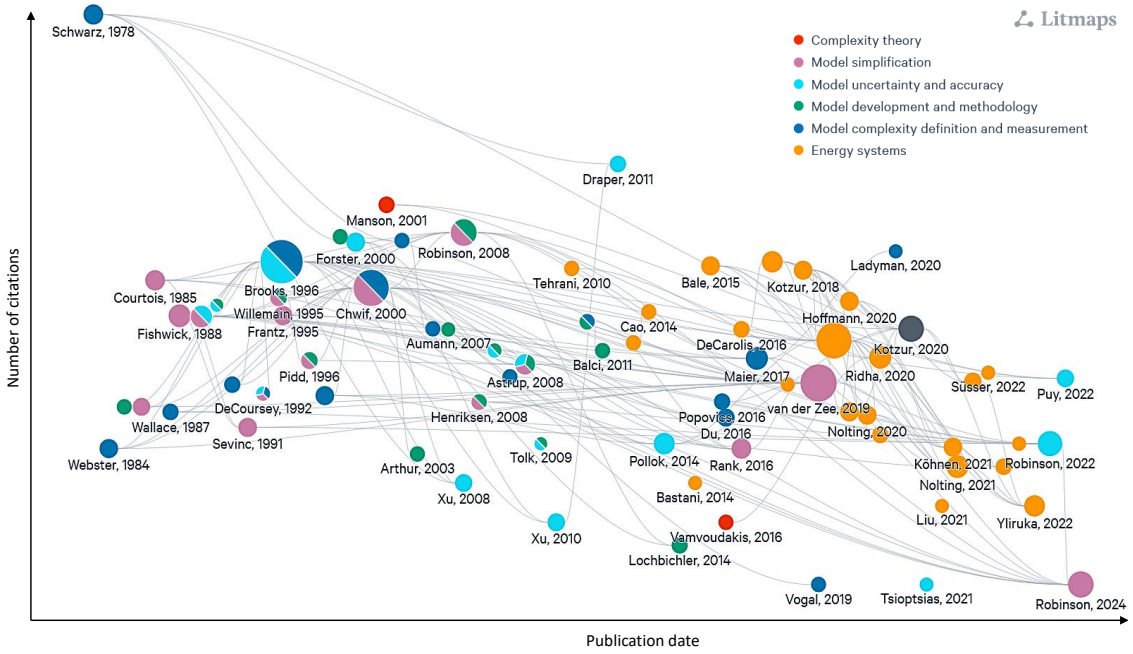

Figure 12: *Self-curated literature map overview of publications regarding simulation and model complexity, visualized with Litmaps [115]. The greater the size of the node, the greater the number of connections in the graph, and thus, the greater its relevance to the topic.*

The lack of research is particularly evident when examining the selection of models for specific use cases. Regarding the topic of energy systems, only a few publications address a more general approach to complexity reduction [116–120], while the majority focus on time resolution and temporal aggregation [67, 121–130]. Spatial resolution is explored in fewer studies [131, 132]. Complexity analysis for energy system simulations remains sparse [133, 134], and only a limited number of publications examine the trade-off between the LoD and accuracy [132, 135, 136]. Most of these publications were released between 2014 and 2022, reflecting a recent surge in interest in these topics.

Furthermore, the topic of simulation and model complexity is explored across various fields, including biomechanics [137], hydrology [93, 138–142], civil engineering [143], neurology [78, 144], marine defense [71], ecology [145], and manufacturing [81], among others.

The importance of analyzing, evaluating, or optimizing simulation models prior to the actual modeling process is recognized as a means to avoid complexity drivers [67, 76, 124], select the optimal resolution, and achieve the best trade-off between complexity and accuracy [105, 119, 133, 135]. However, existing publications that address this step are sparse and often tailored to specific use cases [119, 135], leaving the broader question of how to holistically optimize the simulation complexity vs. accuracy trade-off across multiple components unanswered. This gap in the literature highlights the need for a

Table 3: Publication overview: Simulation model complexity

	Focus topic	**Authors**
Model complexity definition and measurement	Complexity metric for models	Chwif [64], Du [75], Schruben [76], Standish [77], Myung [78], Wallace [79], Schwarz [80], Popovics [81]
	Definition of model complexity/level of detail/granularity	Brooks [63], Webster [65], Standish [77], Du [75], Golay [82], Ladyman [83], Maier [84], Netter [85]
	Model performance evaluation	Brooks [63], Vogal [86]
	(Dis-)advantages of model complexity	Brooks [63], Decoursey [87]
Model development and methodology	Model credibility through verification and validation	Shannon [50], Banks [51], Sargent [56], Arthur [69], Tolk [88]
	Model design and implementation	Shannon [50], Banks [51], Aumann [5], Pidd [74], Zeigler [89], Willemain [54], Robinson [90, 91]
	Reusability	Lochbichler [60], Balci [70]
	Complexity management in modeling	Aumann [5], Henriksen [72], Astrup [73], Netter [85], Zeigler [89]
	Robust modeling	Choi [92]
Model uncertainty and accuracy	Acceptability, credibility, performance assessment	Brooks [63], Astrup [73], Tolk [88], Xu [93], Balci [94], Tsioptsias [95], Forster [96], Ward [97]
	Method to avoid uncertainties	Decoursey [87], Choi [92]
	Influence of complexity on uncertainty/accuracy	Puy [98], Robinson [99]
	Assessment of model uncertainty/accuracy	Puy [98], Apostolakis [100], Draper [101], Xu [102], Pollok [103]

	Focus topic	Authors
Model simplification and abstraction	Models should be parsimonous/ model simple	Willemain [54], Box [59], Chwif [64], Salt [66], Henriksen [72], Astrup [73], Pidd [74], Decoursey [87], Robinson [90], Ward [97], Rexstad [104], van der Zee [105], Fishwick [106], Rank [107]
	Methods for simplification/ abstraction	Pidd [74], Rexstad [104], van der Zee [105], Fishwick [106], Rank [107], Robinson [108], Courtois [109], Sevinc [110], Frantz [111]
Complexity theory	Complex systems - characteristics and approaches	Manson [112], Vamvoudakis [113], Simon [114]

systematic approach, which is why this work focuses on developing a comprehensive methodology to address this challenge.

2.3.3 Requirements for Simulations

In order to study a system using simulation, certain requirements must be met by the simulation to gain a good understanding of the behavior of the real system or for the development of (utilization) strategies [146] as listed in Tab. 4. Compared to field-testing, simulations are quick and inexpensive to conduct, but also require adherence to a cost framework and are expected to deliver results in a short time. First, the model must describe the behavior of the real system in sufficient detail and with a certain accuracy [63, 146]. The resources needed to create the model, simulate it, and analyze the results should be kept to a minimum [54], as should the hardware requirements [63]. High usability and the ability to reuse models can reduce cost and time at this point [54, 147, 148]. The accuracy and validity of the model are important in order to obtain high-quality simulation results. Insofar as possible, simplified minimal models increase understandability and promote better verifiability [147, 149]. To maximize the utility of the results, it is essential to minimize the probability of errors within the model and guarantee a high degree of agreement with known historical or test data. Additionally, the input data used for model development should be of high quality, thereby enhancing the model's credibility [63, 91]. In addition, models should be easy to understand, and their results should be comprehensible. If the model is transferable to other research questions or if its use within other models is conceivable, this is also an advantage [63].

However, these requirements can lead to conflicting goals, as high accuracy typically

Table 4: *Requirements for simulations*

Requirements	**Ideal value**
Computation time	low
Development time	low
Analysis time	low
Hardware requirements	low
Accuracy	high
Detail	as low as possible to reach required accuracy
Portability	high
Understandability	high
Probability of model errors	low
Validity for (historical) data	high
Credibility (theoretical)	high

requires increased resources. A high LoD can reduce comprehensibility and portability, and increase model error probability, yet it offers greater theoretical credibility and potential accuracy. Therefore, a careful trade-off between complexity and accuracy is essential.

2.3.4 Uncertainties in Simulations and Models

Simulations are required to be sufficiently accurate for their respective application [49]. The accuracy corresponds to the deviation between the result of the simulation and the behavior of the real system represented by the simulation by using a reference measurement. A lower complexity of simulation and model usually results in a reduced range of application [146], i.e., it requires a more precise orientation towards a specific application in order to be sufficiently accurate. There is therefore a trade-off between the complexity of a simulation and its accuracy, as shown in Fig. 13. The output variables should always have a certain accuracy in relation to the represented system, but at the same time the simulation model should have the lowest possible complexity [146]. Nevertheless, a simulation always carries an error in comparison to the real system or a Power Hardware-in-the-Loop (PHiL)- or field-test[3].

Sources of error that lead to reduced accuracy can initially be divided into systematic and stochastic errors, but in this work the four categories of data uncertainty, numerical uncertainty, model structure errors, and evaluation errors are additionally used [92], as shown in Fig. 14.

[3]While PHiL- and field-tests are still subject to systematic and measurement uncertainties, they remain the closest attainable approximation

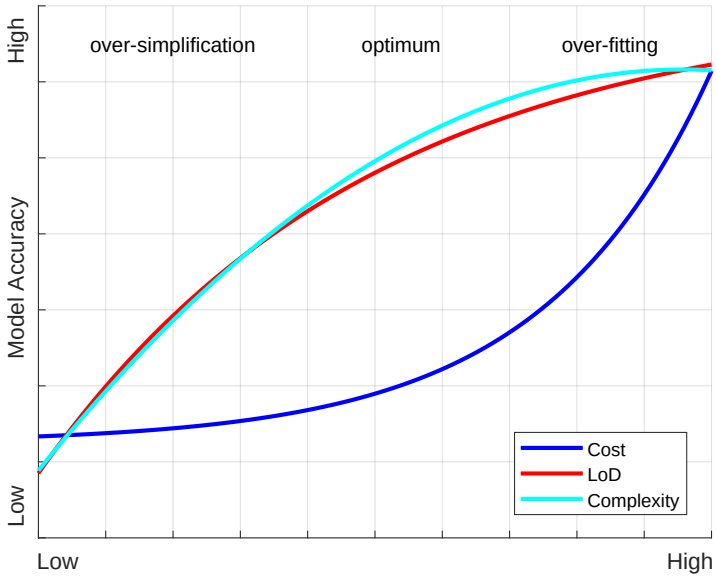

Figure 13: *Model accuracy with regard to level of detail, complexity, and cost*

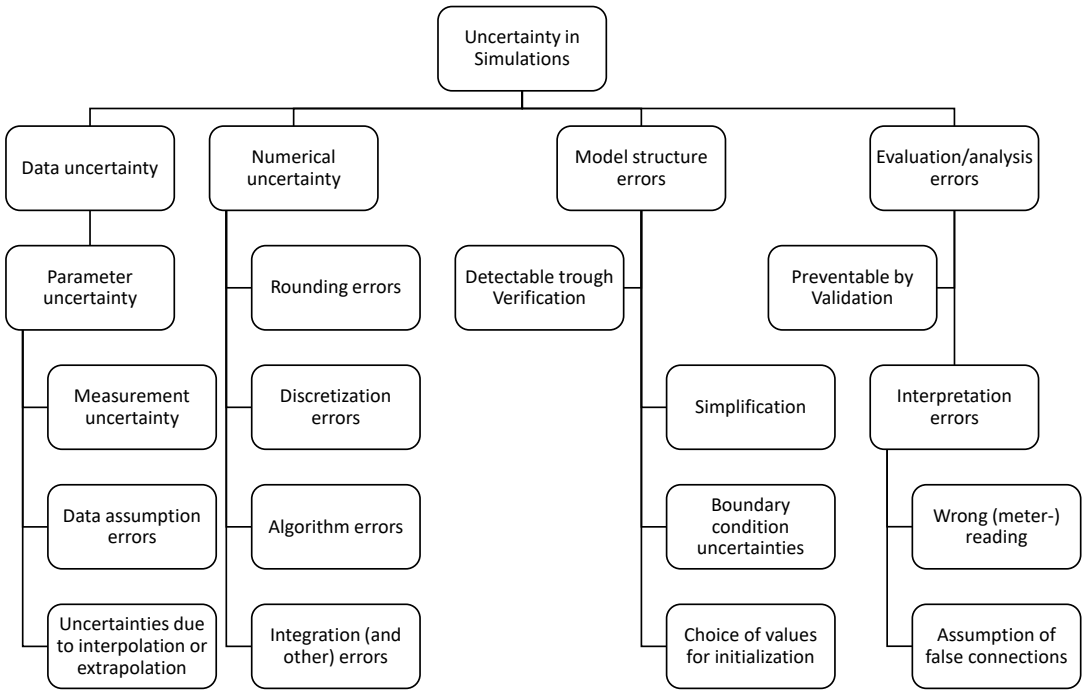

Figure 14: *Overview of different model uncertainties*

Data uncertainty occurs in particular when identifying parameters, this can be due to measurement uncertainties, uncertainties that arise due to interpolation or extrapolation of available data or data assumption errors, where false connections or correlations within the data are assumed. Additionally, data uncertainty can be due to the quantification of the simulation's accuracy by comparison with defective data. Furthermore,

numerical uncertainties can influence the accuracy of a simulation. Rounding errors result from the fact that a computer is only able to represent a finite set of numbers with a limited number of decimal figures. Model structure errors, that may be detected through a thorough verification, arise due to the simplification of the model in comparison to the represented system, a poor choice of initialization values or uncertainties in the selection of boundary conditions. They can be fundamental and endanger the simulations' fidelity [150] but are often difficult to quantify [92]. Evaluation errors may be prevented by a thorough validation process, nevertheless, errors within the interpretation of results may still occur, e.g. wrong metering or the assumption of false connections or correlations within the results f.i. assuming causal behavior, that does not correspond to reality. The propagation and combination of these four classes of errors may lead to an even larger uncertainty in the chain of errors. The worst case for the complete propagated error can be calculated using a Taylor expansion.
Ultimately, all models incorporate errors and are uncertain to a degree, but it is important, that the accuracy is still sufficient to obtain viable results for the specific application [59]. Therefore, a differentiation between epistemic errors that are reducible and aleatory errors (irreducible) is necessary:

- Evaluation and model structure errors are epistemic errors, as they can be diminished by a better model formulation or more careful analysis of results.
- Numerical uncertainties may be epistemic to a certain degree, but there is always an inevitable aleatory numerical error left.
- Data uncertainties are epistemic, if the possibility to gather more or more accurate data exists.

2.3.5 Accuracy of Simulations and Models

The quantification of simulation and model accuracy using a weighted Mean Average Percentage Error (MAPE) is one of the key measures in this work. Since this is a less commonly used error metric, an explanation of its calculation is presented here. In order to quantify the accuracy, a weighted MAPE [151] with the measured reference value at index im_i, the simulated value at index is_i and the weight for the i-th data point w_i are used in this work:

$$wMAPE = \frac{\sum_{i=1}^{n} w_i \cdot |\frac{m_i - s_i}{m_i}|}{\sum_{i=1}^{n} w_i} \tag{1}$$

$$w_i = \begin{cases} 0.02 & \text{if } m_i \leq 0.2 \cdot M_{\max}, \\ 0.98 & \text{if } m_i > 0.2 \cdot M_{\max}, \end{cases} \tag{2}$$

The reference values used originate from measurements of real systems or from measurements in corresponding test benches (e.g. PHiL) using a *Zimmer LMG 671* power analyzer [152] (ZES ZIMMER Electronic Systems GmbH, Germany) for measurements. More complex simulations can also be used as reference values. To enable the comparison of different simulations, only the relative deviation is used here instead of absolute values. Since the data contains noise, outliers should not have a significant impact, and a relative error metric is required to interpret the magnitude of deviations between simulations. Consequently, squared error metrics, such as Root Mean Squared Error (RMSE), are not used. For measured reference values equal to zero, m_i is set to the minimum possible distance in *MATLAB* (eps), that is approximately $2.22 \cdot 10^{-16}$. However, for values near zero, the MAPE can yield disproportionately high and physically meaningless results. To mitigate this, all values where $m_i \leq 0.2 \cdot M_{\max}$ are assigned reduced weights, rather than weights directly proportional to the reference value. This approach reflects the fact that, once the reference measurement approaches zero, the precise value becomes less critical as long as the simulated result remains similarly close to zero since accurately capturing noise in this region is not the objective. The uncertainty expressed as the MAPE is then converted into an accuracy value by subtracting the MAPE value from 100 % for all comparisons of simulations. If the MAPE is greater than 100 %, the accuracy is set to the minimum value of 0 %.

The deviations can now be used to quantify the total uncertainty of a simulation or model, but only very limited statements can be made about the individual proportions of the different types of uncertainty. In addition, this type of error quantification carries the risk of over- or underestimating the deviations from the real system, since the comparison data from measurements or more complex simulations may also be subject to errors and are also only recorded with a certain degree of accuracy [153]. For some cases, more complex simulations can also be used as reference values if no such measurements are available. To enable the comparison of different simulations, only the relative deviation is used here instead of absolute values. To account for inaccuracies in the reference measurements, it is assumed that any differences between the simulation and the reference values that fall below the measurement uncertainty of the device are zero [154].

To adapt the metric for AC systems (for inverter analysis in Ch.4.2.3), an additional scaling factor is applied. This is necessary because frequency behavior, and consequently phase shifts of a signal, have a greater impact in AC systems compared to DC systems. The scaling factor is determined by calculating the MAPE for a reference sine wave and a comparison sine wave with a phase shift of two timesteps and an amplitude reduction by 2 %. The scaling factor is derived from the expected error of 2 % and the resulting MAPE value, resulting in scaling factors[4] $MAPE_{\text{Corr\_V}} = 5.7763$ and $MAPE_{\text{Corr\_I}} = 6.3894$.

[4] different values for current and voltage are implemented due to different measurement uncertainties

2.3.6 Application Scope of Simulations

In the iterative process of ship design, as described in Chapter 2.2, the purpose of modeling and simulation can be divided into different investigation purposes, each of which takes place in different phases of the ship design and guarantees a refinement of the simulation over the individual iteration steps or phases:

- Technology screening, potential analysis, feasibility study, efficiency calculations
- Feasibility/conceptualization
- Design/concept development
- Detailed design
- Optimization

Appropriate LoDs and complexity must be selected for the different purposes, as qualitatively shown in Fig. 15. For example, detailed planning and optimization require both a high LoD and a high level of complexity, while a low level of complexity with a low LoD is sufficient for technology screening. For general grid design and concept development, there should already be an appropriately high level of complexity, but not all details need to be finalized, so a medium LoD is sufficient. Conversely, a higher LoD is required to carry out general feasibility and possibly concept studies on individual components or grid sections, in order to identify critical points of individual concepts, but at the same time, these can be carried out with relatively low complexity, as no overall grid simulation is usually required for this step.

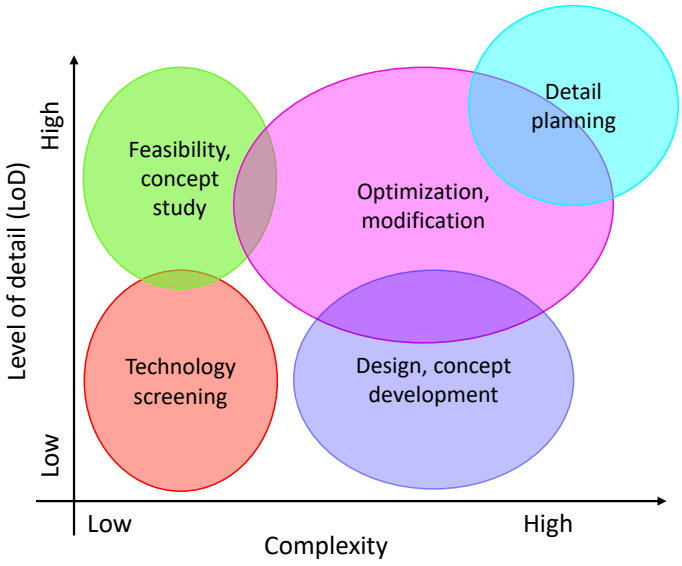

Figure 15: *Classification of application scopes for simulations*

Possible areas of application for these individual investigation purposes include, among others:

- Load flow analysis to assess the load on individual parts of the grid
- Short-circuit analysis to analyze power flows in the event of a fault
- Transient stability analysis to check the general stability of the grid
- Dimensioning of energy sources such as generators, batteries, and fuel cells
- Comparative studies to analyze the feasibility of different variants

All of these application areas require different simulation accuracies to achieve their goals, that can be judged by their safety relevance, risk of failure, possible mitigation/repair and associated costs, and generally by their relevance to compliance with standards. For operational-level investigations, such as dimensioning and feasibility studies, electrical system response times in the order of minutes are often sufficient. For example, the response time of a battery may require smaller simulation time steps to capture its behavior and achieve the desired response time. In contrast, system-level investigations, particularly during early-stage design and optimization processes, demand considerably faster response times, typically around 10 milliseconds [119]. Applications such as short-circuit analysis and other waveform-level studies require even higher temporal resolution, with response times ranging from milliseconds to microseconds [119]. The minimal necessary accuracy, temporal resolution t_s and simulation duration t_{sim} for the different application areas are listed in Appendix E.4.

2.4 Aim of the Work and Hypotheses

As highlighted in Chapter 2.3.2, achieving an optimal balance between complexity and accuracy in simulation and modeling is essential. A holistic a priori optimization of the model's LoD is identified as a research gap that remains largely unexplored. To address this, a comprehensive methodology for creating models and simulations of electrical (DC) power systems to an appropriate level of accuracy is proposed. Simulations are crucial in the development of complex DC grids, where the use of prototypes and field tests is extremely limited. However, simulation carries certain risks due to limited experience with the technology and insufficient validation. In addition, it is often difficult to correct errors, as the systems are usually implemented in their final state. In particular, detailed physics-based models often introduce additional errors, further complicating the choice of complexity. A decision has to be made between accepting risks and possibly oversizing the system to be developed, while striving for a balance between accuracy and complexity. Given the investment involved in such complex

DC grid technologies, this step is important for the successful introduction of this key technology for greener shipping. The proposed methodology aims to avoid unnecessary waste of computing and development resources caused by overly complex models and simulations. Simultaneously, it should provide better comparability between simulation models, improve realism, and reproducibility through the reusability of submodels.

Based on these considerations, the following hypotheses are proposed to serve as a guideline for this work's investigation:

- Hypothesis 1: Simulation models of electrical DC systems can be developed in various degrees of complexity, leading to different levels of accuracy. This complexity can be objectively quantified.
- Hypothesis 2: There is a methodological approach that can be used to achieve minimal simulation costs while keeping the simulation's accuracy sufficient.
- Hypothesis 3: The complexity of simulations and simulation models for shipboard DC grids can be optimized so that sufficient accuracy is achieved at minimum total cost to the owner.
- Hypothesis 4: The developed methodology can also be applied to other systems such as mechatronic systems.

Therefore, in the context of this thesis, a strategy is developed to objectively measure and quantify the complexity of a DC grid simulation by considering several metrics, that are explained and compared in Chapter 3. The complexity caused by certain characteristics of a DC grid, such as the influence of topology, is examined in Chapter 4.3 employing a use case. To assess the accuracy of the simulations, PHiL and hardware tests are used as described in Chapter 4.2. In order to limit the complexity of a simulation model or simulation prior to modeling, a cost function is developed in Chapter 4.4, leading to the optimal complexity of the model and simulation in relation to the costs incurred. To validate the resulting method, the simulation and model complexity of an example ship is optimized in Chapter 5 and subsequently the scalability, sustainability, and flexibility of the method are analyzed.

3 Metrics for the Quantification of Simulation Complexity

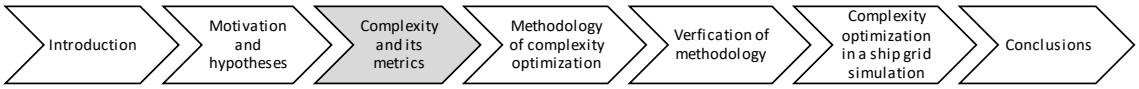

This work presents a selection of relevant complexity metrics for the use case of the complexity of electrical simulations and models, an even more extensive overview can be found in [155]. Although the computational and structural complexities of a simulation or model can be distinguished, they cannot be completely separated. Structural complexity can also be used to determine the human resources required to develop, understand, and analyze a model, so there is a direct link to cognitive complexity [82]. Structural complexity influences computational complexity, as increased structural complexity with stronger interconnection is usually associated with longer computation times. At the same time, computational complexity influences structural complexity; for example, splitting into sub-models to reduce computation time can affect coupling and connectivity within the model. The following sections address various structural and computational complexity metrics for simulations and models, concluding with a comparison to identify the metrics most suitable for electrical simulations. These selected metrics are then applied to measure complexity in Chapter 4.

3.1 Metrics for Structural Complexity

The structural complexity of a simulation can be divided in different categories, as depicted in Fig. 16. Hierarchical influences and the variety and multitude of components compound the structural complexity [156, 157]. The complexity due to hierarchical influences is affected by the coupling of different (sub-)models and the number of interconnections within one (sub-)model [149, 157]. The literature offers a number of methods to quantify the structural complexity of a simulation. Often, the number of parts of a structure in a partial or complete model are analyzed [63, 158] to assess the multitude and variety, but these methods require a specific form of representation in

the model structure [64]. As different representations are used for different types of

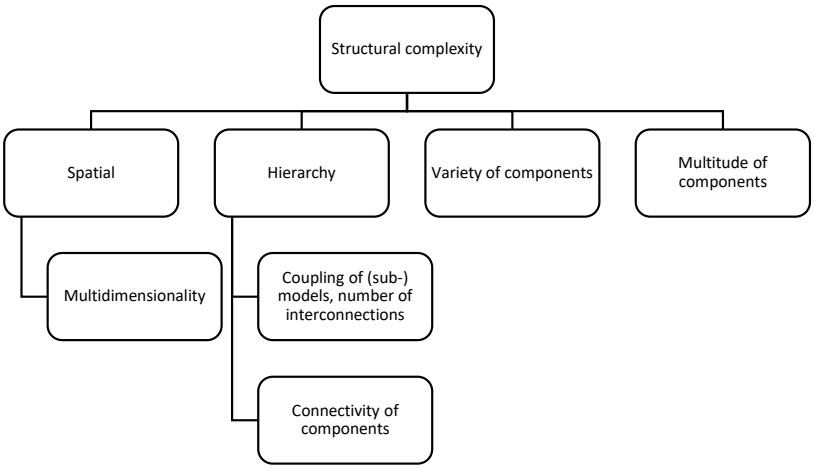

Figure 16: *Breakdown of structural complexity impact factors*

simulation, it is difficult to find a method that is applicable to all representations. In addition, it is generally not possible to translate different types of simulations into a universal representation since, for example, continuous or discrete simulations cannot be represented arbitrarily. Programming languages are a common representation for simulations, and the code complexity can be quantified by measuring the number of lines of code. Considering that simulations often access software libraries, counting lines of code is also limited [159]. Therefore, only metrics that are applicable to a graphical representation are considered in this work. For simulations that have a graphical representation, such as *MATLAB Simulink/ Simscape*® simulations, various metrics can be used to quantify structural complexity in terms of connectivity and coupling [64]. In addition to the cyclomatic complexity metric [158] discussed here, several other metrics can be used, including Control and Transformation Metric (CAT) [79], event graph representations [76], and asymptotic difficulty [157], that are not considered further in this work.

3.1.1 Cyclomatic Complexity/Number of Branches as a Complexity Metric

The cyclomatic complexity indicates the number of linearly independent paths of the program control graph that denote possible paths from the start node to the end node [158]. As long as there are no loops, all paths can be traversed independently. If the graph contains loops, there are infinitely many possible paths, so only the number of linearly independent paths is determined. In this case, the cyclomatic complexity denotes the number of base paths to which each path can be traced by the linear combination of

several base paths [76]. It is mostly used in in software engineering as a test for software quality. The cyclomatic complexity $\eta(G)$ or possible intermodular interaction [76, 158] results for a graph with only one possible input and output, e edges, n nodes and p connected components, or the number of unconnected parts of the flow chart such as subroutines, to be

$$\eta(G) = e - n + 2p. \tag{3}$$

Cyclomatic complexity can therefore be used to measure the resources required to create, test, and maintain a model. This provides a link to the resources required for the simulation process. However, an evaluation is only possible for models that have a graphical representation. The actual application of the cyclomatic complexity metric aims at program control graphs [158], that graphically describe the sequence of application of model equations and computational rules of a simulation. Branches occur at points where decisions are made between the execution of different next model components. These branches form loops. In principle, such a graph can be generated from any code of a simulation, but some components present in machine language cannot be captured, so that the program control graph is incomplete and can therefore only represent a part of the simulation complexity. Such a program control graph with entry vertex a and exit vertex j is shown in Fig. 17 and the linearly independent paths are listed in Tab. 5. One additional edge from exit to entry vertex is added. In Tab. 5 the basis for the set of cycles is set to be ($a\ b\ c\ f\ g\ i\ j$), ($g\ i\ g$), ($a\ b\ c\ f\ g\ h\ i\ j$) and ($a\ b\ d\ e\ j$). Any path through the graph can be represented by a linear combination of these cycles, leading to a cyclomatic complexity of $\eta(G) = 12 - 10 + 2 = 4$.

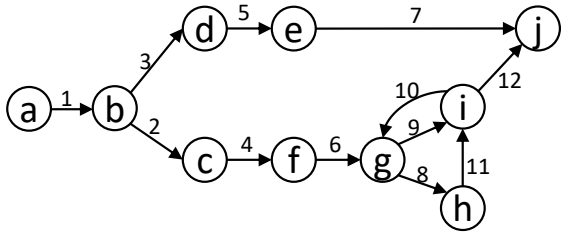

Figure 17: *Example for linear independent paths of program control graph*

Table 5: *Example linear independent paths for cyclomatic complexity*

Vector/Edges	**1**	**2**	**3**	**4**	**5**	**6**	**7**	**8**	**9**	**10**	**11**	**12**
(a b c f g i j)	1	1	0	1	0	1	0	0	1	0	0	1
(g i g)	0	0	0	0	0	0	0	0	1	1	0	0
(a b c f g h i j)	1	1	0	1	0	1	0	1	0	0	1	1
(a b d e j)	1	0	1	0	1	0	1	0	0	0	0	0

3.1.2 Number of Parameters as a Complexity Metric

Independent of the type of model representation, the number of parameters can be used to quantify the complexity of a model. Parameters can be used as scalar-valued model constants or, for example, to parameterize characteristic fields and the like [85]. It is often used for applications in machine learning as an efficiency metric [160]. However, the number of parameters affects not only the structural complexity but also the computational complexity, since parameters are associated with computational operations. Nevertheless, not every change of parameters leads to a change of computational complexity, since parameters can also be combined in the sense of constant folding [161]. The computation time is particularly affected by the parameters whose values are not known in advance but are determined by iterative parameter estimation procedures. This leads to a complexity of the direct solution procedure of $\mathcal{O}(hj^2)$ depending on the number of real measured values h and the number of model parameters j to be estimated. The quadratic influence of the number of parameters on the computational complexity therefore has a relevant influence on the computational complexity, but the influence on the structural complexity should not be diminished as more parameters come with a larger effort of creating and maintaining a model.

3.1.3 Variety and Multitude of Components as a Complexity Metric

When considering structural complexity, the variety and multitude of components or sub-models is an important factor in quantifying a models' complexity [77]. A simulation model that includes more components is more complex because it contains more parts. However, not every component is necessarily the same. There are distinct components or sub-models, f.i. electrical components such as converters for higher-level simulation models and as transistors or resistors for lower-level simulation models. A model containing only one type of component multiple times can lead to a more complex model than having fewer of said component. A model that consists of the same amount of distinct components and a higher variety though, is always more complex than the one set up from identical components [157]. Especially for cognitive complexity, a large number of distinct components is more complex. Variety can be measured by counting distinct components or other sub-parts, but on its own is not a sufficient measure of complexity.

3.2 Metrics for Computational Complexity

The computational complexity can be divided into computation time [76], memory demand of simulation models [76, 162], algorithmic complexity [163], and robustness and error tolerance [83] as shown in Fig. 18. These are influenced by the dynamics as well as the spatial and temporal resolution of the simulation [147]. Robustness to errors can be analyzed retrospectively with regard to modeling using a selectivity analysis/Monte Carlo simulation as described in Chapter C. Using the number of machine operations is

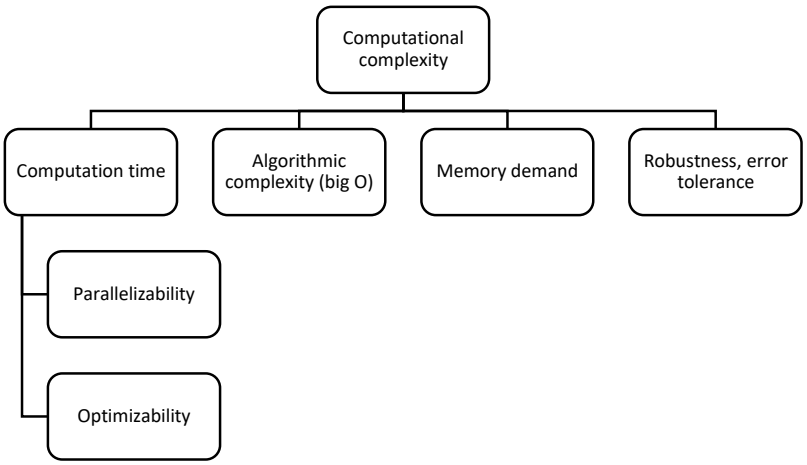

Figure 18: *Breakdown of computational complexity impact factors*

an often used procedure for the quantification of the computational complexity. Each simulation can be broken down into machine operations [159], the number of which correlates with the computation time. The calculations performed on the processor are carried out on data from the working memory. Different machine operations such as memory accesses, arithmetic operations, or logical comparisons are required. Machine operations may take different times and may depend on other results, resulting in latencies [159]. In particular, the use of caches with their dynamic data management can lead to a large variation in the computation times. The number of machine operations is also affected by the number of times the simulation is run. Parts of the simulation or the entire simulation can be looped to iteratively optimize the result. In addition, for simulations of different physical domains, the result of each domain can be dependent on the other, resulting in a higher repetition of simulation steps. In this work, the focus is on purely electrical simulations, so the coupling of different physical domains is not considered here.

3.2.1 Computation Time and its Statistical Analysis as a Complexity Metric

The computation time is widely used in programming, for example to evaluate efficiency [164]. Due to the characteristics of computers as explained in Chapter 3.2, the computation time of simulations is a randomly distributed variable [165, 166]. The simulation execution time is not a normally distributed variable, but follows the Weibull distribution [166]. An analysis of the distribution of the computation times for the simulations in this work is presented in Appendix B. Therefore, in order to guarantee that the computation time is adequately recorded, repeated measurements must be conducted and statistically analyzed. In addition, the median should be used instead of the mean to reduce the influence of outliers. When measuring computation time, the simulation should first be run without time measurement to load it into memory before the actual measurement. All other user programs need to be shut down before the measurement, so that the influence of the operating system is uniform.

In order to evaluate the complexity of a simulation, a comparison of several different simulations is usually carried out. In this case, a hypothesis test is necessary to identify differences in computation time with a certain significance and to avoid chance discoveries. Since the assumption of normally distributed populations is not tenable for fluctuating computation times [165, 166], the Mann-Whitney U-test (also known as the Wilcox rank-sum test), respectively the Kruskal-Wallis H-test for more than two independent groups is used in this work. This significance test is suitable for testing the difference between the central tendencies of independent samples and can be used when the conditions for a t-test are not met, for example, when a parametric procedure cannot be used, but an ordinal scaling is available [167]. The adaptation of the t-test for samples with unequal variances according to Welch is also not suitable in this case because of the necessary assumption of a normal distribution of the populations. The U-test cannot actually detect differences in central tendency for any non-normal distribution, but only for populations with the same shifted distribution form, but it is to be expected that central tendencies are still detectable even with (slightly) different distribution forms [168].The Mann-Whitney U-test, respectively the Kruskal-Wallis H-Test is suitable for determining the existence of differences in computation time. The samples are ordered by size and replaced by ranks, and the calculation of the test is based only on the order of these ranks, ignoring the absolute distances[167]. If samples come from different populations, it is to be expected that the values of one sample will, on average, be ranked higher than those of the others[167]. Finally, for the Mann-Whitney U-test the rank sums of the groups are used to test for significance using the standardization of the test variable (U-value) by comparing it with the critical value of the z-distribution[5]

[5]For a target confidence level of 95 %, the null hypothesis is rejected if the magnitude of the z-value exceeds 1.96. At the 99 % confidence level, the threshold is 2.58.

[167]. With the quantities $x_1,\ldots,x_n$ and $y_1,\ldots,y_m$ in size order and T being the sum of the ranks of the larger quantity, the U-statistic is defined by [167] as

$$U_1 = mk + \frac{m(m+1)}{2} - T. \tag{4}$$

The z-Standardization is then calculated with the mean value of the U distribution μ_U and the standard error of the U-value σ_U [167] as

$$Z = \frac{U - \mu_\mathrm{U}}{\sigma_\mathrm{U}} = \frac{U - \frac{mk}{2}}{\sqrt{\frac{mk(m+k+1)}{m}}}. \tag{5}$$

The Kruskal-Wallis H-test uses the rank sums of the groups to test significance [168, 169] using the test value H with the sample size n, the rank sum of group i R_i, and the number of cases in group i n_i:

$$H = \frac{12}{k\cdot(k+1)} \cdot \sum_{i=1}^{p} \frac{{R_i}^2}{k_i} - 3\cdot(k-1) \tag{6}$$

The H-value is then compared to the critical χ^2-value, resulting in a significance level of rejection of the null hypothesis.

In the case of the computation time comparison, the hypothesis tested is 'the computation time of the compared simulations does not differ'. Since it is not certain which of the compared simulations has a shorter computation time, a two-sided test must be performed.

3.2.2 Memory Demand as a Complexity Metric

Space complexity as a very common complexity measure in software engineering can also be applied to simulation and models, using the memory demand and amount of working storage required for a model, respectively simulation [170]. Since a certain size can cause resource problems, simulations with too high a memory demand are undesirable. Nevertheless, size alone is a necessary but not sufficient condition for complexity, as complex systems tend to have a certain minimal size, but a large system or simulation does not necessarily need to be complex. A rapid increase of complexity can be observed with size [157], but the critical size as stated in [157] may be very small. Additionally, the understandability for humans is also impaired if the models become too large. Analogously to the limited human brain capacities, working storage or cache memory have certain limitations. However, program resources are allocated

by the operating system [171], therefore, working storage usage is a weak complexity measure.

3.2.3 Time Resolution as a Complexity Metric

The resolution of time, voltage, and current is applicable in this work for electrical simulation models. Voltage and current resolutions in *MATLAB Simulink Simscape* simulations are usually set by defining the respective data type, ranging from signed or unsigned integers (8 to 64-bit) to single- or double-precision floating points, but may also be set user-specifically. Therefore, voltage and current resolution are quantified in bits. The time resolution in *MATLAB Simulink Simscape*® simulations is defined in the simulation settings as a time step duration in seconds and highly depends on the application of the simulation. Depending on possible peak duration, the subject to be analyzed, the choice of the time resolution is critical for the accuracy and validity of the simulation results. For models of renewable power systems for AC grids, studies have found no universally acceptable time step, but specific results have been obtained for choosing time resolution in certain cases. Systems, including batteries, that have a larger capacity than necessary to buffer the usual occurring load and supply peaks, can be simulated with a lower temporal resolution without major detriments to simulation accuracy [121, 172]. As easy battery integration is one of the advantages of modern DC grids, this result can also be used in the context of DC simulations. Additionally, a coarser time resolution of 10-min instead of a 1-min time step in an AC grid simulation on the demand side revealed a more pronounced averaging effect than on the generation side [173], leading to the assumption of a similar effect in DC grids. With a coarser time resolution, inaccuracies are likely to be more substantial [121], since peak loads and supplies have the highest inaccuracies, if the temporal resolution is coarse [127]. The time resolution can serve both as a metric for measuring complexity and as a simulation parameter. However, since the required time resolution depends on the specific application and a higher resolution than necessary does not provide additional insights, time resolution is treated solely as a parameter determined by the application area in this work and is not used to quantify complexity.

3.2.4 Algorithmic Complexity as a Complexity Metric

The algorithmic complexity is defined as the minimal difficulty of a program to recreate a number or pattern [157] by the use of a step-by-step procedure, that does not need to be a mathematical procedure. Considering only mathematical procedures, arithmetic complexity can be used, and the minimal number of arithmetic operations for a certain task can be analyzed. Several approaches for measuring algorithmic complexity exist

and are applied in areas such as theoretical logic, machine learning, and compression algorithms [174]. The Kolmogorov-complexity also known as Algorithmic Information Complexity (AIC), is the necessary length of a pattern-producing program divided by the patterns' size. It is defined in [175], similar approaches were presented by Solomonoff [176] and Chaitin [177]. Bennet's [178] logical depth though is defined as the computation time of the nearly minimal length of the shortest program for the task, executable on a Turing machine.
The most relatable definition, in connection with this work, is the big $\mathcal{O}$ notation: Certain algorithms can process a variable number of inputs. Depending on the number of inputs, the big $\mathcal{O}$ notation indicates how the number of operations evolves with respect to the number of inputs or the size of the problem, formally defined for deterministic Turing machines [170]. The dominant term of the equation for the number of operations without constant factors is given in brackets after the $\mathcal{O}$ [179]. Depending on the algorithm used, the same task can be performed with a different number of operations and complexity [179]. For instance, if for an input of size x, the algorithm needs $4x^3 - x^2 + 7log(x)$ units of time, the big $\mathcal{O}$ notation for the algorithms' complexity would be $\mathcal{O}(x^3)$. It is important to note that the big $\mathcal{O}$ notation is useful for comparing different algorithms but can only represent an upper bound of complexity, since different inputs of the same size can lead to different running times[170]. Fig. 19 shows the representation of the dependence between the problem size n and the resulting number of operations for algorithms of different complexity $\mathcal{O}(-)$.

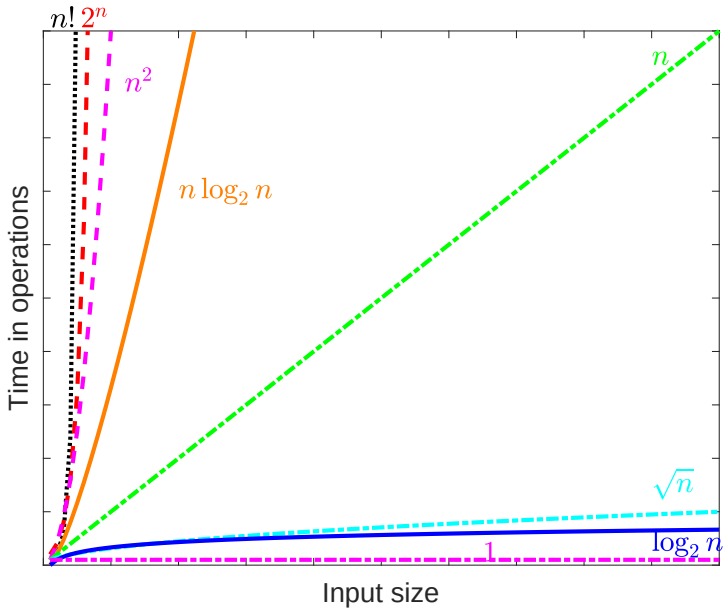

Figure 19: *Double logarithmic representation of the dependence between the problem size n and the resulting number of operations for algorithms of different complexity* $\mathcal{O}(-)$

3.2.5 Informational Entropy as a Complexity Metric

Another approach is to use the informational entropy of a system, where entropy describes the disorder present in a system. Informational entropy is widely used across various fields, such as landscape analysis [180] and network studies [181], to assess randomness, uncertainty, or centrality. The concept of information, defined by Shannon [182] for reliable message transmission with semantic content, can also possibly be applied to measure the complexity of a simulation model. Shannon defined the information for the listener of a message using the probability of the occurrence of said message. A less likely message therefore has high information. This concept can be used in an analogous way to the AIC, where the AIC measures knowledge, and the Shannon information or informational entropy, that is approximately equal to the conditional AIC, is used as a measure of ignorance [183]. The information or informational entropy I of a message of symbols x_i, that have a probability of $p(x_i)$ of occurring in the message, is given by [77, 157, 182] as

$$I_{\text{ent}}(x_1 x_2 ... x - n) = \sum_{i=1}^{n} p(x_i)(x_i) log_2 p(x_i)(x_i). \tag{7}$$

As in digital systems, the information is usually transmitted in bits; the logarithm base two is used in this case. Information content has a high dependence on the listener, who needs to have consensus on certain definitions like what constitutes a component or subsystem.

To analyze the distribution, Turing machines are used as a computational model. As the Turing machine halts after outputting a particular string s, only a number of instructions $l(p)$ are executed. This leads to an identical result for a string starting with the same $l(p)$ bits. Assuming a uniform measure, this gives the universal prior or Solomonoff-Levin distribution [77] of the proportion of strings starting with the same bits $l(p)$ and their probability $2^{l(p)}$

$$P(s) = \sum_{p:U(p)=s_{\text{Turing}}} 2^{-l(p)}. \tag{8}$$

Eq. 7 or the logarithm of Eq. 8 provide the complexity or information content of the description. The complexity C with the size of the encoding alphabet N used, and the number of equivalent descriptions $\omega(s,x)$ with meaning x of a maximum size of s is given

$$C(x) = \lim_{s\to\infty} s \log_2 N_{\text{enc}} - \log_2 \omega(s,x). \tag{9}$$

If the simplicity of understanding a system or, as in this thesis, a simulation, is defined

by the number of questions required to reduce the uncertainty about all states of the system to zero, then the system uncertainty and the informational entropy of the system are proportional to each other [82]. The informational entropy of the simulation can therefore be used as a measure of system complexity in such cases.

3.3 Comparison of Metrics

None of the single metrics for model and simulation complexity presented in Chapter 3.1 and Chapter 3.2 is able to represent all the different aspects of complexity. Only by combining different metrics can all aspects of complexity be considered. Masmali and Badreddin [184] use weighting factors for individual metrics for this combination of different aspects, so that the influence of individual metrics can be balanced accordingly. For this work, it is not necessary to weight metrics to obtain an overall complexity, as the weighting takes place in the cost function that is to be optimized. Only metrics that influence the same type of cost need to be weighted, and this process is performed in the cost function.

The presented metrics provide insight into different aspects of measuring simulation complexity. Structural complexity, that is determined by factors such as cyclomatic complexity, number of parameters, and diversity of components, is particularly relevant for model development and understanding of models and simulations. Therefore, all of these metrics are suitable, as they comprehensively capture the different facets of structural complexity.

In comparison, the metrics of computational complexity, such as computation time, memory requirements, resolution, algorithmic complexity, and information entropy, are less distinct. As algorithmic complexity quantifies the minimal description needed for a lossless reconstruction, it does not account for the actual structural representation of the grid and is often difficult to measure and therefore difficult to handle in further analysis. The computation time is mainly proportional to the memory requirement and the chosen resolution, and hence the computation time can provide a limited representation of both, although the computation time is not always conclusive and cannot cover all aspects of computational complexity. Although it is applicable to networks, metrics like cyclomatic complexity may offer a more intuitive representation of structural complexity, since informational entropy often emphasizes centrality and the analysis of randomness rather than overall system complexity and is dependent on model size. Therefore, in this work, all the presented structural complexity metrics are used, while computational complexity is represented solely by computation time.

3.4 Complexity Reduction Methods

Although the aim of this work is to find the right balance between simulation complexity and accuracy, it is useful to familiarize with techniques for simplifying models in order to reduce the existing model's complexity for possible re-use. Common methods are all grouped into one of six categories:

- Aggregation: By aggregating groups of components into one component that represents the combined overall behavior of the group of components, it is possible to reduce the total number of components, directly affecting the complexity of the simulation models [104, 146, 185]. In addition, temporal or spatial clustering [123, 126] or parameter aggregation [117] can be used. The process of repeated aggregation is referred to as substitution [107].
- Omission: Omitting variables, components, or interactions can reduce the complexity of the simulation model, since the number of components, parameters, or cyclomatic complexity is affected [104, 146, 185]. When omitting certain parameters, it is advantageous to find interdependent parameters that have algebraic representations in terms of other parameters, thus preserving the influence of the omitted parameters in the simulation [104, 146, 185]. In order to maintain simulation accuracy at a feasible level, only system elements that have no or very little influence on the system should be omitted [107].
- Linearization: If a simulation model is used to analyze a component at a particular operating point, it can be linearized around that point [146]. In principle, it is also possible to model an entire system by repro-modeling (e.g. with linear regression) by considering only the transformation from input to output states [104]. However, this requires extensive measurement data on the real system, that is usually not available.
- Deterministic/stochastic replacement: Stochastic model components can be replaced by deterministic descriptions, e.g., by replacing a distribution with the corresponding mean value [146]. Conversely, stochastic descriptions can also be used to replace deterministic model components by replacing complex algorithms with samples from distributions that are easy to compute [146].
- Formalism transformation: A further way to reduce the complexity of a simulation model may be to transform it into a different formalism, e.g., by mapping the model from differential equations into a discrete event model [146]. As this work only uses specific *MATLAB Simulink Simscape*® electrical models in the context of DC ship grids, this reduction technique is not easily applicable here.

- Functional Mock-up Units (FMUs): FMUs offer a modular and standardized approach of simulation model complexity reduction, enabling efficient exchange and integration across different tools and abstraction levels. They facilitate the aggregation of components, support omission by encapsulating simplified submodels, utilize linearized models for specific operating points, and serve as deterministic or stochastic replacements. By adhering to the functional mock-up interface standard, FMUs guarantee compatibility and consistency across diverse simulation environments.

Furthermore, structured programming is a proposed method for complexity reduction [104], applied to the case in this work, it could be interpreted as making the simulation model more comprehensible by achieving a good structure.

4 Complexity based Optimization

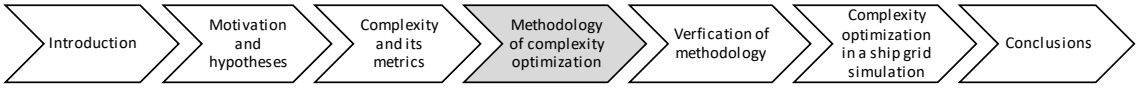

This chapter outlines a methodology for optimizing the complexity of ship grid simulations. This methodology aims to balance accuracy and simulation complexity while ensuring applicability in ship grid design. First, the systematic approach and the requirements are presented. Then, the resulting methodological process is described, enabling said optimization. Different aspects of simulation complexity resulting from specific use cases are analyzed, including the influence of critical components. Finally, a cost function, derived from the previous steps, is introduced along with implementation and optimization.

4.1 Methodological Approach

Although integrated design methods are becoming increasingly popular in shipbuilding, the design spiral still remains the primary method employed, as discussed in Chapter 2.2. It is therefore logical to develop a methodology that can be integrated into ship design using the design spiral but that can also be adapted for integrated development. As the focus of this work lies on the development of electrical grids that can be carried out in a single simulation environment, interface problems and media breaks may only occur at the transition to other development steps such as hydrostatics and trim. Nevertheless, the methodology developed here should be sufficiently flexible to be transferred to other development areas in case sufficient data is available for those areas.

In order to integrate the methodology into the development process in accordance with the design spiral, a series of simulations will be conducted at each stage of the development process, as depicted in Fig. 21. In accordance with the specific requirements of each development phase, the simulation must be tailored to encompass a range of application areas, necessitating the incorporation of varying levels of complexity. It is possible to extend certain parts of the simpler models developed in the early phases, but in other cases it is necessary to create a completely new model because the application

areas are significantly different or additional alternative concepts have to be developed. Moreover, it is not necessary to perform a simulation in all phases for each ship development. In the case of a class of ships, e.g. a number of sister ships, it is sufficient to consider the planned adjustments to the grid design in comparison to previous ships. Even in the case of new developments, it can be assumed that the shipyard will have a certain amount of experience and that only critical new applications and, if necessary, the overall system should be verified by simulation. However, in the case of developing new DC systems for ships, this experience cannot be assumed, leading to the need for a much more extensive analysis.

The methodology to be developed for optimizing the simulation complexity for ship grid design needs to be adaptable to other setups, able to deliver reproducible results, and efficient in pre-simulating the system. Furthermore, it should be understandable, allow flexibility in the development of grids, and have applicability to modularized systems.

The black box model of the methodology in Fig. 20 shows the important input and output variables, as well as the disturbance variables that can influence the methodology. The black box model for the simulation complexity optimization for various application areas in the context of ship grid design takes into account several critical inputs, including costs, boundary conditions and constraints, application area, accuracy requirements of the system, system characteristics such as the use of specific energy sources or topologies, and the potential for cost reduction through possible savings in the system. Additionally, the method must account for disturbances such as risks and regulations, as well as uncertainties in measurements and data, possibly affecting the reliability and compliance of simulation outcomes. Despite these challenges, the method is designed to deliver an output consisting of a minimally complex, cost-optimal simulation strategy reaching adequate accuracy.

In the absence of established methodologies, decisions regarding suitable complexity are typically based on expert judgment [50], complemented by sensitivity analyses that focus on specific application areas and employ either top-down or bottom-up modeling approaches. To minimize simulation costs, traditional methods have relied on cost tracking to monitor and manage simulation expenses until the allocated budget is fully utilized, as well as the use of standardized models and grid concepts to streamline processes. This work proposes an a priori optimization approach to determine the optimal simulation and model complexity, minimizing the total cost of required resources and associated risks while ensuring that accuracy meets the applications requirements. By conducting this optimization prior to model development, the appropriate LoD is defined without depending on subjective expert judgment, that may be unavailable for novel grid designs. This methodology replaces the traditional reliance on expert intuition with a standardized and methodological approach, enhancing consistency, objectivity, and reproducibility in simulation-based grid development.

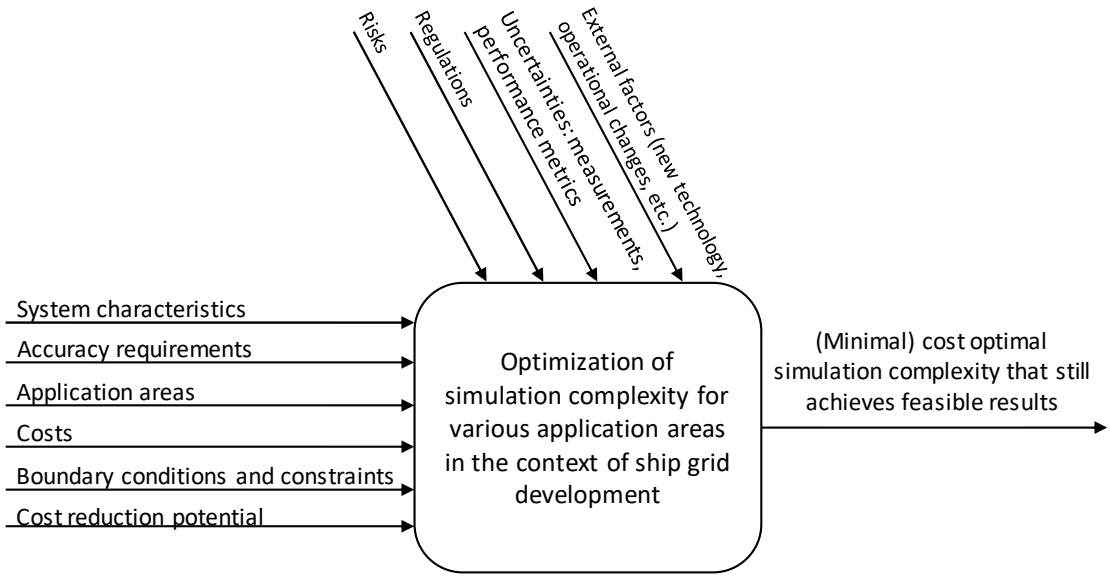

Figure 20: *Black box model of the optimization process with inputs, outputs and disturbances*

To achieve optimal simulation complexity, it is important to account for the modularization and hierarchical structure of the modeled grid. Ship grids are predominantly organized hierarchically, ranging from Medium Voltage (MV) to LV distributions. This hierarchical arrangement facilitates the separation of simulations. For simulations analyzing energy supply and demand in systems where primary energy sources are connected to the MV distribution grid, a single simulation of the MV segment may suffice, with LV sub-distributions aggregated into energy sums.

Additionally, modularization offers further opportunities to divide models into smaller segments, enabling the concurrent execution of multiple partial simulations. In such cases, it is essential to determine the points in the system where splitting models is feasible without compromising simulation accuracy due to lost connections across these points.

Methodology The following procedure represents a possible integration of the methodology into the ship design process according to the design spiral as shown in Fig. 21. As part of the concept design phase, the general feasibility and an idealized functional concept can first be investigated, including an initial feasibility study, with particular attention to the energy supply and its design. In the second phase, the preliminary design phase, basic feasibility studies are carried out, such as load flows, simple short-circuit analyses and, if necessary, a precise design of the energy sources. During the contract design phase, that is typically the auxiliary and main grid design phase, it is imperative to analyze the system-specific behavior. This may necessitate further load

flow and short-circuit simulations, as well as consideration of transient stability and the simulation of various faults to achieve safe operation. In the final phase of the detailed design, the remaining optimization options for the system are the focus of attention.

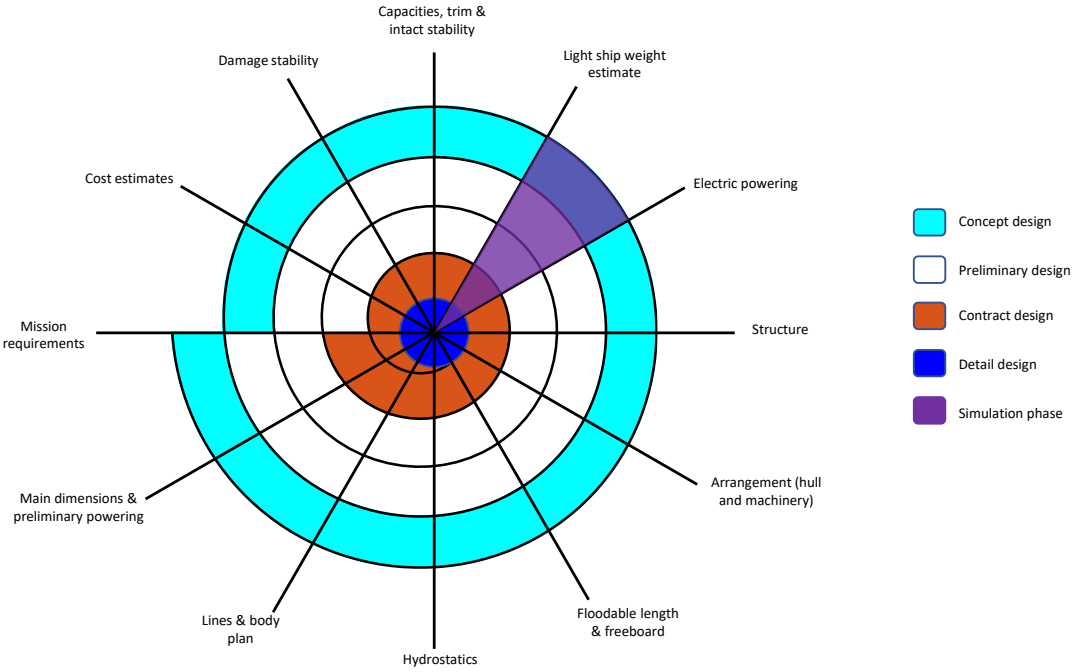

Figure 21: *Design spiral with ship design phases and integrated simulation phases for grid design*

In each of these simulation phases, the method and cost function developed in this work can be applied as shown in Fig. 22. Each simulation phase consists of several steps:

- Definition of the application domain and simulation objectives to clarify the purpose of the simulation
- Identification of relevant variables and parameters for the intended objectives, such as loads, operating conditions and environmental conditions
- Definition of the system boundaries to determine what is relevant and into which subsystems the ship is divided, analysis of modularization (e.g. separation at DC/DC-converters)
- Determination of the optimal simulation accuracy, using the cost function
- Modeling of the ship grid using the defined variables and parameters
- Analyses of critical component models accuracy, comparison with PHiL/Controller Hardware-in-the-Loop (CHiL)

- Analyses of the developed model and, if required, further iteration in the modeling process
- Simulation with realistic operation data and analysis of the simulation result
- Validation of the simulation results with real data if available to check the accuracy and reliability of the complete simulation

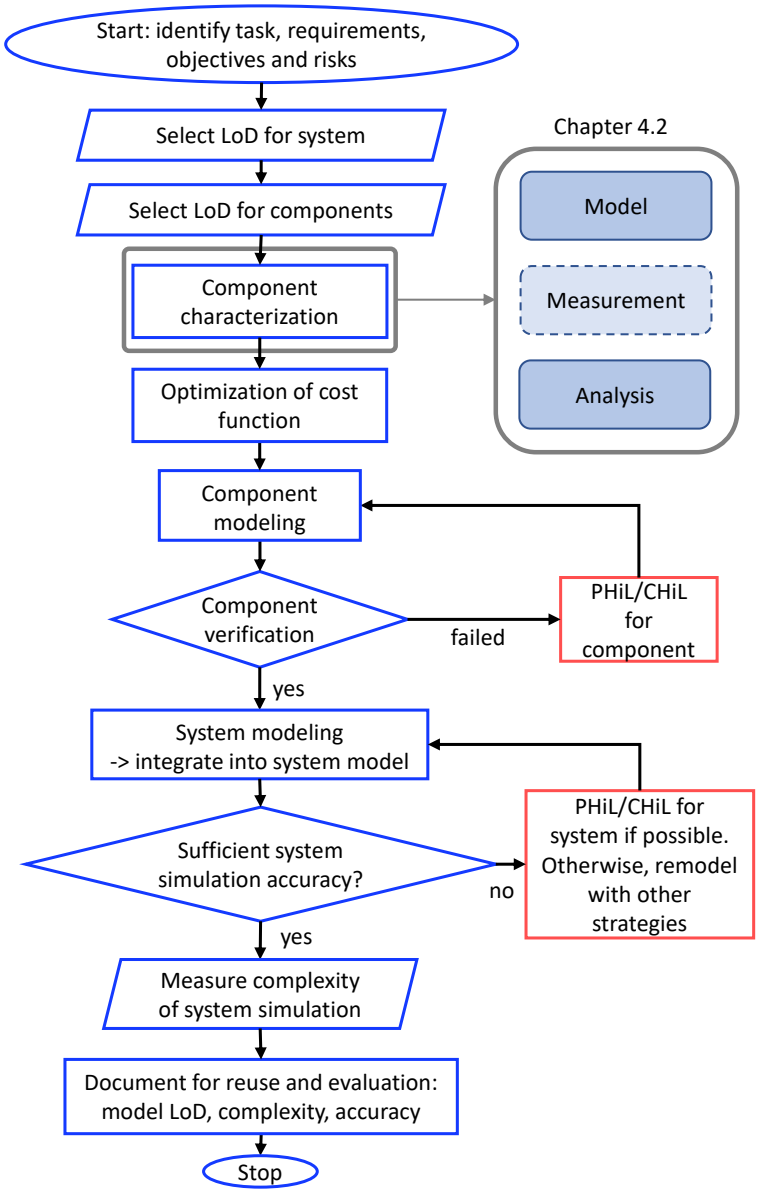

Figure 22: *Proposed methodology for simulation complexity optimization. The process involves identifying tasks, requirements, and risks; selecting the LoD for system and components; characterizing components, optimizing the cost function; verifying component models, integrating them into the system model, and ensuring sufficient simulation accuracy. The component characterization process is detailed in Chapter 4.2 for certain components.*

4.2 Simulation Complexity of Energy Components

In order to implement the cost function, it is necessary to ascertain the interdependence between the achieved accuracy and the complexity of a (component) simulation for different grid components, as measured by the metrics outlined in Chapter 3. To determine this relationship, several key components of DC grids are subjected to examination in a laboratory setting, and then the results of these experiments are compared to simulations at varying levels of complexity. As part of the investigation, simulations with an increasing number of parameters are analyzed in order to determine their simulation accuracy in relation to the investigation conducted in the laboratory. In order to achieve the various levels of complexity, the simple models are gradually expanded by adding parasitic components. The sequence is based on expert knowledge and the observed change in results largely corresponds to the expected increase in accuracy with increasing parameters. Subsequently, the computation time and cyclomatic complexity of the different simulations are subjected to analysis. The determined correlations are then approximated by curve fitting (as described in Appendix D.1) and implemented as a function in the cost function. The accuracy and complexity of the key components are analyzed subsequently. DC/DC-converters and frequency converters are analyzed based on own measurements, whereas batteries, fluctuating loads, constant loads, Heating, Ventilation and Air Conditioning (HVAC), and fuel cells are analyzed based on measurement data from existing publications.

Each analysis includes a description of models with varying complexities, the corresponding measurements for comparison if applicable, and an evaluation of complexity in relation to simulation accuracy, with 100 % accuracy defined by the measured values. As part of the cost function, the relationship between accuracy and the number of parameters is visualized using scatter plots, and a fitting function is approximated for these data points. Four different functions are used for this purpose, as exemplified in Fig. 23.

Fig. 23(a) illustrates a component model that fails entirely for parameter counts below a critical threshold, while Fig. 23(b) depicts a model where even a small number of parameters achieves reasonable accuracy. Fig. 23(c) shows a model with no significant accuracy gains for medium parameter counts. Finally, Fig. 23(d) represents a model in which a specific parameter count achieves high accuracy, but additional parameters provide little to no improvement.

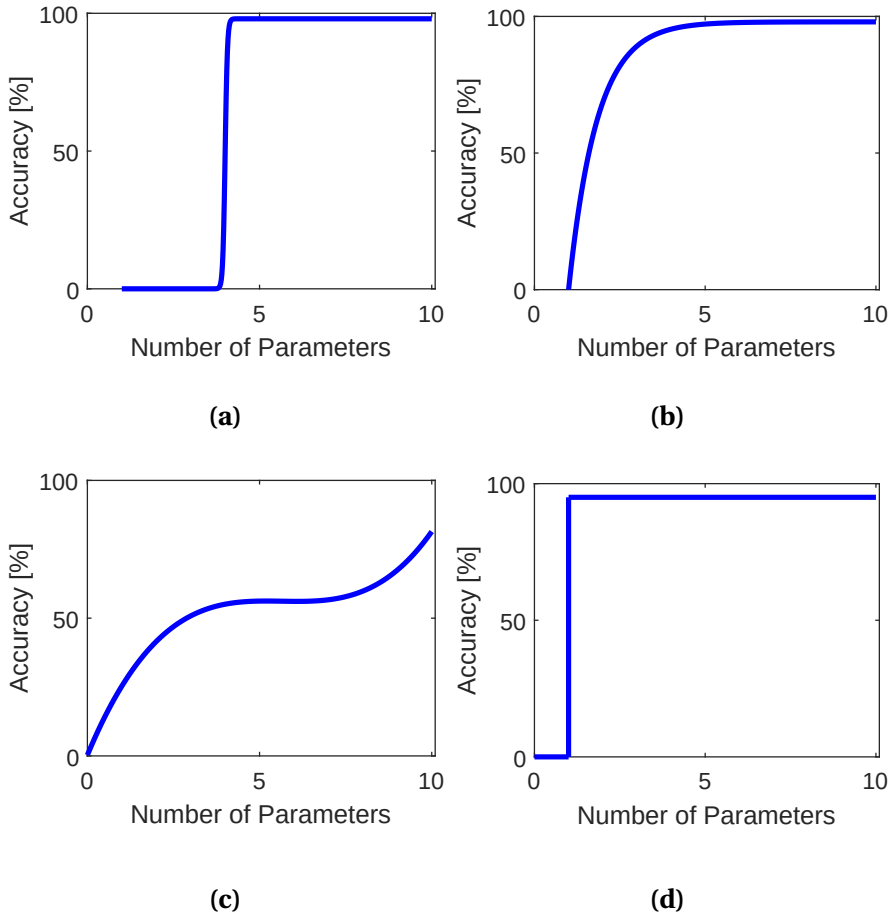

Figure 23: *Exemplary representations of accuracy curves for different parameter numbers: (a) symmetric sigmoidal curve, (b) fast initial increase that gradually levels off, (c) polynomial trend with an initial rise, short plateau and renewed stronger increase, (d) step function*

4.2.1 DC/DC-Converters (Experimental Basis)

DC/DC-converters represent a critical component in DC grids as shown in Chapter 4.3.2, and thus the ratio of complexity to accuracy of the simulation of this component is of particular relevance for the design of the grid.

Model A minimal model (Fig. 24) comprising 15 parameters is expanded with up to 13 additional parasitic components in nine steps to create various intermediate stages of complexity, that are then compared with the measurement of a converter in order to analyze the accuracy in relation to this. The respective models are analyzed in order to gain understanding of peak overshoots and settling times, that can affect system stability. Additionally, the effects of voltage fluctuations that can be caused by

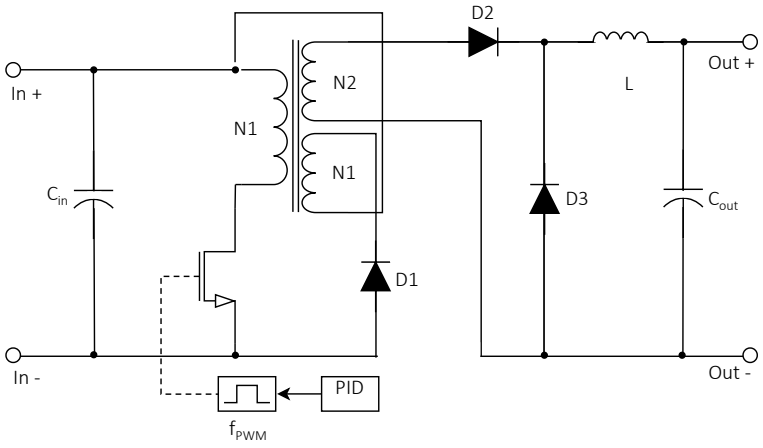

Figure 24: *Forward converter simulation model with 15 parameters*

harmonics generated by converters, motors, or generators are considered, giving rise to instabilities due to resonances.

The models are created in *MATLAB Simulink® Specialized Power Systems*, that is specifically tailored to power converters. The parameters used are defined or calculated based on the information provided in the datasheet and are listed in Appendix D.3. The simple model is extended by a capacitance model, also including an equivalent series resistance and an equivalent series inductance [186]. The Metal–Oxide–Semiconductor Field-Effect Transistors (MOSFETs) are extended by parasitic capacitances between gate, drain, and source [187]. An equivalent parallel capacitance and a series resistor are also added to the inductance [186]. In addition, further parameters are activated that are included in the components already contained in the simple model as described in Appendix D.3, leading to the most complex model depicted in Fig. 25. These additional 14 parameters are also listed in Appendix D.3. If capacitances (C_{in} and C_{out}) and diodes (D_1, D_2, and D_3) are selected differently, this results in a total of 28 parameters.

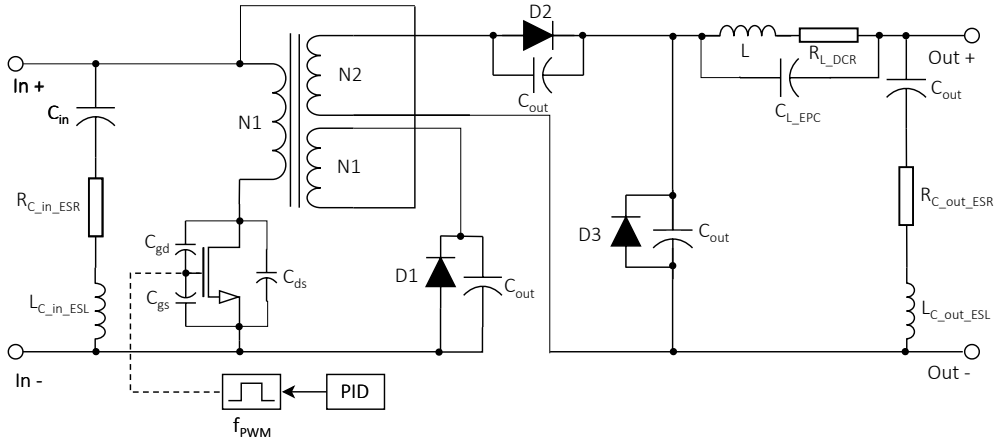

Figure 25: *Complex forward converter simulation model with 28 parameters*

In order to analyze the differences between the different models, a sensitivity analysis is used to determine the influence on the mean and variance of the input current and output voltage (see Appendix D.3). The parasitic components are arranged in order of their impact on the complexity metrics. This allows for the additional parasitic components that have the greatest influence on the result to be inserted into the simulation first, if lower parameter numbers are used.

Measurement This measurement is conducted with two different DC/DC-converters — one prototype 350 V to 24 V converter and a *Bauer* 24 V to 12 V converter (Dennis Bauer United, Germany). The input is connected to an *EA DC voltage source* [188] (EA Elektro-Automatik GmbH, Germany) and the output is connected to a *Spitzenberger & Spieß AC Amplifier*[189] (Spitzenberger & Spies GmbH & Co. KG, Germany) in sink mode, that is controlled via SCPI protocol as shown in Fig. 26.

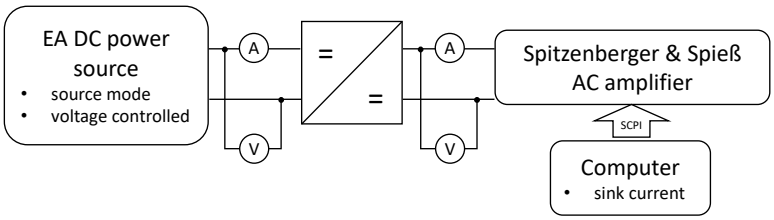

Figure 26: *DC/DC-converter measurement setup including a power source, an AC amplifier functioning as a load to provide a specific sink current, and two measurement points for data acquisition*

Analysis To optimize the various complexity metrics, the accuracy of the simulation is shown as a function of the metrics. This is achieved by curve fitting. The accuracy of the DC/DC-converter simulation as a function of the number of parameters is shown in Fig. 27. A minimum number of parameters of 18 must be assumed for the model of a forward converter to be able to map the physical functionality to a certain extent and is therefore defined for the cost function.

The parameters for the curve fitting of the DC/DC-converter accuracy function are presented in Apx. D.1.The prototype converter data and fit are used for the cost function and further analysis, as its power rating and voltage range align better with the ship grid use case compared to the Bauer converter, that serves as a verification of the component analysis.

The measured computation times (median values of 10 measurements, each under identical conditions) of the simple model (15 parameters) and the complex model (28 parameters) are shown in Fig. 28.

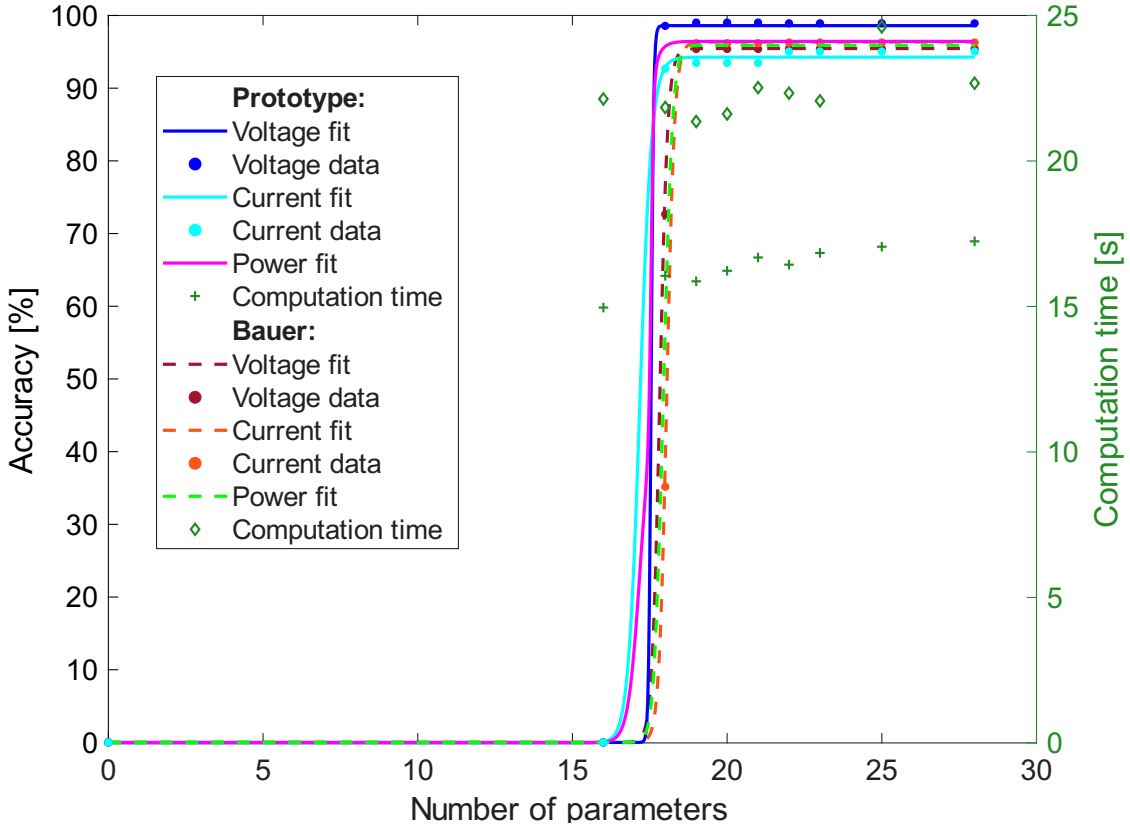

Figure 27: *Simulation accuracy for different numbers of parameters for DC/DC-converters, showing data points and corresponding fits for voltage, current, and power accuracy.*

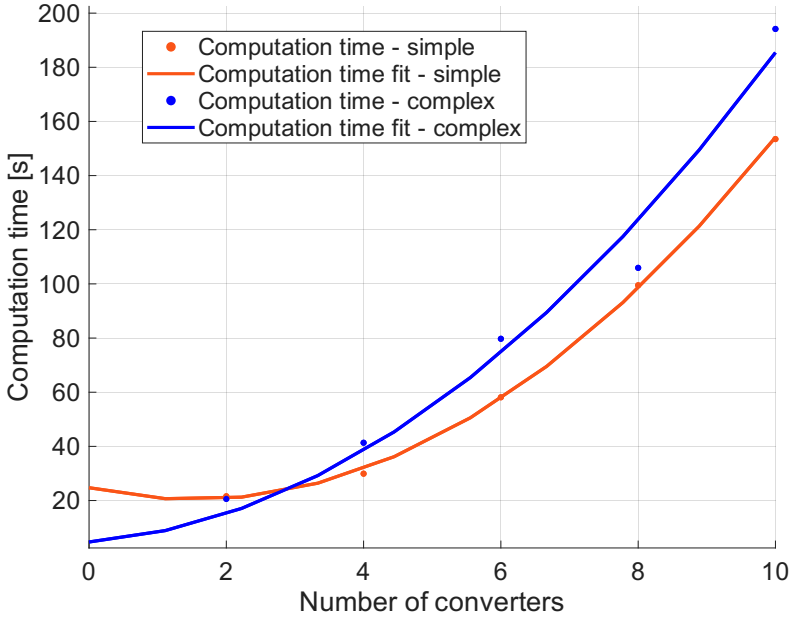

Figure 28: *Simulation time of the simplified and complex model of the DC/DC-converter with increasing number of implemented DC/DC-converters*

To approximate the function for the computation time, a second-degree polynomial as in Eq. 10 is used with x as the number of DC/DC-converters in the simulation:

$$t_{\text{Calc,Simp.}} = 2.230x^2 + 0.968x + 14.910 \tag{10}$$

$$t_{\text{Calc,Comp.}} = 0.582x^3 - 1.169x^2 + 15.490x + 2.335 \tag{11}$$

The third metric, cyclomatic complexity, has an identical value of three for the initial model of a DC/DC-converter and three for each subsequent converter in the model, both for the simple and the complex model.

4.2.2 Batteries

Batteries are also important components for the simulation of DC electrical grids due to the factors outlined in Chapter 4.3.3.

Model To assess the ratio of complexity to accuracy of the simulation for batteries, a simulation of the discharging process of a $LiFePO_4$ cell is simulated, a table-based battery model based on a characteristic curve [190] is used as a reference model with 100 % accuracy. It is compared to a linearized model and a polynomial-based model with four coefficients, all described in Appendix D.2.

The resulting computation time (median values of 10 measurements, each under identical conditions) and the numbers of parameters are given in Tab. 6.

Table 6: *Characteristic values and simulation values of the different battery simulations*

	Table-based	**Linear**	**Polynomial-based 4 coeff.**
Computation time	31.64 s	38.23 s	38.22 s
Number of parameters	2000	4	8
Cyclomatic complexity	2	2	2
Accuracy	100 %	49.99 %	75.73 %

Analysis The simulation accuracy with regard to the number of implemented parameters is shown in Fig. 29 and can be approximated using the curve fitting function in Apx. D.1.

For the computation time, first the dependence on the number of parameters is analyzed as shown in Fig. 30.

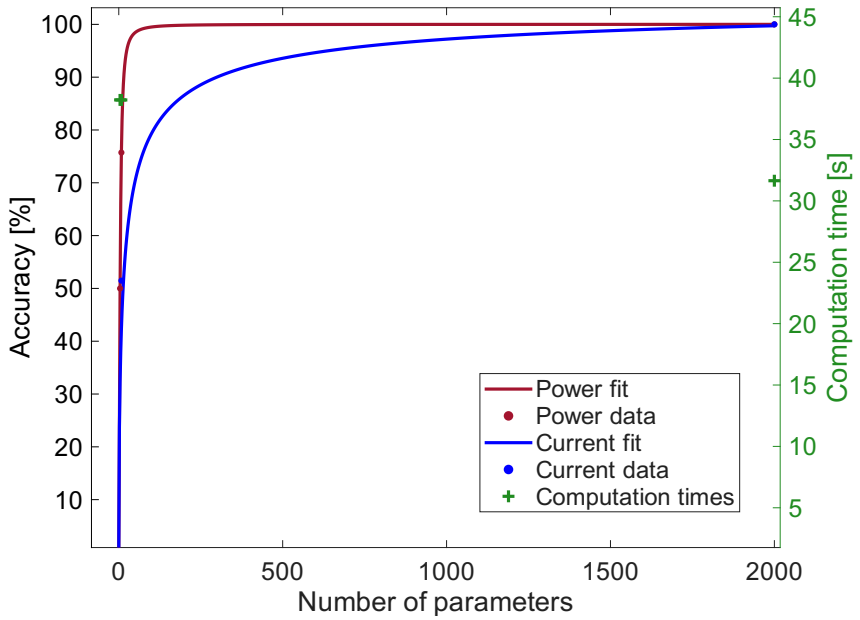

Figure 29: *Accuracy and computation times achieved in battery simulation for implemented number of parameters, showing data points and corresponding fits for current and power accuracy.*

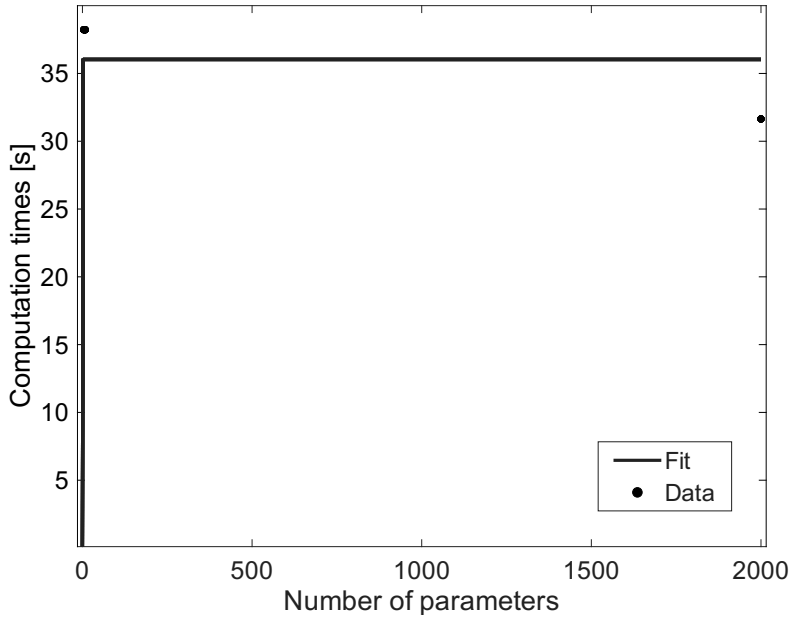

Figure 30: *Computation time of the battery simulation, depending on the implemented number of parameters. While the table-based model (2000 parameters) requires only* 31.64 s*, the linear and polynomial models (4 and 8 parameters) take* 38.23 s *and* 38.22 s*, resulting in a step-like behavior in the fitted function*

As the number of batteries has an influence on the bidirectionality and the total computation time of the simulation can differ due to the bidirectionality, as discussed in Chapter 4.3.3, this influence is analyzed. To evaluate it, different numbers of batteries are implemented in a small grid with 10 randomly varying loads. For the resulting data, a curve for the correlation between the computation time and the number of batteries implemented is approximated and shown in Fig. 31.

An exponential function is used for this approximation as shown in Eq. 12 and Eq. 13 with x as the number of batteries in the simulation.

$$t_{\text{Calc,Simp.}} = -128.354 + 196.3058 \cdot e^{+0.08844572 \cdot x} \tag{12}$$

$$t_{\text{Calc,Comp.}} = -180.3336 + 247.7803 \cdot e^{+0.07705182 \cdot x} \tag{13}$$

In the cost function, Eq. 12, valid for the table-based model, is used to determine the influence of bidirectionality f_{Bidirect} as the table-based model has achieved the highest accuracy and the lowest computation time.

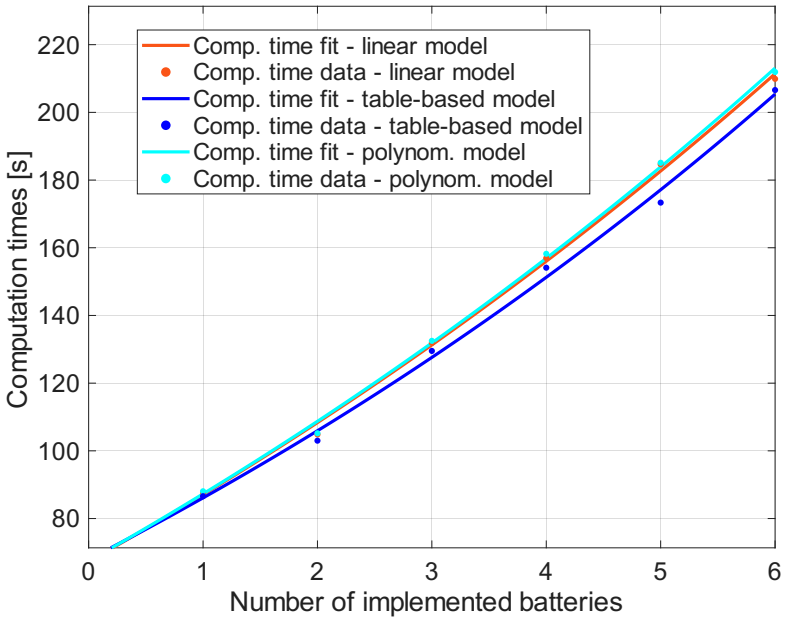

Figure 31: *Required computation time depending on the number of batteries implemented*

The cyclomatic complexity of each battery implemented in the simulation is identical, with a value of two.

4.2.3 Frequency Converters (Experimental Basis)

Model A model of an inverter in *MATLAB Simulink Simscape®* is analyzed with respect to complexity metrics. Three sub-components with varying LoD are used to model the measured setup: The Pulse Width Modulation (PWM) generation, the inverter, and the asynchronous machines, each available in multiple LoD configurations. The PWM generation with and without a deadtime, the inverter represented by an ideal switch, an ideal switch and a diode, and a MOSFET including a diode. The asynchronous machine is represented by a resistance inductivity combination or a *MATLAB Simulink Simscape®* block including stator and rotor parameters, inertia, friction, mutual inductance, and initial conditions. These sub-models are combined in all possible variations to explore the impact of different combinations of LoD on the overall system behavior.

Measurement A measurement is performed on two different real components. For this purpose, the respective frequency converter is connected directly to an *EA DC voltage source* [188] (EA Elektro-Automatik GmbH, Germany) at the intermediate circuit, as shown in Fig. 32. In the case of the 7.5 kW *Danfoss inverter VLT FC 302* (Danfoss Drives A/S, Denmark), a 4.3 kW *Siemens* asynchronous machine of type LA5133-6SA80-Z (Siemens AG, Germany) is connected (Fig. 32(a)). In the case of the *Siemens Micromaster 440* (Siemens AG, Germany) frequency converter, three 4 kW Perske KNS 51,14-2 (Walter Perske GmbH, Germany) asynchronous machines are connected to the output of three frequency converters running against an additional asynchronous machine (26,4 kW Lenze MDFMA_160-32B (Lenze SE, Germany)) as a load using a belt for connection of the four machines (Fig. 32(b)). Only one of the identical machines and converters is connected to the measurement equipment. All measurements are conducted using a *Zimmer LMG 671* power analyzer [191] (ZES ZIMMER Electronic Systems GmbH, Germany).

Analysis The respective models show a cyclomatic complexity of four for the simplified asynchronous machine model and five for the more complex asynchronous machine model, with the number of parameters ranging from 12 to 35. As illustrated in Fig. 33, computation times tend to increase with higher parameter counts, accompanied by improvements in accuracy. However, there are outliers, where the combination of different complexity levels in the frequency converter's sub-components results in lower accuracy despite increased computation time and parameter count.

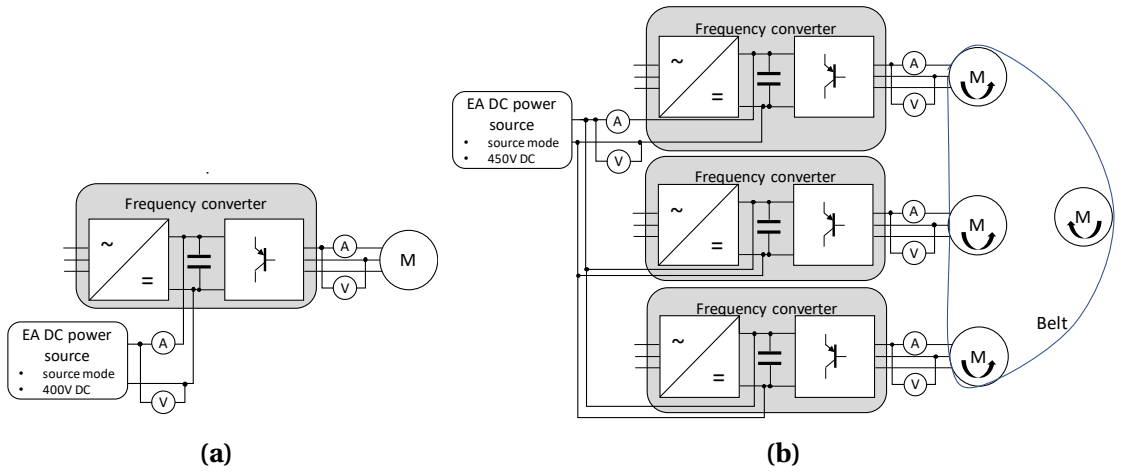

Figure 32: *Frequency converter measurement setup, (a) a Danfoss VLT FC 302 inverter with a 4.3 kW asynchronous machine in idle operation (b) three Siemens Micromaster 440 with three 4 kW Perske asynchronous machines running against an additional asynchronous machine as a load connected via belt*

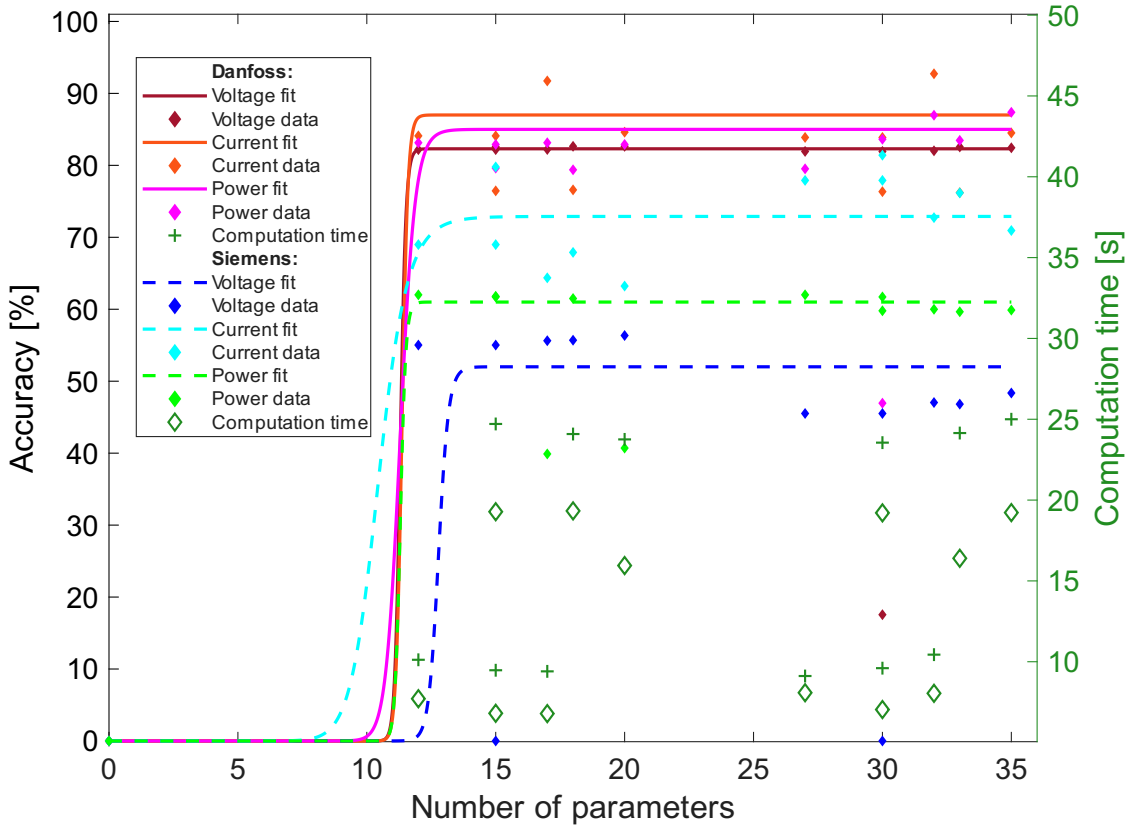

Figure 33: *Frequency converter accuracy and computation times for different frequency converter simulation models and their number of parameters, showing data points and corresponding fits for voltage, current, and power accuracy.*

A comparison of the frequency converter simulations reveals that the *Siemens* converters have considerably lower simulation accuracy compared to the *Danfoss* converters used. This discrepancy can be attributed to two factors: either the parameterization of the *Siemens* device models is suboptimal, or the control strategy employed by *Siemens* could not be adequately captured in the simulation model. As a result, the *Danfoss* converter values are chosen for further analysis and as input for the cost function, as their superior accuracy offers a more reliable foundation for optimizing the grid design process. The *Siemens* frequency converter serves as a verification of the component analysis.

The measured computation times (median values of 10 measurements each under identical conditions) of the simple model and the complex model of the *Danfoss* frequency converters are shown in Fig. 34.

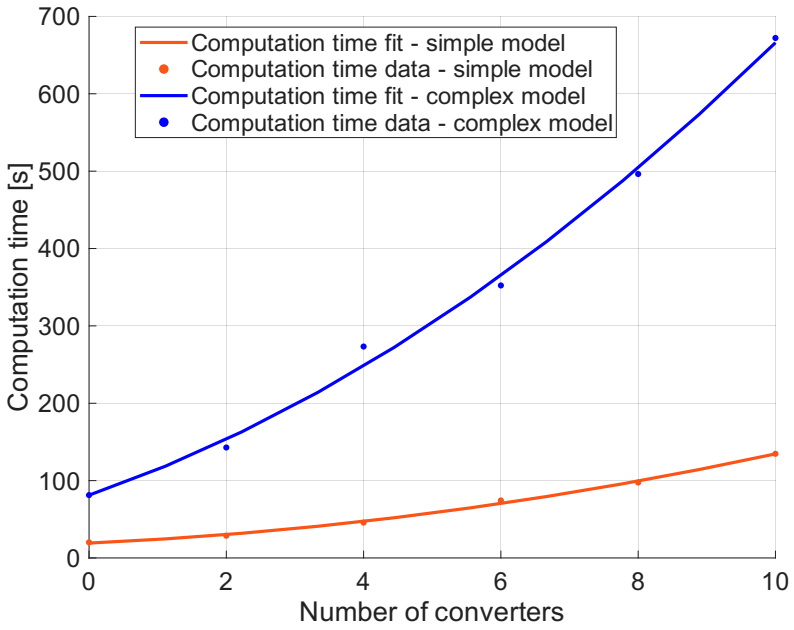

Figure 34: *Simulation time of the simplified and complex model of the frequency converter with increasing number of implemented frequency converters*

The computation time in the cost function is approximated by

$$t_{\text{Calc,Comp.}} = 81.17633 + 30.55108 * x + 2.793124 * x^2 \tag{14}$$

with x representing the number of inverters implemented.

4.2.4 Fluctuating loads

One of the most important fluctuating loads onboard a cruise or passenger ship is the cabin load. It is determined by the number of passengers using various electrical devices.

Model To achieve generic load profiles of different degrees of complexity, data from [192] regarding the passenger presence and the expected loads for a typical set of electrical devices is used. A detailed account of the methodology employed to derive a generic cabin load can be found in Appendix D.5, the resulting sum of 1025 cabins with a granularity of 3 minutes is shown in Fig. 35, other granularities are shown in Appendix D.5.

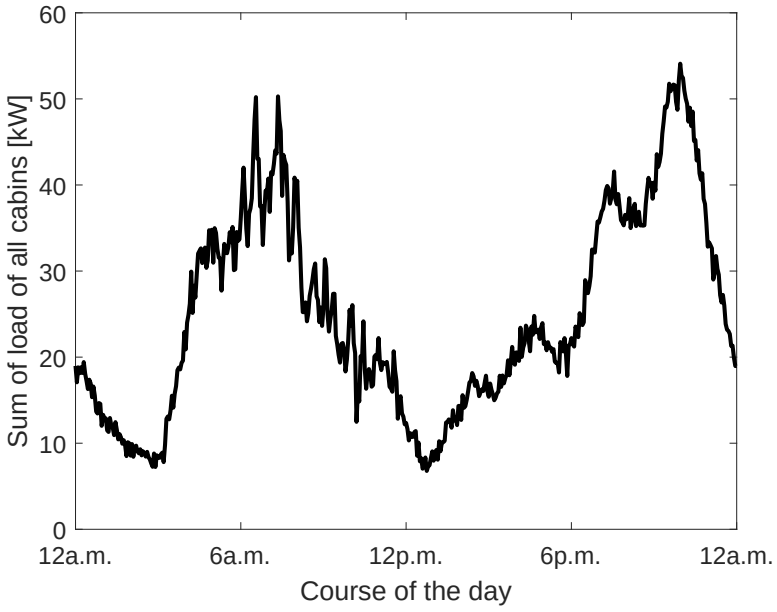

Figure 35: *Resulting total load of 1025 cabins for the model with 480 parameters (3 minute granularity)*

Analysis In order to map different degrees of complexity of the cabin load, the number of implemented parameters is varied by determining the cabin load with different time intervals. The resulting accuracy is shown in Tab. 7. As resolution and number of parameters increase, load spikes are represented with greater accuracy, resulting in a function of accuracy dependent on the number of parameters, as illustrated in Fig. 36.

Table 7: *Achieved accuracy of the cabin load for different numbers of parameters*

Number of parameters for 24 h	0	24	48	96	120	160	240	480
Accuracy [%]	0	88.77	91.75	94.30	94.79	95.43	96.65	100

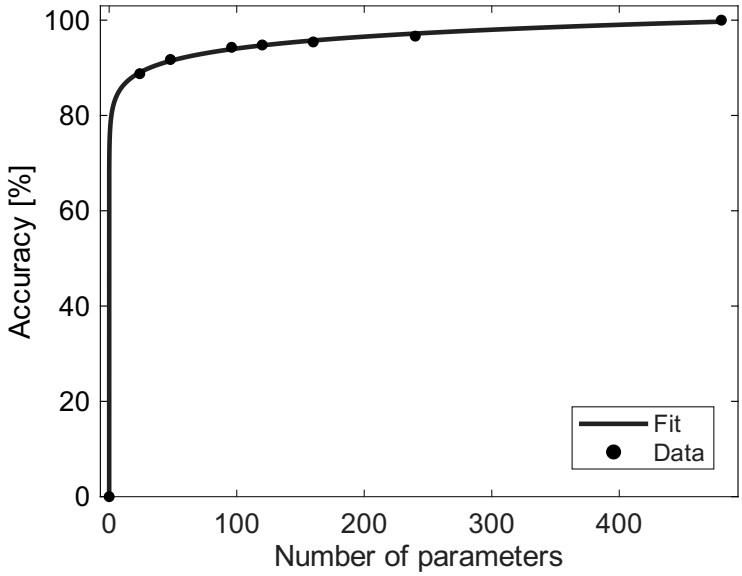

Figure 36: *Achieved accuracy of the cabin load for increasing numbers of parameters*

To assess the computation time in relation to the number of cabins and the number of parameters, a *MATLAB Simulink*® model is created. Five cabins with varying numbers of parameters are simulated 10 times, leading to a median computation time as listed in Tab. 8. A Kruskal-Wallis test confirms that there is no significant difference in computation times for different numbers of parameters.

Table 8: *Average computation time of five cabins with different numbers of parameters*

Number of parameters	4	12	24	48	480
Average computation time [s]	28.14	28.47	28.40	28.60	28.00

For the evaluation of the impact of the number of cabins on the computation time, blocks of five to 25 cabins are simulated 10 times each. The resulting computation times are listed in Tab. 9.

Table 9: *Average computation time of increasing number of cabins simulated with four parameters each*

Number of cabins	5	10	15	20	25
Average computation time [s]	28.14	33.74	36.80	44.54	50.75

The expected computation time can be calculated from the data depending on the number x of cabins implemented with

$$t_{\text{Calc}} = 1{,}1204 \cdot x + 21{,}988. \tag{15}$$

The last metric of complexity is the cyclomatic complexity V_{cyc} of the *MATLAB Simulink®* model of a cabin. This value is four for each cabin implemented.

4.2.5 Constant loads

Model Constant loads occur very frequently in ship grids. Since these can be accurately represented with only one parameter, it is assumed that the simulation accuracy of constant loads for the cost function is 100 %. However, it should be noted that a minimal deviation is possible due to the variable type on the simulation side leading to quantization errors and due to measurement or dimensioning inaccuracies (and component inaccuracies) in the analysis of the real system.

Analysis The computation time is determined as a function of the number of constant loads implemented, for this purpose, the cabin load model from Chapter 4.2.4 is adapted to constant loads, and 10 simulations are run for each of the numbers of implemented loads shown in Tab. 10.

Table 10: *Average computation time for increasing number of constant loads*

Number of loads	5	10	15	20	25	30
Average computation time [s]	27.78	30.79	33.46	37.37	41.02	43.57

From the computation times of the simulations performed, the expected computation time is calculated depending on the number x of constant loads implemented with

$$t_{\text{Calc}} = 0.6489 \cdot x + 24.31. \tag{16}$$

The cyclomatic complexity V_{cyc} of a constant load is one.

4.2.6 HVAC

Model The load through the HVAC system is a fluctuating load and is analyzed using the example of a cruise ship and the analysis from [192]. The total load of the HVAC system during a day at sea with a resolution of 30 minutes (corresponding to 48 parameters for 24 hours) is shown in Fig. 37, other resolutions with lower parameter numbers are shown in Appendix D.4.

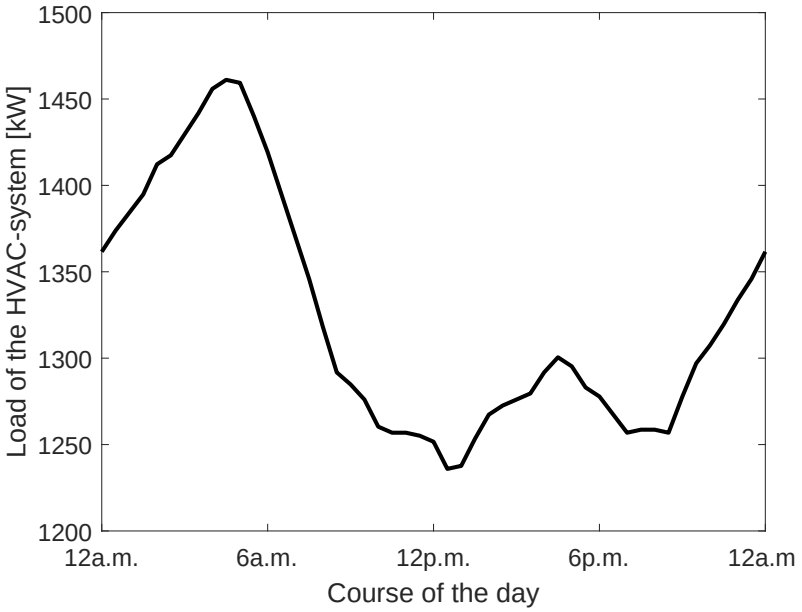

Figure 37: *30-minute load of the HVAC-system for a day at sea according to [192].*

Analysis The accuracy is determined analogously to the procedure in Chapter 4.2.4 and the accuracy function generated by curve fitting as a function of the number of parameters used is shown in Fig. 38. As the HVAC load is also a fluctuating load like the cabin load, the same principle is used for the simulation, leading to the same cyclomatic complexity and the same computation time, since there were no discernible differences due to the number of parameters.

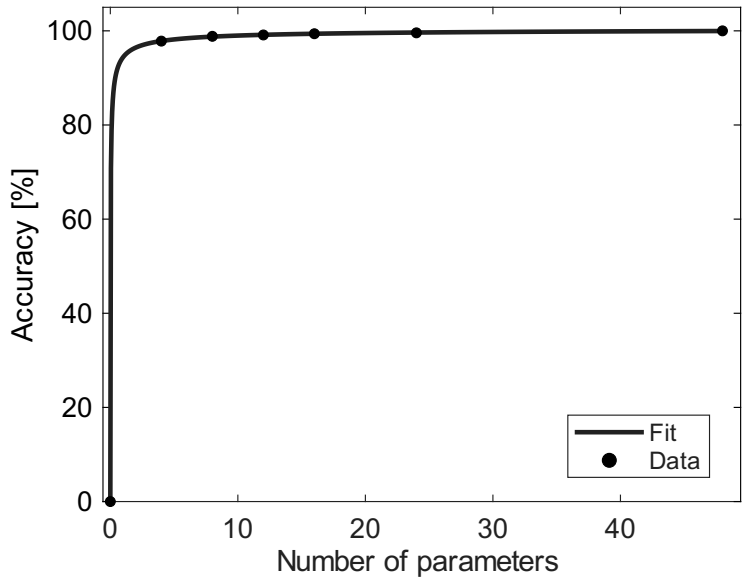

Figure 38: *Achieved accuracy for increasing number of parameters of the HVAC system*

4.2.7 Fuel Cells (Literature Basis)

Model In the absence of a fuel cell suitable for corresponding experiments, the models and analysis of those of Barać *et al.* [193] are used for characterization, presenting six different simulation models for fuel cells of various degrees of complexity. To implement the fuel cell model in the cost function, the assumptions of [193] are used, as the accuracies cannot be determined for the individual models. The simulation models exhibit a high degree of similarity in their load behavior, resulting in identical frequency and voltage dynamics. The differences only become apparent in the perspective at the device level. For example, simplified models neglect the influence of temperature on the fuel cell, resulting in higher cell voltages and lower currents within the cell. Models that are simplified to a certain degree are nevertheless sufficient for simulations of electrical grids as long as no thermal analysis is to take place [193].

Analysis The simulation models presented in [193] are analyzed with regard to the relevant complexity metrics, with the results presented in Tab. 11.

Table 11: *Characteristic data for the various simulation models of a fuel cell from [193]*

Number of model	**1**	**2**	**3**	**4**	**5**	**6**
Number of parameters	55	44	27	4	4	2
Average computation time [s]	2.400	1.300	1.224	0.970	0.889	0.777
Cyclomatic complexity	3	1	1	1	1	1

For fuel cells, the computation time is omitted from the cost function because the data available from the literature lacks comparability to the own measurements of the computation time performed for the other types of components. The cost function therefore includes only the cyclomatic complexity and the number of parameters as complexity metrics for this type of component.

4.3 Simulation Complexity of Maritime Energy Systems

The inherent simulation complexity of maritime energy systems arises from the various requirements and configurations of shipboard electrical grids. This subsection explores how specific use cases influence simulation complexity, focusing on model partitioning, critical components, bidirectionality, and the impact of system topology.

4.3.1 Modularization via System Partitioning

The modularization of the grid facilitates the division of simulations into smaller independent segments, enabling faster and parallelized simulation. In DC grids, where DC/DC-converters are used to interconnect subsystems at various locations, they serve as ideal points for splitting into distinct simulation models. However, to maintain reliability and accuracy, it is necessary to investigate how different dynamics propagate through DC/DC-converters to avoid compromising the simulation accuracy due to a lost connection across these points. The propagation of different dynamics through DC/DC-converters is analyzed in [194]. An experimental setup is employed, where a DC/DC-converter is configured to allow the application of harmonic distortions on both the input and output sides. In one experiment, an *EA DC power source* [188] (EA Elektro-Automatik GmbH, Germany) supplying 350 V DC is connected to the primary side, while a 4-quadrant *Spitzenberger & Spieß AC Amplifier* [189] (Spitzenberger & Spies GmbH & Co. KG, Germany) is used on the secondary side to impose a load current with a ripple of 500 mA. The ripple frequency is varied across the range of 1 Hz to 100 kHz. As shown in Fig. 39(a) and (b), the transmission of low frequencies from the secondary to

the primary side is observed, while frequencies above 100 Hz have no significant impact on the primary side.

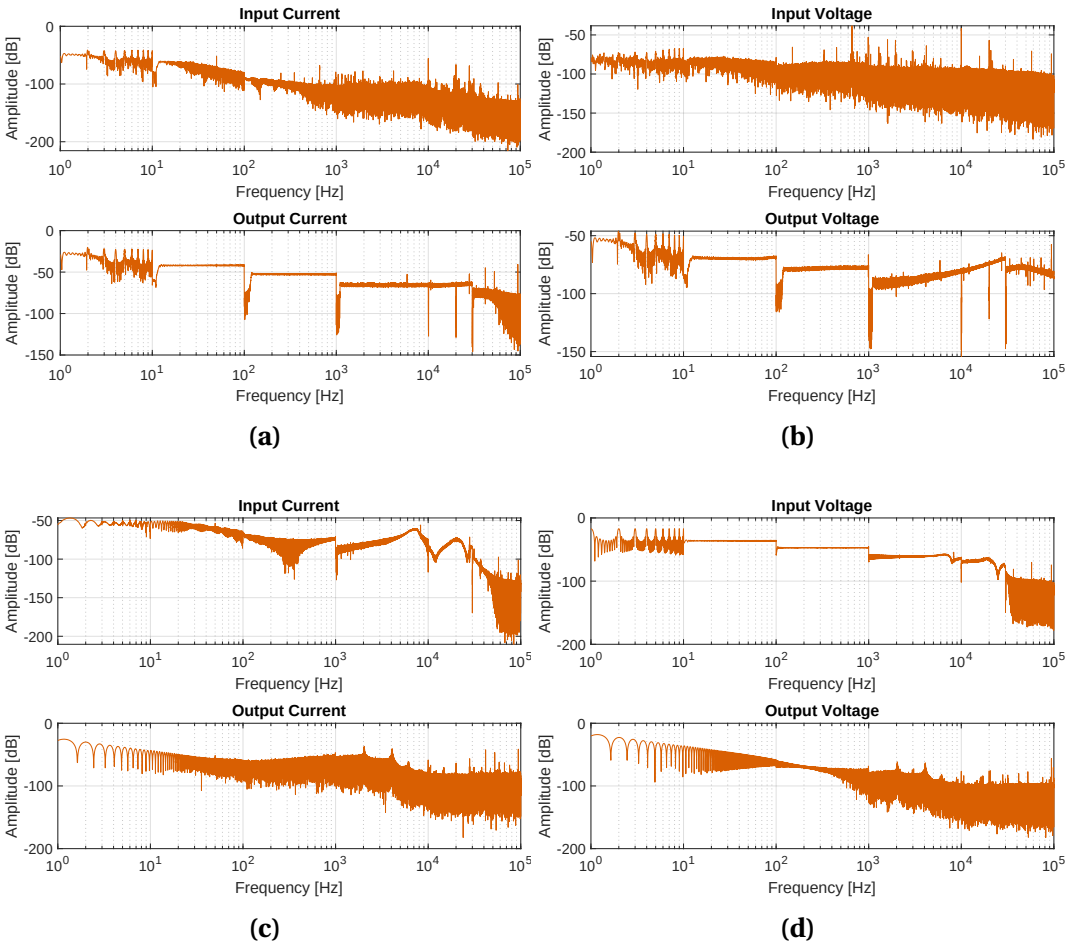

Figure 39: *Frequency response analysis of the converter for harmonic ripples applied at the input and output across a frequency range of* 1 Hz *to* 100 kHz *according to [194] . The amplitude in dB is relative to 1 (*V*, respectively* A*). (a) Current response of the output current to harmonic current ripples of* 500 mA *applied at the output. The results show resonance frequencies at the output and the propagation of low frequencies to the primary side. (b) Voltage response of the output voltage to harmonic current ripples of* 500 mA *applied at the output. The results show resonance frequencies at the output and the propagation of low frequencies to the primary side. (c) Current response of the output current to harmonic voltage ripples of* 1 V *applied at the input. The results indicate that only low-frequency components are transmitted to the output, with resonance peaks observed at* 7 kHz *and* 20 kHz*. (d) Voltage response of the output voltage to harmonic voltage ripples of* 1 V *applied at the input. The results indicate that only low-frequency components are transmitted to the output, with resonance peaks observed at* 7 kHz *and* 20 kHz*.*

In another experiment, a constant load current is applied using an *EA DC power source*

[188] (EA Elektro-Automatik GmbH, Germany) operating in sink mode, while the 4-quadrant *Spitzenberger & Spieß AC Amplifier* [189] (Spitzenberger & Spies GmbH & Co. KG, Germany), set to 350 V DC, is connected to the primary side for the power supply. Voltage ripples of 1 V are introduced on the primary side, with frequencies ranging from 1 Hz to 100 kHz. The frequency response of the DC/DC-converter, depicted in Fig. 39(c) and (d), indicates that only low-frequency components are transmitted to the output. Additionally, resonance frequencies are identified at 7 kHz and 20 kHz.

These experiments show that DC/DC-converters are mostly decoupling the dynamic interactions between their primary and secondary sides, as they attenuate the propagation of harmonic distortions across a wide frequency range. Thus, making them an ideal location for the partitioning of system simulations by modeling the DC/DC-converters as boundary elements. Especially in maritime DC grids, this allows the separation of simulations into different voltage levels and subsystems.

4.3.2 Identification of Critical Components

Maritime energy systems are characterized by their diversity, as the specific requirements of each type of ship vary according to its individual task [39, 195]. To cope with this complexity, the concept of modularization, as described in Chapter 2.1, is often applied. Standardized modules and interfaces are used. In this context, the question arises as to which of these elements or modules should be modeled with high complexity and LoD in order to enable a valid simulation without requiring excessive simulation resources.

Considering the exemplary modularized ship power system presented in Chapter 2.1, most of the elements can be categorized according to their functionality:

- Power generation: The power required during the operation of (diesel electric) ships is primarily generated by AC generators and then converted to DC by using rectifiers. In addition, fuel cells, distributed energy storage or energy storage systems can be connected directly to the Medium Voltage Direct Current (MVDC) or LVDC bus due to their inherent DC architecture, although a DC/DC-converter is usually used for connection.
- Propulsion and motors: The propulsion system is mainly based on variable-frequency AC motors, usually powered from the MVDC bus via a frequency converter. Various other motors and pumps are used on board for heating, ventilation, air conditioning, and bilge pumps, connected to the MVDC or LVDC bus via frequency converters.

- Switches and circuit breakers: These are critical to the safety and redundancy of onboard power systems, whether AC or DC. Circuit breakers and switches require a more sophisticated design than their AC counterparts due to the missing zero crossing [3, 196].
- Resistive loads: Small to medium electrical appliances such as lighting, galley equipment, laundry, and various other appliances connected to low-voltage sockets make up the largest group of consumers in the case of cruise ships and can be described as purely resistive.

System safety is a particular focus of the assessment. For components with a considerable impact on system stability, accurate modeling is more critical than for other components, to warrant that the systems designed on the basis of this simulation achieve stable operation with high power quality, while complying with all regulations. The modeling of functionality and understanding of components for safety-related functions or the handling of fault scenarios should also be more accurate. Components that are frequently installed in the system can have a substantial impact on the overall system if small deviations add up due to the large number of components installed in different locations. High power components, on the other hand, can have a large impact in the event of a failure or disturbance, even for limited installed numbers. In addition, the inherent complexity of a component can also influence its criticality, as the dynamic interactions of the various parts pose a challenge in correctly mapping the real behavior of the component, especially in cases where there is a lack of information on individual parameters. This highlights that a combination of properties contributes to the component criticality and its contribution to system safety and stability.

As shown in the overview in Tab. 12, the various types of components have very different influences on the factors that are important for component criticality.

Complexity While *resistive loads* have a low level of complexity, even though they are distributed in large numbers throughout the ship and there are continuous variations in the load profile, the complexity of *motors* and *generators* is considerably higher. As the motors/generators are predominantly AC components (DC motors are rarely used), they are connected to the DC grid via frequency converters or rectifiers, only transferring the corresponding characteristics of the components to the grid to a limited extent. Therefore, the relevance of the complexity of the *converters* is much higher at this point and their accurate modeling must be given priority. Frequency converters or rectifiers also have a high level of complexity that is relevant to almost all simulation applications. Numerous active elements, high switching frequencies, and complex software control are responsible for the high level of complexity. Although *circuit breakers* can be modeled as switches for many simulation scenarios, they are much

more complex, especially for fault scenarios, as they must be designed to switch DC fault currents in a much more complex way than their AC counterparts.

Number of occurrence The number of *generators* used in the ship grid is very small, as there are typically only a few large main generators. The number of *switches/breakers* and *motors* is in the medium range, as these are mainly used in the primary system. The number of *DC/DC-converters*, in contrast, is high because they must be used for each voltage change, and many of these conversions take place in parallel with several converters to keep power levels low and achieve greater redundancy. *Resistive loads* are by far the most common as they are distributed throughout the ship from low to high power and include equipment such as lighting, galley, and entertainment systems.

Power The power density of the *resistive loads* is in the W to kW range, while the *converters* cover the wide range from W/kW to MW, as they are also used to connect propulsion *motors* and *generators*, that account for the majority of the ship's power and are in the kW to MW range. As *switches/circuit breakers* are not consumers in the narrower sense, they have no consumption or generation of power, although the power range can be defined. They are primarily used in the higher voltage ranges to protect whole sub-segments where power in the kW to MW range needs to be safely disconnected.

Table 12: *Overview of components in DC grids and their properties according to [194]*

Component	**Complexity**	**Number of occurrences**	**Power**	**Contribution to electrical system safety**	**Contribution to system stability**
Resistive loads	low	very high	W-kW	low	during load spikes/drops
Switches/ breakers	higher than in AC	medium	kW-MW	high	during switching operation
Motors	high	medium	kW-MW	low	high via frequency converter
Generators	high	low	kW-MW	low	high via rectifier
DC/DC-converters	high	high	W-MW	low	high

Contribution to electrical system safety Although *resistive loads*, *motors*, *generators*, and *converters* are important to the functionality of the system, they have little impact on the safety of the system, as they have no direct role in the context of fault scenarios. *Switches/breakers*, on the other hand, are essential for the connection and protection of subsystems and therefore make a decisive contribution to system safety and redundancy.

Contribution to system stability Load peaks or dips in the area of uncontrolled *resistive loads* are relevant to the system stability factor, but the influence of *motors* and *generators* through the introduction of oscillations is also high, even if these can be controlled via frequency *converters* or rectifiers. *Switches/circuit breakers* only contribute to system stability at their respective switching times. Frequency converters, on the other hand, have a major impact on system stability, as the high frequency switching operations can lead to substantial voltage and current ripple and high current peaks from their charged capacitors can be possible.

Critical component assessment Based on the previous comparison, it can be concluded that power electronic converters are the most relevant critical components for the simulation of DC grids. This is due to their use for interfaces, their complex design/structure, their software-based control, their frequent occurrence in DC grids, and their pronounced influence on system stability and power quality. This effect is also visible in the scaled-ship grid analysis of Chapter 5.1.1.

4.3.3 Influence of Topology

From certain use cases, it is known that the topology of a grid can have an impact on the necessary resolution and therefore on the simulation and model complexity [121]. To analyze the influence of topology, an exemplary analysis of a maritime DC grid onboard a cruise ship is conducted by analyzing the influence of the use of bidirectional load flows through the use of components such as battery storage systems, and the influence of grid enmeshment.

A cruise ship with a DC grid is analyzed that has two propulsion motors in the primary grid connected to the redundant DC bus structure via inverters as shown in Fig. 40. Two AC generators are used for the main supply, connected to the DC bus via AC/DC-converters. From the two DC buses in the primary system, each FZ has a DC/DC-converter that converts from MVDC to LVDC and supplies the FZ via vertical busbars. The actual structure of the FZ may vary depending on the ship's structure and existing equipment.

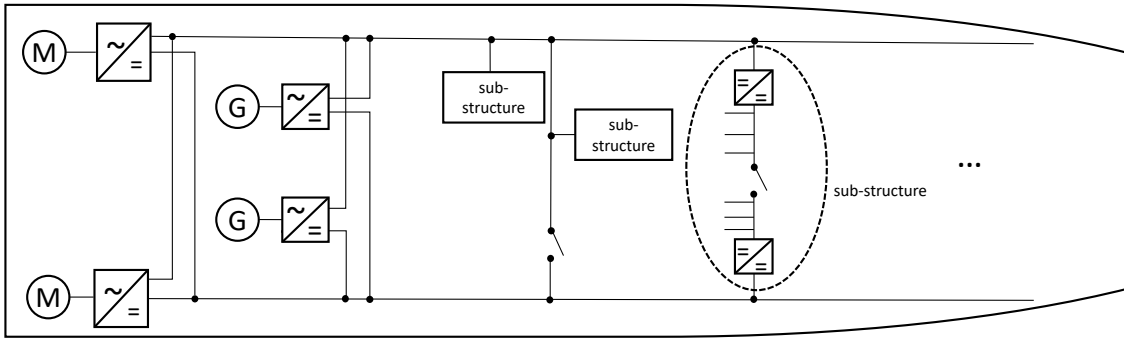

Figure 40: *Simplified SL ship distribution for the analysis of topology influences*

In order to analyze the topological influences on the simulation and the model complexity, a simulation model of a deck section of a FZ in the hotel area with a total of 60 cabins with fluctuating loads is used.

Bidirectionality The influence of bidirectionality is analyzed by connecting different numbers of battery storage units to the simulated hotel area. The batteries are connected to the hotel area DC bus at different positions via a DC/DC-converter, as depicted in Fig. 41. Each additional battery leads to a natural increase in the number of

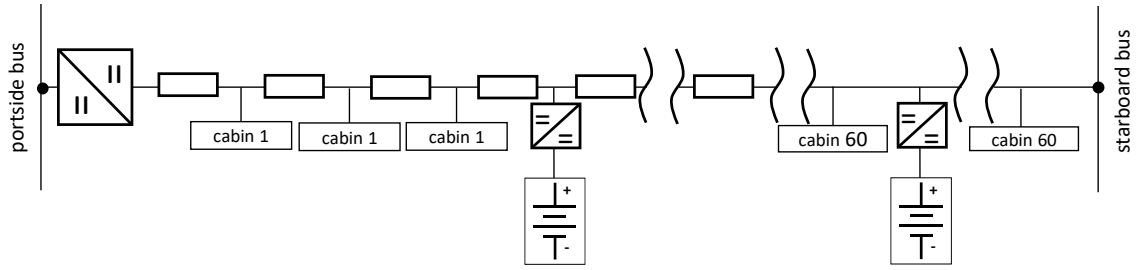

Figure 41: *Hotel Area Ship Distribution System for Bidirectionality Analysis*

components and therefore in the number of simulation parameters. The effects of the different numbers of batteries on the model and simulation complexity are shown in Fig. 42. In the simulation performed in [195], the number of parameters increases by 13 with each additional battery. The cyclomatic complexity increases by eight with each additional battery. An in-depth analysis of the computation time in relation to the number of parameters, cyclomatic complexity, and the number of components shows that the computation time and the number of parameters do not have a constant ratio. However, the additional computation time per additional battery increases proportionally to the increase in cyclomatic complexity. This relationship shows that bidirectionality has a substantial impact on the complexity of a simulation and therefore on the resources required to perform it.

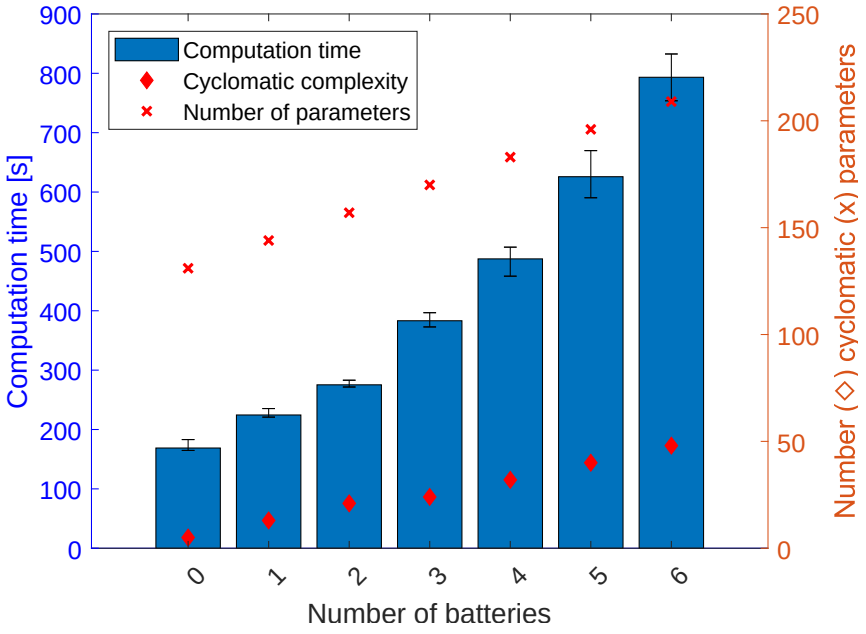

Figure 42: *Complexity Measures for Different Numbers of Batteries*

There are two opposing effects in terms of the simulation complexity of batteries, depending on the specific application. The higher the complexity of the simulation, the higher the cost of running a simulation with many bidirectional components compared to simulations with otherwise identical properties. This is due to the increased computation time required. However, investigations in [121, 172] show that the use of storage components can ensure that lower time resolutions are possible without loss of accuracy, as peaks are compensated by them. Therefore, the influence of increasing the simulation effort through longer simulation times must be weighed against the risks of lower simulation accuracy or maintaining simulation accuracy through the possibility of reducing the time resolution. When designing DC grids, the use of fewer batteries with larger capacities can be advantageous in terms of simulation complexity and thus resources, as well as in terms of installation, control, and maintenance efforts.

Enmeshment The same subsystem of the exemplary cruise ship hotel area deck is used to analyze the effects of enmeshment on small DC grids. As the grid does not have a high enmeshment under normal operating conditions, a special operating point is chosen for analysis. In normal operation, each load is supplied from one busbar only, and the additional connection to the second busbar for redundancy purposes is provided by a coupling switch. This coupling switch closes in the event of a fault to make sure that the load can continue to operate at full power. To investigate the case of high enmeshment, this paper therefore analyzes the case where the coupling switch is closed in normal operating mode, thus creating a ring topology as shown in Fig. 43. Even

if this mode of operation does not occur in reality, the corresponding setup permits the analysis of the differences in complexity of simulation models with different degrees of enmeshment. The analysis of the effect of enmeshment is carried out for three

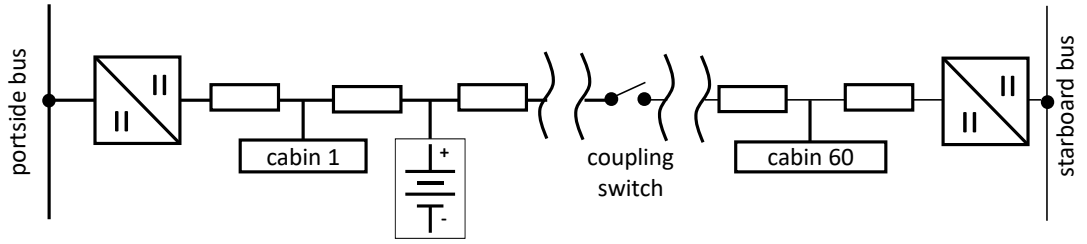

Figure 43: *Exemplary hotel area SL ship distribution system for analysis of enmeshment*

different topologies in order to compare the influence of the degree of enmeshment: A bus topology with a single converter and an open coupling switch is considered the normal operating case. A ring topology with two DC/DC-converters is used to achieve a higher level of enmeshment, consisting of loads connected to both busbars via one DC/DC-converter per bus. To isolate the impact of increased enmeshment, a bus system with an open coupling switch and parallel DC/DC-converters on one bus is analyzed. The three topologies analyzed show different cyclomatic complexities that are only due to the change in the number of DC/DC-converters used, resulting in a number of five for the bus topology with only one converter and a number of 10 for both topologies with two converters. Considering the number of parameters for the topologies, again only the number of DC/DC-converters present changes, with 130 parameters for the single-converter topologies and 135 for the two-converter topologies. A higher degree of enmeshment only increases the number of line resistances, so the simulation complexity for these metrics remains similar. In terms of computation time, the bus topology with two converters shows the longest duration.While the computation times show a statistically significant difference between all three topologies investigated in a Kruskal-Wallis test, the assertion that higher enmeshment in small DC grids leads to increased simulation complexity cannot be supported, as no significant increase or decrease due to enmeshment is found. A more detailed analysis of the influence of bidirectionality and enmeshment on simulation and model complexity can be found in [195].

4.3.4 Influence of Simulation Resolution

Temporal Resolution The temporal resolution of the simulation is not employed as a metric (see Chapter 3); however, it directly influences the simulation's deviation from reality. This is because load or source peaks can only be represented inaccurately at lower temporal resolutions. Cao *et al.* [121] analyzes this effect and evaluates the impact

of buffering/peak shaving on simulation accuracy due to the use of batteries. In their study, Cao *et al.* investigated 16 different groups of simulations involving Photovoltaics (PV) systems and batteries. For this thesis, only groups H2, representing a hypothetical constant generation unit with 0.82 kW, and P2, modeling a PV system with an area of 17.8 m^2 and an approximate generation of 0.29 kWh, are considered. The corresponding data is provided in Appendix D.7. Fig. 44 shows the ratio of simulation errors for H2 and P2, depending on the temporal resolution. In this thesis, the influence of temporal resolution F_{ts} on the cost function is derived as an average of the results for H2 and P2. The usage of batteries can lead to an increased simulation accuracy while maintaining

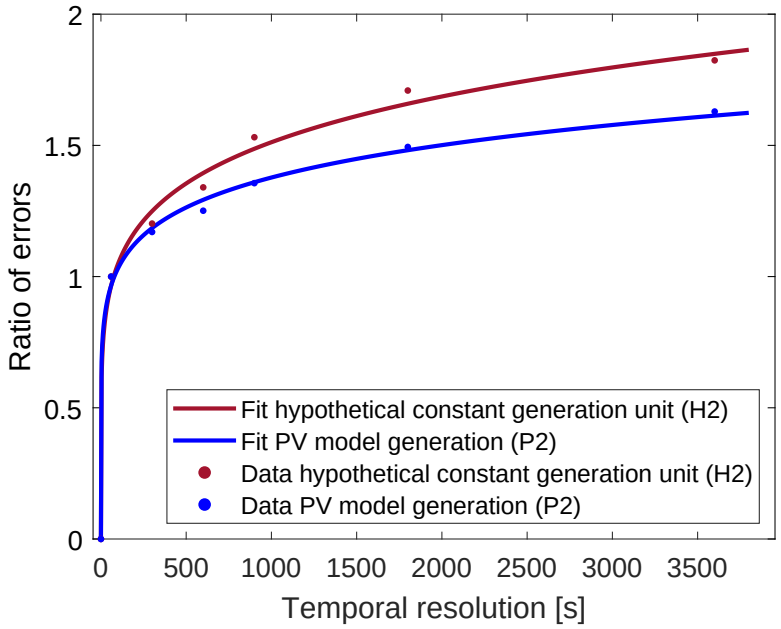

Figure 44: *Ratio of different simulation errors compared to the simulation with 60 s resolution for a hypothetical constant power generation unit (H2) and a PV simulation example (P2) according to the data from Cao et al. [121]*

or even reducing the temporal resolution, as illustrated in Fig. 45. By appropriately scaling the battery capacity to match the expected load peaks, the batteries are able to reduce the simulation error through peak shaving. This result can be applied to cruise ships, where the battery capacity can be scaled to accommodate load peaks of approximately 39 kWh [192]. However, onboard battery capacities may well go beyond the capacitance necessary for peak shaving. The factor for the influence of the battery capacity F_{Bat} for the cost function in this work is derived as the average of the results for H2 and P2.

Minimal Accuracy for Components To avoid neglecting more complex models in the cost function, a minimal accuracy is defined for both the individual components

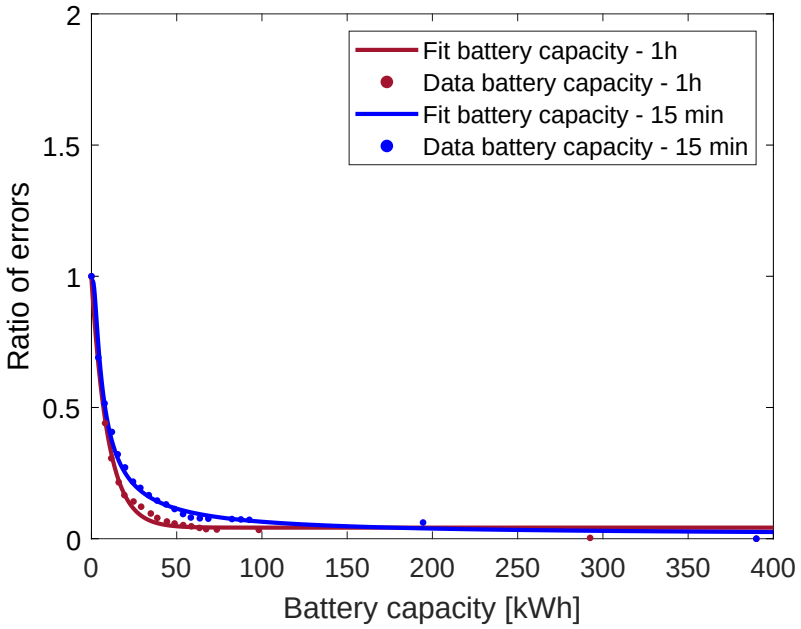

Figure 45: *Ratio of simulation error compared to the simulation without batteries for distinct battery capacities for a simulation with 1 h and 15 min time steps according to the data from Cao et al. [121]. The investigation conducted in [121] assumes peak loads between 0.15 kWh and 0.40 kWh.*

and the overall system to be simulated. The system accuracy depends on the specific application and is therefore defined before the use of the cost function. For the minimal component accuracy, a number of possible "wrong" components n_{false} is defined as

$$n_{\text{false}} = a + max(0, \left\lfloor \frac{N_{\text{Comp}} - b}{c} \right\rfloor), \tag{17}$$

to guarantee a minimal accuracy that can be below 100 % in the optimization. Here, the parameter a defines the baseline value of n_{false}, b specifies the number of components at which n_{false} begins to increase and c determines the rate at which n_{false} grows as the number of components exceeds b. The values of these factors are specified in Appendix D.7. Further, the condition

$$A_{\text{min,Comp}} \geq A_{\text{min,sys}} \tag{18}$$

is defined with the minimal component accuracy $A_{\text{min,Comp}}$ and the minimal system accuracy $A_{\text{min,sys}}$. The probability $P(E)$ of simulating fewer than n_{false} components incorrectly when simulating N_{Comp} components

$$P(E) = \sum_{i=0}^{n_{\text{false}}} B(N_{\text{Comp}}, A_{\text{min,Comp}}, i) \tag{19}$$

is defined with the binomial distribution B, given in Appendix D.7. The optimization is performed for the component accuracy $A_{\text{min,Comp}}$, ensuring that $P(E) \geq A_{\text{min,sys}}$. This approach balances the minimal simulation accuracy, ensuring it is not unnecessarily high for complex but infrequently used components, while also avoiding excessively low accuracy for frequently used components.

System accuracy The overall system accuracy is determined by the component accuracies, an implementation factor F_{Imp}, an inaccuracy penalty f_{U}, and the factors for simulation resolution F_{ts} and battery capacity F_{Bat}.

The system accuracy, A_{Sys}, is derived from the component accuracies as the average of the component accuracies $A_{\text{Comp,tot}}$ and is finally adjusted by the factors for the battery capacity F_{Bat} and the influence of the temporal resolution F_{ts} defined in Chapter 4.3.4 and a penalty factor f_{U} (see Appendix D.7) to obtain the total resulting system accuracy $A_{\text{Sys,tot}}$ as shown in Eq. 20.

$$A_{\text{Sys,tot}} = A_{\text{Sys}} \cdot f_{\text{U}} \cdot (1 - F_{\text{Bat}} \cdot F_{\text{ts}}) \tag{20}$$

4.4 Defining the Cost Function

A cost function is developed, that can be employed within the presented methodology for the purpose of minimizing the associated costs of modeling and simulation, while ensuring that the simulations remain sufficiently accurate. The area of application of the simulation, the simulation objectives, the assessment of different cost categories and boundary conditions are all accounted for in this cost function. Moreover, the employed optimization algorithm and its capacity to identify all pertinent local minima, particularly the global minimum, are of importance. Common components in DC grids are analyzed to include their relationship between accuracy and complexity in the cost function (Chapter 4.2). The cost function optimum corresponds to the lowest cost. The total costs are shown in Eq. 21 and consist of the development cost C_{Dev}, the computation cost C_{Calc}, the fixed cost C_{Fix}, the risk cost C_{Risk} and the potential savings C_{Sav}. The weighting of the individual cost factors is carried out within these separate costs, in order to guarantee that the individual cost factors always result in a total sum in euros.

$$C_{\text{tot}} = \sum_{i=1}^{n} C_i = C_{\text{Dev}} + C_{\text{Calc}} + C_{\text{Fix}} + C_{\text{Risk}} - C_{\text{Sav}} \tag{21}$$

A graphical representation of the cost function is shown in Fig. 46.

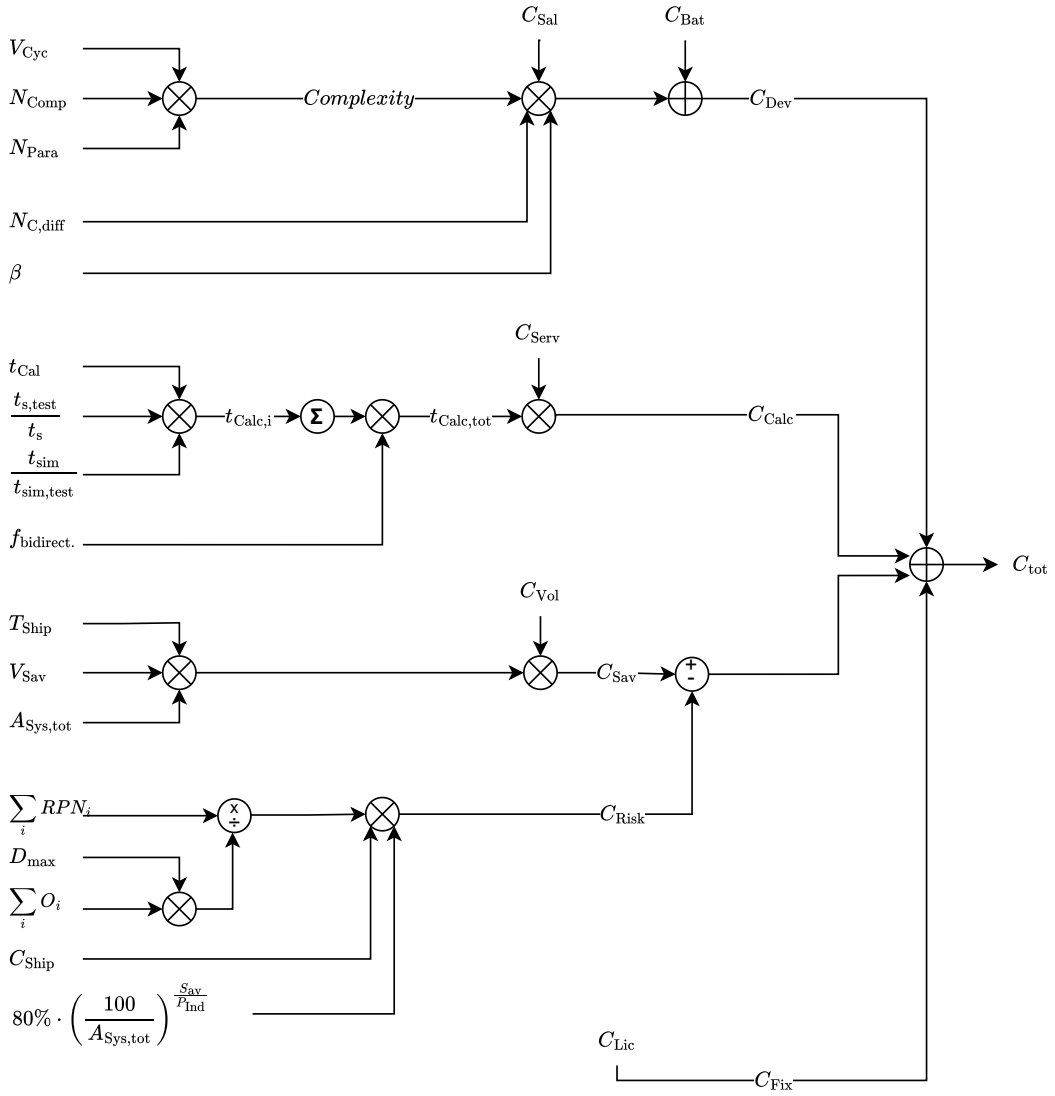

Figure 46: *Graphical representation of the cost function*

4.4.1 Development Cost

The complexity metrics defined in Chapter 3 are employed to estimate the development cost of the model. The total development cost is determined according to the function shown in Eq. 22. The development cost comprises the hourly wage of the engineers C_{Sal}, the cyclomatic complexity V_{cyc}, the number of multiple implemented components $N_{\mathrm{Comp,Mult}}$, the number of parameters N_{Para}, a scaling factor β (as defined in Appendix E.3), the number of different components $N_{\mathrm{C,diff}}$ that are realized in the system (as defined in Appendix E.2), and the cost of the battery capacity optimized

according to Chapter 4.3.4.

$$C_{\text{Dev}} = C_{\text{Sal}} \cdot \left(V_{\text{cyc}} \cdot N_{\text{Comp,Mult}} \cdot N_{\text{Para}} \right) \cdot \beta \cdot N_{\text{C,diff}} + C_{\text{Bat}} \tag{22}$$

4.4.2 Computation Cost

The computation cost C_{Calc} results from the server cost C_{Serv}, that is required for the simulation, and the expected simulation time $t_{\text{Calc,tot}}$. The computation cost is shown in Eq. 23 and includes a conversion of the simulation time from seconds to hours:

$$C_{\text{Calc}} = C_{\text{Serv}} \cdot \frac{t_{\text{Calc,tot}}}{360} \tag{23}$$

The expected computation time $t_{\text{Calc,tot}}$ is composed of the computation times of the components $t_{\text{Calc},i}$ and the factor of bidirectionality f_{Bidirect} established in Ch.s 4.3.3 and 4.2.2. The following therefore applies to $t_{\text{Calc,tot}}$:

$$t_{\text{Calc,tot}} = f_{\text{Bidirect}} \cdot \sum_{i=1}^{n} t_{\text{Calc,i}} \tag{24}$$

The computation time of the individual components is determined according to the data established in Chapter 4.2. In order to adapt these to the application area, they are scaled with the simulation period t_{sim} and the simulation resolution t_{s}. Accordingly, the following applies

$$t_{\text{Calc},i} = t_{\text{Calc},i} \cdot \frac{t_{\text{s,test}}}{t_{\text{s}}} \cdot \frac{t_{\text{sim}}}{t_{\text{sim,test}}}, \tag{25}$$

where $t_{\text{s,test}}$ and $t_{\text{sim,test}}$ represent the simulation resolution and time used in the simulation analyzed to obtain the computation time. The scaling is based on the assumption of a linear dependency between computation time and simulation resolution.

4.4.3 Fixed Cost

The fixed cost C_{Fix} represents expenses that remain constant for all computation times and amounts of simulations. They include expenses for software, maintenance contracts and all license fees C_{Lic} incurred for the simulation that usually only occur once and remain constant across simulation scenarios.

$$C_{\text{Fix}} = C_{\text{Lic}} \tag{26}$$

4.4.4 Risk Cost

To quantify the risk cost, a Failure Mode and Effects Analysis (FMEA) is conducted, that is detailed in Appendix H. A highly reduced excerpt from the FMEA is provided in Tab. 13. In total, 1,345 potential failure modes, their effects, and failure cause combinations are identified and their Risk Priority Numbers (RPNs) calculated.

Risk cost is calculated using Eq. 27, incorporating the total ship cost C_{Ship}, and the occurrence O_i, severity S_i, and detectability D_i of each distinct failure cause, effect, and mode combination throughout the ship's life cycle. To derive probabilities for both occurrence and detection, the resulting value is divided by the maximum detectability, D_{max}, and the sum of all occurrences. To account for the fact that the FMEA results are based on an 80 % simulation accuracy, the value is multiplied by 80 %. The total simulation accuracy $A_{\text{Sys,tot}}$ is also considered and raised to the power of the average severity value divided by the industry-specific scaling factor P_{Ind}. For the shipbuilding industry, this scaling factor is set to one.

$$C_{\text{Risk}} = \sum_i \frac{O_i \cdot S_i \cdot D_i}{D_{\text{max}} \cdot \sum_i O_i} \cdot C_{\text{Ship}} \cdot 0.8 \cdot \left(\frac{100}{A_{\text{Sys,tot}}} \right)^{\frac{S_{\text{av}}}{P_{\text{Ind}}}} \tag{27}$$

Since the different application areas have varying impacts on the potential risk cost, the resulting risk cost from Eq. 27 is weighted by the respective share of the total risk, as defined in Tab. 23. This results in the complete risk cost from Eq. 27, when all simulation applications are considered.

4.4.5 Emerging Cost Reduction Potentials

In addition to the advantages of DC grids listed in Chapter 2.1, a simulation can also prevent the oversizing of components. The potential for savings is comprised of the volume savings price C_{Vol}, the service life of a cruise ship T_{Ship}, the maximum possible volume reduction V_{Sav} and the simulation accuracy achieved $A_{\text{Sys,tot}}$

$$C_{\text{Sav}} = C_{\text{Vol}} \cdot T_{\text{Ship}} \cdot V_{\text{Sav}} \cdot \frac{A_{\text{Sys,tot}}}{100}. \tag{28}$$

The approach shown in [197] leads to a volume saving price of €$0.35 m^{-3} h^{-1}$, assuming that a cruise ship is in use for 40 years and that a maximum total volume of 20 m^3 can be saved, this results in a maximum savings potential C_{Sav} of €6.132 M for an average cruise ship.

Table 13: *Excerpt from the FMEA to determine the risk cost, full FMEA shown in Appendix H*

Potential failure mode	Potential effects of failure	Potential Causes of failure	Sev.	Occ.	Det.	RPN
Higher current than simulated	faster ageing	incorrect dimensioning	4	9	5	180
Slower reaction, lower frequencies	faster degeneration					180
Load flow changes not correctly simulated	lower efficiency					180
Numerical problems	lower speed					180
Lower current than simulated	insufficient available power	system based simulation	8	7	4	224
Faster reaction, higher frequencies simulated than real	higher reaction time	incorrect dimensioning	5	9	5	225
Higher current than simulated	overload - connection destruction	system based simulation	9	7	4	252
Shifting of behaviors to other time, incorrect event synchronization	overload - destruction		9	7	4	252
Load flow changes (e.g. of direction) not correctly simulated	capacity too low	incorrect dimensioning	6	9	5	270
Slower reaction, lower frequencies	overload - loss of propulsion	system based simulation	10	7	4	280
Faster reaction, higher frequencies simulated than real	insufficient available power	incorrect dimensioning	8	9	5	360
Numerical problems	safety hazard - fire risk, overheating	incorrect dimensioning	9	9	5	405
Slower reaction, lower frequencies	complete power outage	incorrect dimensioning	10	9	5	450
Higher current than simulated	safety hazard - passengers/crew					450

4.4.6 Cost Function Boundary Constraints

In order to apply the cost function, it is necessary to know the minimum accuracy required for each simulation area, as well as the simulation duration and resolution. In certain applications of simulation, such as load flow analyses and energy source dimensioning, longer simulation durations are necessary. In contrast, short-circuit and transient stability analyses only require short simulation durations until the system has reached a steady state. In terms of resolution, the usage of double variables is assumed for current and voltage values. With regard to time resolution, in particular the relevance of the activation and usage of semiconductors and power switches must be taken into account. Feasibility studies that only analyze basic load flows do not require extensive time resolution. In contrast, short-circuit analyses that lead to tripping of solid-state circuit breakers require much higher time resolutions. The resulting minimal accuracies and resolutions for different simulation applications are presented in Chapter 4.3.4.

All optimization variables must be defined, including the specification of the lower and upper bounds and their type. A set of variables for an exemplary cruise ship is provided in Chapter E.1.

4.4.7 Implementation

The implementation of the methodology involves several decisions, specifically the selection of an appropriate time resolution for the simulation. In selecting an appropriate simulation time resolution, it is essential to acknowledge the direct impact that this choice has on the accuracy of the simulation in relation to the real system. For instance, load peaks can be represented less precisely in a simulation with a lower resolution. If batteries of a certain capacity are available in the simulated system, they can serve to buffer long-lasting intermittent spikes, both in the real system and in the simulation, thereby reducing the error and increasing the accuracy of the simulation [121]. The same behavior is observed for photovoltaic systems [173] and hybrid configurations [172], but the effect is less pronounced for diesel generators [172]. Although these studies have been conducted on the suitability of different time resolution settings for simulations, there is no consensus on the optimal time resolution for a given simulation. Therefore, the implemented battery capacity is taken into account when optimizing the cost function.

5 Method Application

The application of the methodology is necessary to prove its reliability and robustness. This is performed by analyzing a scaled-ship grid test setup and applying the methodology to a mechatronic use case. The methodology and optimization of the cost function are applied to an exemplary ship grid.

5.1 Complexity Analysis with Real-Life Examples

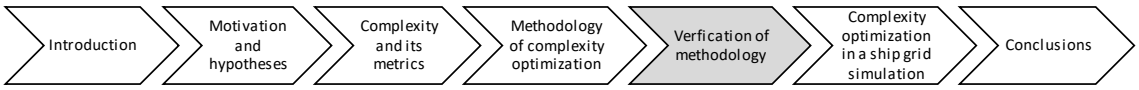

This work was conducted as part of the research project *Sustainable DC-Systems (SuSy) - Direct Current Energy Supply on Ships*, that aimed to develop concepts and technologies for future hybrid on-board power systems integrating AC and DC components [31]. As part of this project, *Meyer Werft GmbH & Co. KG*, *Siemens Energy Global GmbH & Co. KG*, *Lloyd's Register EMEA*, and *morEnergy GmbH* worked alongside research partners *German Aerospace Center (Institute for Networked Energy Systems)* and *Hamburg University of Technology*, represented by the *Institute for Mechatronics in Mechanics (iMEK)* and the *Institute for Electrical Power and Energy Technology*. Associated partners *Schneider Electric GmbH* and *Damen Shipyards* further collaborated with the partners to achieve the project goals of increasing energy efficiency, reducing conversion costs, and improving the system integration of DC loads and sources.

During the project, that relied exclusively on simulations and laboratory tests due to the unavailability of prototypes, the challenge of determining an appropriate simulation depth and accuracy without access to validation measurements on a real DC ship became evident. To address this issue, the methodology developed in this thesis is specifically tailored to the application of ship grid development and is validated within this context. The analysis of the methodology is critical to ensure consistent results by confirming that the influence of the implemented LoD of the simulation has the expected influence on the simulation accuracy. To achieve this in the absence of real ship prototypes with DC grids, a scaled-ship grid is designed, constructed, and measured

for validation purposes (Chapter 5.1.1). The cost optimization methodology is applied to a cruise ship, as this ship type was the focus of the SuSy project and relevant data for such a ship is available (Chapter 5.2).

Furthermore, since the research focus of the iMEK lies primarily in mechatronic actuators, applying the developed methodology to this field was a logical extension. To explore its broader applicability, the methodology was tested on a mechatronic use case, demonstrating its potential for use in other domains (Chapter 5.1.2).

5.1.1 Scaled-Ship Grid Test Setup

To validate the overall methodology of the various simulations LoDs, a scaled version of a ship grid section within a FZ is used, containing the most important components of the grid, DC/DC-converters, ohmic loads, fans, batteries and a long line equivalent. To construct the scaled-ship grid, each component is integrated into a dedicated Printed Circuit Board (PCB) unit. These units include the respective component, the necessary circuitry for connection to the measurement equipment, connectors to the scaled-ship grid bus, and, depending on the component, additional electrical elements such as LEDs or transistors to enable switching the unit on and off and detecting its current mode. The measurements using the scaled-ship grid are compared with the results from different LoD models, Fig. 47 shows the DC/DC-converter PCB unit, its schematic diagram, and a low and high LoD model. A detailed description of the other units is provided in Appendix F.

These individual units can be connected to three separate segments, each with its own bus. The entire setup, including the segments, is powered by an EA laboratory power source (EA Elektro-Automatik GmbH, Germany). Each segment is supplied with 24 V from the laboratory power source when using a DC/DC-converter unit, or with 12 V directly from the laboratory power source. Each segment can accommodate up to five units, resulting in the most complex possible setup shown in Fig. 48.

For each unit, simulation models with varying LoDs are developed. Most individual simulations of the units, as described in Appendix F, reveal only minor differences in accuracy between adjacent levels of model complexity. The inclusion of parasitic components typically results in marginal changes. Consequently, the scaled-ship grid test setup uses only the minimally complex, low LoD model and the most complex, high LoD model for analysis. This approach reduces the number of combinations to a manageable level, ensuring the feasibility of the investigation.

The analysis of the three-segment setups, as well as configurations with more units than those shown in Fig. 49 and Fig. 91 in Appendix G, demonstrates that the relevant behaviors and their impact on accuracy can already be observed in setups with fewer

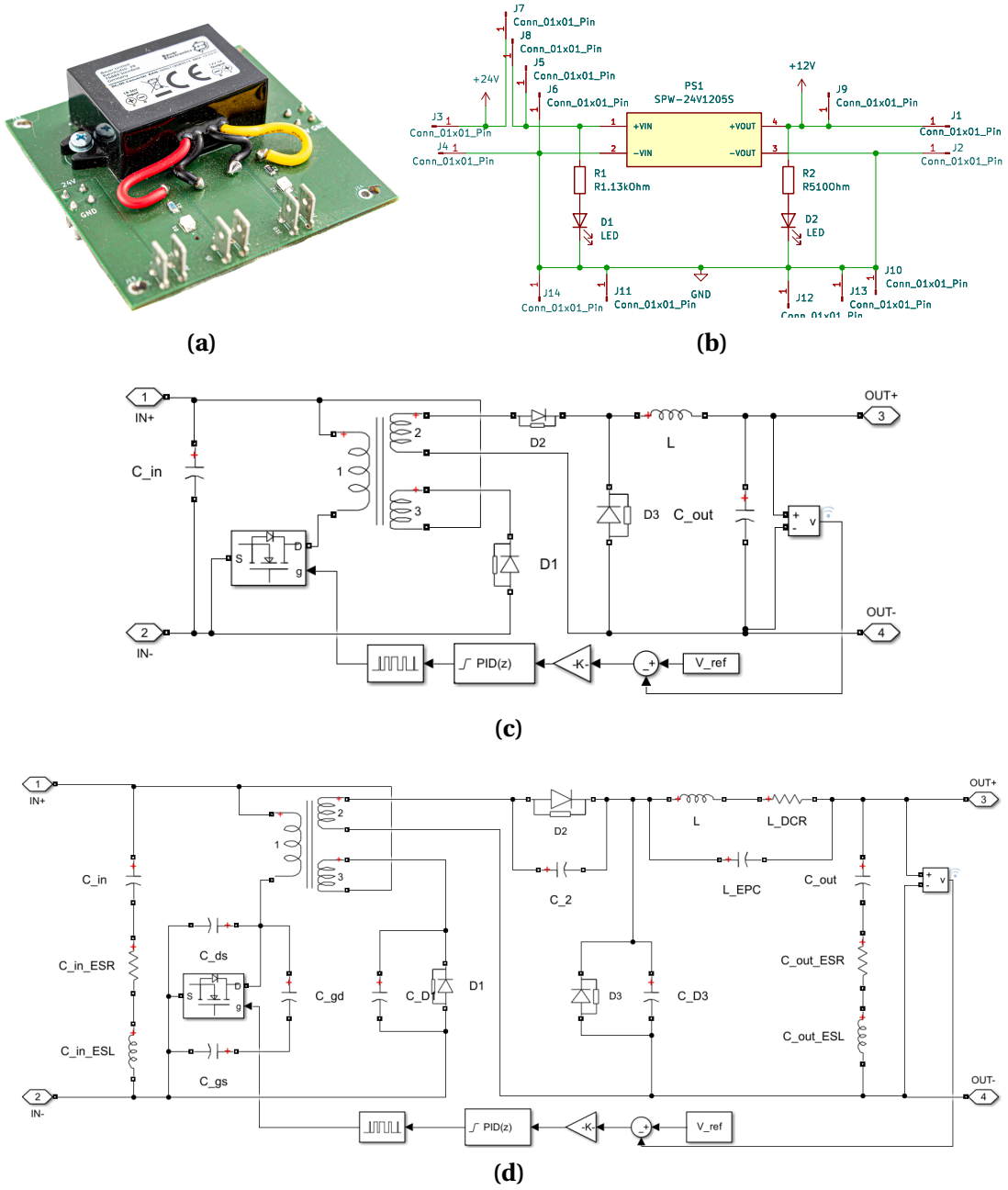

Figure 47: *DC/DC-converter unit (a) photo, (b) schematic diagram of PCB, (c) low LoD model, (d) high LoD model*

components and segments. As a result, this analysis focuses on these smaller and simpler setups to make the investigation more efficient while capturing the essential dynamics.

The influence of the DC/DC-converter and several batteries is analyzed, as is the impact

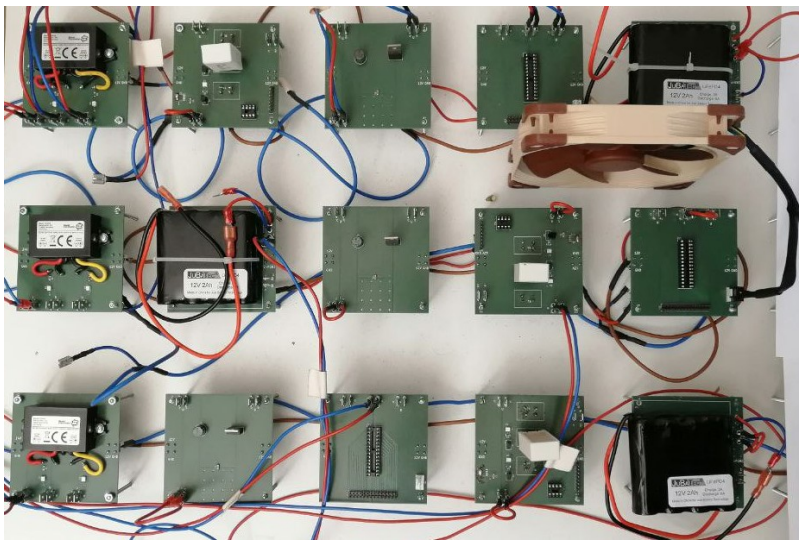

Figure 48: *Most complex possible setup of the scaled-ship grid test setup. Each of the three segments includes five PCB units.*

of an additional long line, an additional grid segment, and a redundant connection of both grid segments. Fig. 49 shows the first set of test setups, a second set of test setups is shown in Appendix G.

In principle, it can be seen from comparison between Fig. 50(b) (with DC/DC-converter) and Fig. 50(c) (without DC/DC-converter) that all experimental setups containing DC/DC-converters show significantly larger voltage fluctuations due to the change in load, than those using the laboratory power supply. This supports the result of Chapter 4.3.2, that the DC/DC-converter is a critical component in DC grids since it requires a higher LoD for sufficiently accurate simulation results. The influence of the LoD of the fan simulation is particularly evident here, as highlighted by the marker 'F' in Fig. 50(a), 50(c) and 50(d), since it is primarily responsible for the load fluctuations. Consequently, the insertion of the long cable, damping the vibrations, is also noticeable. The influence of the LoD of the long line, with or without parasitic components, is almost imperceptible within the overall system, indicated by the marker 'L' in Fig. 50(b). Almost all LoD combinations of this setup including a long line unit result in higher simulation accuracies than those of the similar setup in Fig. 50(a) without a long line unit. However, a the LoD of the simulation of the ohmic loads does not have a constant influence on the overall simulation accuracy, as shown in Fig. 50(c).

A comparison of the structures with one segment and the structures with two segments, further emphasizes the significance of the LoD of the fan simulation and the DC/DC-converter, but the influence of a high LoD of the simulation of the ohmic loads is not reflected in the simulation accuracy for larger systems anymore as shown in Fig. 50(d). In general, it can be observed that higher parameter numbers also lead to higher accuracies.

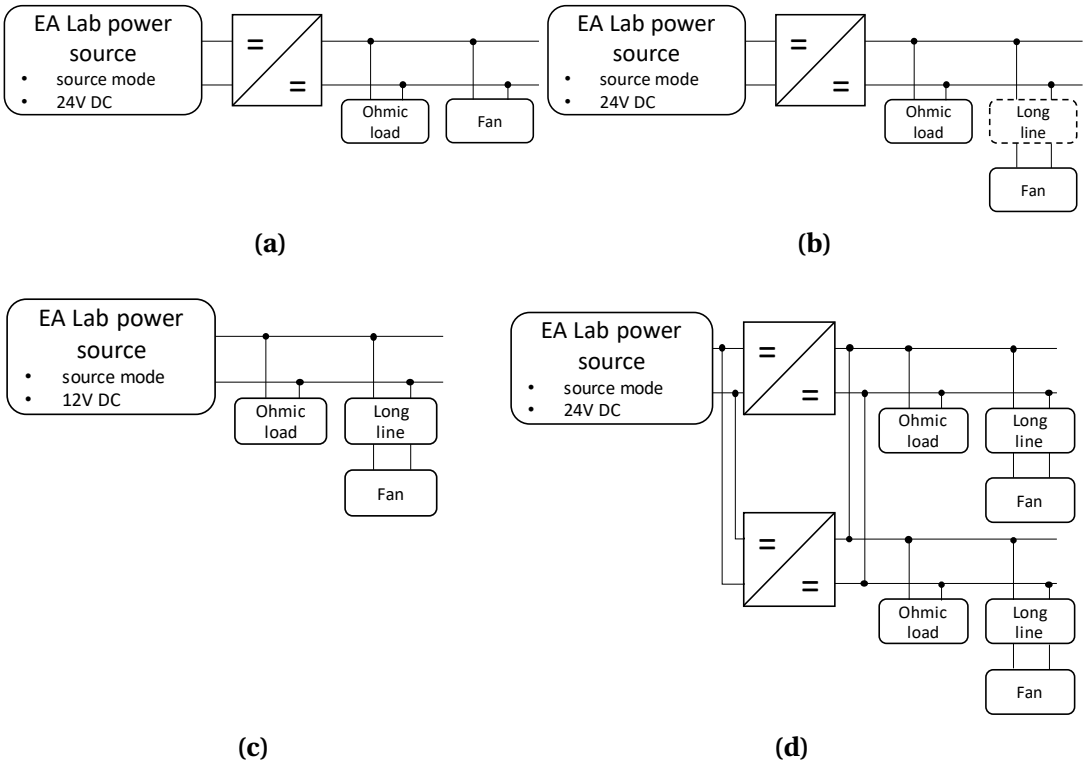

Figure 49: *Setup of the scaled-ship grid system, supplied by a lab power source: (a) DC/DC-converter connected to one segment with an ohmic load and a fan, (b) DC/DC-converter connected to one segment with an ohmic load and a fan connected via a long line, (c) one segment with an ohmic load and a fan connected via a long line, (d) two DC/DC-converters connected to two segments in a redundant configuration, each segment with an ohmic load and a fan connected via a long line*

Specifically, the setup with several batteries shows that higher parameter numbers tend to result in higher accuracy. With an increasing numbers of parameters, the computation time generally tends to increase, as shown in Fig. 51.

Furthermore, it is demonstrated that an increase in the number of parameters does not necessarily result in a corresponding increase in computation time and accuracy, as illustrated in Fig. 52, Fig. 53 and Fig. 54. However, given that all three metrics reflect a particular form of complexity, it is validated that the utilization of a single metric is insufficient to adequately capture both computational and structural complexity. The integration of all three metrics is therefore necessary.

Further graphs describing the analysis of the scaled-ship grid setup are shown in Appendix G.

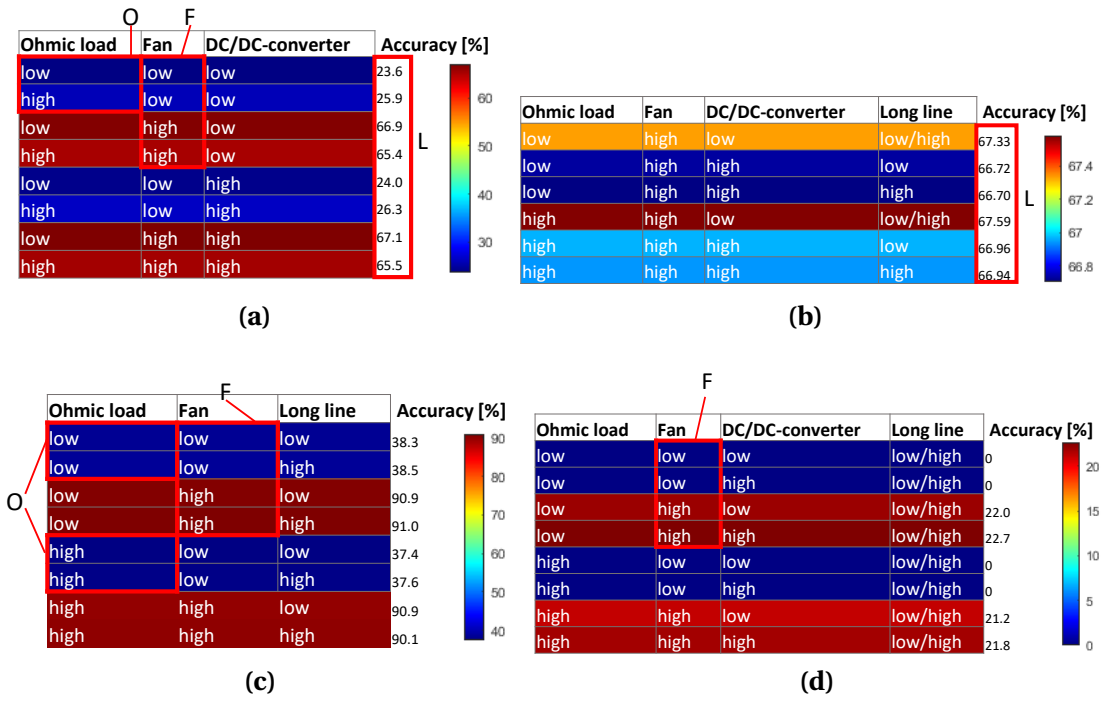

Figure 50: *Accuracy heatmaps of all simulation LoD combinations in the setups displayed in Fig. 49, where (a), (b), (c), and (d) correspond to the respective subfigures. Each row represents a specific combination of low and high LoDs of the different units, with accuracy indicated by the heatmap color.*

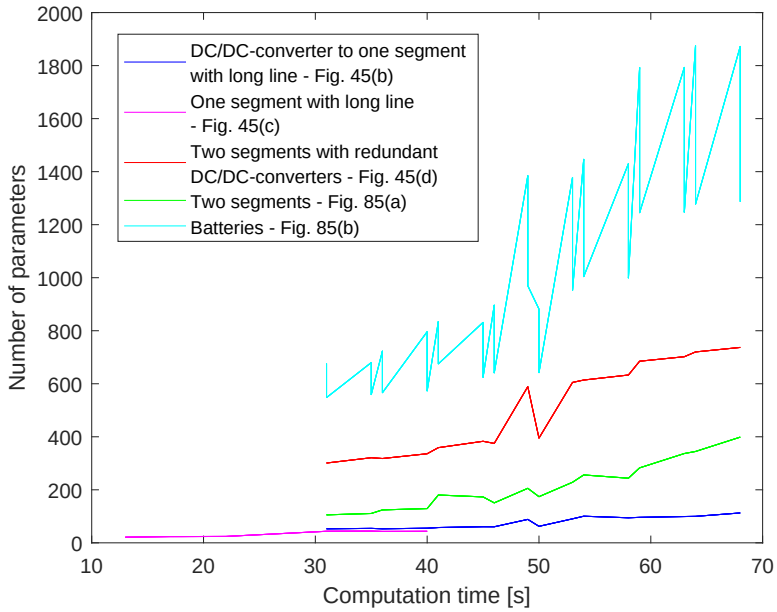

Figure 51: *Simulation times and parameter numbers of all scaled-ship grid simulations*

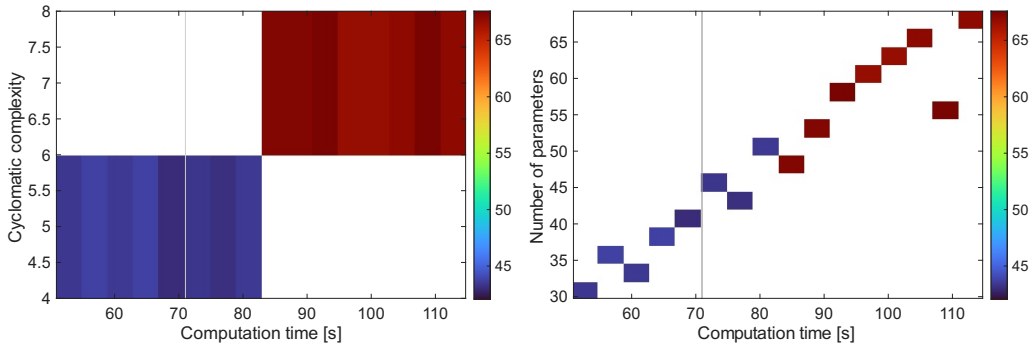

Figure 52: *Accuracy heatmap of (a) cyclomatic complexity and (b) parameter number and computation time of the setup displayed in Fig. 49(b)*

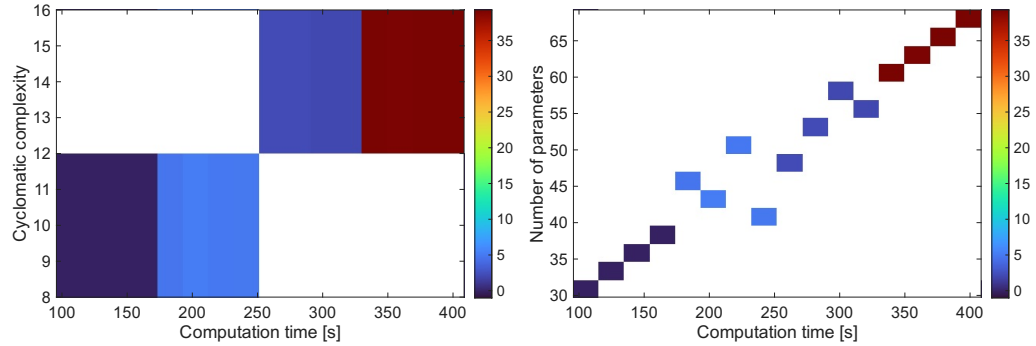

Figure 53: *Accuracy heatmap of (a) cyclomatic complexity and (b) parameter number and computation time of the setup displayed in Fig. 91(a)*

The investigation of the scaled-ship test setup supports the significance of the DC/DC-converter as stated in Chapter 4.3.2. The influence of different components on system accuracy by varying their LoD and parameter counts is systematically analyzed with the test setup, using the developed methodology. The results demonstrate that, for applications in electrical DC grids, components such as DC/DC-converters, fans, and other fluctuating loads have a significant impact on system performance and should therefore be modeled with a comparatively high LoD. In contrast, components like ohmic loads, which have a minimal effect on total system accuracy, can be modeled with a reduced LoD, leading to more efficient simulations. This differentiation in LoD, as implemented by the methodology, ensures that computational resources are efficiently allocated based on the characteristics and criticality of each component. The investigation also revealed that while a higher number of parameters does not always result in increased computation time, it generally raises the LoD and contributes to greater complexity. To achieve a deeper understanding of the accuracy-to-complexity relationship for specific components, investigations such as those described in Chapter 4.2 are invaluable. These

investigations not only verify the methodology but also provide insights for adapting the component model LoD. The structured approach of the methodology aids in the decision, which models to select for high LoD to achieve a sufficient accuracy without unnecessarily increasing the complexity.

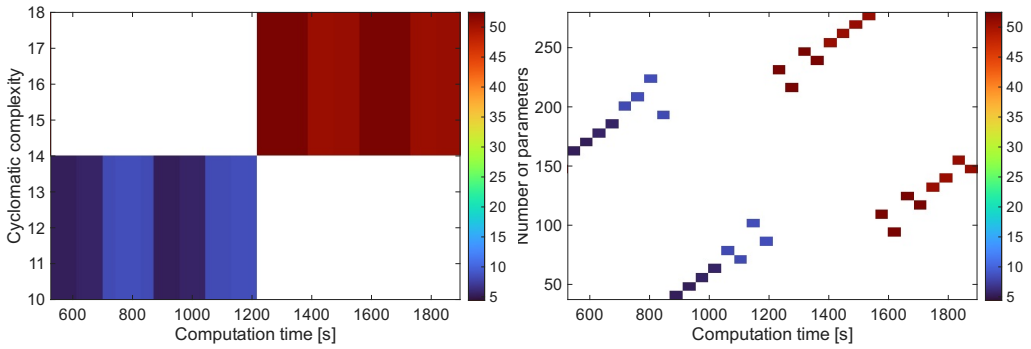

Figure 54: *Accuracy heatmap of (a) cyclomatic complexity and (b) parameter number and computation time of the setup displayed in Fig. 91(b)*

5.1.2 Mechatronic Use Case

The presented methodology is primarily designed for electrical grid simulation, but its potential application to other domains is also of interest. Beyond electrical systems, mechanical systems can be represented as lumped models of concentrated electrical elements through analogies [198], as illustrated in Tab. 14. In the force-voltage analogy, force F_{mech} is represented as a potential difference analogous to voltage V_{elec} in electrical systems, and velocity $\dot{x}$ is represented as a flow analogous to current I_{elec}. In the force-current analogy, force F_{mech} is represented as a flow analogous to current I_{elec}, and velocity $\dot{x}$ corresponding to potential difference is analogous to voltage V_{elec}.

To evaluate the applicability of the methodology to mechatronic systems, a case study of the vibrotactile haptic actuator *Grewus* EXS2608 (Grewus GmbH, Germany), shown in Fig. 55, is conducted. Vibrotactile actuators are essential for delivering haptic feedback in various applications, such as gaming consoles. Actuator performance is measured in two distinct configurations: an unloaded (idle) state and a loaded (blocked) state [198]. The idle state measurement determines the maximum acceleration with minimal force output, while the blocked state measurement determines the maximum force the actuator can generate. The actuator's characteristics across the frequency bandwidth are investigated using a discrete sweep from 10 Hz to 1 kHz. In the unloaded configuration, the actuator is suspended to remove its weight and springs are attached to

Table 14: *Analogy between electromechanical models and lump-sum-concentrated electrical elements according to [199]*

Mechanical System	**Unit**	**Electrical System**	**Unit**	
Velocity $\dot{x}$	[m/s]	Voltage V_{elec}	[V]	
Force F_{mech}	[N]	Current I_{elec}	[A]	
Compliance $c_{\text{mech}} = \frac{1}{k}$	[m/N]	Inductance L_{elec}	[F]	
Mass m_{mech}	[kg]	Capacitance C_{elec}	[H]	
Damper/Friction $d_{\text{mech}} = \frac{1}{R}$	[m/Ns]	Conductance R^{-1}	[Ω]	

both sides to neutralize tension in the rope [199]. For this measurement, a *PCB 352C65 acceleration sensor* (PCB Piezotronics, United States of America) [200] is used. In the blocked configuration, the actuator is fixed to a mass within a rigid system to restrict its motion, allowing for force exertion at minimal velocity [199]. This measurement is performed using a *PCB 208C03 force sensor* [201] (PCB Piezotronics, United States of America). For both setups, an *EX682A40 ICP amplifier* [202] (PCB Piezotronics, United States of America) and a *DAQ USB-1608GX-2AO* [203] (Measurement Computing Corp., United States of America) are used for data acquisition.

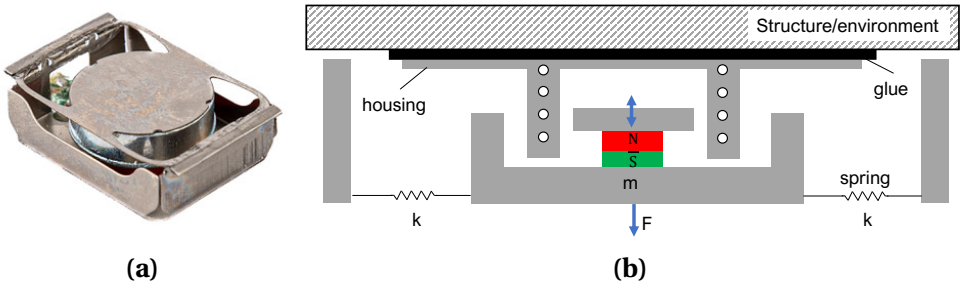

Figure 55: *Linear-Resonant-Actuator (LRA) Grewus EXS2608 (a) photo, (b) actuator design schematic*

A simulation model consisting of eight elements, as shown in Fig. 56, is used to represent the actuator [199]. Specifically, the elements c_{W}, d_{W}, and m_{W} model the environment as a load, while c_{int}, d_{int}, and m_{int} represent the internal mass-spring-damper system of the linear resonant actuator. Additionally, d_{M} and c_{M} capture the internal compliance and damping. The model is systematically reduced step by step by removing the least relevant elements to create simplified models, that are depicted in Fig. 57. The eight-element model is subsequently parameterized in two distinct ways: in the physics-informed variant, all components are designed according to realistic values of the

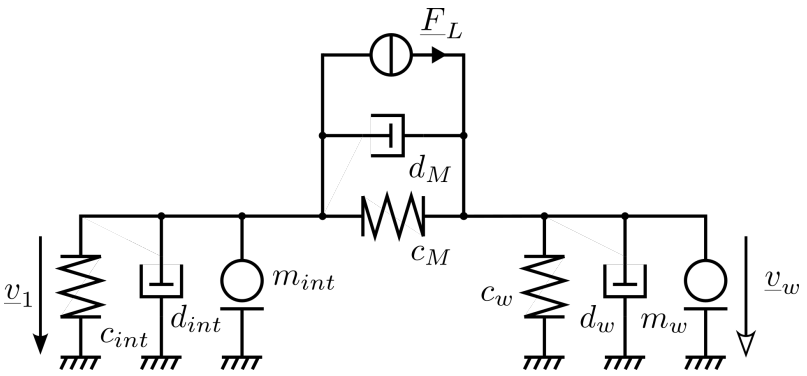

Figure 56: *Model of the LRA Grewus EXS2608 with eight elements according to [199]*

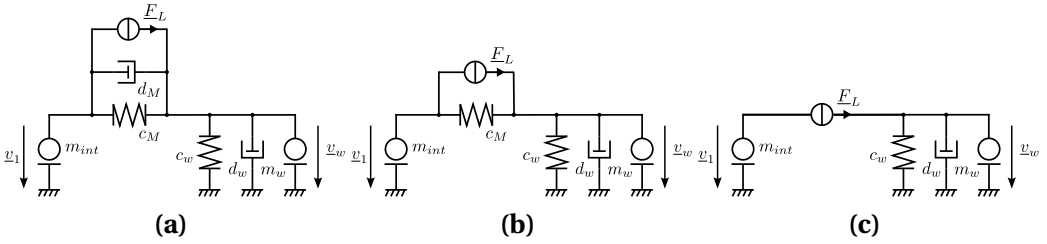

Figure 57: *Model of the LRA Grewus EXS2608 with (a) six elements, (b) five elements, and (c) four elements*

respective individual components of the actuator, while the free-optimum variant freely fitted all nine parameters to the data.

Fig. 58 shows the measurement data from the *Grewus* EXS2608 in comparison to the simulations, both acceleration measurements in idle operation and force measurements in blocked operation are shown. In idle operation, the physics-informed optimized models with eight, six, and five elements perform relatively well compared to the measurement data. However, none of these models can accurately capture the behavior between 610 and 900 Hz. The four-element physics-informed model performs poorly at both lower and higher frequencies but aligns reasonably well with the measurement data in the medium frequency range. The free-optimum model with eight elements achieves a better fit in the 610 to 730 Hz range and performs well at lower frequencies. However, it fails to reproduce the second peak at higher frequencies, though it is still more accurate than the eight-element physics-informed model. The six-element free-optimum model performs similarly to its physics-informed counterpart, but free-optimum models with fewer than six elements deviate significantly from the measurement data.

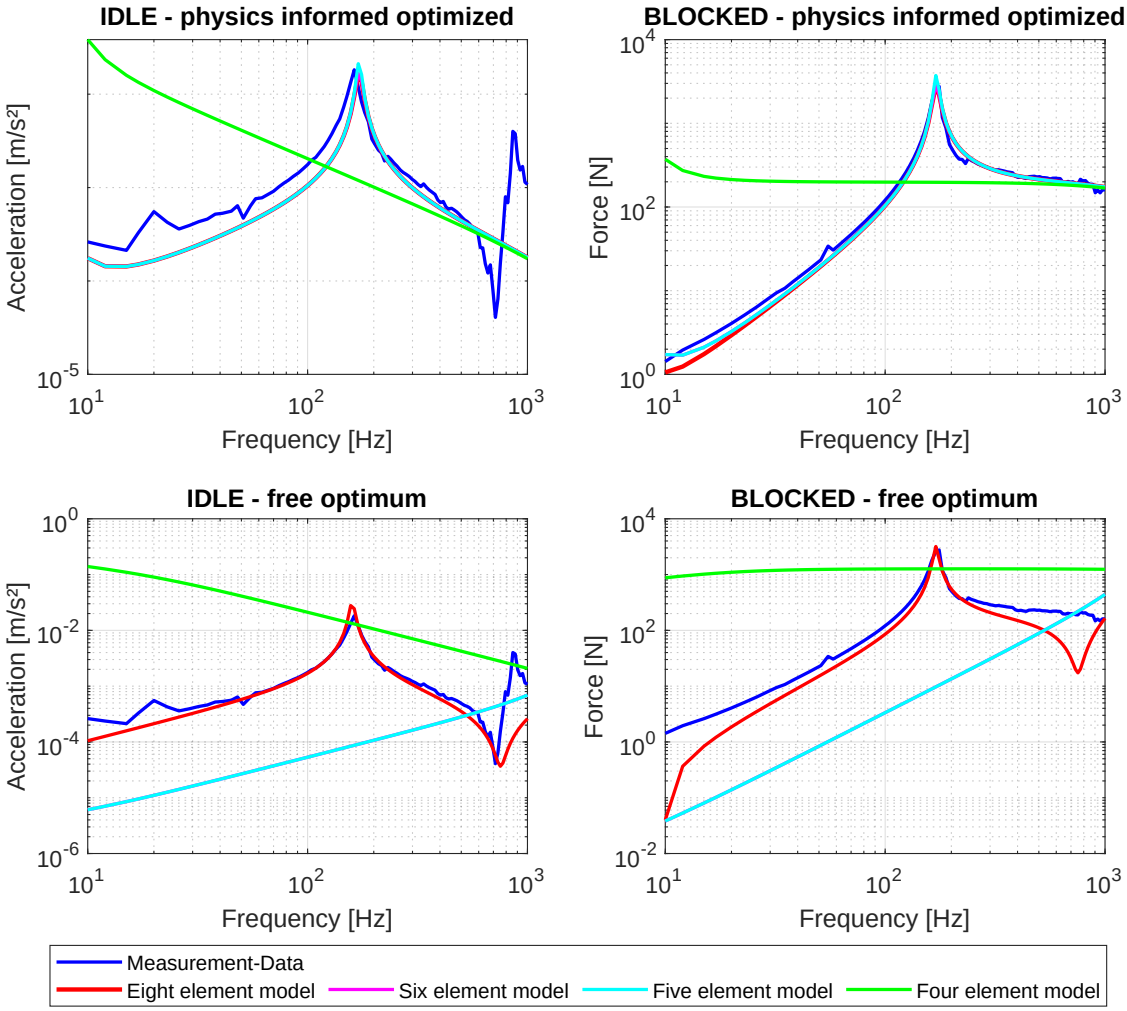

Figure 58: *Measurement data of the LRA Grewus EXS2608 and simulation results of 9, 6, 5 and 4 element models in a physics-informed and free-optimum variant*

A similar pattern is observed in blocked operation. Only the eight-element physics-informed model performs well across all frequencies. In contrast, the eight-element free-optimum model performs worse in this scenario, exhibiting behavior at higher frequencies that is not reflected in the measurement data. Likewise, the five- and four-element free-optimum models show significant deviations from the measurement data, while the four-element physics-informed model provides a reasonable accuracy at higher frequencies at least.

Absolute differences provide a clearer comparison of model performance and are shown in Fig. 59 and Fig. 60. The resulting data of the simulation of the different models is analyzed using the MAPE as described in Chapter 2.3.5 and shown in Fig. 59 and 60. However, a modified uncertainty interval as shown in Appendix I is used, as different measurement devices are utilized than for the electrical measurements. For both the

acceleration measurement and the force measurement, the uncertainty is taken into account in a point-wise manner. The absolute differences and the resulting MAPE in Fig. 59 reveal that the four-element free-optimum model performs particularly poorly, with a MAPE of approximately 7000 % at the 715 Hz peak and only a narrow frequency range where the MAPE falls below 100 %. The free-optimum models, as well as the four- and five-element physics-informed models, also exhibit significant issues at the 715 Hz peak, with MAPEs ranging from 539 % to 578 %. In contrast, all other models perform better, with many results falling within the measurement accuracy.

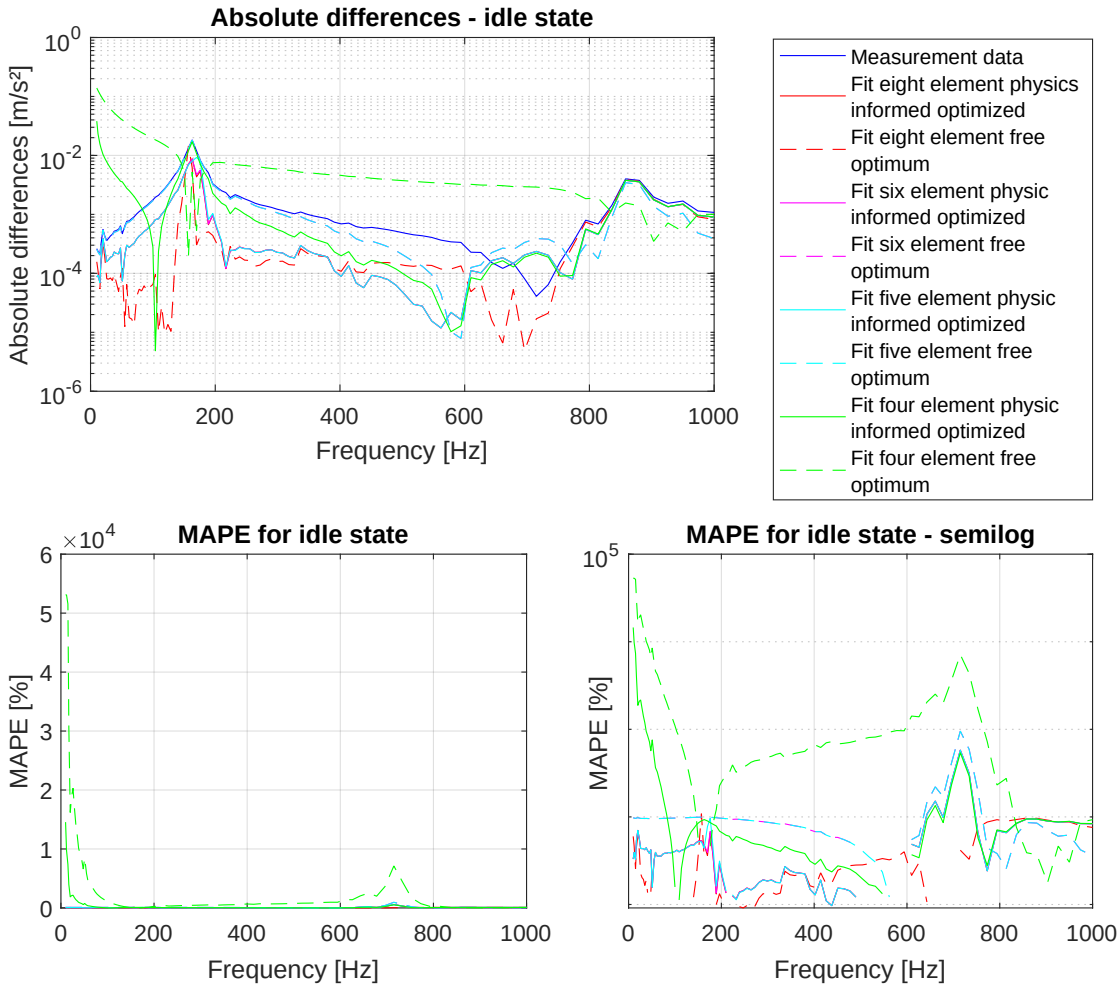

Figure 59: *Difference between measurement data of the LRA Grewus EXS2608 and 9, 6, 5 and 4 element models in a physics-informed and free-optimum variant in idle mode. For better context, the measurement data is included for direct comparison, even though it does not represent a difference.*

In blocked operation, shown in Fig. 60, the absolute differences and resulting MAPE again highlight the poor performance of the four-element free-optimum model, which reaches a MAPE of approximately 530 % at medium frequencies and only achieves a

MAPE below 100 % in a limited frequency range. The free-optimum models and the four-element physics-informed model show MAPEs between 43 % and 180 %. However, all other models perform significantly better, with a peak MAPE of only 43 % at a specific frequency and generally much lower values across the frequency range.

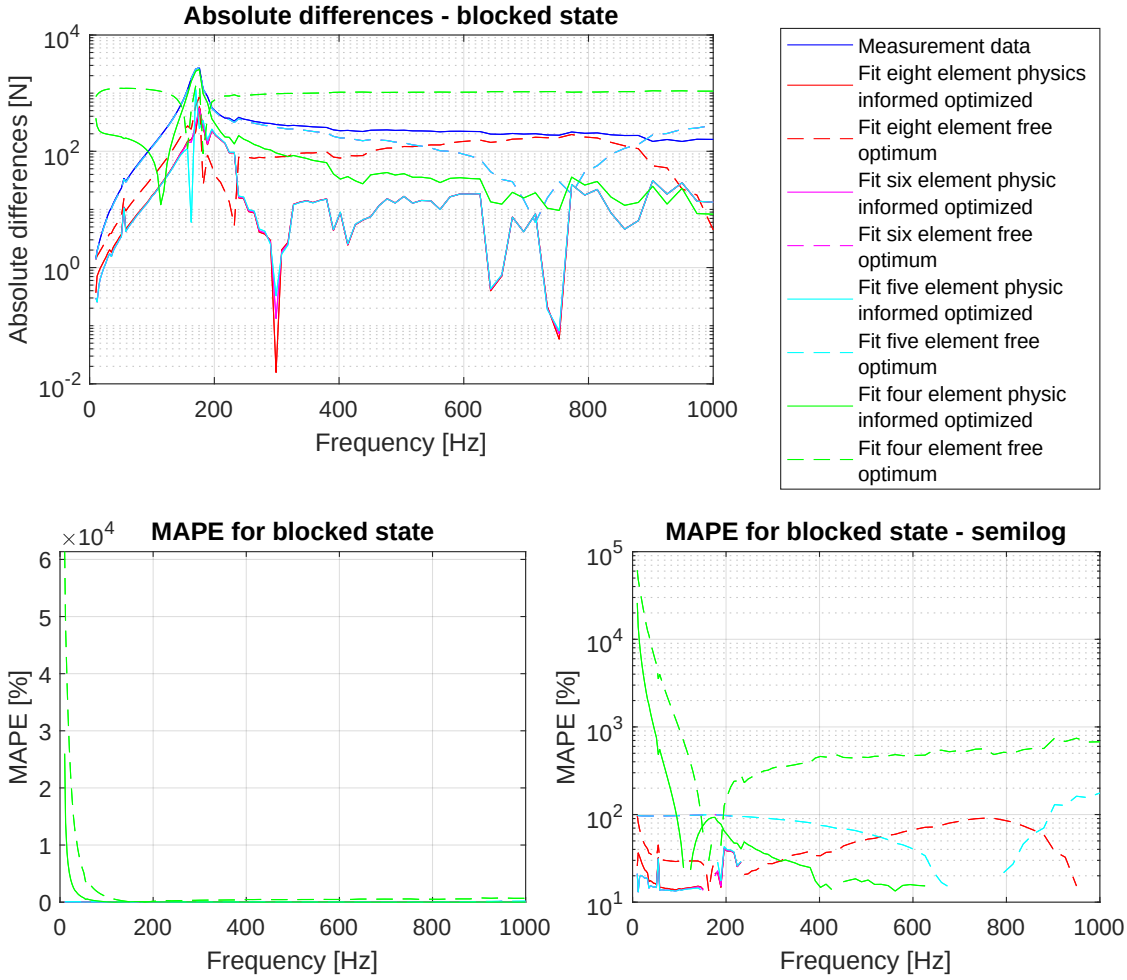

Figure 60: *Difference between measurement data of the LRA Grewus EXS2608 and 9, 6, 5 and 4 element models in a physics-informed and free-optimum variant in blocked mode. For better context, the measurement data is included to provide a direct comparison even though it is not a difference.*

It is noteworthy, that the physics-informed parameterization maintains stability and generates valid values even when individual parameters are removed up to and including the five-element variant as shown in Fig. 61. In contrast, the free-optimum variant shows a considerable loss of accuracy in the five-element variant. The four-element free-optimum variant generates insufficient usable data. The free optimum variant demonstrates better performance in blocked operation, while the physics-optimized variants exhibit better performance in idle operation.

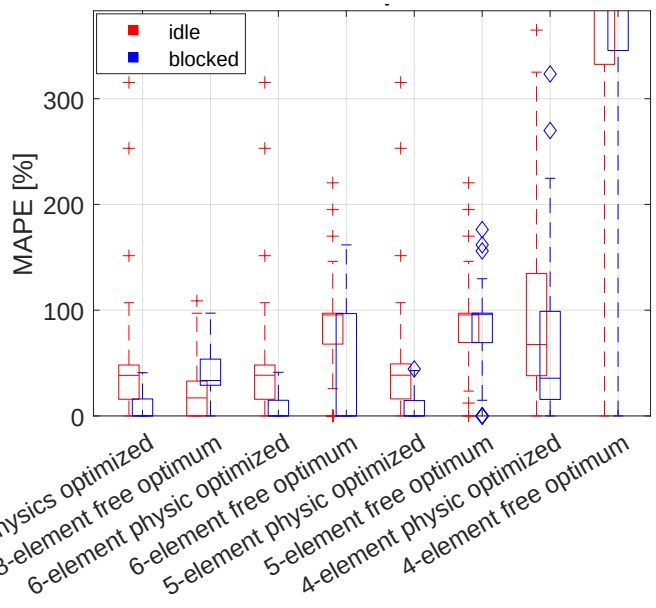

Figure 61: *MAPE of different models of the LRA Grewus EXS2608, showing larger MAPE for free optimum variants*

Analogous to electrical simulations, the complexity of mechatronic simulation models can be quantified and put into relation with their respective simulation accuracy when compared to measurement data. Fig. 62 illustrates this relationship, that can serve as an input for optimizing a cost function similar to the one described in Chapter 4.4. However, the presented cost function is not applied to the specific mechatronic use case. For haptic actuators, single simulations of individual components are sufficient for most applications, making extended simulation models with multiple components unnecessary. Furthermore, due to the small number of parameters involved, the development, simulation, and analysis of such models can be completed efficiently within a short time frame.

This analysis shows, that the relation between complexity and accuracy is applicable beyond the domain of electrical grids and can support decision-making for various types of models. In the case of mechatronic component models based on the electrical-mechanical analogy, the inclusion of parasitic elements generally improves accuracy. To minimize the number of parameters, a free-optimum parametrization approach may be more effective than a low-parameter, physics-based alternative, provided it is carefully tuned for the specific application. However, if the model is intended for use across multiple application cases or component operating states, a physics-based model is recommended, as it offers greater robustness and consistency across diverse scenarios.

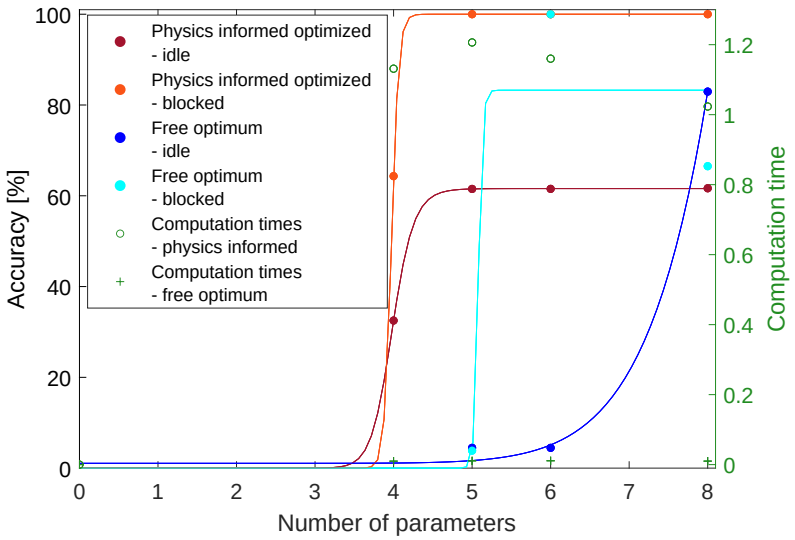

Figure 62: *Accuracy in relation to complexity of different models of the LRA Grewus EXS2608*

5.2 Complexity Optimization in a Ship Grid Simulation

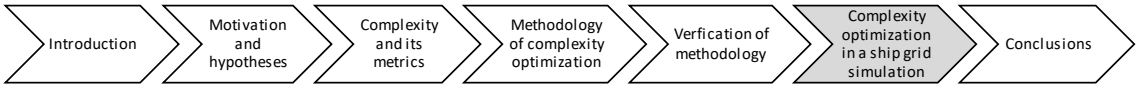

To assess the accuracy of the optimization results, a comparison with real-life data is necessary to evaluate the performance in a realistic scenario. Given that the methodology targets the ship grid development process, an existing ship is used for an exemplary calculation, as most of this ship's cost factors are known.

To validate the methodology, an exemplary calculation of the optimal simulation complexity-to-cost ratio for a DC ship grid is performed. Given the availability of sufficient information, the AIDAbella is selected as the reference ship. The AIDAbella is a medium sized cruise ship with 1025 cabins and five FZs. The two propulsion engines and four thrusters are powered by four diesel generators. Further information about the possible DC setup and the related number of components are provided in Appendix E.1. The values for all cost types required for the cost function are provided in Tab. 15.

All optimization variables are constrained within specific bounds, defined by the real ship scenario as outlined in Appendix E.1. The optimization is performed for each application area, with the results presented in Tab. 16.

The total cost varies depending on the application area, ranging from €0.44 M to €2.21 M, with a total cost of €6.79 M for a complete analysis across all application areas. All results achieve an accuracy higher than the defined minimum accuracy, with an average accuracy of 91.35 %. Notably, higher simulation accuracy does not always

Table 15: *Cost types for the exemplary simulation of the AIDAbella grid*

Type of cost	Value	Data source
Computation cost		
On-demand-prices for computation capacities per hour	€0.125/h	Cost for 16GiB working memory at Amazon EC2 (region: Europe)[204]
Development cost		
Salary per hour	€150	[205]
Risk cost		
Ship building cost	€315 M	according to [206]
Resulting $\frac{RPN}{D_{\max} \cdot \Sigma O_i}$ of FMEA	19.12	Appendix H
Resulting average severity of FMEA	5.75	Appendix H
Savings potential		
Savings potential for material	€1 M	4.4.5
Savings potential for volume	€1.23 M	according to [197]
Savings potential for assembly	€0.3 M	Chapter 4.4.5
Fixed cost		
MATLAB® license	€10,000	assumption for necessary packages [207]

correlate with higher total costs. For instance, the short-circuit analysis achieves the highest accuracy but not the highest cost, whereas the dimensioning of generators and batteries results in the lowest accuracy but relatively high costs. This demonstrates that the optimization effectively balances accuracy and cost, depending on the application area, the respective minimum accuracies, and total simulation durations, while prioritizing cost reduction.

Development and calculation costs are the primary contributors to total costs, emphasizing the importance of reducing computational and structural complexity. Fixed costs remain identical across all application areas, while the savings potential consistently lies within the same range. In most cases, the savings potential significantly reduces the total cost, as it is comparable to the calculation cost. The highest savings potential is observed in the transient stability and short-circuit analyses, highlighting the economic benefits of more accurate simulations. Risk costs, on the other hand, are relatively small across all application areas, ranging from €0.11 M (transient stability analysis and short-circuit analysis) to €0.25 M (dimensioning of generators and batteries). This indicates that risk cost is not the dominant factor in the total cost structure.

Table 16: *Results of optimization for exemplary ship grid development*

Application area	**Total cost** [M€]	**Simulation accuracy** [%]	**Development cost** [M€]	**Calculation cost** [M€]	**Risk cost** [M€]	**Savings potential** [M€]	**Fix cost** [€]
Transient stability analysis	0.65	95.85	1.09	1.76	0.11	2.32	10,000
Dimensioning of generators/batteries	1.66	83.63	0.36	2.80	0.25	1.76	10,000
Short-circuit analysis	2.21	96.63	1.53	2.93	0.11	2.36	10,000
Load flow analysis	0.44	89.38	0.50	1.78	0.17	2.02	10,000
Comparative feasibility study	1.83	91.46	0.84	2.95	0.15	2.12	10,000
Complete analysis	6.79	91.35 (average)	4.32	12.22	0.78	10.58	50,000

In order to analyze the optimization results, it is also necessary to classify the results within the framework of the ship design in order to verify the realism of the results. The total development cost of €4.32 M corresponds to approximately 3,200 person-days at the assumed hourly rate; the transient stability analysis, for example, contributes 481 person-days to this. Within the framework of the four ship design phases, a new cruise ship design with an innovative grid can be estimated at over 10,000 person-days for the entire ship design [41]. The proportion of the total simulation of the electrical grid is therefore realistic within the overall ship design. Taking into account the total construction cost of the example ship AIDAbella of €315 M, the total cost of a simulation across all areas of application of €6.79 M are within a realistic range, especially since they also include the existing risks over the ship's operating life.

To evaluate the benefits of the proposed optimization methodology, a comparison with a simulation that does not utilize this approach is necessary. For the exemplary case of the AIDAbella, assuming a theoretical simulation accuracy of 100 % yields a total simulation cost of €96.8 M - an entirely unrealistic value. In practice, such high costs would necessitate the use of lower simulation accuracies based on expert judgment

to ensure feasibility. To exemplify, in the case of load flow analysis, achieving 100 % accuracy would incur costs of €8.4 M. In contrast, the optimized simulation using the proposed methodology requires only €0.44 M, as the necessary simulation accuracy can be drastically reduced without compromising the results. For simulations across all application areas, the theoretical cost of €96.8 M for maximum accuracy is reduced to just €6.79 M when applying the optimized methodology. This demonstrates the substantial cost savings achieved by adapting simulation accuracy to practical and necessary levels rather than striving for an impractical 100 % accuracy.

Fig. 63 illustrates the accuracy-parameter relationship for all component types and the resulting cost-optimal simulation accuracies for each component in a load flow analysis. For the battery model, a high number of parameters is selected, whereas the optimization results for HVAC and cabin models indicate a medium number of parameters relative to the maximum possible number as defined in Chapter 4.2. These models achieve sufficient accuracy with fewer parameters. In contrast, the optimization results for frequency converters and DC/DC-converters approach the maximum defined number of parameters for their respective components.

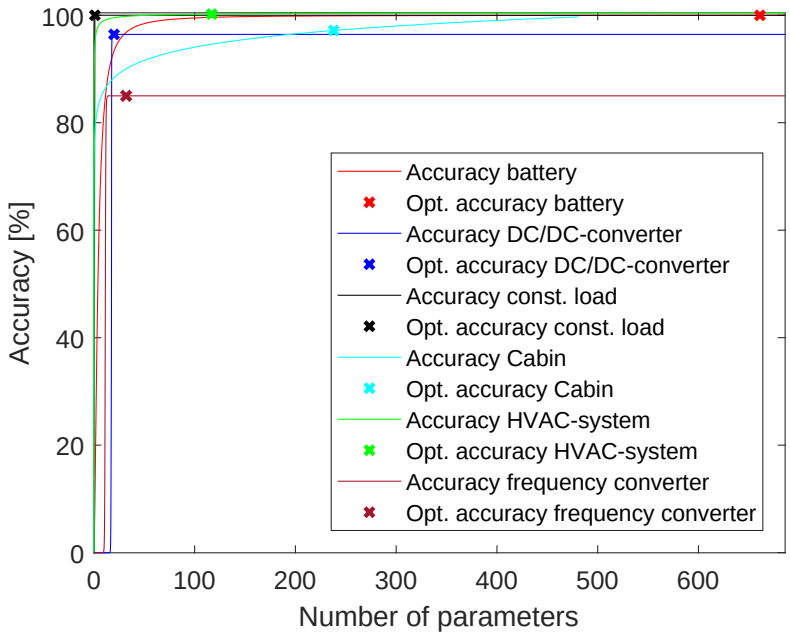

Figure 63: *Accuracies resulting from the optimization of the cost function for the application area of load flow analysis*

The exemplary optimization of the grid design for the AIDAbella demonstrates that the costs for a comprehensive simulation across all application areas can be significantly reduced compared to a maximum-accuracy simulation, which is associated with prohibitively high costs. The traditional approach of relying on subjective expert judgment to determine the simulation complexity cannot consistently identify the optimal LoD

and model complexity required for a simulation. By structuring the modeling process using the proposed methodology, it is possible to achieve substantially lower simulation costs while maintaining associated risks at an acceptable level.

5.3 Method Analysis

To evaluate the developed methodology, a sensitivity analysis and a Pareto analysis are conducted. The aim is to identify potentially critical parameters for optimization that may lead to greater uncertainties and less robust solutions.

Additionally, the Pareto fronts for the various application cases are calculated to visualize the possibilities within the entire solution space. This also helps to identify the point at which costs increase sharply without yielding significant improvements in accuracy.

Sensitivity Analysis To ensure that no single parameter is critical for the optimization, a Monte-Carlo sensitivity analysis is performed for all optimization variables. Latin hypercube sampling is employed to distribute parameter variations as evenly as possible, enabling coverage of the parameter space with fewer calculations, as detailed in Appendix C. For this analysis, a total of 140 calculations were performed, derived from 10 samples per parameter across 14 optimization variables. All parameters are varied within their reasonable limits for the selected example ship to analyze their impact on the total costs.

The results of the sensitivity analysis are shown in Fig. 64. It is evident that no single optimization variable has a dominant influence on the total costs; instead, a multivariate dependency is observed. This analysis demonstrates that the cost function of the developed methodology is robust against changes in individual parameters, with significant cost differences arising only from the combination of multiple system parameters. The subsequent Pareto analysis further illustrates the optimal trade-offs between accuracy, cost, and complexity.

Following the sensitivity analysis, the correlation between total costs and individual optimization variables is examined, as shown in Fig. 65. The number of parameters of the battery model, the number of batteries, and the number of parameters of the cabin model exhibit a higher influence compared to other variables. Most parameters exhibit a minor influence on total costs. The number of cabins simulated, the number of fuel cells, and the number of parameters of the constant loads, however, show a slight negative correlation, indicating compensatory effects within the system.

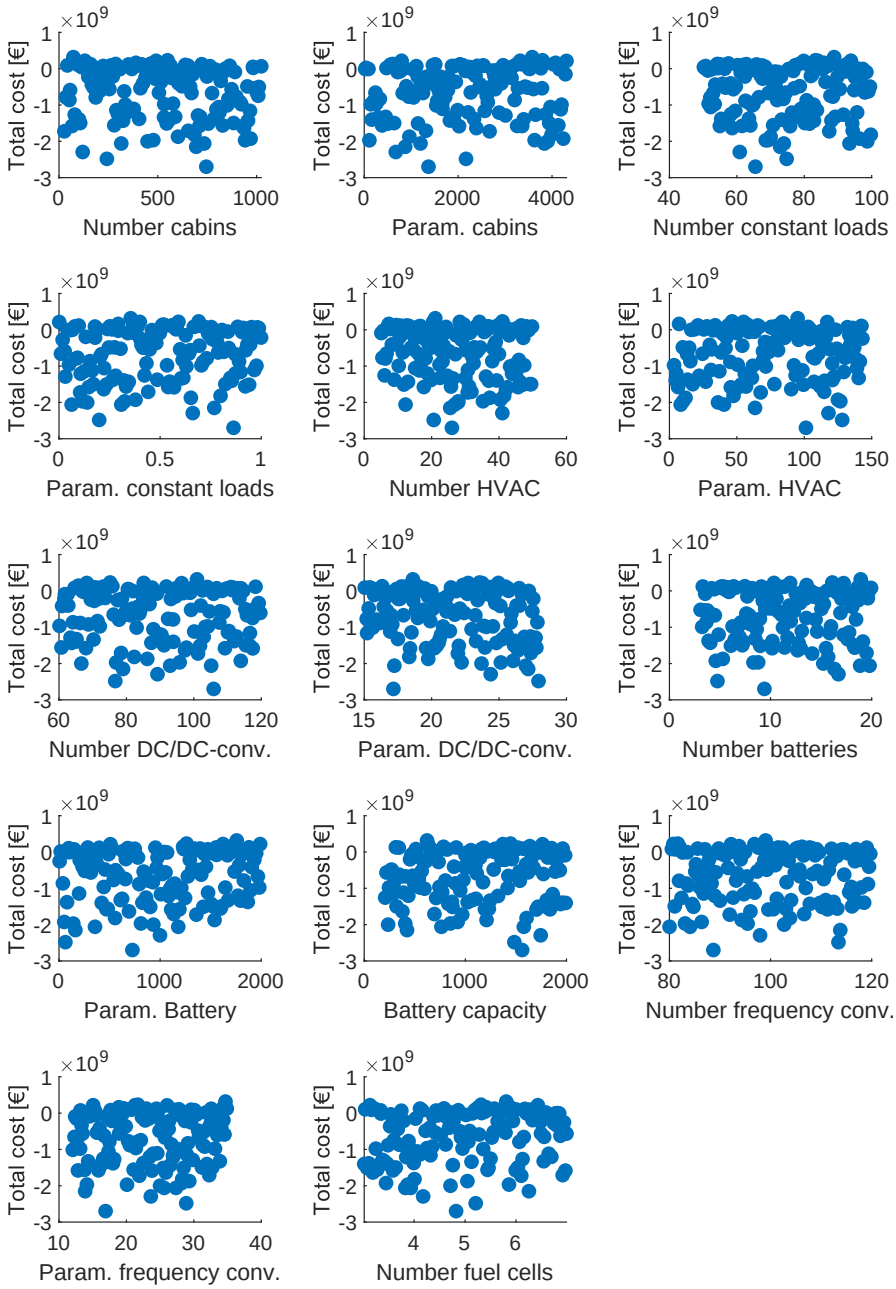

Figure 64: *Sensitivity analysis of the optimization variables of the cost function*

Pareto Analysis To analyze the optimization of the cost function presented in Chapter 4.4, a Pareto analysis is conducted for each application area. In the Pareto front depicted in Fig. 66, each point represents a solution where neither accuracy nor cost can be improved without compromising the other. As accuracy increases, costs rise, with a sharp increase observed between 97.5 and 98 percent, highlighting the optimally balanced solution near the knee point.

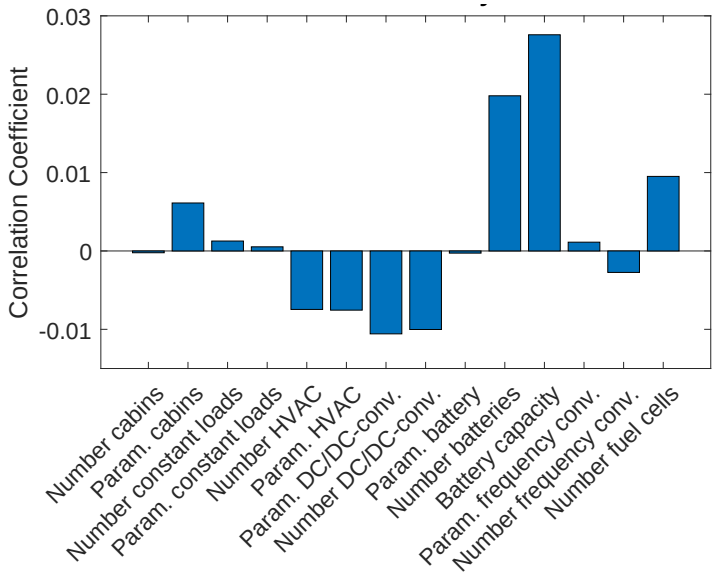

Figure 65: *Correlation analysis of the optimization values of the cost function, derived from 8000 samples per parameter*

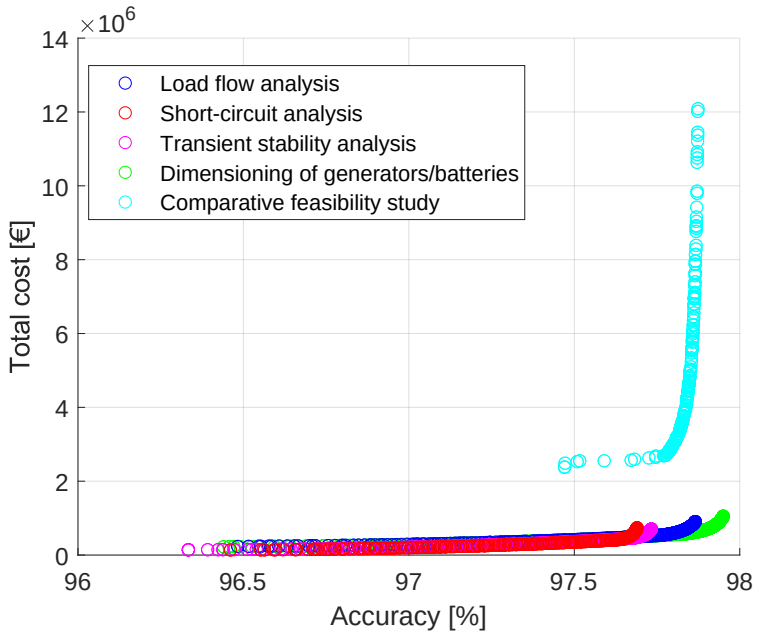

Figure 66: *Pareto fronts of the trade-off between total simulation cost and simulation accuracy for the different application areas, showing a disproportionately higher cost for the higher percentages of accuracy*

The knee point of the Pareto front demonstrates higher levels of accuracy and cost efficiency in comparison to the optimization results presented in Chapter 5.2, as the optimization is designed to minimize the total cost rather than achieving an optimal balance between accuracy and costs. In order to mitigate risk, it may be reasonable to

use the knee point of the Pareto front. This is because it represents a balanced trade-off between cost and accuracy. Nonetheless, risk costs are already incorporated into the cost function, thereby ensuring that risks are taken into account during the optimization process. However, achieving an accuracy level beyond the knee point is not recommended, as this would result in a disproportionate increase in costs without providing a significant additional benefit in terms of accuracy. The steep rise in costs beyond the knee point highlights the diminishing returns of higher accuracy, making it inefficient and impractical for most applications. In this specific example, even with high risk aversion, an accuracy of 97.7 percent across all use cases should not be exceeded, as it is associated with a sharp rise in costs. The cost-optimal simulation accuracy is significantly lower and is already achieved at 96.63 percent for the application area with the highest requirements. This shows that using the developed method, comprising the optimization of the cost function, is instrumental in maintaining low costs and ensuring the efficacy of the simulation.

The methodology can be applied in ship grid design in two distinct ways, either iteratively in each design phase by allocating risk costs accordingly, or as a single, upfront optimization prior to the initial modeling in the concept design phase to determine a global cost-optimal simulation accuracy. Regardless of the chosen approach, the application of the methodology within a given design phase follows a structured process as shown in Fig. 67.

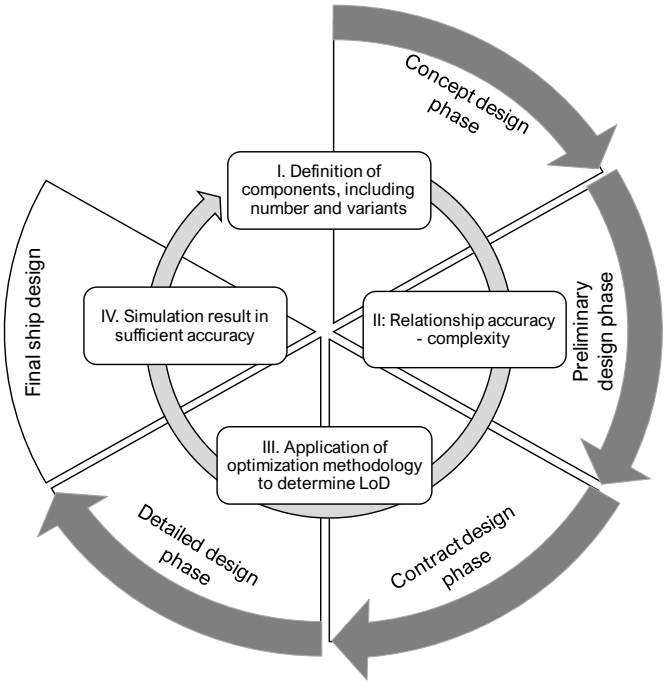

Figure 67: *Methodology embedded in ship (grid) design process. In each design phase the developed methodology is applied.*

First, the system's components are defined, including their quantities and variants. Second, the relationship between accuracy and complexity is established for each component. Third, the optimization methodology is applied to determine the cost-optimal (LoD) for each component model, based on the inputs from the previous steps. Finally, the models are developed to the specified LoD, and the simulation is executed, ensuring sufficient accuracy for the respective application area.

6 Summary and Outlook

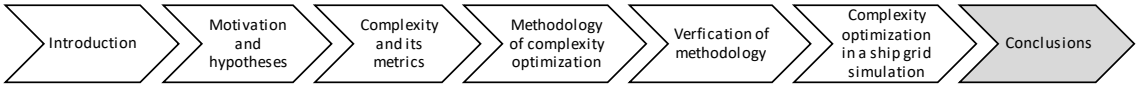

6.1 Summary

In tackling the climate crisis, innovative solutions for energy systems are vital to lower GHG emissions. In the shipping industry, the ship grid design is of importance, since the increased adoption of DC grids and other new grid technologies on ships contributes to the achievement of climate goals by achieving a higher efficiency. The methodology developed supports the United Nations Agenda 2030 goals of climate action (goal 13) and conserving and sustainably using oceans (goal 14) by lowering emissions in ship grids [208]. Simulations are a valuable tool to investigate the appropriate design for ship grids and as these grid options are explored, efficient and accurate models and simulations are necessary. Traditionally, the LoD and accuracy of models and simulations are determined by using expert judgment as no standardized methodology for this process exists. This lack of methodology is an issue across various domains and applications. With growing complexity of new grid solutions, simulation efforts are similarly growing, demanding increased computational resources. Therefore, balancing accuracy and complexity of simulation models becomes more relevant to limit the used resources to a reasonable level. A methodology for the a priori optimization of this trade-off was developed and presented, addressing the need for systematic and efficient simulation strategies.

This work addresses the identified gap in the simulation-based grid design process by the introduction of a methodology to balance the simulation and model accuracy and complexity. This standardized approach reduces reliance on subjective expert judgment and ensures appropriate accuracy while minimizing required resources.

The developed methodology is based on the measurability of complexity for simulations and thus introduces metrics for both structural and computational complexity in

Chapter 3. This is essential to not only address the computational characteristics but also the understandability for humans to analyze, adapt and maintain the models. The methodology further requires established relations between accuracy and complexity for the used components, e.g., energy components as presented in Chapter 4.2. A cost function is then employed to account for all relevant cost factors in the development and usage of a simulation in ship grid design as discussed in Chapter 4.4, including potential risks occurring due to insufficient simulation accuracy. By minimizing this cost function, the optimal cost and the corresponding complexity of the simulation and models of the distinct components are identified. Applying this methodology reduces computational effort, development effort, and maintenance efforts for the models, while the reusability is improved. This is achieved while maintaining the quality of results and without increasing risk cost beyond the levels already accounted for in the optimization, since the cost function explicitly includes risk cost and allows for a deliberate acceptance of certain risks in the minimization of overall costs. Consequently, a higher efficiency in the simulation and grid design process can be achieved that results in higher understandability of simulation models and a reduced complexity.

The established methodology is grounded in the analysis of the model's relationship between LoD and accuracy. The investigation revealed that for components like DC/DC-converters, achieving sufficient accuracy requires precise modeling of parasitic elements, such as the on-resistances of diodes and MOSFETs. For batteries , table-based models were found to be superior to polynomial approaches in terms of accuracy, computational speed, and intuitive understanding. Linearization is feasible in some cases, if only a certain part of the characteristic curve is necessary because neither low nor high State of Charges (SOCs) are used. The analysis of frequency converters shows the importance of matching the LoD of the inverter and the machine to prevent simulation artifacts. Furthermore, it was noted that the modeling of fluctuating loads and HVAC systems is highly dependent on user behavior, necessitating the development of generic usage profiles for broader applicability and investigation of possibilities of influencing the usage. Building on these component-level insights, two crucial system-level strategies are emphasized, modularization and the identification of critical components. Partitioning the system at points of low interaction proved to be an effective way to manage complexity. The identification of critical components, based on their impact on power, safety, stability, and frequency of occurrence, allows for a targeted application of high LoD models where they are most needed. The integration of bidirectional components, such as energy storage, was also identified as an important factor that can enhance system stability and potentially lower the required simulation resolution. All these factors converge in the cost function, the key of the methodology. This function integrates the costs of engineering work, computational resources, and the quantifiable risks associated with insufficient simulation accuracy. The effectiveness of the optimization is highly dependent on the quality of these inputs, supporting the need for

meticulous risk assessment, ideally informed by a thorough FMEA and a broad data basis. For domains like shipping, emerging cost reduction potentials, such as the revenue gained from saved space, can be quantified and integrated directly. The methodology presented provides a structured, data-driven approach to modeling and simulation beyond traditional expert judgment and enables a systematic integration of the component analysis into an optimization framework. However, to align the methodology with other domains, modifications may be required.

An exemplary optimization of the cost of the simulation process is carried out and discussed in Chapter 5.2 and a significant reduction of 93 % in total cost by reducing the accuracy for the less critical components and simulating only the most critical components with a high accuracy is demonstrated. A scaled-ship test setup is investigated in Chapter 5.1.1 to analyze the effects of the LoD of different component types, leading to a similar outcome in critical components as the optimization. Additionally, the methodology is applied to a mechatronic actuator in Chapter 5.1.2 to assess the applicability to other systems. For the electrical representation of this mechatronic actuator, the applicability of the methodology is shown, confirming its potential for use in other systems.

The methodology is specifically applicable for maritime grid design, since this use case, components and data are primarily analyzed. Additionally, the stepwise addition of further parameters is helpful in achieving different levels of complexity. For other domains, specific risk cost and other costs may differ, and the data for the relation between complexity and accuracy of components requires further investigation. When applying the methodology to other domains, different time constants or frequencies may be of interest and certain non-linearities may be apparent, that are not obvious elements within an electrical representation. It is required that the electrical representation is valid in all necessary operation modes to ensure reliability. However, for smaller systems, the application of the methodology may not always be practical since the optimization process and data acquisition require time and effort. In these cases, the simpler expert judgment approach may be more suitable.

Hypotheses The hypotheses formulated at the beginning of this thesis are validated as follows: First, it was demonstrated that simulation models of electrical DC systems can be modeled with varying degrees of complexity, resulting in different levels of accuracy. This was proven through measurements of seven types of physical components and their comparison to different simulation models, as detailed in Chapter 4.2. The analysis is based on the objective quantification of complexity by using the metrics number of parameters, cyclomatic complexity, and computation time, as discussed in Chapter 3. Second, a methodological approach to achieve minimal simulation costs

while maintaining sufficient accuracy was developed, that is based on the relation between accuracy and the complexity of models and simulations, as well as a cost function including all needed resources for the simulation. Third, it was shown, that shipboard DC grid simulations can be optimized to ensure minimum total cost to the owner while maintaining sufficient accuracy. The optimization methodology was applied to a maritime use case, demonstrating its practical relevance. A Pareto front was identified for each application area for this use case, illustrating the trade-off between accuracy and complexity and showing that accuracies beyond 97.7 % come with a disproportionate increase in costs for this use case. A 93 % reduction in simulation cost is achieved for the maritime use case when compared to the theoretical cost of a 100 % accurate simulation. Finally, the methodology developed is not limited to maritime DC grids, but can also be extended to other domains, as demonstrated by the application for a mechatronic use case in Chapter 5.1.2. This emphasizes the versatility of the methodology and its potential for broader use in systems that can be represented as electrical circuits.

Generally, the presented approach is scalable and has the potential to reduce the energy and resource usage of the simulation itself and keep simulations manageable despite slowing progress of miniaturization in chip transistors. Optimized energy system setups can be identified more quickly and flexible. Additionally, alternative simplification strategies, such as selecting hierarchy levels, could complement the methodology.

6.2 Outlook

While this work has demonstrated the applicability of the proposed method to two domains, further opportunities for future research and application to other domains remain. Land-based (micro-)grids and grids in other transportation modes, such as airplanes and trains, could benefit significantly from the structured approach to modeling, enabling a reduction in simulation and modeling resources. Additionally, domains such as fluid mechanics, structural mechanics, biology, hydrology, and many others should explore the feasibility of the optimization methodology since there are representations of their systems with electrical analogies. This would allow them to leverage the developed methodology or adapt similar methodologies tailored to their specific needs.

Moreover, extending the methodology to systems that cannot be represented electrically has the potential to significantly broaden its applicability. Developing analogous approaches for these domains would open new opportunities for systematic optimization of simulation and modeling processes across a wider range of disciplines. Further enhancement of the optimization through the use of more refined data on the relationship between accuracy and complexity from larger component investigations could enable

finding an even more precise balance between accuracy and complexity. A broader range of components should be analyzed, to investigate the influence of the modeling of electrical connections, controllers, safety elements such as SSCBs, and measurement architecture. Additionally, comparisons between multiple components of the same type should be conducted to improve the data basis. Refinements to the cost and risk analysis, based on real-world data for different ship types, different domains, or systems, could further enhance the optimization. Specifically, analyzing the risk cost associated with insufficient simulation accuracy, the use of actual error data from incidents on ships and in other grids, along with their impact on the respective systems, could provide a more exact risk cost assessment. Applying the methodology to real-world ship grid developments would allow a direct comparison of the results from grids developed using the presented methodology and the optimized models and simulations, with those developed using the traditional process and relying on expert judgment. Extending this comparison to other types of ship and grids could further validate the methodology and emphasize its potential for a wider adoption across applications and domains.

On the way to the integration of the developed methodology into the design process in the industry, there are several approaches to be considered. The least resistance path for the end users in e.g. shipyards would entail integration into simulation software solutions, such as *MATLAB*® that could directly offer it as an extension. This would facilitate rapid access and an easy integration into the modeling process, as it would pick up the modelers in the environment where they model anyway. Especially in shipyards, but also in other industries, the integration as an internal company standard could be pushed. Additionally, a standalone tool or a consulting service could be used to bring the methodology and optimization to use, although the access to the modelers would be much more difficult in this case and data availability could be problematic.

From an academic perspective, the methodology could benefit from further research into how adaptability can be increased. The utilization of machine learning could aid in predicting e.g. risk costs. A particularly intriguing research topic would be investigations of how to apply the methodology to multi-domain simulations and their transitions.

In light of the growing demand for sustainable energy systems and their expansion, the developed methodology has the potential to facilitate the development and design of new grid solutions by providing an efficient and cost-effective strategy for modeling and simulation. Integrating further data and applying the methodology to other domains could further enhance the applicability of the methodology and holds promise for a changed approach to the simulation process.

Appendix

List of Figures

List of Tables

A Literature Research

A methodical search of the existing literature was conducted using the keywords within the IEEE database, Web of Science, and Google Scholar. An initial selection of sources was made based on the titles. Subsequently, the summaries/abstracts were utilized for further filtering. The remaining articles were analyzed in their entirety, and their content is evaluated for this work.

Web of Science - Energy related: (TI=(simulation) OR TI=(model) OR TI=(simulating) OR TI=(modeling) OR TI=(modelling)) AND (ALL=(accuracy) OR ALL=(accurate) OR ALL=(uncertainty) OR ALL=(error) OR ALL=(performance) OR ALL=(sensitivity) OR ALL=(effectivess) OR ALL=(efficacy) OR ALL=(impact) OR ALL=(complexity) OR ALL=(complex) OR ALL=(level of detail)) AND (ALL=(aggregation) OR ALL=(simplification) OR ALL=(simplify) OR ALL=(reduction) OR ALL=(reduce) OR ALL=(resolution) OR ALL=(optimization) OR ALL=(optimisation) OR ALL=(optimal) OR ALL=(hierarchical) OR ALL=(hierarchy) OR ALL=(cluster) OR ALL=(trade-off)) AND (ALL=(power) OR ALL=(power system) OR ALL=(energy) OR ALL=(energy system) OR ALL=(electric)) AND (TI=(complexity) OR TI=(complex) OR TI=(level of detail))

https://www.webofscience.com/wos/woscc/summary/540e96f2-ed55-42bb-a6fb-08c6bf2c7a53-0154f23208/relevance/1

IEEE - Energy related: (allintitle:simulation OR allintitle:model OR allintitle:simulating OR allintitle:modeling OR allintitle:modelling) AND (ALL=(accuracy) OR ALL=(accurate) OR ALL=(uncertainty) OR ALL=(error) OR ALL=(performance) OR ALL=(sensitivity) OR ALL=(effectivess) OR ALL=(efficacy) OR ALL=(impact) OR ALL=(complexity) OR ALL=(complex) OR ALL=(level of detail)) AND (ALL=(aggregation) OR ALL=(simplification) OR ALL=(simplify) OR ALL=(reduction) OR ALL=(reduce) OR ALL=(resolution) OR ALL=(optimization) OR ALL=(optimisation) OR ALL=(optimal) OR ALL=(hierarchical) OR ALL=(hierarchy) OR ALL=(cluster) OR ALL=(trade-off)) AND (ALL=(power) OR ALL=(power system) OR ALL=(energy) OR ALL=(energy system) OR ALL=(electric)) AND (TI=(complexity) OR TI=(complex) OR TI=(level of detail))

Web of Science - Complexity in general: (TI=(simulation) OR TI=(model) OR TI=(simulating) OR TI=(modeling) OR TI=(modelling)) AND (ALL=(accuracy) OR ALL=(uncertainty) OR ALL=(error) OR ALL=(complexity) OR ALL=(complex) OR ALL=(level of detail)) AND (TI=(complexity) OR TI=(complex) OR TI=(level of detail))

https://www.webofscience.com/wos/woscc/summary/cdfe5b21-be2d-460a-8951-7ec78c107d7b-0154f46089/relevance/1

IEEE - Complexity in general: (("Document Title":simulation) OR ("Document Title":model) OR ("Document Title":simulating) OR ("Document Title":modeling) OR ("Document Title":modelling)) AND (("Document Title":complexity) OR ("Document Title":complex) OR ("Document Title":level of detail))

Table 17: *Key findings and topics of publications from literature overview in Chapter 2.3.2*

Author	Key findings
Apostolakis [100]	goodness of fit as a probability
Arthur [69]	verification, validation, and confidence levels
Astrup [73]	estimations of prediction error for functions with different complexities
Aumann [5]	simple models have equal prediction output but require less data and validation, lead to fewer errors and are more likely to achieve understanding
Balci [94]	model credibility by verification and validation steps
Bale [209]	energy system models are interrelated, heterogenous elements, no autonomous control over whole system, self-organisation is complex behavior
Banks [51]	sufficient complexity for application needed, but not higher complexity. (Dis)advantages of simulation
Box [59]	all models have errors, some can be useful for a specific application
Brooks [63]	ways for model comparison and their relation: model performance, LoD and further complexity metrics
Choi [92]	methodology to avoid model structure uncertainties
Chwif [64]	computational power allows complex models that have disadvantages in managing etc. complex, detailed models that are imprecise are possible
Courtois [109]	reduction to smaller subsystems, time and space division
Decoursey [87]	classification of models, analysis of algorithm performance and uncertainty sources
Draper [101]	reasons for model uncertainties
Du [75]	holistic complexity measurement
Fishwick [106]	aggregation, trade-off complexity and data sufficiency must be favorable to remain useful
Forster [96]	model selection, performance, trade-off of fit and simplicity

Author	Key findings
Frantz [111]	model abstraction approaches
Golay [82]	definition of classes of complexity, measurement of uncertainty with informational entropy
Henriksen [72]	maximize applicability, correctness, obedience, performance, and usability while keeping cost and complexity low
Ladyman [83]	essential traits of complexity: non-linearity, feedback, robustness and lack of central control, emergence, hierarchy
Law [55]	simulation approach, advantages and disadvantages of simulations
Lochbichler [60]	index to describe model depth for combined models
Maier [84]	granularity can be separated into structural and information granularity
Manson [112]	complexity approaches: deterministic, algorithmic, aggregate
Netter [85]	quantification and adaptation of complexity in terms of flexibility - number and range of parameters and functional form, including accuracy analysis
North [210]	model integration process for reusability
Pidd [74]	modeling principles: as simple as possible, think complicated
Myung [78]	goodness of fit can limit generalizability, more model selection criteria are necessary
Pollok [103]	pareto optimum of computation time and accuracy
Popovics [81]	preliminary estimation of model complexity is advantageous, structural and software complexity measure
Puy [98]	models with higher dimensions come with more uncertainties, analysis of relation between complexity and uncertainty
Rank [107]	appropriate level of complexity is essential, appropriate data necessary, careful abstraction
Rexstad [104]	model simplification by repro-modeling, structured programming, variable aggregation, interdependent parameters, graph theory, and generalizations
Robinson [90]	model requirements, model scope, and simplification methods. The benefits of simplicity outweigh accuracy losses
Robinson [108]	identification of assumptions and simplifications is essential for analysis of suitability, simplification definition, methods, and (dis-) advantages
Salt [66]	simple models are easier to validate and analyze
Sargent [56]	relation model accuracy and cost, verification and validation
Schruben [76]	graph theoretic complexity measurement

Author	Key findings
Schwarz [80]	Bayesian Information Criterion as model complexity measurement
Sevinc [110]	model abstraction definition, motivation, and methods
Shannon [50]	model development, validation, insufficient methodology in modeling
Simon [114]	complex systems are hierarchical, representation is key to achieve simpler systems
Standish [77]	complexity definition, measurement using graph theoretic approach and information theoretical approach
Tolk [88]	engineering simulation management: modeling approach, verification and validation,
Tsioptsias [95]	model acceptance and usefulness do not necessarily concur
Vamvoudakis [113]	characteristics of complex systems
van der Zee [105]	review: model simplification approaches and benefits, drivers of complexity
Vogal [86]	modeling steps, model performance, and LoD/complexity definition
Wallace [79]	measurement of model complexity
Ward [97]	avoid overly complex models, distinction between constructive simplicity and transparency
Webster [65]	determining degree of model complexity
Willemain [54]	model accuracy acceptance should be judges by user or tests
Xu [93]	appropriateness framework
Xu [102]	bias-variance trade-off
Zeigler [146]	partial models are helpful to deal with irreducible complexity of real systems

B Computation Time Distribution

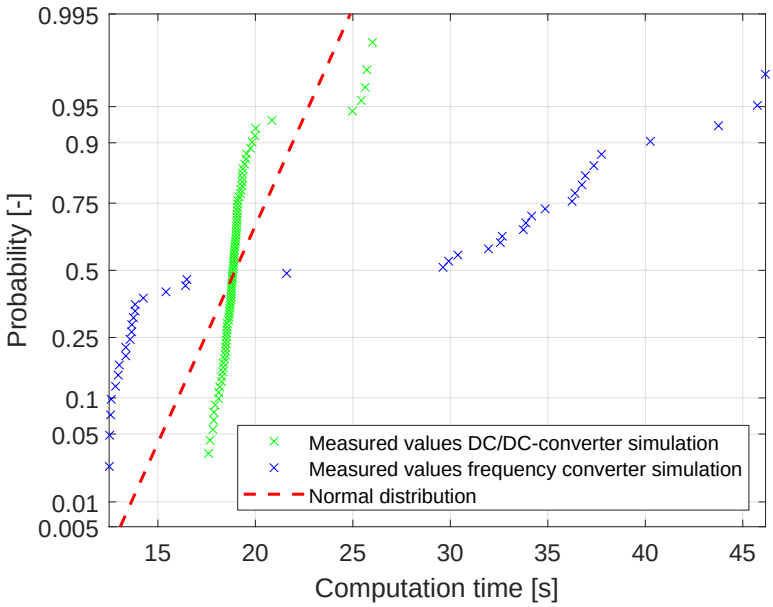

Figure 68: *Normal distribution plot for the measurement results of the computation time for the DC/DC-converter simulations and the frequency converter simulations. The measured values do not follow a normal distribution.*

C Sensitivity Analysis

For the analysis of a simulation model's sensitivity regarding different input parameters or measurement/reference data, the Monte-Carlo method can be utilized. For simulations including many continuous values, it is not feasible to analyze the impact of each input parameter individually. The Monte-Carlo method involves randomly sampling the input parameters within their defined probability distributions and running multiple simulations to observe the effect on the output variables of interest. This method allows statistically sound statements about a wide range of values to be made without the need for explicit calculation of all possible combinations. One way of ensuring comprehensive coverage of the value range is the use of Latin hypercube sampling. To quantify the dependence between input and output variables, the correlation coefficient R is used in this work. In addition, a correlation analysis can be performed to identify the input variables with minor influence on the simulation results. In order to reduce the number of calculations for the correlation analysis, Monte-Carlo methods are also used for this calculation.

D Component Model Complexity

In Appendix D further information for the component analysis presented in Chapter 4.2 is given.

D.1 Curve Fitting

DC/DC-converter:

$$f_{\text{DCDC\_P}} = 96.4350 - \frac{1}{2}\left(\frac{94.2700}{1+\left(0.0582\,N_{\text{ParaDCDC}}\right)^{90.3}} + \frac{98.6000}{1+\left(0.0570\,N_{\text{ParaDCDC}}\right)^{442.3}}\right) \tag{29}$$

$$f_{\text{DCDC\_I}} = 94.2700 + \frac{-0.0660 - 94.2700}{1+(0.0582 * N_{\text{ParaDCDC}})^{90.3000}} \tag{30}$$

Battery:

$$f_{\text{Batt\_P}} = 100.0037 + (4.3290e-15 - 100.0037)/(1+(N_{\text{ParaBatt}}/4.0011)^{1.6418}) \tag{31}$$

$$f_{\text{Batt\_I}} = 105 + (0.5297 - 105)/(1+(N_{\text{ParaBatt}}/15.6865)^{0.6058}) \tag{32}$$

D.2 Battery Models

Table-based Simscape Model The table-based Simscape battery model from the Simscape library maps the non-linear behavior of the battery during the discharging process and uses table values between which linear interpolation takes place. The behavior of the battery is described by the no-load voltage V_0 and the internal resistance R_0. The input variables of the model are the current I and the initial state of charge S_0. The output variables are the voltage at the battery V and the state of charge SOC. The table-based battery model consists of a total of 2000 parameters[6]. The current I is used to calculate the values for V_0 and R_0 and is integrated into the circuit via an adjustable resistor or a voltage source. The respective state of charge SOC is calculated from the current I and the previous state of charge SOC (respectively S_0 for the first step) in order to determine the zero load voltage V_0 and the internal resistance R_0 can then be calculated and integrated as an adjustable resistor and adjustable voltage source.

[6] 1000 values each for V_0 and R_0

Linearized Model To reduce the complexity, a linearized model can be used, that leads to a reduced number of parameters by simplifying the corresponding model equations. In this model, the parameters of the linear equalization lines for the dependencies of the variables V_0 and R_0 are determined from the 2000 parameters of the table-based model. This results in a reduction of the number of parameters for the linear model to four. The accuracy is determined in comparison to the table-based model based on measurement data.

Polynomial-based Model As the linear equalization line represents the simplest case and therefore a model with a high deviation, the polynomial degree is increased for the polynomial-based model in order to reduce the deviation.

The accuracy improves for polynomial degrees four but higher degrees do not lead to significant further improvements in accuracy and have similar computation times. Therefore, only the polynomials with degree four are used for further analysis. These adjustments result in a model parameter count of 8. In the areas of particularly low and high states of charge ($< 20\,\%$ and $> 80\,\%$), there are larger deviations, as shown in Fig. 69. However, these ranges in particular are usually rarely used so as not to damage the batteries.

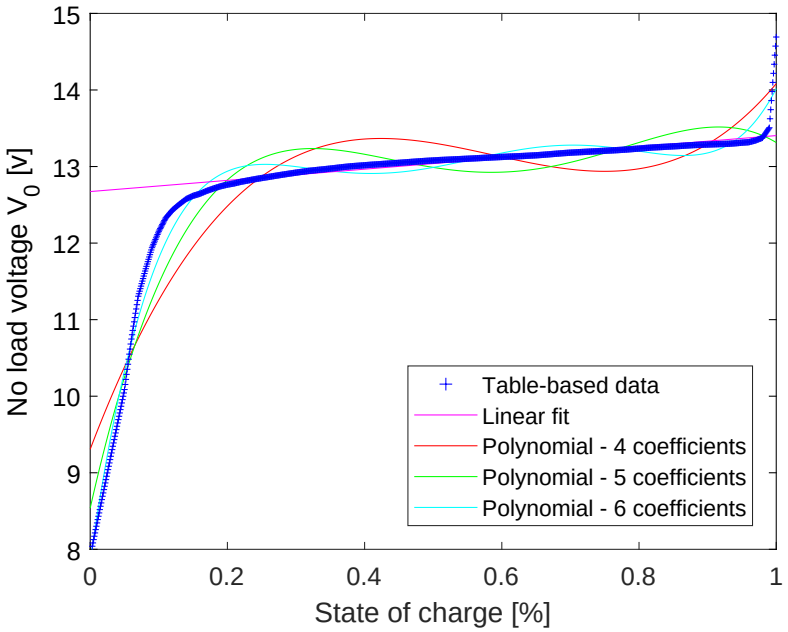

Figure 69: *The polynomials for the no-load voltage V_0 compared with the table values for the battery. In some areas, the deviations between the polynomial and table values are significantly higher than the average*

D.3 Parameters DC/DC-Converter

The PWM frequency f_{PWM} of the controller is set to 100 kHz and the output inductance L is calculated with the desired output voltage V_{out} and the maximum power P of the converter.

$$L = \frac{{V_{\mathrm{out}}}^2}{0.4 * P * f_{\mathrm{PWM}}} \tag{33}$$

Using the input voltage V_{in}, the output voltage V_{out} and the maximum on-time of the transistor $t_{\mathrm{on,max}}$, the number of secondary windings $N2$ is calculated with

$$N2 = N1 * \frac{V_{\mathrm{out}}}{V_{\mathrm{in}}} * \frac{1}{t_{\mathrm{on,max}}} \tag{34}$$

[211, 212]. To ensure full demagnetization of the coil, the maximum duration the transistor can be switched on per one duty cycle $t_{\mathrm{on,max}}$ is set to 0.5 [212].

Table 18: *DC/DC-converter simulation model parameters*

Parameter	**Value**
Input voltage V_{in}	350 V
Output voltage V_{out}	24 V
Power P	480 W
Transistor on-time $t_{\mathrm{on,max}}$	0.5
Controller P_{PID}	2
Controller I_{PID}	200
Controller D_{PID}	0
Controller Frequency f_{PWM}	100 kHz
Input Capacitance C_{in}	150 mF
Output capacitance C_{out}	100 μF
Inductance L	0.045 mH
Primary Windings $N1$	794
Secondary Windings $N2$	109
Magnetization Inductance L_{m}	100 mH
Forward Voltage V_{f}	0.9 V

The additional parameters resulting from the insertion of parasitic components and the activation of further parameters are listed in Tab. 19. It is considerably more challenging to estimate, or even calculate the parasitic parameters of components such as capacitors, inductances, or MOSFETs without data from the converter manufacturer. This is

because these parameters are mostly component specific and often depend on factors such as power density or operating temperature. Consequently, sensible base values are selected and their effect on the input and output quantities over a broad range of values is investigated using a sensitivity analysis. The value range is also mentioned in Tab. 19.

Table 19: *Complex DC/DC-converter simulation model parameters*

Parameter	Value	Value Range
Diode		
On-Resistance $R_{\text{on,diode}}$	10 mΩ	10-100 mΩ
On Inductance $L_{\text{on,diode}}$	5 nH	5-50 nH
Capacitance C_{diode}	10 pF	10-1000 pF
Inductor		
Parallel Capacitance L_{EPC}	50 nF	10-90 nF
Series Resistance L_{DCR}	10 mΩ	10-100 mΩ
Capacitor		
Series Inductance C_{ESL}	1 nH	1-10 nH
Serial Resistance C_{ESR}	1 mΩ	1-20 mΩ
MOSFET		
On-Resistance $R_{\text{on,MOSFET}}$	1 mΩ	1-100 mΩ
On Inductance $L_{\text{on,MOSFET}}$	5 nH	5-100 nH
Drain Source Capacitance C_{ds}	10 pF	10-1000 pF
Drain Gate Capacitance C_{gd}	10 nF	10-1000 pF
Gate Source Capacitance C_{gs}	1 nF	1-3 nF
Transformer		
Winding Resistance R_{winding}	50 mΩ	10-100 mΩ

The results of this investigation are shown in Fig. 70 and 71, and it can be seen that most of the parasitic components have only an extremely small influence on the overall result of the simulation.

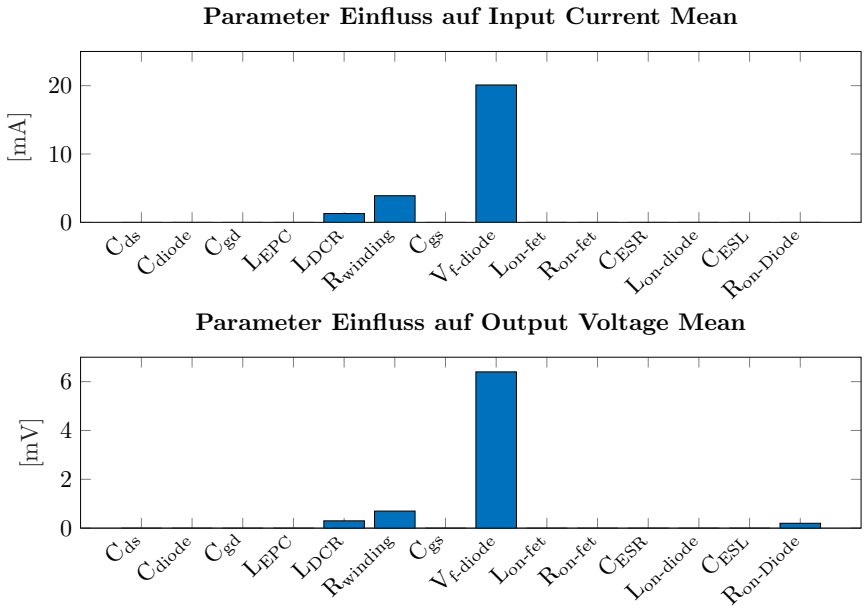

Figure 70: *Influence of the parameters on the mean input current and output voltage of the DC/DC-Converter*

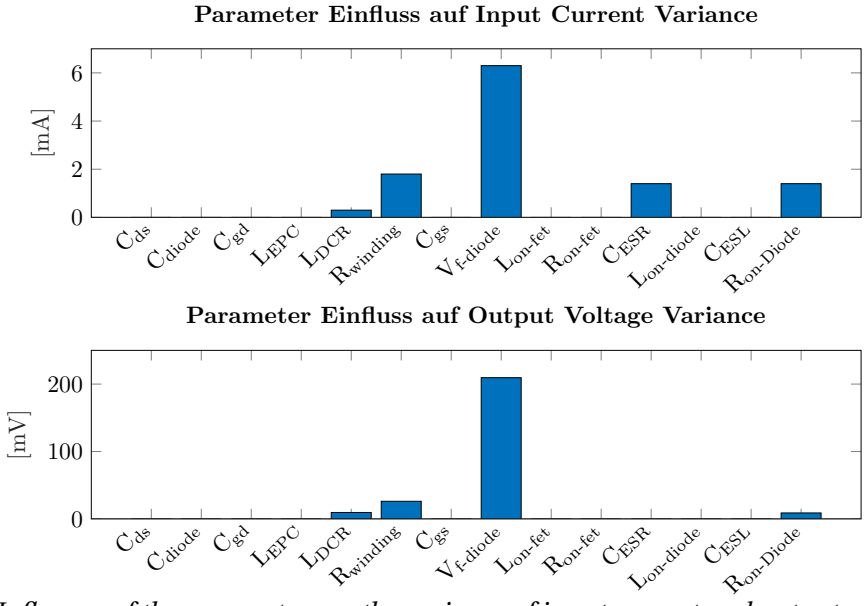

Figure 71: *Influence of the parameters on the variance of input current and output voltage of the DC/DC-converter*

A sensitivity analysis of the DC/DC-converter design parameters is shown in Fig. 72, showing the strong influence of input capacitance C_{in} and inductance L.

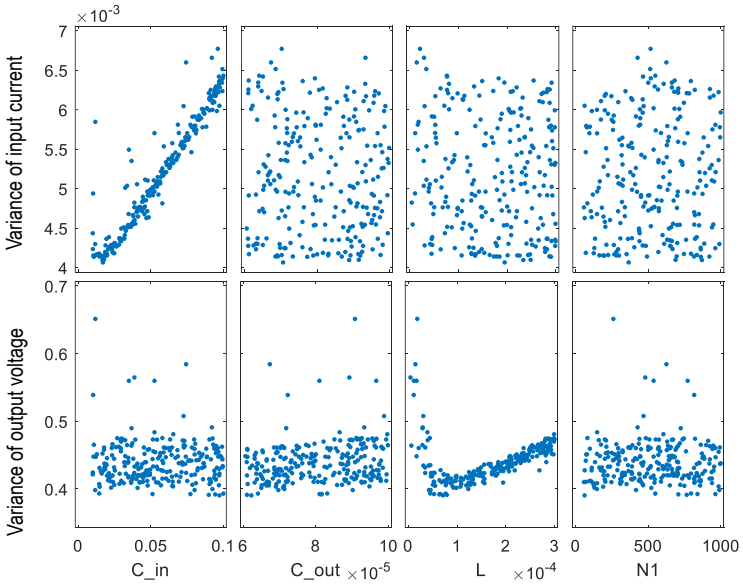

Figure 72: *Sensitivity Analysis of the DC/DC-converter design parameters*

D.4 HVAC Load

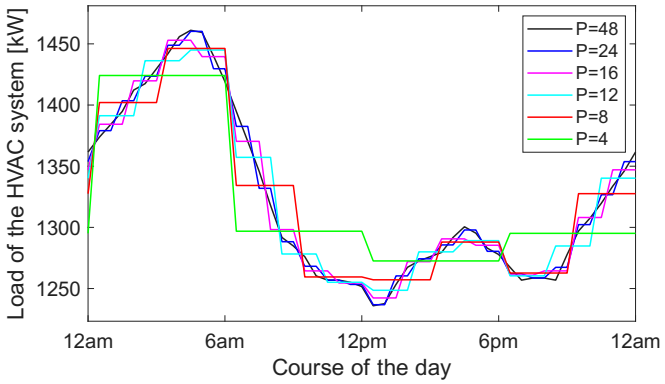

Figure 73: *Load of HVAC system for different number of parameters*

D.5 Cabin Load

The cabin load is based on the use of various electrical devices (lighting, TV, hairdryer, charging of electrical devices such as mobile phones), that is determined based on the presence of passengers. The presence of passengers in the cabins is modeled stochastically using the data from [192] as shown in Fig. 75 and 76.

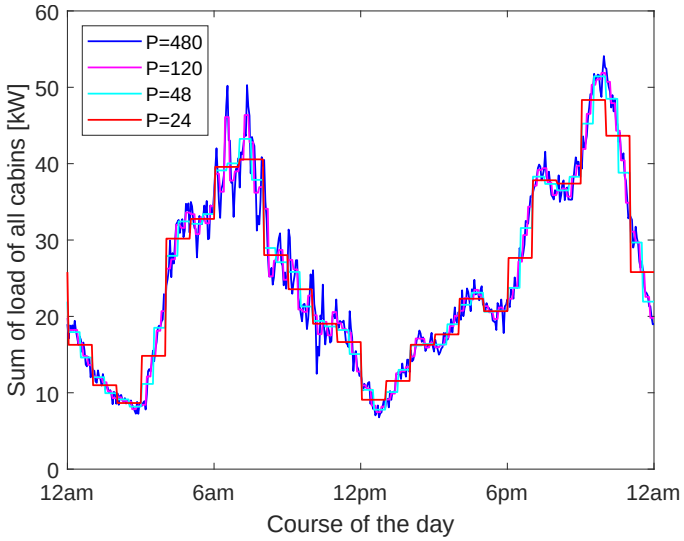

Figure 74: *Sum of load of all cabins for different numbers of parameters of the model*

In order to prevent the generation of excessive noise and the imposition of unrealistically brief periods of cabin occupancy, a minimum resolution of 3 minutes is employed.

To calculate the lighting, it is necessary to distinguish between no lighting, medium lighting (50 W) and full lighting (105 W). For the purpose of charging electrical devices, it is assumed that the majority of overnight charging will be completed within a period of two to three hours, with an average of 5 W per device and two devices per cabin. For the load from televisions, one hour of use per day with an output of 100 W is assumed. Two superimposed normally distributed probability density functions with peaks at 7 p.m. and 9 p.m. are employed. In order to calculate the load caused by the use of the hairdryer, two superimposed normally distributed probability density functions with peaks at 7 a.m. and 10 a.m. are employed in the same manner as for the television. It is assumed that the average usage time is nine minutes at 1200 W.

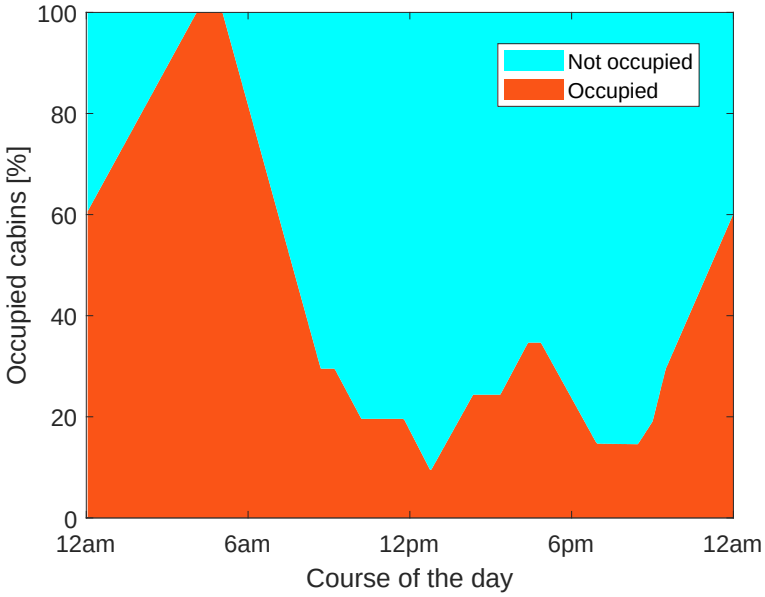

Figure 75: *Occupied cabins over the course of day*

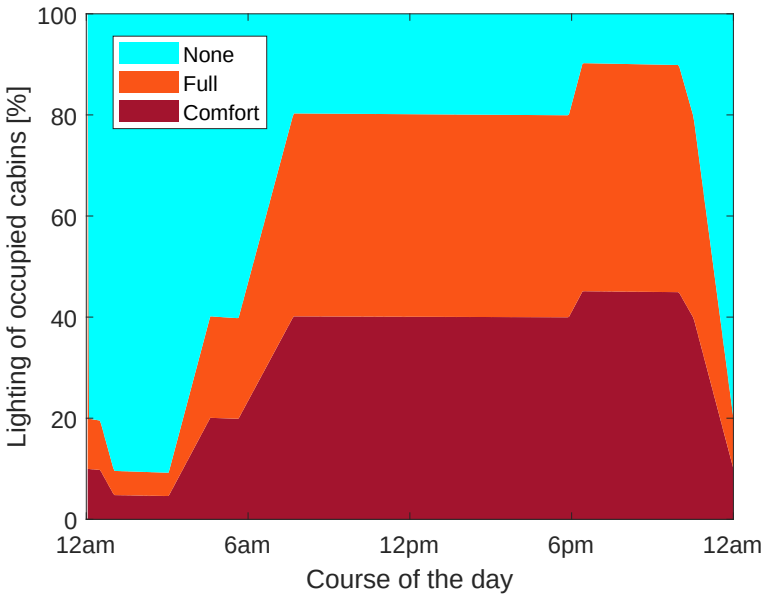

Figure 76: *Lighting in the cabins over the course of day*

D.6 Computation Time Analysis using Kruskal-Wallis

The Chi-squared statistic for the Kruskal-Wallis test of the different Danfoss frequency converter simulations is 31.67 (Fig. 77), indicating a significance level of 99.999 999 385 3 % for the hypothesis that the values in each group originate from distinct populations.

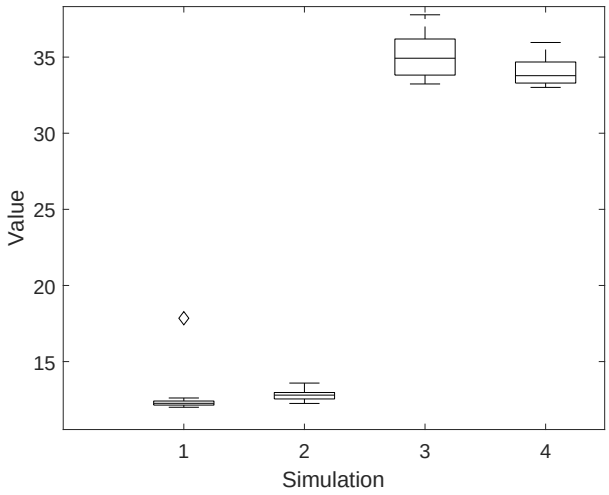

Figure 77: *Kruskal-Wallis analysis of the computation times of the Danfoss frequency converter,* $\chi^2 = 31.67$

The Chi-squared statistic for the Kruskal-Wallis test of the different Siemens frequency converter simulations is 31.45 (Fig. 78), indicating a significance level of 99.999 999 317 7 % for the hypothesis that the values in each group originate from distinct populations.

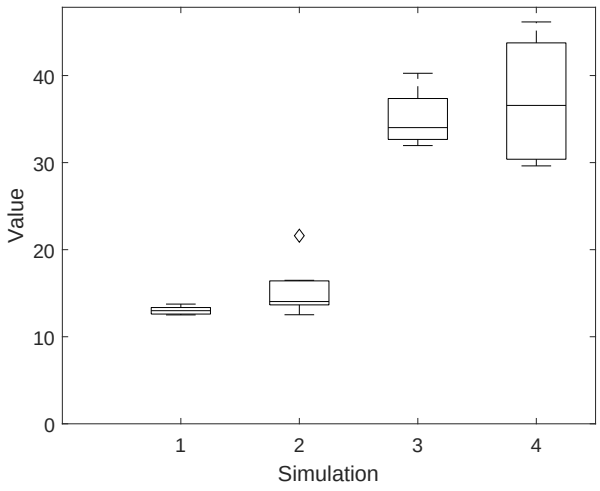

Figure 78: *Kruskal-Wallis analysis of the computation times of the Siemens frequency converter,* $\chi^2 = 31.45$

The Chi-squared statistic for the Kruskal-Wallis test of the different battery simulations is 16.34 (Fig. 79), indicating a significance level of 0.9997 % for the hypothesis that the values in each group originate from distinct populations.

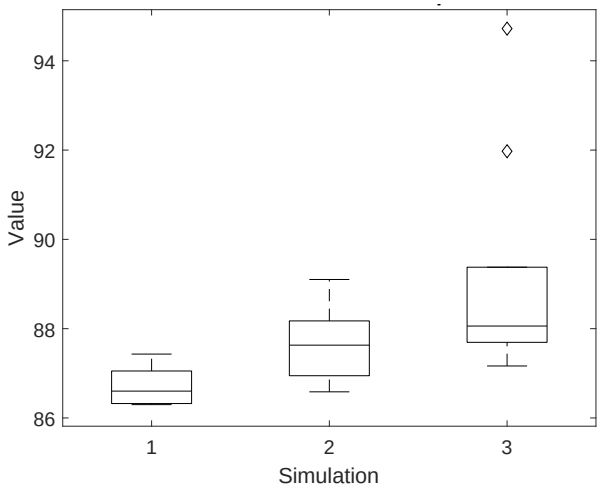

Figure 79: *Kruskal-Wallis analysis of the computation times of the different battery simulations,* $\chi^2 = 16.34$

The Chi-squared statistic for the Kruskal-Wallis test of the different prototype DC/DC-converter simulations is 53.3 (Fig. 80), indicating a significance level of 99.999 999 06 % for the hypothesis that the values in each group originate from distinct populations.

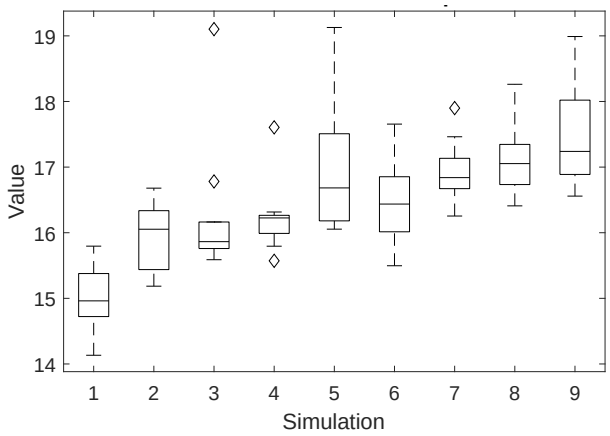

Figure 80: *Kruskal-Wallis analysis of the computation times of the prototype DC/DC-converter,* $\chi^2 = 53.3$

The Chi-squared statistic for the Kruskal-Wallis test of the different Bauer DC/DC-converter simulations is 23.84 (Fig. 81), indicating a significance level of 99.76 % for the hypothesis that the values in each group originate from distinct populations.

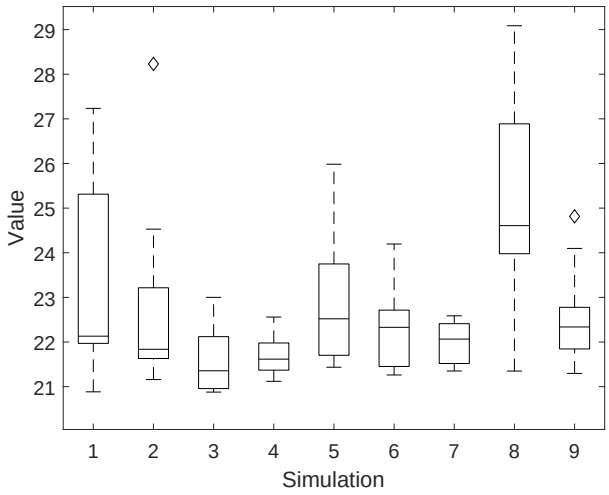

Figure 81: *Kruskal-Wallis analysis of the computation times of the Bauer DC/DC-converter,* $\chi^2 = 31.67$

D.7 Resolution

In [121], various simulations of PV systems and the influence of batteries on simulation accuracy are examined. This thesis focuses on group H2, representing a hypothetical constant generation unit with 0.82 kW, and group P2, modeling a PV system with an area of 17.8 m^2, resulting in an approximate generation of 0.29 kWh. The relevant data from [121] utilized in this thesis is summarized in Table 20.

Table 20: *Ratio of simulation error for different temporal resolutions according to [121]*

Group	**Temporal resolution [s]**					
	60	300	600	900	1800	3600
	Ratio of simulation error					
H2	1	1.202	1.340	1.531	1.709	1.824
P2	1	1.17	1.251	1.356	1.494	1.629

The coefficients for the calculation of n_{false} are chosen such that the minimum accuracy for frequently implemented components stabilizes at approximately 95 % as this value seems reasonable from the analysis of components.

Table 21: *Values for minimal accuracy factors*

Factor	a	b	c
Value	5	40	20

$$B(N_{\text{Comp}}, A_{\text{min,Comp}}, i) = \binom{N_{\text{Comp}}}{i} \cdot (1 - A_{\text{min,Comp}})^{i} \cdot {A_{\text{min,Comp}}}^{N_{\text{Comp}} - i} \tag{35}$$

An inaccuracy penalty f_{U} is incorporated into the function and needs to be specified for the respective application. For the calculations in Chapter 5.2 it is set to 0.998 to ensure a maximum possible total simulation accuracy of 99.8 %.

E Cost Function

E.1 Optimization Variables

The optimization is solved using 'fmincon' with the interior-point algorithm, as the problem includes constraints on minimum accuracy, non-linear dependencies within the cost function, and requires relative solution tolerances. Tests with alternative solution algorithms showed minimal differences in both optimization time and results.

The variables for the optimization are presented in Tab. 22. For the optimization variables, limits are defined based on reasonable values for a ship the size of the AIDAbella. Although these limits are derived from real components of the ship, the variables represent only the simulation model. For instance, the maximum number of cabins, set at 1025, corresponds to the actual number of cabins on the ship. However, this value is used to represent the number of cabins to be modeled for optimal simulation cost in ship design. Consequently, this number cannot exceed the actual number of cabins.

The number of cabins is therefore constrained to a range of 25 to 1025 cabins (the maximum on the AIDAbella). This range assumes that there are 25 distinct cabin types, each with different electrical loads and usage patterns. The number of constant loads is constrained to a range of 50 to 100, as this category includes components such as emergency lighting systems, small heating elements (e.g., for fuel), computers, and other minor equipment. The exact number can vary significantly depending on how these components are grouped. DC/DC-converters are essential for connecting the MVDC to the LVDC in each FZ and should be redundant. Additionally, public areas (decks 4–12, 14) can be equipped with DC/DC-converters, either one per deck per FZ or fewer, depending on the distribution system. Machine rooms and other technical equipment require approximately 20 additional DC/DC-converters. This results in a total range of 60 converters (if only certain decks are equipped) to 120 converters (if all decks and extensive technical equipment are included). The number of HVAC systems

Table 22: *Optimization variables*

Optimization Variable	Min. Value	Max. Value
Number of cabins	25	1025
Number of parameters fluctuating load	1	4320
Number of constant loads	50	100
Number of parameters constant load	0	1
Number of DC/DC-converters	60	120
Number of parameters DC/DC-converter	15	28
Number of batteries	3	20
Number of parameters Batteries	1	2000
Capacity batteries	200 kWh	2000 kWh
Number of frequency converters	80	120
Number of parameters frequency converters	12	35
Number of HVAC	5	50
Number of parameters HVAC	3	144
Number of fuel cells	3	7

ranges from 5 to 50, depending on the ship's requirements. This range accounts for configurations from one system per FZ to one system per FZ per deck. For batteries, the minimum number is set to three, equipping three out of five FZs, as the remaining two FZs are assumed to have generators. The maximum is limited to 20 batteries, as larger batteries should not be placed in public spaces for safety reasons and are therefore restricted to decks 1–3. While smaller batteries could technically be installed in public spaces due to their lower safety risks, high numbers would lead to increased installation and maintenance costs. Battery capacities for these lower numbers of batteries range between 200 kWh and 2000 kWh since the electrical load of a FZ typically varies between 200 - 800 kW. Frequency converters are required for generators, propulsion systems, thrusters, pumps, smaller machinery, and fans. For a ship the size of the AIDAbella, this results in a range of 80 to 120 converters. Fuel cells, on the other hand, are expected to be sparingly integrated due to specific safety requirements at a maximum of one per FZ, with a range of 3 to 7 per ship.

E.2 Multiple implemented components

The function in Eq. 36 is used to represent the fact that the initial development of a model for a component is significantly more complex than its subsequent implementations. The number of implemented components x is used as a variable, leading to

$$f(x) = 10.71883 - 9.889301 * e^{-0.02375583 * x} \tag{36}$$

E.3 Scaling factor β

From the development of the model for the frequency converter with 35 parameters and a cyclomatic complexity of 5, in a total of 12 component variants, that required approximately 20 hours within the scope of this work, the scaling factor β is determined as:

$$\beta = \frac{t_{\mathrm{Dev}}}{N_{\mathrm{Para}} \cdot V_{\mathrm{cyc}} \cdot N_{\mathrm{Comp,imp}}} = \frac{20h}{2100} = 0.0095 \tag{37}$$

E.4 Application Area Specifications

Table 23: *Definition of minimal accuracy, simulation duration and temporal resolution for different applications*

Application area	$A_{\mathrm{min,sys}}$ [%]	t_{s} [s]	t_{sim} [s]
Dimensioning of energy generators/batteries	70	$1 \cdot 10^{-4}$	14400
Load flow analysis	85	$1 \cdot 10^{-4}$	14400
Comparative feasibility studies	90	$1 \cdot 10^{-5}$	14400
Transient stability analysis	95	$1 \cdot 10^{-6}$	60
Short-circuit analysis	96	$1 \cdot 10^{-6}$	60

F Scaled-Ship Grid Test Setup Units

This section provides a detailed description of the individual units of the scaled-ship setup, highlighting their role and representation within the simulation framework. In some of the simulation models, an increase in complexity does not necessarily lead to an improvement in accuracy. This phenomenon can be attributed to the fact that individual components are not always represented with sufficient precision. Achieving a complete characterization of each component is often resource-intensive, making it impractical in many cases. Additionally, inherent variations in the properties of individual components can introduce distortions into the results, further limiting the accuracy of the simulation.

F.1 DC/DC-Conversion Unit

Table 24: *Accuracy and cyclomatic complexity for DC/DC-converter models*

Number of parameters	16	18	19	20	21	22	23	25	28
Accuracy [%]	4.71	91.2	98.31	98.31	98.31	98.34	98.34	98.34	98.34
Cyclomatic complexity	3	3	3	3	3	3	3	3	3

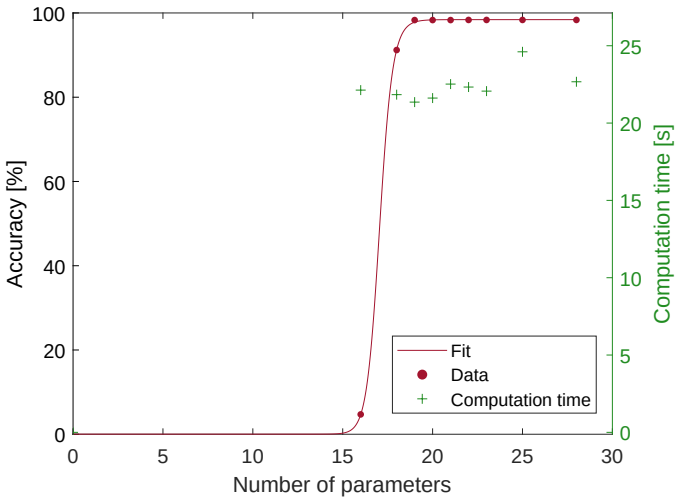

Figure 82: *DC/DC-converter unit simulation accuracy for different numbers of parameters*

F.2 Long Line Unit

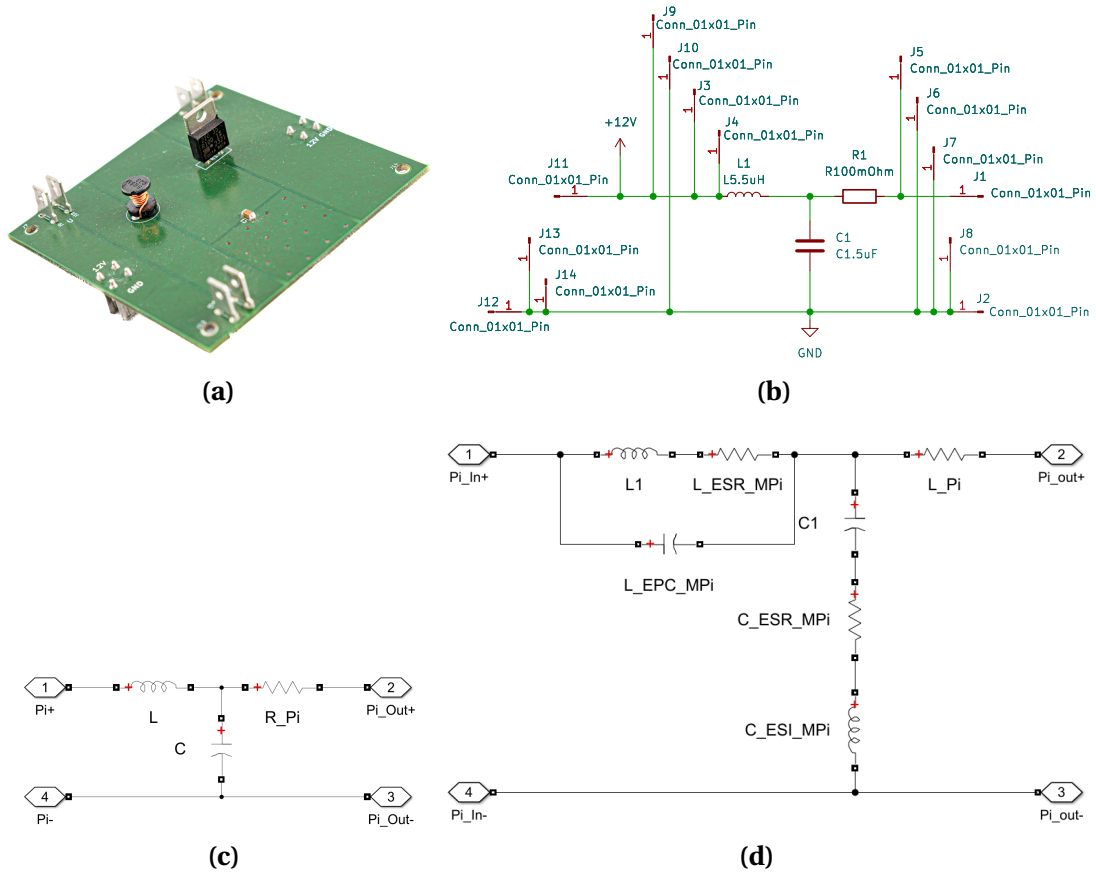

Figure 83: *Long line unit (a) photo, (b) schematic diagram of PCB, (c) low LoD model, (d) high LoD model*

Table 25: *Accuracy and cyclomatic complexity for long line models*

Number of parameters	3	4	5	6	7
Accuracy [%]	99.99	99.99	99.99	99.37	99.59
Cyclomatic complexity	1	1	1	1	1

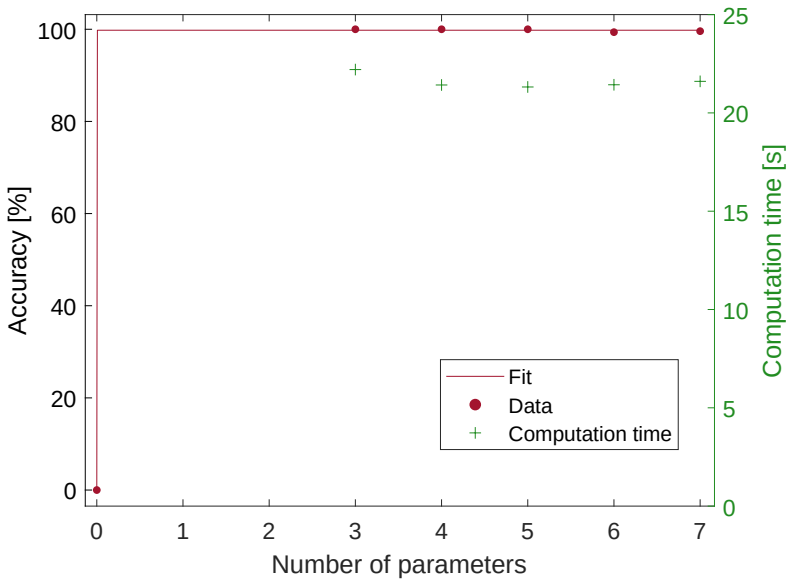

Figure 84: *Long line unit simulation accuracy for different numbers of parameters*

F.3 Fan Unit

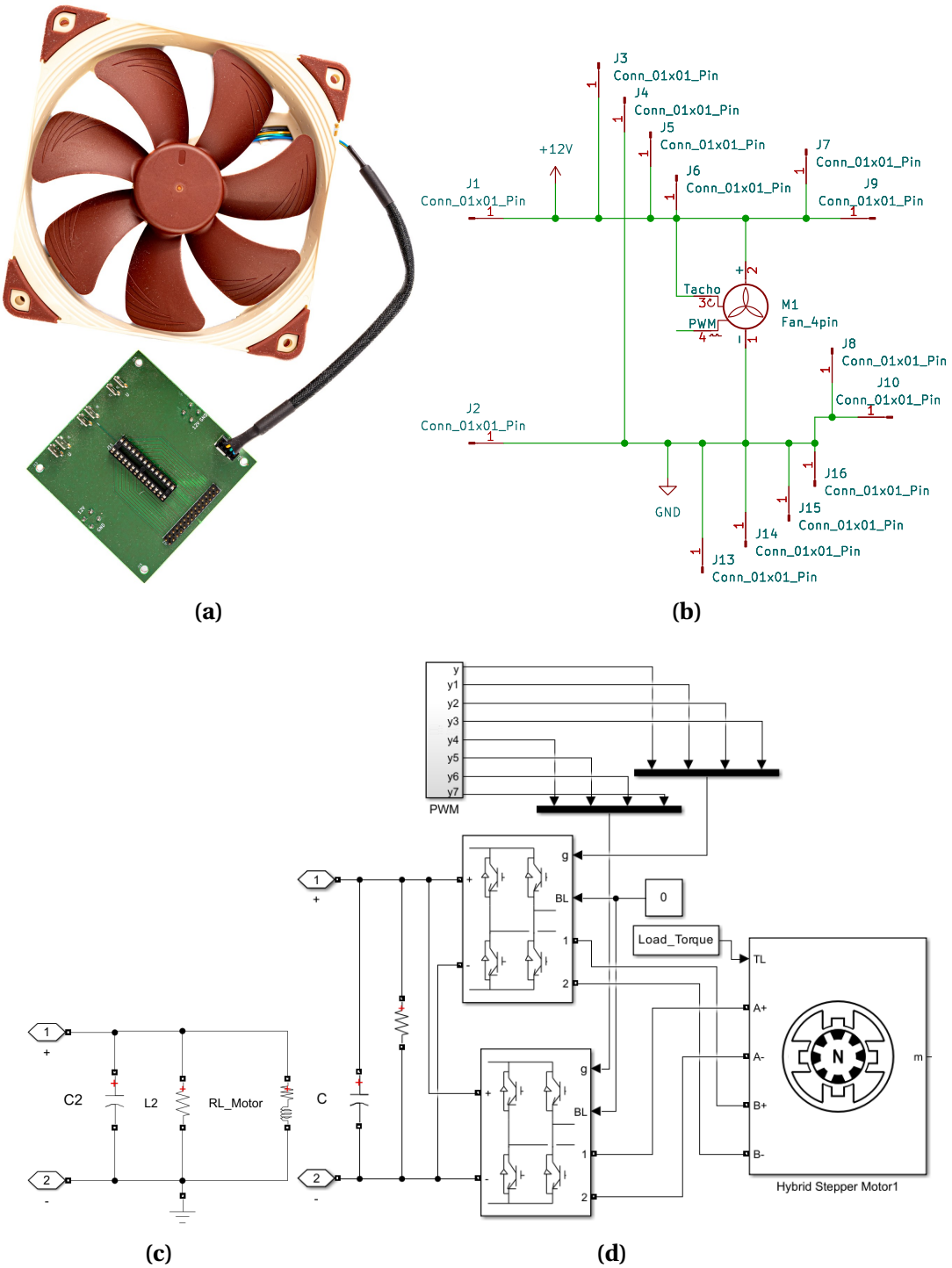

Figure 85: *Fan unit (a) photo, (b) schematic diagram of PCB, (c) low LoD model, (d) high LoD model*

Table 26: *Accuracy and cyclomatic complexity for fan models*

Number of parameters	4	18	19	20	22
Accuracy [%]	49.61	66.24	66.16	78.59	78.51
Cyclomatic complexity	1	2	2	3	3

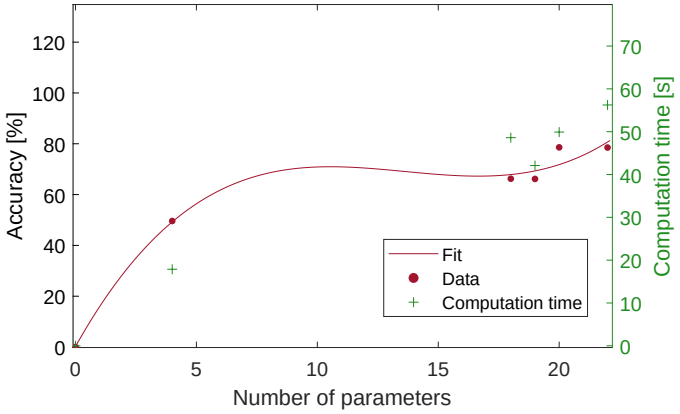

Figure 86: *Fan unit simulation accuracy for different numbers of parameters*

F.4 Ohmic Load Unit

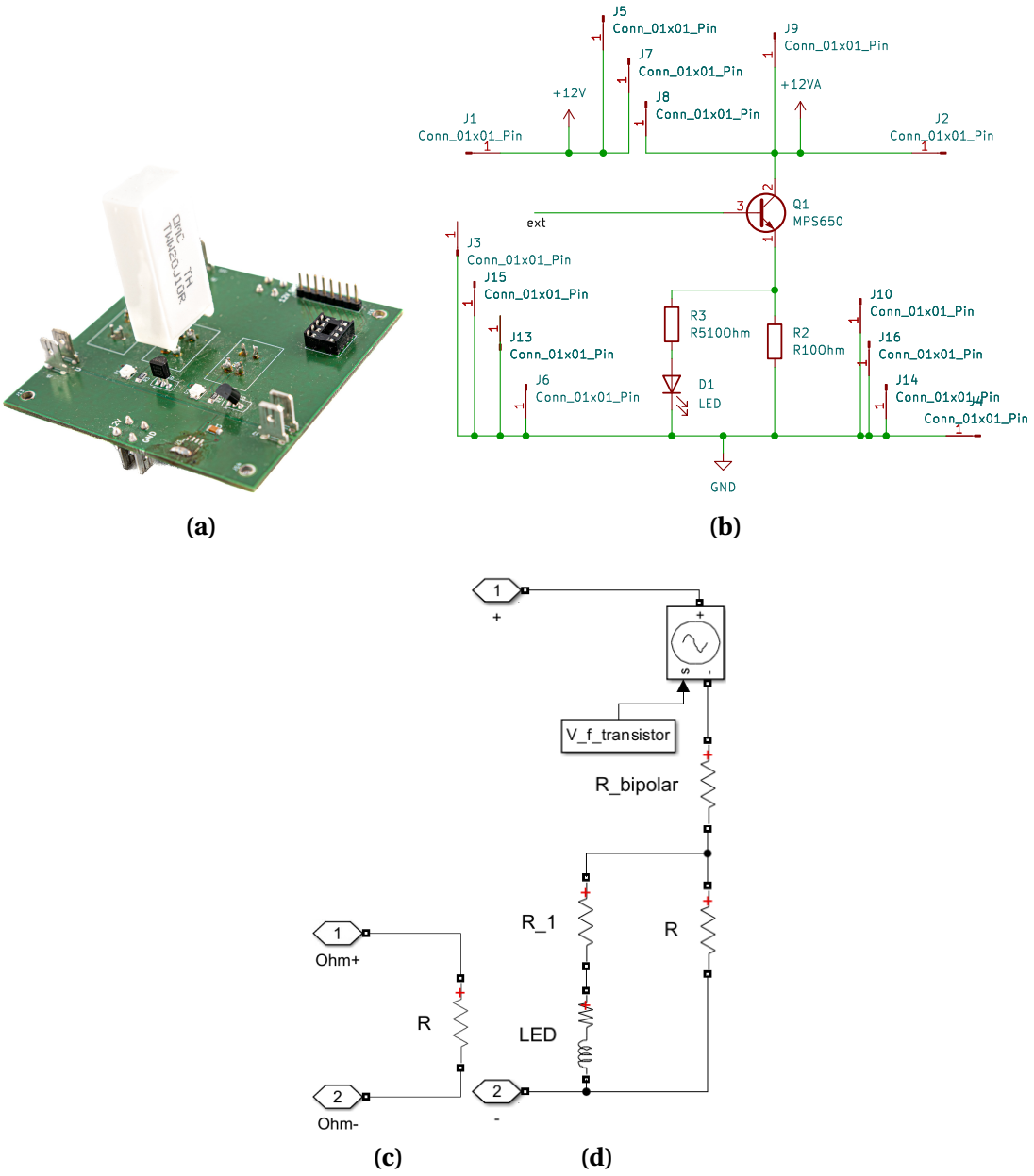

Figure 87: *Ohmic load unit (a) photo, (b) schematic diagram of PCB, (c) low LoD model, (d) high LoD model*

Table 27: *Accuracy and cyclomatic complexity for ohmic load models*

Number of parameters	1	4	5	6
Accuracy [%]	95.14	95.14	95.14	95.14
Cyclomatic complexity	1	1	1	1

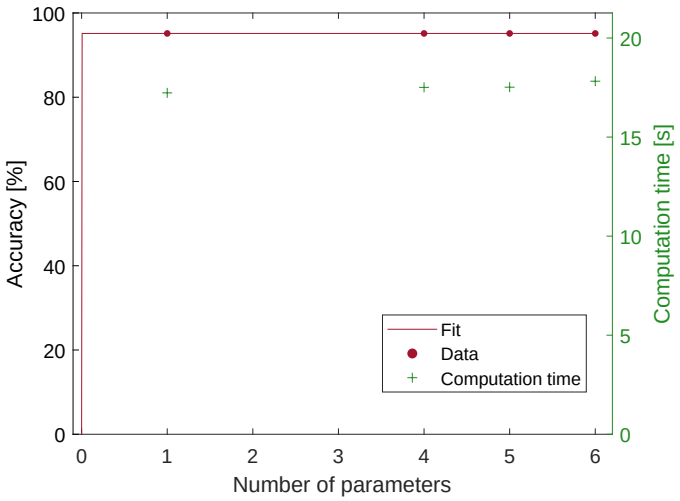

Figure 88: *Ohmic load unit*

F.5 Battery Unit

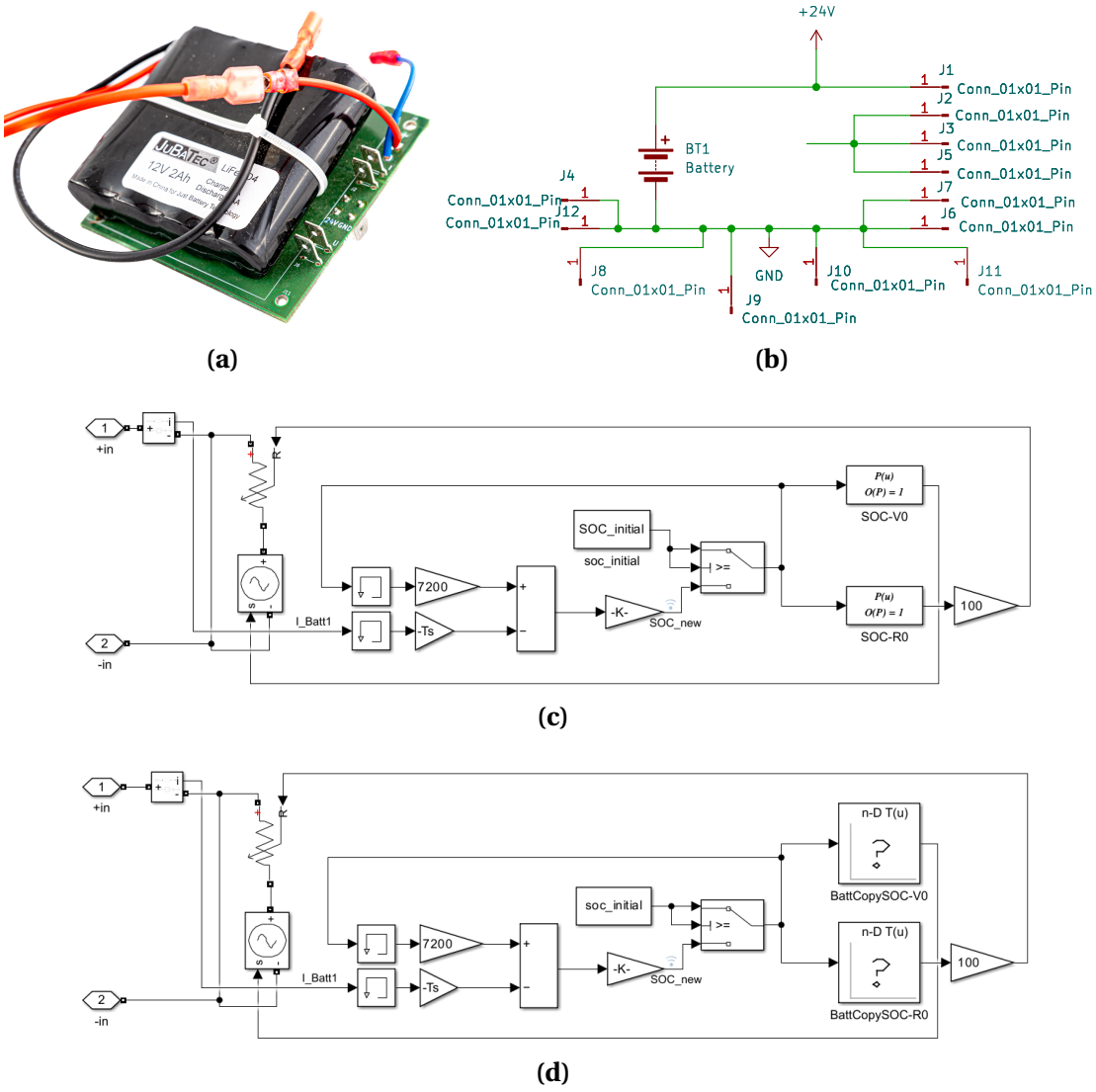

(a) **(b)**

(c)

(d)

Figure 89: *Battery unit (a) photo, (b) schematic diagram of PCB, (c) low LoD model, (d) high LoD model*

Table 28: *Accuracy and cyclomatic complexity for battery models*

Number of parameters	4	8	10	12	2000
Accuracy [%]	49.99	75.73	67.79	59.36	100
Cyclomatic complexity	2	2	2	2	2

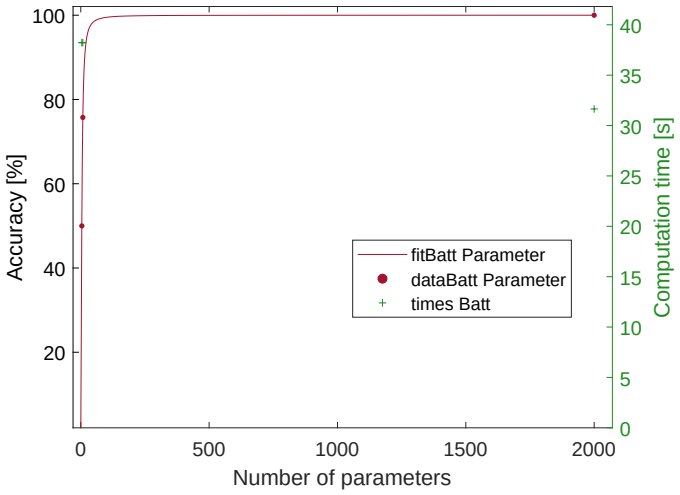

Figure 90: *Battery unit*

G Scaled-Ship Grid Results

The analysis of the scaled-ship grid, detailed in Chapter 5.1.1, resulted in additional test setups as shown in Fig. 91 and additional accuracy heatmaps, that are shown in Fig. 92b, 92a, 93, 94, and 95.

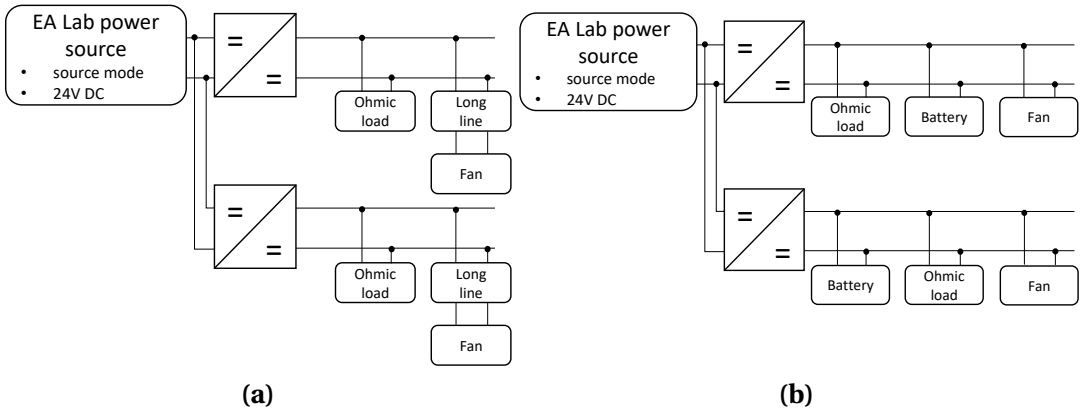

Figure 91: *Setup of the scaled-ship grid system, supplied by a lab power source: (a) two DC/DC-converters connected to two segments, each with an ohmic load, and a fan connected via a long line, (b) two DC/DC-converters connected to two segments, each with an ohmic load, a battery, and a fan*

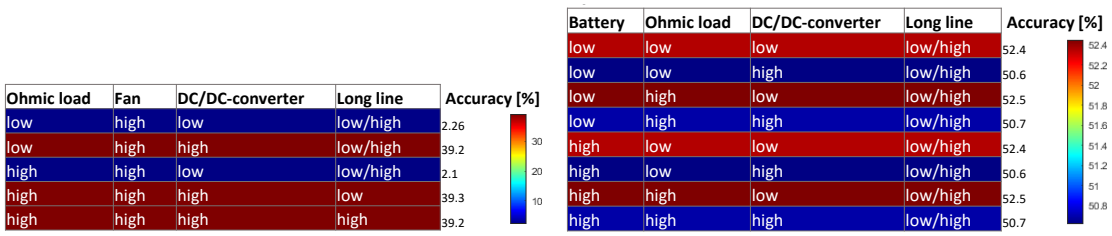

(a) **(b)**

Figure 92: *Accuracy heatmap of all simulation LoD combinations in the setup displayed in Fig. 91(a) and (b)*

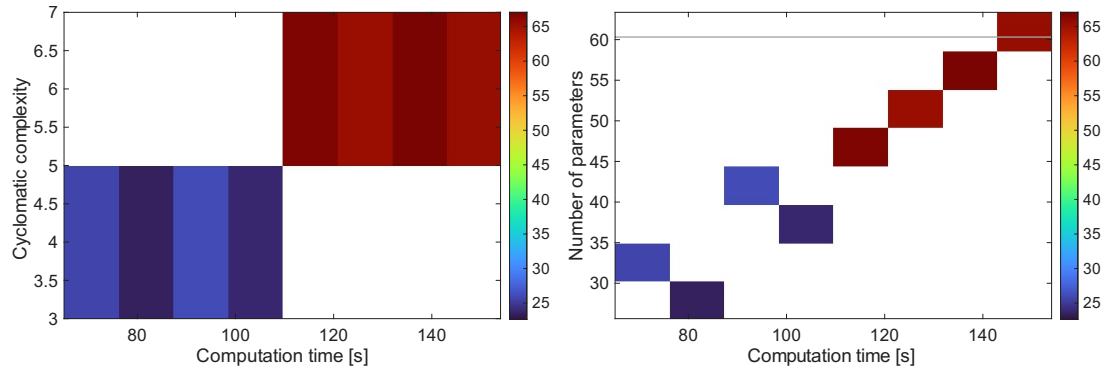

(a) **(b)**

Figure 93: *Accuracy heatmap of (a) cyclomatic complexity and (b) parameter number and computation time of setup Fig. 49(a)*

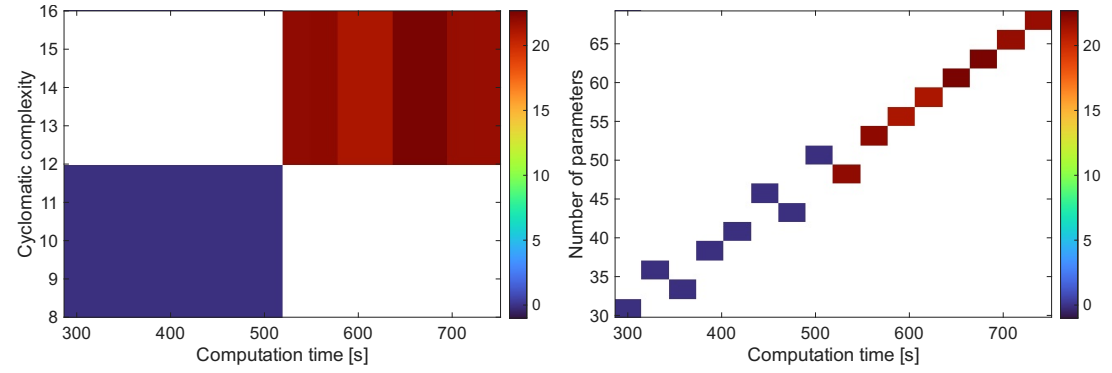

(a) **(b)**

Figure 95: *Accuracy heatmap of (a) cyclomatic complexity and (b) parameter number and computation time of setup Fig. 49(d)*

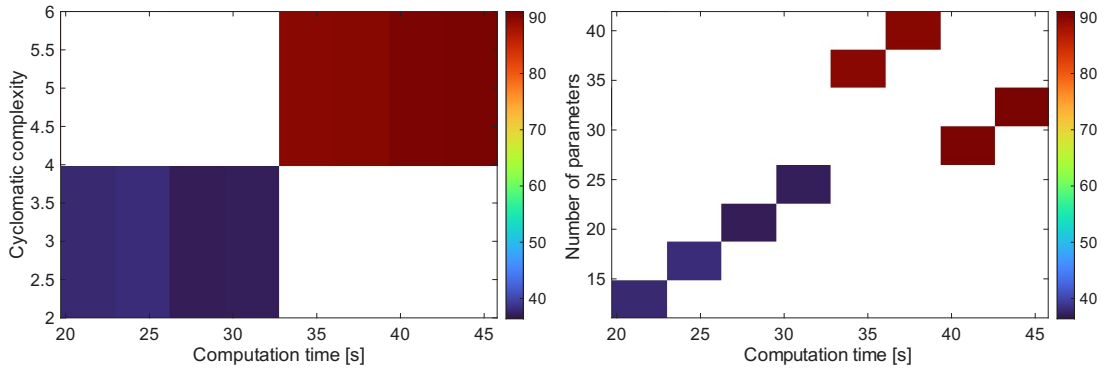

(a) **(b)**

Figure 94: *Accuracy heatmap of (a) cyclomatic complexity and (b) parameter number and computation time of setup Fig. 49(c)*

H FMEA

In order to gain a more detailed understanding of the potential risks and savings associated with the cost function, an FMEA analysis according to [213] is conducted. The severity scale is utilized in accordance with Tab. 29, the occurrence scale in accordance with Tab. 30, and the detection scale in accordance with Tab. 31.

Table 29: *Severity evaluation criteria for FMEA*

Effect	Severity	Rank
Failure to meet safety and/or regulatory requirements	Failure mode affects safe/reliable operation, danger to passengers/crew possible, involves noncompliance with regulations, without warning	10
	Failure mode affects safe/reliable operation, danger to passengers/crew possible, involves noncompliance with regulations, with warning	9
Loss or degradation of primary function	Loss of primary function, that does not affect safety	8
	Degradation of primary function	7
Loss or degradation of secondary function	Loss of secondary function, subsystem or part malfunctions	6
	Degradation of secondary function	5
Annoyance	Minor performance loss, that can be overcome by modifications	4
	Minor performance loss, that can be overcome, so there is no performance loss anymore	3
	Minor effects, that are rarely noticed	2
No effect	No discernible effect	1

The occurrence of failure causes varies significantly in simulations, Tab. 32 shows the ratings for large passenger ship grid simulations as used for the FMEA. One of the most frequent causes is incorrect dimensioning, that has an occurrence rating of 9 and directly impacts system accuracy. Using an inaccurate resolution, rated at 8, is a frequent issue, particularly in simulations requiring high precision, and it can lead to significant errors in the results. Using system-based simulations instead of physics-based simulations is a common simplification, especially in complex systems like ship grids, and it is rated at 7. Using the wrong components is relatively common, with an occurrence rating of 5; this often results from miscommunication or incorrect assumptions during the design phase. Using an insufficient number of components has an occurrence rating of 4. Using the wrong "network" and placing components incorrectly in relation to other components has a much lower occurrence rating of 3. Wrong solvers or solver settings (rated 1) and rate transition issues (rated 2) are rare but can occur due to improper configuration or lack of expertise in simulation tools. Fundamental *MATLAB*® bugs, rated at 1, are extremely rare, but they can occasionally arise due to software limitations or unpatched issues.

Table 30: *Occurrence evaluation criteria for FMEA*

Likelihood of Failure	Occurrence of Cause (Reliability/Design Life)	Occurrence of Cause (Incidents per Ship in Lifetime)	Rank
Very High	Failure almost inevitable, due to new design/ technology/no history	25	10
High	Failure highly likely, due to new design/technology/no history or change in operating conditions	5	9
	Failure likely, due to (partly) new design/technology/limited history or change in operating conditions	1	8
	Failure uncertain, due to (partly) new design/ technology/limited history or change in operating conditions	0.5	7
Moderate	Failure occasional, due to similar designs/technology/history or simulation and testing	0.1	6
	Failure improbable, due to similar designs/technology/history or simulation and testing	0.02	5
	Failure isolated in similar designs/technology/history or simulation and testing	0.005	4
Low	Only isolated failures in almost identical designs/ technology/history or simulation and testing	0.001	3
	No observed failures in almost identical designs/ technology/history or simulation and testing	0.0002	2
Very Low	Eliminated through preventive control	<0.0001	1

Severity ratings for the DC grid ship simulation used for the FMEA are shown in Tab. 33. As they come with major operational and safety implications and noncompliance with regulations, power outages, overloads to the point of destruction and/or loss of propulsion, destruction of connection, and any safety hazards are assigned a severity of 9 or 10, depending on the availability of a warning. Severity of insufficient available power are assigned a severity of 8, as it directly affects other safety relevant systems and can result in cascading failures but does not inherently affect safety. Lower capacities than intended and other component overloads due to re-routing carry the risk of affecting other systems, however, as there is no loss of primary function, the severity assigned is 6. Degradation of secondary functions such as higher power flows than simulated

Table 31: *Detection evaluation criteria for FMEA*

Opportunity for Detection	**Likelihood of Detection**	**Rank**
No detection opportunity	Almost impossible	10
Not likely at any stage	Very remote	9
Remote chance that design/technology analysis or simulation and testing will detect failure after usage/construction	Remote	8
Very low chance that design/technology analysis or simulation and testing will detect failure after usage/construction	Very low	7
Low chance that design/technology analysis or simulation and testing will detect failure after usage/construction	Low	6
Moderate chance that design/technology analysis or simulation and testing will detect failure prior to usage/construction	Moderate	5
Moderately high chance that design/technology analysis or simulation and testing will detect failure prior to usage/construction	Moderately high	4
High chance that design/technology analysis or simulation and testing will detect failure prior to usage/construction	High	3
Very high chance that design/technology analysis or simulation and testing will detect failure prior to usage/construction	Very high	2
Obvious detection	Almost certain	1

and higher reaction times, is assigned a severity of 5. Severities of 4 are associated with a minor performance loss, that can be overcome by modifications, faster aging and degeneration, lower efficiency and lower speed are in this category. Minor performance losses, that can be overcome completely, thus assigned a severity of 3, include incorrect energy quantities adding up for the optimization calculations, reduced power ratings of components, unused capacities, and a limited usability of end consumer equipment. A lower system efficiency caused by the discarding of better systems in simulation due to numerical issues can range from a severity of 1 to 4, but in this case is assigned 2 as these effects will rarely be noticed at all, given a thorough simulation by experts.

Table 32: *Occurrence rating for FMEA*

Occurrence	**Rating**
Incorrect dimensioning	9
Inaccurate resolution used	8
System based simulation instead of physics based simulation	7
Usage of wrong components	5
Insufficient number of components used	4
Wrong network — component in the wrong location relative to other components	3
Rate transition issues	2
Wrong solver or solver settings	1
Fundamental *MATLAB*® bug	1

The detectability of failure causes is important to account for the associated risk and rating for the use case of the FMEA are shown in Tab. 34. Fundamental *MATLAB*® bugs are undetectable for users, although extremely rare, and therefore assigned a detectability of 10. Incorrect dimensioning, while not always obvious unless extreme, is assigned a detectability of 5. Detectabilities of 4 are assigned to the insufficient number of components used, and system based simulations instead of a physics based ones, as these can typically be detected through verification and validation of the simulations. Inaccurate resolutions, wrong solvers or solver settings, and wrong networks (component in the wrong location relative to other components) are assigned a detectability of 2 as these issues often result in instable simulations or other noticeable effects in simulation. Rate transition issues typically trigger warnings or error messages, making them highly detectable and therefore assigned a detectability of 1.

Only the most relevant parts of the complete FMEA, with RPN numbers in the unacceptable area higher than 175 and up to a maximum of 450 [214], are displayed here in an aggregated format. Incorrect dimensioning and system based simulation instead of physics based simulation account for the lowest detectability probability (therefore highest detectability rating) and highest occurrence, resulting in the highest overall RPN. The most critical failure effects include any safety hazards and overloads or outages. Furthermore, insufficient power availability/capacity, excessive power flows, insufficient reaction times and reduced machine speeds or efficiency, and accelerated aging or degeneration of components lead to high RPN. The main failure modes consist of frequencies in simulation being higher or lower than in reality - leading to undetected oscillations and aliasing, respectively producing nonexistent oscillations-, currents being smaller or larger in simulation than in reality, incorrect simulations of load flow changes

Table 33: *Severity rating for FMEA*

Severity	**Rating**
Complete power outage	10
Overload — loss of propulsion	10
Safety hazard — passengers/crew	10
Earthing problem	10
Overload — connection destruction/loss	9
Overload — destruction	9
Safety hazard — fire risk, overheating	9
Insufficient available power due to lower power flow	8
Capacity too low	6
Other component overload due to re-routing of power flows	6
Higher reaction time	5
Power flow too high	5
Faster aging	4
Lower efficiency	4
Lower speed	4
Faster degeneration	3
Incorrect energy quantities	3
Reduced power rating	3
Unused capacity	3
Usability of equipment limited	3
Lower system efficiency	2

(e.g. fast switching direction changes that are not simulated), numerical problems, and incorrect event synchronization.

Table 34: *Detectability rating for FMEA*

Detectability	**Rating**
Fundamental *MATLAB*® bug	10
Incorrect dimensioning	5
System based simulation instead of physics based simulation	4
Insufficient number of components used	4
Usage of wrong components	3
Wrong solver or solver settings	2
Wrong "network"	2
Inaccurate resolution used	2
Rate transition issues	1

Table 35: *FMEA of ship design process using simulation*

Potential failure mode	Potential effects of failure	Potential causes of failure	S	O	D	RPN
Higher current than simulated	faster aging	incorrect dimensioning	4	9	5	180
Slower reaction, lower frequencies						180
Load flow changes not correctly simulated						180
Numerical problems						180
Higher current than simulated	faster degeneration					180
Slower reaction, lower frequencies						180
Numerical problems						180
Higher current than simulated	lower efficiency					180
Lower current than simulated						180
Slower reaction, lower frequencies						180
Faster reaction, higher frequencies simulated than real						180
Load flow changes not correctly simulated						180
Numerical problems						180
Lower current than simulated						180
Faster reaction, higher frequencies simulated than real						180
Numerical problems						180
Lower current than simulated	lower speed					180
Faster reaction, higher frequencies simulated than real						180
Numerical problems						180

Potential failure mode	Potential effects of failure	Potential causes of failure	S	O	D	RPN
Load flow changes not correctly simulated	insufficient available power	system based simulation instead of physics based simulation	8	7	4	224
Lower current than simulated						224
Faster reaction, higher frequencies simulated than real						224
Load flow changes not correctly simulated						224
Shifting of behaviors, incorrect event synchronization						224
Faster reaction, higher frequencies simulated than real	higher reaction time	incorrect dimensioning	5	9	5	225
Higher current than simulated	power flow too high					225
Slower reaction, lower frequencies						225
Numerical problems						225
Slower reaction, lower frequencies						225
Higher current than simulated	overload — connection destruction	system based simulation instead of physics based simulation	9	7	4	252
Slower reaction, lower frequencies						252
Shifting of behaviors, incorrect event synchronization						252
Higher current than simulated	overload - destruction					252
Slower reaction, lower frequencies						252
Shifting of behaviors, incorrect event synchronization						252

Potential failure mode	Potential effects of failure	Potential causes of failure	S	O	D	RPN
Numerical problems	capacity too low	incorrect dimensioning	6	9	5	270
Load flow changes not correctly simulated						270
Higher current than simulated	other component overload due to re-routing of power flows					270
Slower reaction, lower frequencies						270
Numerical problems						270
Higher current than simulated	complete power outage	system based simulation instead of physics based simulation	10	7	4	280
Slower reaction, lower frequencies						280
Shifting of behaviors, incorrect event synchronization						280
Higher current than simulated	overload — loss of propulsion					280
Slower reaction, lower frequencies						280
Shifting of behaviors, incorrect event synchronization						280
Higher current than simulated	safety hazard — passengers/crew					280
Slower reaction, lower frequencies						280
Shifting of behaviors, incorrect event synchronization						280
Load flow changes not correctly simulated	insufficient available power	incorrect dimensioning	8	9	5	360
Lower current than simulated						360
Faster reaction, higher frequencies simulated than real						360
Load flow changes not correctly simulated						360
Numerical problems						360

Potential failure mode	Potential effects of failure	Potential causes of failure	S	O	D	RPN
Higher current than simulated	overload - connection destruction	incorrect dimensioning				405
Slower reaction, lower frequencies						405
Numerical problems						405
Higher current than simulated	overload — destruction of component					405
Slower reaction, lower frequencies			9	9	5	405
Numerical problems						405
Higher current than simulated	safety hazard — fire risk, overheating					405
Slower reaction, lower frequencies						405
Numerical problems						405
Higher current than simulated	complete power outage					450
Slower reaction, lower frequencies						450
Numerical problems						450
Higher current than simulated	overload — loss of propulsion					450
Slower reaction, lower frequencies			10	9	5	450
Numerical problems						450
Higher current than simulated	safety hazard — passengers/crew					450
Slower reaction, lower frequencies						450
Numerical problems						450

In order to ascertain the potential for cost savings in the development of the ship grid, it is necessary to consider the areas of material, installation, and volume savings. A more precise simulation can lead to significant cost savings by designing grid components as ideally as possible. This can be achieved by reducing the number of cables that need to be installed (material and installation cost savings) or by eliminating or reducing the size of large/heavy components through skillful planning, resulting in volume savings.

Since using the cost function itself carries a certain risk, an additional FMEA is performed to more precisely assess the risk associated with the cost function itself, as shown in Tab. 36.

Table 36: *FMEA for cost function*

Potential failure mode	Potential effects of failure	Potential causes of failure	S	O	D	RPN
False estimation of C_Bat	incorrect development costs	inadequate analysis of battery influence	3	3	3	27
False estimation of salaries		inadequate data from ship yard/engineering company	3	1	1	3
False estimation of number of multiple implemented components		inadequate data from ship yard/engineering company	3	1	2	6
False estimation of cyclomatic complexity in component analysis		inadequate analysis of components	3	3	3	27
False estimation of number of parameters in component analysis		inadequate analysis of components	3	3	3	27
False estimation of number of components		inadequate data from ship yard/engineering company	3	1	2	6
False estimation of scaling factor		inadequate analysis of system	3	4	2	24
False estimation of server cost	incorrect computation	inadequate data from ship yard/engineering company	3	1	1	3
False estimation of influence of bidirectionality		inadequate analysis of bidirectionality influence	3	3	3	27
False estimation of computation times in component analysis		inadequate analysis of components	3	3	3	27

Potential failure mode	Potential effects of failure	Potential causes of failure	S	O	D	RPN
Incorrect FMEA results	incorrect risk costs	inadequate data from ship yard/engineering company	5	1	1	5
Incorrect estimation of ship value		inadequate data from ship yard	5	1	1	5
Incorrect estimation of license costs	incorrect fixed cost	inadequate data from ship yard/engineering company	1	1	1	1
Reduction of material costs not equal to cost savings	incorrect possible savings	ship grid consists of different components	2	2	2	8
		component costs vary according to supply chains	2	2	1	4
Component dimensioning not equal to lower amount of work		different installation effort	2	3	3	18
		other components have to be installed nevertheless	2	2	2	8
Volume saving not equal to cost reduction		volume savings need to be taken into account with their location	2	2	2	8

I Uncertainty of Haptic Actuator

Relative uncertainty force measurement:

$$e_{rel} = \frac{F_{max,abs}}{F_{nom}} - 1 \Rightarrow e_{rel} = \frac{\frac{F * 2.248 \cdot 1.15 \cdot 1.0001 \cdot 1.00024 + 915\mu V}{2.248}}{F_{nom}} - 1 \quad (38)$$

$$= \frac{\frac{7.1421}{2.248}}{2.7589N} - 1 = \frac{3.1771N}{2.7589N} - 1 = 1.15 - 1 = 15\% \quad (39)$$

Relative uncertainty acceleration measurement:

$$e_{rel} = \frac{a_{max,abs}}{a_{nom}} - 1 \Rightarrow e_{rel} = \frac{\frac{a * 10.2 * 10^{-}3 \cdot 10 \cdot 1.1 \cdot 1.0001 \cdot 1.00024 + 915\mu V}{10 \cdot 10.2 \cdot 10^{-}3}}{a_{nom}} - 1 \quad (40)$$

$$= \frac{\frac{2.0481V}{0.102}}{18.24m/s^2} - 1 = \frac{20.079m/s^2}{18.24m/s^2} - 1 = 1.101 - 1 = 10.1\% \quad (41)$$

References

[1] Jasper Faber, Shinichi Hanayama, Shuang Zhang, Paula Pereda, Bryan Comer, Elena Hauerhof, Schim van der Loeff, Wendela, Tristan Smith, Yan Zhang, Hiroyuko Kosaka, Masaki Adachi, Jean-Marc Bonello, Connor Galbraith, Ziheng Gong, Koichi Hirata, David Hummels, Anne Kleijn, David S. Lee, Yiming Liu, Andrea Lucchesi, Xiaoli Mao, Eiichi Muraoka, Liudmila Osipova, Haoqi Qian, Dan Rutherford, Suárez de la Fuente, Santiago, Haichao Yuan, Camilo Velandia Perico, Libo Wu, Deping Sun, Dong-Hoon Yoo, and Hui Xing. *Fourth IMO GHG Study 2020: Full Report*. London, 2020.

[2] IMO. *IMO's work to cut GHG emissions from ships*. 2023. URL: https://www.imo.org/en/MediaCentre/HotTopics/Pages/Cutting-GHG-emissions.aspx (visited on 2023-04-18).

[3] Kyunghwa Kim, Kido Park, Gilltae Roh, and Kangwoo Chun. "DC-grid system for ships: a study of benefits and technical considerations". In: *Journal of International Maritime Safety, Environmental Affairs, and Shipping* 2.1 (2018), pp. 1–12. DOI: 10.1080/25725084.2018.1490239.

[4] Mehrad Bastani, Aristotelis E. Thanos, Nurcin Celik, and Chun-Hung Chen. "Efficient design selection in microgrid simulations". In: *Proceedings of the Winter Simulation Conference 2014*. IEEE, 2014, pp. 2762–2773. ISBN: 978-1-4799-7486-3. DOI: 10.1109/WSC.2014.7020119.

[5] Craig A. Aumann. "A methodology for developing simulation models of complex systems". In: *Ecological Modelling* 202.3-4 (2007), pp. 385–396. DOI: 10.1016/j.ecolmodel.2006.11.005.

[6] Dirk Abel and Alexander Bollig. *Rapid control prototyping: Methoden und Anwendungen ; mit 16 Tabellen*. 1. Aufl. Berlin and Heidelberg: Springer, 2006. ISBN: 978-3-540-29524-2.

[7] Charles E. Leiserson, Neil C. Thompson, Joel S. Emer, Bradley C. Kuszmaul, Butler W. Lampson, Daniel Sanchez, and Tao B. Schardl. "There's plenty of room at the Top What will drive computer performance after Moore's law". In: *Science* 368.6495 (2020).

[8] Michael C. Fu, Guzin Bayraksan, Shane G. Henderson, Barry L. Nelson, Warren B. Powell, Ilya O. Ryzhov, and Ben Thengvall. “Simulation optimization: A panel on the state of the art in research and practice”. In: *Proceedings of the Winter Simulation Conference 2014*. IEEE, 2014, pp. 3696–3706. ISBN: 978-1-4799-7486-3. DOI: 10.1109/WSC.2014.7020198.

[9] Thomas L. Delworth, Anthony Rosati, Whit Anderson, Alistair J. Adcroft, V. Balaji, Rusty Benson, Keith Dixon, Stephen M. Griffies, Hyun-Chul Lee, Ronald C. Pacanowski, Gabriel A. Vecchi, Andrew T. Wittenberg, Fanrong Zeng, and Rong Zhang. “Simulated Climate and Climate Change in the GFDL CM2.5 High-Resolution Coupled Climate Model”. In: *Journal of Climate* 25.8 (2012), pp. 2755–2781. ISSN: 0894-8755. DOI: 10.1175/JCLI-D-11-00316.1.

[10] Rene Prenc, Aleksandar Cuculić, and Ivan Baumgartner. “Advantages of using a DC power system on board ship”. In: *Journal of Maritime & Transportation Science* 52.1 (2016), pp. 83–97. ISSN: 0554-6397. DOI: 10.18048/2016.52.05.

[11] Sohaib Qazi, Prasanth Venugopal, Gert Rietveld, Thiago Batista Soeiro, Udai Shipurkar, Alex Grasman, Alan J. Watson, and Patrick Wheeler. “Powering Maritime: Challenges and prospects in ship electrification”. In: *IEEE Electrification Magazine* 11.2 (2023), pp. 74–87. ISSN: 2325-5897. DOI: 10.1109/MELE.2023.3264926.

[12] Giorgio Sulligoi, Andrea Vicenzutti, and Roberto Menis. “All-Electric Ship Design: From Electrical Propulsion to Integrated Electrical and Electronic Power Systems”. In: *IEEE Transactions on Transportation Electrification* 2.4 (2016), pp. 507–521. DOI: 10.1109/TTE.2016.2598078.

[13] S. S. Kalsi and O. Nayak. “Ship electrical system simulation”. In: *IEEE Electric Ship Technologies Symposium, 2005*. IEEE, 2005, pp. 63–69. ISBN: 0-7803-9259-0. DOI: 10.1109/ESTS.2005.1524654.

[14] Hans-Jürgen Reuß. “Brennstoffzellen an Bord von Schiffen. Stand der Technik und Perspektiven eines alternativen Antriebs”. In: *Hansa. International Maritime Journal* 145.9 (2008), pp. 131–137.

[15] Simone Castellan, Roberto Menis, Alberto Tessarolo, Fabio Luise, and Teresa Mazzuca. “A review of power electronics equipment for all-electric ship MVDC power systems”. In: *International Journal of Electrical Power & Energy Systems* 96 (2018), pp. 306–323. ISSN: 01420615. DOI: 10.1016/j.ijepes.2017.09.040.

[16] Karlijn Pott. *Waterbus 2907*.

[17] Guomei Chang, Yunxiang Wu, Shiyi Shao, Zhaoxia Huang, and Teng Long. “DC Bus Systems for Electrical Ships: Recent Advances and Analysis of a Real Case”. In: *IEEE Electrification Magazine* 8.3 (2020), pp. 28–39. ISSN: 2325-5897. DOI: 10.1109/MELE.2020.3005697.

[18] Daniele Bosich, Massimiliano Chiandone, Giorgio Sulligoi, Andrea A. Tavagnutti, and Andrea Vicenzutti. “High-Performance Megawatt-Scale MVDC Zonal Electrical Distribution System Based on Power Electronics Open System Interfaces”. In: *IEEE Transactions on Transportation Electrification* 9.3 (2023), pp. 4541–4551. DOI: 10.1109/TTE.2023.3244360.

[19] Dinesh Kumar and Firuz Zare. “A Comprehensive Review of Maritime Microgrids: System Architectures, Energy Efficiency, Power Quality, and Regulations”. In: *IEEE Access* 7 (2019), pp. 67249–67277. DOI: 10.1109/ACCESS.2019.2917082.

[20] Luona Xu, Josep Guerrero, Abderezak Lashab, Baoze Wei, Najmeh Bazmohammadi, Juan Vasquez, and Abdullah Abusorrah. “A Review of DC Shipboard Microgrids—Part I: Power Architectures, Energy Storage, and Power Converters”. In: *IEEE Transactions on Power Electronics* 37.5 (2022), pp. 5155–5172. ISSN: 0885-8993. DOI: 10.1109/TPEL.2021.3128417.

[21] M. Saeedifard, M. Graovac, R. F. Dias, and R. Iravani. “DC power systems: Challenges and opportunities”. In: *IEEE PES General Meeting*. IEEE, 2010, pp. 1–7. ISBN: 978-1-4244-6549-1. DOI: 10.1109/PES.2010.5589736.

[22] Zheming Jin, Mehdi Savaghebi, Juan C. Vasquez, Lexuan Meng, and Josep M. Guerrero. “Maritime DC microgrids - a combination of microgrid technologies and maritime onboard power system for future ships”. In: *2016 IEEE 8th International Power Electronics and Motion Control Conference (IPEMC-ECCE Asia)*. IEEE, 2016, pp. 179–184. ISBN: 978-1-5090-1210-7. DOI: 10.1109/IPEMC.2016.7512282.

[23] Zheming Jin, Giorgio Sulligoi, Rob Cuzner, Lexuan Meng, Juan C. Vasquez, and Josep M. Guerrero. “Next-Generation Shipboard DC Power System: Introduction Smart Grid and dc Microgrid Technologies into Maritime Electrical Netowrks”. In: *IEEE Electrification Magazine* 4.2 (2016), pp. 45–57. ISSN: 2325-5897. DOI: 10.1109/MELE.2016.2544203.

[24] Nesimi Ertugrul and Derek Abbott. “DC is the Future [Point of View]”. In: *Proceedings of the IEEE* 108.5 (2020), pp. 615–624. ISSN: 0018-9219. DOI: 10.1109/JPROC.2020.2982707.

[25] Aditya Shekhar, Laura Ramirez-Elizondo, and Pavol Bauer. “DC microgrid islands on ships”. In: *2017 IEEE Second International Conference on DC Microgrids (ICDCM)*. IEEE, 2017, pp. 111–118. ISBN: 978-1-5090-4479-5. DOI: 10.1109/ICDCM.2017.8001031.

[26] Luona Xu, Josep Guerrero, Abderezak Lashab, Baoze Wei, Najmeh Bazmohammadi, Juan Vasquez, and Abdullah Abusorrah. “A Review of DC Shipboard Microgrids—Part II: Control Architectures, Stability Analysis, and Protection

Schemes". In: *IEEE Transactions on Power Electronics* 37.4 (2022), pp. 4105–4120. ISSN: 0885-8993. DOI: 10.1109/TPEL.2021.3128409.

[27] Evangelos Grigoroudis and Michael Doumpos, eds. *Operational Research in Business and Economics*. Cham: Springer International Publishing, 2017. ISBN: 978-3-319-33001-3. DOI: 10.1007/978-3-319-33003-7.

[28] G. T. T. Vieira, M. B. C. Salles, Renato M. Monaro, and Bruno S. Carmo. *7th International Conference on Clean Electrical Power: Renewable Energy Resources Impact: Otranto, 2-4 July 2019*. Piscataway, NJ: IEEE, 2019. ISBN: 978-1-7281-1356-2. DOI: 10.1109/ICCEP46073.2019.

[29] Volker Staudt, Roman Bartelt, and Carsten Heising. "Fault Scenarios in DC Ship Grids: The advantages and disadvantages of modular multilevel converters". In: *IEEE Electrification Magazine* 3.2 (2015), pp. 40–48. ISSN: 2325-5897. DOI: 10.1109/MELE.2015.2413436.

[30] Mirsajed Pourmirasghariyan, Seyed Fariborz Zarei, and Mohsen Hamzeh. "DC-system grounding: Existing strategies, performance analysis, functional characteristics, technical challenges, and selection criteria - a review". In: *Electric Power Systems Research* 206 (2022), p. 107769. ISSN: 0378-7796. DOI: 10.1016/j.epsr.2021.107769.

[31] Robert Annuth, Timon Samuel Hartwich, Jana Ihrens, Christoph Klie, Mattis Molinski, Thorsten A. Kern, and Christian Becker. *SuSy Abschlussbericht Sustainable DC-Systems - Gleichstrom-Energieversorgung auf Schiffen: Abschlussbericht Technische Universität Hamburg*. DOI: 10.34657/18060.

[32] Andrea Alessia Tavagnutti, Andrea Vicenzutti, Davide Comugnaro, Daniele Bosich, Massimiliano Chiandone, and Giorgio Sulligoi. "Reduced Order Model of Zonal DC Microgrid for Open Source Real-time Emulation". In: *2024 Open Source Modelling and Simulation of Energy Systems (OSMSES)*. IEEE, 2024, pp. 1–6. ISBN: 979-8-3503-8468-0. DOI: 10.1109/OSMSES62085.2024.10668972.

[33] Sachin Yadav, Zian Qin, and Pavol Bauer. "Bipolar DC grids on ships: possibilities and challenges". In: *e & i Elektrotechnik und Informationstechnik* 139.4-5 (2022), pp. 458–467. ISSN: 0932-383X. DOI: 10.1007/s00502-022-01036-x.

[34] Yunjie Gu, Wuhua Li, and Xiangning He. "Analysis and Control of Bipolar LVDC Grid With DC Symmetrical Component Method". In: *IEEE Transactions on Power Systems* 31.1 (2016), pp. 685–694. ISSN: 0885-8950. DOI: 10.1109/TPWRS.2015.2403310.

[35] Walter F. Daenzer, ed. *Systems Engineering: Methodik und Praxis*. 11. durchges. Aufl. Zürich: Verl. Industrielle Organisation, 2002. ISBN: 3-857-43998-X.

[36] Horst Wildemann. *Komplexitätsmanagement: In Vertrieb, Beschaffung, Produkt, Entwicklung und Produktion*. 15. Aufl. Vol. 49. Leitfaden / TCW Transfer-Centrum für Produktions-Logistik und Technologie-Management. München: TCW Transfer-Centrum Verl., 2014. ISBN: 978-3-9315-1130-2.

[37] Ubaldo La Monaca, Serena Bertagna, Alberto Marinò, and Vittorio Bucci. "Integrated ship design: an innovative methodological approach enabled by new generation computer tools". In: *International Journal on Interactive Design and Manufacturing (IJIDeM)* 14.1 (2020), pp. 59–76. ISSN: 1955-2513. DOI: 10.1007/s12008-019-00612-4.

[38] Stefan Krueger. *Allgemeines zum Entwurfsumfeld [Lecture notes]*. 2001. URL: https://www.tuhh.de/t3resources/ssi/layout01INSTITUTE/Lehre/Numerische_Methoden_im_Schiffsentwurf/Vorlesungsunterlagen/01_Allgemeines_zum_Entwurfsumfeld.pdf (visited on 2025-09-23).

[39] Timon Samuel Hartwich, Kurt Sommer, Thorsten Alexander Kern, and Laura Haffner. *DC-Netze : ein ganzheitlicher Systementwurf für verschiedene Schiffstypen*. 2023. DOI: 10.15480/882.4392.

[40] gogiart. *Cruise Ship 07, liensed under CC BY 4.0*. URL: https://skfb.ly/oABWS (visited on 2025-07-04).

[41] Apostolos Papanikolaou. *Ship Design*. Dordrecht: Springer Netherlands, 2014. ISBN: 978-94-017-8750-5. DOI: 10.1007/978-94-017-8751-2.

[42] Baoyu Ni and Lingdong Zeng. "Ship Design Process". In: *Encyclopedia of Ocean Engineering*. Ed. by Weicheng Cui, Shixiao Fu, and Zhiqiang Hu. Singapore: Springer Singapore, 2019, pp. 1–8. ISBN: 978-981-10-6963-5. DOI: 10.1007/978-981-10-6963-5_36-1.

[43] J. Harvey Evans. "Basic Design Concepts". In: *Journal of the American Society for Naval Engineers* 71.4 (1959), pp. 671–678. DOI: 10.1111/j.1559-3584.1959.tb01836.x.

[44] Rachel Pawling, David Andrews, and Victoria Percival. "A Study into the Validity of the Ship Design Spiral in Early Stage Ship Design". In: *Journal of Ship Production and Design* 33.2 (2017), pp. 81–100. DOI: 10.5957/JSPD.33.2.160008.

[45] Giuseppe Nicosia, Panos Pardalos, Giovanni Giuffrida, Renato Umeton, and Vincenzo Sciacca, eds. *Machine Learning, Optimization, and Data Science*. Vol. 11331. Cham: Springer International Publishing, 2019. ISBN: 978-3-030-13708-3. DOI: 10.1007/978-3-030-13709-0.

[46] *[White Paper] Simulation-driven ship design: Rethinking marine design to increase productivity and early*. 2022. URL: https://static.sw.cdn.siemens.com/siemens-disw-assets/public/6LguukHruu2cXE5J67D5kb/en-US/Siemens%20SW%20Simulation%20driven%20ship%20design%20White%20Paper.pdf (visited on 2025-09-18).

[47] Lampros Nikolopoulos and Evangelos Boulougouris, eds. *A Methodology for the Holistic, Simulation Driven Ship Design Optimization under uncertainty*. 2018.

[48] A. Papanikolaou, G. Zaraphonitis, S. Harries, and M. Wilken. "Integrated Design and Multiobjective Optimization Approach to Ship Design". In: *ICCAS 2011: International Conference on Computer Applications in Shipbuilding*. RINA, 9202011, pp. 31–42. ISBN: 978-1-905-040872. DOI: 10.3940/rina.iccas.2011.50.

[49] Ulrich Gähde, Stephan Hartmann, and Jörn Henning Wolf, eds. *Models, simulations, and the reduction of complexity*. Online-Ausg. Vol. v.4. Abhandlungen der Akademie der Wissenschaften in Hamburg Ser. Berlin and Boston: De Gruyter, 2013. ISBN: 978-3-1103-1368-0. URL: http://site.ebrary.com/lib/alltitles/Doc?id=10819943.

[50] R. E. Shannon. "Introduction to the art and science of simulation". In: *1998 Winter Simulation Conference. Proceedings (Cat. No.98CH36274)*. IEEE, 1998, pp. 7–14. ISBN: 0-7803-5133-9. DOI: 10.1109/WSC.1998.744892.

[51] Jerry Banks, ed. *Handbook of simulation: Principles, Methodology, Advances, Applications, and Practice*. A Wiley-Interscience publication. New York and Weinheim: Wiley, 1998. ISBN: 0.471- 13403-1.

[52] Marvin Minsky. "Matter, Mind and Models". In: *Proc. IFIP Congress Information* 1 (1965). URL: http://hdl.handle.net/1721.1/6119.

[53] Michael Glöckler. *Simulation mechatronischer Systeme*. Wiesbaden: Springer Fachmedien Wiesbaden, 2014. ISBN: 978-3-658-05383-3. DOI: 10.1007/978-3-658-05384-0.

[54] Thomas R. Willemain. "Model Formulation: What Experts Think About and When". In: *Operations Research* 43.6 (1995), pp. 916–932. ISSN: 0030-364X. DOI: 10.1287/opre.43.6.916.

[55] Averill M. Law. *Simulation Modeling and Analysis*. 1st Random House ed. // Fifth edition. McGraw-Hill series in industrial engineering and management science. New York: Golden Book and McGraw-Hill Education, 2013. ISBN: 978-0-07-340132-4.

[56] Robert G. Sargent. *Winter Simulation Conference, 2007: 9 - 12 Dec. 2007, [Washington, DC] ; [proceedings*. Piscataway, NJ: IEEE Operations Center, 2007. ISBN: 978-1-4244-1306-5. URL: http://ieeexplore.ieee.org/servlet/opac?punumber=4419575.

[57] Aliki Ott. “System Testing in the Avionics Domain”. PhD thesis. Bremen: Universität Bremen.

[58] Andreas Markus Müsing. “Multi-Domain-Simulation in der Leistungselektronik”. Dissertation. Zürich: ETH Zürich, 2012.

[59] George E. P. Box. “Science and Statistics”. In: *Journal of the American Statistical Association* 71.356 (1976), p. 791. ISSN: 01621459. DOI: 10.2307/2286841.

[60] M. Lochbichler, F. Oestersotebier, A. Trachtler, M. Lochbichler, F. Oestersötebier, and A. Trächtler. “Dynamic Behavior Models and Their Modeling Depth in the Design Process of Mechatronic Systems”. In: (). DOI: 10.1115/IMECE2014-37040.

[61] Anastasia Gogi, Antuela A. Tako, and Stewart Robinson. “A preliminary study on the role of simulation models in generating insights”. In: *Proceedings of the Winter Simulation Conference 2014*. IEEE, 2014, pp. 3618–3629. ISBN: 978-1-4799-7486-3. DOI: 10.1109/WSC.2014.7020191.

[62] Martin Halle and Frank Thielecke. “Avionics Next-Gen Engineering Tools (AvioNET): Experiences With Highly Automised and Digital Processes for Avionics Platform Development”. In: *2021 IEEE/AIAA 40th Digital Avionics Systems Conference (DASC)*. IEEE, 2021, pp. 1–8. ISBN: 978-1-6654-3420-1. DOI: 10.1109/DASC52595.2021.9594509.

[63] R. J. Brooks and A. M. Tobias. “Choosing the Best Model: Level of Detail, Complexity, and Model Performance”. In: *Mathl. Comput. Modelling* Vol. 24.4 (1996), pp. 1–14.

[64] L. Chwif, M.R.P. Barretto, and R. J. Paul. “On simulation model complexity”. In: *2000 Winter Simulation Conference Proceedings (Cat. No.00CH37165)*. IEEE, 2000, pp. 449–455. ISBN: 0-7803-6579-8. DOI: 10.1109/WSC.2000.899751.

[65] Dennis B. Webster, Mary L. Padgett, Gail S. Hines, and Donald L. Sirois. “Determining the level of detail in a simulation model - a case study”. In: *Computing & Industry Engineering* Vol. 8 // 8.3/4 // 3-4 (1984), pp. 215–225. DOI: 10.1016/0360-8352(84)90014-7.

[66] John D. Salt. “Keynote Address: Simulation should be easy and fun!” In: *Proceedings of the 1993 Winter Simulation Conference, IEEE, New York* (1993), pp. 1–5.

[67] Leander Kotzur, Lars Nolting, Maximilian Hoffmann, Theresa Groß, Andreas Smolenko, Jan Priesmann, Henrik Büsing, Robin Beer, Felix Kullmann, Bismark Singh, Aaron Praktiknjo, Detlef Stolten, and Martin Robinius. “A modeler’s guide to handle complexity in energy systems optimization”. In: *Advances in Applied Energy* 4 (2021), p. 100063. ISSN: 26667924. DOI: 10.1016/j.adapen.2021.100063.

[68] R. Ahmed, M. Shah, and M. Umar. “Concepts of Simulation Model Size and Complexity”. In: *International Journal of Simulation Modelling* 15.2 (2016), pp. 213–222. ISSN: 17264529. DOI: 10.2507/IJSIMM15(2)2.317.

[69] J. D. Arthur, R. G. Sargent, J. B. Dabney, A. M. Law, and J. D. Morrison. “Verification and validation: what impact should project size and complexity have on attendant V&V activities and supporting infrastructure?” In: *WSC'99. 1999 Winter Simulation Conference Proceedings. 'Simulation - A Bridge to the Future' (Cat. No.99CH37038)*. IEEE, 1999, 148–155 vol.1. ISBN: 0-7803-5780-9. DOI: 10.1109/WSC.1999.823064.

[70] O. Balci, J. D. Arthur, and W. F. Ormsby. “Achieving reusability and composability with a simulation conceptual model”. In: *Journal of Simulation* 5.3 (2011), pp. 157–165. ISSN: 1747-7778. DOI: 10.1057/jos.2011.7.

[71] Thomas W. Lucas and John E. McGunnigle. “When is model complexity too much? Illustrating the benefits of simple models with Hughes' salvo equations”. In: *Naval Research Logistics (NRL)* 50.3 (2003), pp. 197–217. ISSN: 0894-069X. DOI: 10.1002/nav.10062.

[72] J. O. Henriksen. “Taming the Complexity Dragon”. In: *Journal of Simulation* 2.1 (2008), pp. 3–17. ISSN: 1747-7778. DOI: 10.1057/palgrave.jos.4250029.

[73] Rasmus Astrup, K. David Coates, and Erin Hall. “Finding the appropriate level of complexity for a simulation model: An example with a forest growth model”. In: *Forest Ecology and Management* 256.10 (2008), pp. 1659–1665. ISSN: 03781127. DOI: 10.1016/j.foreco.2008.07.016.

[74] M. Pidd and Mike Pidd. “Five simple principle of modelling”. In: Proceedings of the 1996 Winter Simulation Conference (), pp. 721–728. DOI: 10.1145/256562.256794.

[75] Jing Du. “The “weight” of models and complexity”. In: *Complexity* 21.3 (2016), pp. 21–35. ISSN: 10762787. DOI: 10.1002/cplx.21612.

[76] Lee Schruben and Enver Yücesan. “Complexity of Simulation Models: A Graph Theoretic Approach”. In: *Proceedings of the 1993 Winter Simulation Conference*. Vol. 10, pp. 94–106. DOI: 10.1287/ijoc.10.1.94.

[77] Russell K. Standish, Ang Yang, and Yin Shan, eds. *Concept and Definition of Complexity // Intelligent complex adaptive systems*. Hershey, PA: IGI Publishing, 2008. ISBN: 978-1-5990-4717-1. DOI: 10.4018/978-1-59904-717-1.ch004.

[78] Jay I. Myung, Mark A. Pitt, and In Jae Myung. “When a good fit can be bad”. In: *Trends in cognitive sciences* 6.10 (2002), pp. 421–425. DOI: 10.1016/s1364-6613(02)01964-2.

[79] Jack C. Wallace. “The control and transformation metric: toward the measurement of simulation model complexity”. In: *Proceedings of the 1987 Winter Simulation Conference* (), pp. 597–603. DOI: 10.1145/318371.318670.

[80] Gideon Schwarz. “Estimating the Dimension of a Model”. In: *The Annals of Statistics* 6.2 (1978), pp. 461–464. DOI: 10.1214/aos/1176344136.

[81] Gergely Popovics and László Monostori. “An approach to Determine Simulation Model Complexity”. In: *Procedia CIRP* 52 (2016), pp. 257–261. ISSN: 22128271. DOI: 10.1016/j.procir.2016.07.072.

[82] Michael W. Golay, Poong H. Seong, and Vincent P. Manno. “A Measure of the Difficulty of System Diagnosis and its Relationship to Complexity”. In: *International Journal of General Systems* 16.1 (1989), pp. 1–23. ISSN: 0308-1079. DOI: 10.1080/03081078908935060.

[83] James Ladyman, James Lambert, and Karoline Wiesner. “What is a complex system?” In: *European Journal for Philosophy of Science* 3.1 (2013), pp. 33–67. ISSN: 1879-4912. DOI: 10.1007/s13194-012-0056-8.

[84] Jakob Maier, C. M. Eckert, and John Clarkson. “Model granularity in engineering design – concepts and framework”. In: (2017). DOI: 10.17863/CAM.7973.

[85] Florian Netter, Frank Gauterin, and Chu Xu. “Complexity adaptation of simulation models in a function-based modular framework”. In: *2013 5th International Conference on Modeling, Simulation and Applied Optimization (ICMSAO)*. IEEE, 2013, pp. 1–6. ISBN: 978-1-4673-5814-9. DOI: 10.1109/ICMSAO.2013.6552642.

[86] Lukas Vogal and Miroslav Pecina. “Modeling theory and the level of model complexity”. In: *Vojnotehnicki glasnik* 67.2 (2019), pp. 365–373. ISSN: 0042-8469. DOI: 10.5937/vojtehg67-20537.

[87] Donn G. Decoursey. “Developing Models with More Detail: Do More Algorithms Give More Truth?” In: *Weed Technology* 6.3 (1992), pp. 709–715. ISSN: 0890-037X. DOI: 10.1017/S0890037X00036095.

[88] Andreas Tolk, ed. *Engineering management challenges for applying simulation as a green technology*. 2010.

[89] Bernard P. Zeigler. “Multifaceted modeling methodology: Grappling with the irreducible complexity of systems”. In: *Behavioral Science* 29.3 (1984), pp. 169–178. ISSN: 00057940. DOI: 10.1002/bs.3830290305.

[90] S. Robinson. “Conceptual modelling for simulation Part I: definition and requirements”. In: *Journal of the Operational Research Society* 59.3 (2008), pp. 278–290. ISSN: 0160-5682. DOI: 10.1057/palgrave.jors.2602368.

[91] Stewart Robinson. *Conceptual modeling for discrete-event simulation*. Boca Raton: CRC Press, 2011. ISBN: 978-1-4398-1037-8.

[92] Hae-Jin Choi, David L. Mcdowell, Janet K. Allen, and Farrokh Mistree. “An inductive design exploration method for hierarchical systems design under uncertainty”. In: *Engineering Optimization* 40.4 (2008), pp. 287–307. ISSN: 0305-215X. DOI: 10.1080/03052150701742201.

[93] Yue-Ping Xu and Martijn J. Booij. “Validation of a Model Appropriateness Framework Using the Elbe Decision Support System”. In: *Decision Support Systems in Agriculture, Food and the Environment*. Ed. by Yuchi Wang, Basil Manos, Nikolaos Matsatsinis, Konstantinos Paparrizos, and Jason Papathanasiou. Advances in Environmental Engineering and Green Technologies. IGI Global, 2010, pp. 193–218. ISBN: 978-1-6152-0881-4. DOI: 10.4018/978-1-61520-881-4.ch010.

[94] Oman Balci and O. Balci. “How To Assess The Acceptability And Credibility Of Simulation Results”. In: *Proceedings of the 1989 Winter Simulation Conference* (1989), pp. 62–71. DOI: 10.1109/WSC.1989.718663.

[95] Naoum Tsioptsias, Antuela Tako, and Stewart Robinson. “An Exploratory Study on the Uses of "Wrong" Simulation Models in Practice”. In: *Proceedings of SW21 The OR Society Simulation Workshop*. Operational Research Society, 3222021. DOI: 10.36819/SW21.018.

[96] Malcolm R. Forster. “Key Concepts in Model Selection: Performance and Generalizability”. In: *Journal of Mathematical Psychology* 44 (2000), pp. 205–231.

[97] S. C. Ward. “Arguments for Constructively Simple Models”. In: *Journal of the Operational Research Society* 40.2 (1989), pp. 141–153. ISSN: 0160-5682. DOI: 10.1057/jors.1989.19.

[98] Arnald Puy, Pierfrancesco Beneventano, Simon A. Levin, Samuele Lo Piano, Tommaso Portaluri, and Andrea Saltelli. “Models with higher effective dimensions tend to produce more uncertain estimates”. In: *Science advances* 8.42 (2022), eabn9450. DOI: 10.1126/sciadv.abn9450.

[99] Stewart Robinson. “Exploring the relationship between simulation model accuracy and complexity”. In: *Journal of the Operational Research Society* 74.9 (2023), pp. 1992–2011. ISSN: 0160-5682. DOI: 10.1080/01605682.2022.2122740.

[100] George Apostolakis. “A Commentary on Model Uncertainty: Report NUREG/CP-0138, US Nuclear Regulatory Commission, Washington, DC, 1994”. In: *Proceedings of Workshop on Model Uncertainty: Its Characterization and Quantification, Maryland* (1993).

[101] David Draper. “Assessment and Propagation of Model Uncertainty”. In: *Journal of the Royal Statistical Society Series B: Statistical Methodology* 57.1 (1995), pp. 45–70. ISSN: 1369-7412. DOI: 10.1111/j.2517-6161.1995.tb02015.x.

[102] Mingyang Xu, MW. Golay, and Michael Golay. “Survey of Model Selection and Model Combination”. In: *SSRN Electronic Journal* (2008). DOI: 10.2139/ssrn.1742033.

[103] Alexander Pollok and Daniel Bender. “Using multi-objective optimization to balance system-level model complexity”. In: *Proceedings of the 6th International Workshop on Equation-Based Object-Oriented Modeling Languages and Tools - EOOLT ’14*. Ed. by Peter Pepper and David Broman. New York, New York, USA: ACM Press, 2014, pp. 69–78. ISBN: 978-1-450-329538. DOI: 10.1145/2666202.2666213.

[104] E. Rexstad, G. S. Innis, Eric Rexstad, and George S. Innis. “Model simplification — Three applications”. In: *Ecological Modelling* 27.27 // 1-2 (1985), pp. 1–13. DOI: 10.1016/0304-3800(85)90021-3.

[105] Durk-Jouke van der Zee. “Model simplification in manufacturing simulation – Review and framework”. In: *Computers & Industrial Engineering* 127 (2019), pp. 1056–1067. ISSN: 03608352. DOI: 10.1016/j.cie.2018.11.038.

[106] P. A. Fishwick. “The role of process abstraction in simulation”. In: *IEEE Transactions on Systems, Man, and Cybernetics* 18.1 (1988), pp. 18–39. ISSN: 00189472. DOI: 10.1109/21.87052.

[107] Sebastian Rank, Christian Hammel, Thorsten Schmidt, Jan Muller, Andre Wenzel, Rainer Lasch, and Germar Schneider. “The correct level of model complexity in semiconductor fab simulation — Lessons learned from practice”. In: *2016 27th Annual SEMI Advanced Semiconductor Manufacturing Conference (ASMC)*. IEEE, 2016, pp. 133–139. ISBN: 978-1-5090-0270-2. DOI: 10.1109/ASMC.2016.7491145.

[108] Stewart Robinson and Roger Brooks. “Assumptions and simplifications in discrete-event simulation modelling”. In: *Journal of Simulation* (2024), pp. 1–18. ISSN: 1747-7778. DOI: 10.1080/17477778.2024.2407369.

[109] P. J. Courtois. “On time and space decomposition of complex structures”. In: *Communications of the ACM* 28.6 (1985), pp. 590–603. ISSN: 0001-0782. DOI: 10.1145/3812.3814.

[110] Suleyman Sevinc. “Theories of discrete event model abstraction”. In: *Proceedings of the 23rd Conference on Winter Simulation*, pp. 1115–1119.

[111] F. K. Frantz. “A taxonomy of model abstraction techniques”. In: (), pp. 1413–1420. DOI: 10.1109/WSC.1995.479055.

[112] Steven M. Manson. “Simplifying complexity: a review of complexity theory”. In: *Geoforum* 32.32 // 3 (2001), pp. 405–414. DOI: 10.1016/S0016-7185(00)00035-X.

[113] K. G. Vamvoudakis and S. Jagannathan. “Introduction to Complex Systems and Feedback Control”. In: *Control of Complex Systems*. Elsevier, 2016, pp. 3–30. ISBN: 978-0-1280-5246-4. DOI: 10.1016/B978-0-12-805246-4.00001-X.

[114] Herbert A. Simon. “The architecture of complexity”. In: *Proceedings of the American Philosophical Society* 106.6 (1962), pp. 467–482.

[115] Litmaps. *Litmaps*. (Version 2025-03-21) [Search Tool]. URL: https://app.litmaps.com/.

[116] Clara Sophie Köhnen, Jan Priesmann, Lars Nolting, Leander Kotzur, Martin Robinius, and Aaron Praktiknjo. “The potential of deep learning to reduce complexity in energy system modeling”. In: *International Journal of Energy Research* 46.4 (2022), pp. 4550–4571. ISSN: 0363-907X. DOI: 10.1002/er.7448.

[117] Hongpeng Liu, Jiageng Liu, and Wei Zhang. “Dynamic Aggregation Modeling for Droop Control Inverter Based on Slow Coherency Algorithm”. In: *2021 IEEE 16th Conference on Industrial Electronics and Applications (ICIEA)*. IEEE, 2021, pp. 983–988. ISBN: 978-1-6654-2248-2. DOI: 10.1109/ICIEA51954.2021.9516262.

[118] Lars Nolting, Thomas Spiegel, Marius Reich, Mario Adam, and Aaron Praktiknjo. “Can energy system modeling benefit from artificial neural networks? Application of two-stage metamodels to reduce computation of security of supply assessments”. In: *Computers & Industrial Engineering* 142 (2020), p. 106334. ISSN: 03608352. DOI: 10.1016/j.cie.2020.106334.

[119] Wanlu Zhu, Jian Shi, and Sherif Abdelwahed. “End-to-end system level modeling and simulation for medium-voltage DC electric ship power systems”. In: *International Journal of Naval Architecture and Ocean Engineering* 10.1 (2018), pp. 37–47. ISSN: 20926782. DOI: 10.1016/j.ijnaoe.2017.04.003.

[120] J. F. DeCarolis, S. Babaee, B. Li, and S. Kanungo. “Modelling to generate alternatives with an energy system optimization model”. In: *Environmental Modelling & Software* 79 (2016), pp. 300–310. ISSN: 13648152. DOI: 10.1016/j.envsoft.2015.11.019.

[121] Sunliang Cao and Kai Sirén. “Impact of simulation time-resolution on the matching of PV production and household electric demand”. In: *Applied Energy* 128 (2014), pp. 192–208. ISSN: 03062619. DOI: 10.1016/j.apenergy.2014.04.075.

[122] Adriaan P. Hilbers, David J. Brayshaw, and Axel Gandy. “Importance subsampling for power system planning under multi-year demand and weather uncertainty: August 18-21, 2020, Liège, Belgium : conference proceedings”. In: *2020 International Conference on Probabilistic Methods Applied to Power Systems (PMAPS)*. DOI: 10.1109/PMAPS47429.2020.

[123] Maximilian Hoffmann, Leander Kotzur, Detlef Stolten, and Martin Robinius. “A Review on Time Series Aggregation Methods for Energy System Models”. In: *Energies* 13.3 (2020), p. 641. DOI: 10.3390/en13030641.

[124] Maximilian Hoffmann, Jan Priesmann, Lars Nolting, Aaron Praktiknjo, Leander Kotzur, and Detlef Stolten. “Typical periods or typical time steps? A multi-model analysis to determine the optimal temporal aggregation for energy system models”. In: *Applied Energy* 304 (2021), p. 117825. ISSN: 03062619. DOI: 10.1016/j.apenergy.2021.117825.

[125] Leander Kotzur, Peter Markewitz, Martin Robinius, and Detlef Stolten. “Impact of different time series aggregation methods on optimal energy system design”. In: *Renewable Energy* 117 (2018), pp. 474–487. ISSN: 09601481. DOI: 10.1016/j.renene.2017.10.017.

[126] Oriol Raventós and Julian Bartels. “Evaluation of Temporal Complexity Reduction Techniques Applied to Storage Expansion Planning in Power System Models”. In: *Energies* 13.4 (2020), p. 988. DOI: 10.3390/en13040988.

[127] Toni Simolin, Kalle Rauma, Antti Rautiainen, Pertti Järventausta, and Christian Rehtanz. “Assessing the influence of the temporal resolution on the electric vehicle charging load modeling accuracy”. In: *Electric Power Systems Research* 208 (2022), p. 107913. ISSN: 0378-7796. DOI: 10.1016/j.epsr.2022.107913.

[128] Lukas Weimann and Matteo Gazzani. “A novel time discretization method for solving complex multi-energy system design and operation problems with high penetration of renewable energy”. In: *Computers & Chemical Engineering* 163 (2022), p. 107816. ISSN: 00981354. DOI: 10.1016/j.compchemeng.2022.107816.

[129] Koen van Greevenbroek, Chiara Bordin, and Sambeet Mishra. “Flexible time aggregation for energy systems modelling”. In: *Abstracts from the Energy Informatics.Academy Asia 2021 conference and PhD workshop*. Vol. 39 // 4. 2021, pp. 5850–5870.

[130] Stefanie Buchholz, Mette Gamst, and David Pisinger. “Sensitivity analysis of time aggregation techniques applied to capacity expansion energy system models”. In: *Applied Energy* 269 (2020), p. 114938. ISSN: 03062619. DOI: 10.1016/j.apenergy.2020.114938.

[131] Kais Siala. “Spatial Complexity in Energy System Modeling”. PhD thesis. Technische Universität München. URL: https://mediatum.ub.tum.de/doc/1547211/1547211.pdf (visited on 2025-03-27).

[132] Maria Yliruka, Stefano Moret, and Nilay Shah. *Detail or uncertainty? Applying global sensitivity analysis to strike a balance in energy system models*. 2023. DOI: 10.1016/j.compchemeng.2023.108287.

[133] Elias Ridha, Lars Nolting, and Aaron Praktiknjo. “Complexity profiles: A large-scale review of energy system models in terms of complexity”. In: *Energy Strategy Reviews* 30 (2020), p. 100515. ISSN: 2211467X. DOI: 10.1016/j.esr.2020.100515.

[134] Diana Süsser, Hannes Gaschnig, Andrzej Ceglarz, Vassilis Stavrakas, Alexandros Flamos, and Johan Lilliestam. “Better suited or just more complex? On the fit between user needs and modeller-driven improvements of energy system models”. In: *Energy* 239 (2022), p. 121909. ISSN: 03605442. DOI: 10.1016/j.energy.2021.121909.

[135] Jan Priesmann, Lars Nolting, and Aaron Praktiknjo. “Are complex energy system models more accurate? An intra-model comparison of power system optimization models”. In: *Applied Energy* 255 (2019), p. 113783. ISSN: 03062619. DOI: 10.1016/j.apenergy.2019.113783.

[136] Ali Soltani Tehrani, Haiying Cao, Sepideh Afsardoost, Thomas Eriksson, Magnus Isaksson, and Christian Fager. “A Comparative Analysis of the Complexity/Accuracy Tradeoff in Power Amplifier Behavioral Models”. In: *IEEE Transactions on Microwave Theory and Techniques* 58.6 (2010), pp. 1510–1520. ISSN: 0018-9480. DOI: 10.1109/TMTT.2010.2047920.

[137] Casey A. Myers, Peter J. Laz, Kevin B. Shelburne, and Bradley S. Davidson. “A probabilistic approach to quantify the impact of uncertainty propagation in musculoskeletal simulations”. In: *Annals of biomedical engineering* 43.5 (2015), pp. 1098–1111. DOI: 10.1007/s10439-014-1181-7.

[138] Rene Orth, Maria Staudinger, Sonia I. Seneviratne, Jan Seibert, and Massimiliano Zappa. “Does model performance improve with complexity? A case study with three hydrological models”. In: *Journal of Hydrology* 523 (2015), pp. 147–159. ISSN: 00221694. DOI: 10.1016/j.jhydrol.2015.01.044.

[139] Eun-Mi Hong, Yakov A. Pachepsky, Gene Whelan, and Thomas Nicholson. “Simpler models in environmental studies and predictions”. In: *Critical Reviews in Environmental Science and Technology* 47.18 (2017), pp. 1669–1712. ISSN: 1064-3389. DOI: 10.1080/10643389.2017.1393264.

[140] Hong Li, C.-Y. Xu, and Stein Beldring. “How much can we gain with increasing model complexity with the same model concepts?” In: *Journal of Hydrology* 527 (2015), pp. 858–871. ISSN: 00221694. DOI: 10.1016/j.jhydrol.2015.05.044.

[141] A. L. Hojberg and J. C. Refsgaard. “Model uncertainty – parameter uncertainty versus conceptual models”. In: *Water Science & Technology* 52.6 (2005), pp. 177–186.

[142] Saeideh Samani, Ming Ye, Fan Zhang, Yong-zhen Pei, Guo-ping Tang, Ahmed Elshall, and Asghar A. Moghaddam. “Impacts of prior parameter distributions on Bayesian evaluation of groundwater model complexity”. In: *Water Science and Engineering* 11.2 (2018), pp. 89–100. ISSN: 16742370. DOI: 10.1016/j.wse.2018.06.001.

[143] Larissa Kühn, Benani Zoumba, Tobias Spratte, Laura Maier, and Dirk Müller. "Level of Detail in Dynamic Simulation Models: A Comparison for Multi-Family Houses". In: *Proceedings of BauSim Conference 2024: 10th Conference of IBPSA-Germany and Austria*. Vol. 10, pp. 215–222. DOI: 10.26868/29761662.2024.28.

[144] Jay I. Myung and Mark A. Pitt. "Model comparison methods". In: *METHODS IN ENZYMOLOGY* 383 (2004), pp. 351–366. DOI: 10.1016/S0076-6879(04)83014-3.

[145] R. A. Stillman, S. McGrorty, J. D. Goss-Custard, and A. D. West. "Marine Ecology Progress Series 208:131 // Predicting mussel population density and age structure: the relationship between model complexity and predictive power". In: *Marine Ecology Progress Series* 208 (2000), pp. 131–145. ISSN: 0171-8630. DOI: 10.3354/meps208131.

[146] Bernard P. Zeigler, Alexandre Muzy, and Ernesto Kofman, eds. *Theory of Modeling and Simulation: Discrete event and iterative system computational foundations*. Third edition. London, San Diego, Cambridge, MA, Oxford, UK: Academic Press an imprint of Elsevier, 2019. ISBN: 978-0-1281-3370-5.

[147] Petra Winzer. *Generic Systems Engineering: Ein methodischer Ansatz zur Komplexitätsbewältigung*. New York: Springer and Springer Vieweg, 2013. ISBN: 978-3-6423-0364-7. DOI: 10.1007/978-3-642-30365-4.

[148] Richard E. Nance. "The Conical Methodology and the evolution of simulation model development". In: *Annals of Operations Research* 53.1 (1994), pp. 1–45. DOI: 10.1007/BF02136825.

[149] Rolf Böhm. *System-Entwicklung in der Wirtschaftsinformatik*. 5th ed. Zürich: vdf Hochschulverlag AG an der ETH Zürich, 2015. ISBN: 978-3-7281-3668-8.

[150] Klaus Gürlebeck, Dmitrii Legatiuk, Henrik Nilsson, and Kai Smarsly. "Conceptual modelling: Towards detecting modelling errors in engineering applications". In: ().

[151] Stephan Kolassa and Wolfgang Schütz. "Advantages of the MAD/Mean Ration over the MAPE". In: *Foresight: The International Journal of Applied Forecasting*. Vol. 6. 2007, pp. 40–43.

[152] "LMG 671 Datenblatt". In: ().

[153] Stewart Robinson. "Tutorial on Simulation Model Verification and Validation". In: *Proceedings of SW21 The OR Society Simulation Workshop*. Operational Research Society, 3222021. DOI: 10.36819/SW21.006.

[154] Joint Committee for Guides in Metrology. *Guide to the Expression of Uncertainty in Measurement (GUM)*. 2008. URL: https://www.iso.org/sites/JCGM/GUM/JCGM100/C045315e-html/C045315e.html?csnumber=50461 (visited on 2025-09-18).

[155] M. Couture. *Complexity and Chaos: State-of-the-Art; Formulations and Measures of Complexity*. 2007. URL: https://apps.dtic.mil/sti/tr/pdf/ADA475275.pdf (visited on 2025-09-18).

[156] Joel J. Luna and J. J. Luna. "Hierarchical Relations in Simulation Models". In: *Proceedings of the 1993 Winter Simulation Conference* (), pp. 132–137. DOI: 10.1109/WSC.1993.718038.

[157] Bruce Edmonds. "Syntactic Measures of Complexity". PhD thesis. University of Manchester, 1999.

[158] Thomas J. McCabe. "A Complexity Measure". In: *IEEE Transactions on Software Engineering* VOL. SE-2.4 (1976).

[159] John L. Hennessy, David A. Patterson, Krste Asanović, Jason D. Bakos, Robert P. Colwell, Thomas M. Conte, José Duato, Diana Franklin, David Goldberg, Norman P. Jouppi, Sheng Li, Naveen Muralimanohar, Gregory D. Peterson, Timothy M. Pinkston, Parthasarathy Ranganathan, David A. Wood, and Amr Zaky. *Computer Architecture: A quantitative approach*. Amsterdam, 2011.

[160] Juan Tapia, Marta Gomez-Barrero, and Christoph Busch. "An Efficient Super-Resolution Single Image Network using Sharpness Loss Metrics for Iris". In: *2020 IEEE International Workshop on Information Forensics and Security (WIFS)*. IEEE, 2020, pp. 1–6. ISBN: 978-1-7281-9930-6. DOI: 10.1109/WIFS49906.2020.9360886.

[161] Steven S. Muchnick. *Advanced compiler design and implementation*. [Nachdr.] San Francisco, Calif.: Morgan Kaufmann, 2007. ISBN: 978-1-558-603202.

[162] Juraj Hromkovič. *Theoretische Informatik: Formale Sprachen, Berechenbarkeit, Komplexitätstheorie, Algorithmik, Kommunikation und Kryptographie*. 4., aktualisierte Aufl. Studium. Wiesbaden: Vieweg-+-Teubner, 2011. ISBN: 978-3-8348-0650-5.

[163] S. Lloyd. "Measures of complexity: a nonexhaustive list". In: *IEEE Control Systems* 21.4 (2001), pp. 7–8. ISSN: 1066-033X. DOI: 10.1109/MCS.2001.939938.

[164] Peilun Yang, Hanchen Wang, Jianye Yang, Zhengping Qian, Ying Zhang, and Xuemin Lin. "Deep Learning Approaches for Similarity Computation: A Survey". In: *IEEE Transactions on Knowledge and Data Engineering* 36.12 (2024), pp. 7893–7912. ISSN: 1041-4347. DOI: 10.1109/TKDE.2024.3422484.

[165] Paulo Eduardo Nogueira, Rivalino Matias, and Elder Vicente. "An experimental study on execution time variation in computer experiments". In: *Proceedings of the 29th Annual ACM Symposium on Applied Computing*. Ed. by Yookun Cho, Sung Y. Shin, Sangwook Kim, Chih-Cheng Hung, and Jiman Hong. New York, NY, USA: ACM, 3242014, pp. 1529–1534. ISBN: 978-1-450-324694. DOI: 10.1145/2554850.2555022.

[166] Matheus Henrique Junqueira Saldanha and Adriano Kamimura Suzuki. “Determining the Probability Distribution of Execution Times”. In: *2021 IEEE Symposium on Computers and Communications (ISCC)*. IEEE, 2021, pp. 1–6. ISBN: 978-1-6654-2744-9. DOI: 10.1109/ISCC53001.2021.9631411.

[167] H. B. Mann and Whitney. D. R. “on a Test of Whether one of two random variables is stochastically larger than the other”. In: *The Annals of Mathematical Statistics* 18.1 (1947).

[168] Jürgen Bortz, Gustav A. Lienert, and Klaus Boehnke. *Verteilungsfreie Methoden in der Biostatistik*. 3., korrigierte Aufl. Springer-Lehrbuch Bachelor, Master. Heidelberg: Springer Medizin Verl., 2008. ISBN: 978-3-5407-4706-2.

[169] William H. Kruskal and W. Allen Wallis. “Use of Ranks in One-Criterion Variance Analysis”. In: *Journal of the American Statistical Association* 47.260 (1952), pp. 583–621. ISSN: 01621459. DOI: 10.1080/01621459.1952.10483441.

[170] Meysam Aghighi. “Computational Complexity of some Optimization Problems in Planning”. In: ().

[171] Ling Huang, Jinzhu Jia, Bin Yu, Byung-gon Chun, Petros Maniatis, and Mayur Naik. “Predicting Execution Time of Computer Programs Using Sparse Polynomial Regression”. In: *ResearchGate* (2010).

[172] Eric J. Hoevenaars and Curran A. Crawford. “Implications of temporal resolution for modeling renewables-based power systems”. In: *Renewable Energy* 41 (2012), pp. 285–293. ISSN: 09601481. DOI: 10.1016/j.renene.2011.11.013.

[173] Joakim Widén, Ewa Wäckelgård, Jukka Paatero, and Peter Lund. “Impacts of different data averaging times on statistical analysis of distributed domestic photovoltaic systems”. In: *Solar Energy* 84.3 (2010), pp. 492–500. ISSN: 0038092X. DOI: 10.1016/j.solener.2010.01.011.

[174] Hector Zenil. “A Review of Methods for Estimating Algorithmic Complexity: Options, Challenges, and New Directions”. In: *Entropy (Basel, Switzerland)* 22.6 (2020). DOI: 10.3390/e22060612.

[175] A. N. Kolmogorov. “On tables of random numbers”. In: *Theoretical Computer Science* 207.2 (1998), pp. 387–395. ISSN: 03043975. DOI: 10.1016/S0304-3975(98)00075-9.

[176] R. J. Solomonoff. “A formal theory of inductive inference. Part I”. In: *Information and Control* 7.1 (1964), pp. 1–22. ISSN: 00199958. DOI: 10.1016/S0019-9958(64)90223-2.

[177] Gregory J. Chaitin. “On the Simplicity and Speed of Programs for Computing Infinite Sets of Natural Numbers”. In: *Journal of the ACM* 16.3 (1969), pp. 407–422. ISSN: 0004-5411. DOI: 10.1145/321526.321530.

[178] Charles H. Bennett. “Logical Depth and Physical Complexity”. In: *The Universal Turing Machine– a Half-Century Survey*. Ed. by Rolf Herken. Oxford University Press, 1988.

[179] Wolfgang Dahmen and Arnold Reusken. *Numerik für Ingenieure und Naturwissenschaftler*. 2., korrigierte Aufl. Springer-Lehrbuch. Berlin, Heidelberg: Springer Berlin Heidelberg and Springer, 2008. ISBN: 978-3-540-76492-2. DOI: 10.1007/978-3-540-76493-9.

[180] Sérgio Henrique Vannucchi Leme de Mattos, Luiz Eduardo Vicente, Andrea Koga Vicente, Cláudio Bielenki Júnior, and José Roberto Castilho Piqueira. “Metrics based on information entropy applied to evaluate complexity of landscape patterns”. In: *PloS one* 17.1 (2022), e0262680. DOI: 10.1371/journal.pone.0262680.

[181] Yamila M. Omar and Peter Plapper. “A Survey of Information Entropy Metrics for Complex Networks”. In: *Entropy (Basel, Switzerland)* 22.12 (2020). DOI: 10.3390/e22121417.

[182] C. E. Shannon and W. Weaver. *The Mathematical Theory of Communication*. Urbana: University of Illinois Press, 1949.

[183] Murray Gell-Mann and Seth Lloyd. “Information measures, effective complexity, and total information”. In: *Complexity* 2.1 (1996), pp. 44–52. ISSN: 10762787. DOI: 10.1002/(SICI)1099-0526(199609/10)2:1{\%}3C44::AID-CPLX10{\%}3E3.0.CO;2-X.

[184] Omar Masmali and Omar Badreddin. “Comprehensive Model-Driven Complexity Metrics for Software Systems”. In: *2020 IEEE 20th International Conference on Software Quality, Reliability and Security Companion (QRS-C)*, pp. 674–675. DOI: 10.1109/QRS-C51114.2020.00115.

[185] Stewart Robinson. *Issues in conceptual modelling for simulation: setting a research agenda*. Ed. by S. Robinson, S. Taylor, S. Brailsford, and J. Garnett.

[186] S. Wang, R. Chen, J. D. VanWyk, F. C. Lee, and W. G. Odendaal. “Developing Parasitic Cancellation Technologies to Improve EMI Filter Performance for Switching Mode Power Supplies”. In: *IEEE Transactions on Electromagnetic Compatibility* 47.4 (2005), pp. 921–929. ISSN: 0018-9375. DOI: 10.1109/TEMC.2005.857367.

[187] Jianjing Wang, Henry Shu-hung Chung, and River Tin-ho Li. “Characterization and Experimental Assessment of the Effects of Parasitic Elements on the MOSFET Switching Performance”. In: *IEEE Transactions on Power Electronics* 28.1 (2013), pp. 573–590. ISSN: 0885-8993. DOI: 10.1109/TPEL.2012.2195332.

[188] Hamburg University of Technology, Institute for Mechatronics in Mechanics. *EA-PSB 11500-60 4U Elektroautomatik Bidirectional Power Supply*. 2024. DOI: 10.15480/882.14713.

[189] Hamburg University of Technology, Institute for Electrical Power and Energy Technology. *DM APS/22500 Spitzenberger & Spies 3-Phase Power System*. 2024. DOI: 10.15480/882.14630.

[190] *LiFePO4 Datasheet: JB-LFP12-2C*. Datasheet (accessed 2025-07-16). Just Battery Technology UG. URL: https://www.jubatec.net/img/2424m1.pdf.

[191] *LMG671 Precision Power Analyzer*. 671. Datasheet (accessed 2025-09-18). Zimmer. URL: https://www.zes.com/de/content/download/1663/19541/file/Brochure-LMG671-EN.pdf.

[192] Clemens Boertz. "Energy demand of a fuel cell-driven cruise ship: Analysis and improved prediction method of the operational power variation under different loading and environmental conditions". Master Thesis. Delft: Delft University of Technology, 2020. URL: http://resolver.tudelft.nl/uuid:1526765e-8491-4576-910d-1c0f38d15b53.

[193] Bojana Barać, Matej Krpan, and Tomislav Capuder. "Modelling of PEM Fuel Cell for Power System Dynamic Studies". In: *IEEE Transactions on Power Systems* 39.2 (2024), pp. 3286–3298. ISSN: 0885-8950. DOI: 10.1109/TPWRS.2023.3297741.

[194] Marlin Malpricht, Jana Ihrens, and Thorsten A. Kern. "Analysis of DC–DC converters as critical components for maritime DC grid simulation". In: *Electric Power Systems Research* 247 (2025), p. 111788. ISSN: 0378-7796. DOI: 10.1016/j.epsr.2025.111788.

[195] Jana Ihrens, Shayan Bahadori Rad, and Thorsten A. Kern. "Complexity of meshed and bidirectional maritime DC-System Simulations". In: *2023 International Conference on Future Energy Solutions (FES)*. IEEE, 2023, pp. 1–6. ISBN: 979-8-3503-3230-8. DOI: 10.1109/FES57669.2023.10182908.

[196] ABB AS. "The step forward Onboard DC Grid". In: (2014). URL: https://new.abb.com/docs/librariesprovider91/articles/lm00614-onboard-dc-grid-brochure_june2014_1.pdf (visited on 2023-01-05).

[197] Timon Hartwich. "Potential der Sektorenkopplung in dezentralen DC-Schiffsbordnetzen". Master Thesis. Hamburg: Technische Universität Hamburg, 2020.

[198] Juliana Lüer, Ali Elnwegy, Maximilian Becker, Ornella Tortorici, and Thorsten Alexander Kern. "Toward a Standardized Characterization of Vibrotactile Actuators under Coupled-Resonance-Dynamics [Preprint]". In: *SSRN Electronic Journal* (2026). Available at SSRN: https://ssrn.com/abstract=5669010. DOI: 10.2139/ssrn.5669010. URL: http://dx.doi.org/10.2139/ssrn.5669010.

[199] Ali Elnwegy, Maximilian Becker, Juliana Lüer, Ornella Tortorici, and Thorsten Alexander Kern. “A systematic method to characterize the frequency response of vibrotactile actuators for coupled-system-dynamics [Preprint]”. In: *SSRN Electronic Journal* (2026). Available at SSRN: https://ssrn.com/abstract=5669010. DOI: 10.2139/ssrn.5669010. URL: http://dx.doi.org/10.2139/ssrn.5669010.

[200] *Model 352C65 Accelerometer Manual*. 352C65. Datasheet (accessed 2025-07-16). PCB Piezotronics. URL: https://www.pcb.com/contentStore/docs/pcb_corporate/vibration/products/manuals/352c65.pdf.

[201] *Model 208C03 Force Sensor Manual*. 208C03. Datasheet (accessed 2025-07-16). PCB Piezotronics. URL: https://www.pcb.com/contentstore/docs/pcb_corporate/forcetorque/products/manuals/208c03.pdf.

[202] *Model EX682A40 Signal Conditioner Manual*. EX682A40. Datasheet (accessed 2025-07-16). PCB Piezotronics. URL: https://www.pcb.com/contentstore/docs/pcb_corporate/electronics/products/manuals/ex682a40.pdf.

[203] *USB-1608G-Series-data Manual*. DAQ USB-1608GX-2AO. Datasheet (accessed 2025-07-16). Measurement Computing Corp. URL: https://files.digilent.com/datasheets/USB-1608G-Series-data.pdf.

[204] Amazon Web Services, Inc., ed. *AWS On-Demand Instances – Amazon Web Services (AWS)*. URL: https://aws.amazon.com/de/ec2/pricing/on-demand/ (visited on 2025-08-02).

[205] Digital Experts, ed. *Softwareentwicklung Kosten: Welchen Preis hat eine Individualsoftware? Stundenlohn Programmierer*. URL: https://www.digital-experts.com/micro-blog/softwareentwicklung-kosten-was-kostet-eine-individualsoftware (visited on 2022-12-18).

[206] WELT, ed. *Neues Kreuzfahrtschiff: Wie "AIDAbella" die Ems-Überführung meisterte*. 2008. URL: https://www.welt.de/reise/article1845637/Neues-Kreuzfahrtschiff-Wie-AIDAbella-die-Ems-Ueberfuehrung-meisterte.html (visited on 2025-07-11).

[207] *Pricing and Licensing*. URL: https://de.mathworks.com/pricing-licensing.html?prodcode=ML&intendeduse=undefined (visited on 2022-12-18).

[208] United Nations. “Transforming our World: The 2030 Agenda for Sustainable Development: A/RES/70/1”. In: (). URL: https://sdgs.un.org/sites/default/files/publications/21252030%20Agenda%20for%20Sustainable%20Development%20web.pdf (visited on 2025-10-06).

[209] Catherine S.E. Bale, Liz Varga, and Timothy J. Foxon. “Energy and complexity: New ways forward”. In: *Applied Energy* 138 (2015), pp. 150–159. ISSN: 03062619. DOI: 10.1016/j.apenergy.2014.10.057.

[210] Michael J. North. “A time and space complexity analysis of model integration”. In: *Proceedings of the Winter Simulation Conference 2014*. IEEE, 2014, pp. 1644–1651. ISBN: 978-1-4799-7486-3. DOI: 10.1109/WSC.2014.7020015.

[211] Ulrich Schlienz. *Schaltnetzteile und ihre Peripherie*. Wiesbaden: Springer Fachmedien Wiesbaden, 2020. ISBN: 978-3-658-29489-2. DOI: 10.1007/978-3-658-29490-8.

[212] Ralf Kories and Heinz Schmidt-Walter. *Taschenbuch der Elektrotechnik: Grundlagen und Elektronik*. 11., überarbeitete Auflage. Europa Lehrmittel. Haan-Gruiten: Verlag Europa-Lehrmittel Nourney Vollmer GmbH & Co. KG, 2017. ISBN: 978-3-80-855865-2.

[213] Carl Carlson. *Effective FMEAs: Achieving safe, reliable, and economical products and processes using failure mode and effects analysis*. Vol. 1. Quality and reliability engineering series. Hoboken N.J.: Wiley, 2012. ISBN: 978-1-1180-0743-3.

[214] Annick Melanson and Sylvie Nadeau. “Resilience Engineering for Sustainable Prevention in the Manufacturing Sector: A Comparative Study of Two Methods of Risk Analysis”. In: *American Journal of Industrial and Business Management* 09.01 (2019), pp. 267–281. ISSN: 2164-5167. DOI: 10.4236/ajibm.2019.91017.